ISSN: 2408-2384 (Online)
ISSN: 1686-5456 (Print)

Environment and Natural Resources Journal

Volume 19, Number 1, January - February 2021

Environment and Natural Resources Journal (EnNRJ)

Volume 19, Number 1, January - February 2021 ISSN: 1686-5456 (Print)
ISSN: 2408-2384 (Online)

AIMS AND SCOPE

The Environment and Natural Resources Journal is a peer-reviewed journal, which provides insight scientific knowledge into the diverse dimensions of integrated environmental and natural resource management. The journal aims to provide a platform for exchange and distribution of the knowledge and cutting-edge research in the fields of environmental science and natural resource management to academicians, scientists and researchers. The journal accepts a varied array of manuscripts on all aspects of environmental science and natural resource management. The journal scope covers the integration of multidisciplinary sciences for prevention, control, treatment, environmental clean-up and restoration. The study of the existing or emerging problems of environment and natural resources in the region of Southeast Asia and the creation of novel knowledge and/or recommendations of mitigation measures for sustainable development policies are emphasized.

The subject areas are diverse, but specific topics of interest include:

- Biodiversity
- Climate change
- Detection and monitoring of polluted sources e.g., industry, mining
- Disaster e.g., forest fire, flooding, earthquake, tsunami, or tidal wave
- Ecological/Environmental modelling
- Emerging contaminants/hazardous wastes investigation and remediation
- Environmental dynamics e.g., coastal erosion, sea level rise
- Environmental assessment tools, policy and management e.g., GIS, remote sensing, Environmental Management System (EMS)
- Environmental pollution and other novel solutions to pollution
- Remediation technology of contaminated environments
- Transboundary pollution
- Waste and wastewater treatments and disposal technology

Schedule

Environment and Natural Resources Journal (EnNRJ) is published 6 issues per year in January-February, March-April, May-June, July-August, September-October, and November-December.

Publication Fees

There is no cost of the article-processing and publication.

Ethics in publishing

EnNRJ follows closely a set of guidelines and recommendations published by Committee on Publication Ethics (COPE).

Environment and Natural Resources Journal (EnNRJ)

Volume 19, Number 1, January - February 2021 ISSN: 1686-5456 (Print)
ISSN: 2408-2384 (Online)

Editorial Office Address
Research Management and Administration Section,
Faculty of Environment and Resource Studies, Mahidol University
999, Phutthamonthon Sai 4 Road, Salaya, Phutthamonthon, Nakhon Pathom, Thailand, 73170
Phone +662 441 5000 ext. 2108 Fax. +662 441 9509-10
Website: https://ph02.tci-thaijo.org/index.php/ennrj/index
E-mail: ennrjournal@gmail.com

Environment and Natural Resources Journal (EnNRJ)

Volume 19, Number 1, January - February 2021 ISSN: 1686-5456 (Print)
ISSN: 2408-2384 (Online)

CONTENT

Organic Carbon in Wetland Soil: Seasonal Flooded Forest, Northeastern Thailand

Piyakarn Teartisup[1*], Prapeut Kerdsueb[1], and Suwalee Worakhunpiset[2]

[1]*Faculty of Environment and Resource Studies, Mahidol University, Nakhon Pathom 73170, Thailand*
[2]*Faculty of Tropical Medicine, Mahidol University, Nakhon Pathom 73170, Thailand*

ARTICLE INFO

Received: 19 Feb 2020
Received in revised: 20 Jul 2020
Accepted: 13 Aug 2020
Published online: 28 Oct 2020
DOI: 10.32526/ennrj/19/2020035

Keywords:
Soil organic carbon/ Wetlands/ Seasonal flooded forest

*** Corresponding author:**
E-mail: tpiyakarn@gmail.com

ABSTRACT

Seasonal flooded forest is one of the most important wetlands in northeastern Thailand, not only for its abundant biodiversity, but also as a source of carbon sequestration. Organic carbon plays an specially important role in the soil carbon cycle. To reinforce comprehension on soil organic carbon, five profiles in a northeast plateau were observed and determined. The most common trees were *Albizzia Odoratissima*, *Combretum quadrangulare Kurz*, and *Streblus asper Lour*. The contents of Soil Organic Carbon (SOC) varied from 3.52 g⁄kg to 5.90 g⁄kg in top soil and varied from 4.01 g⁄kg to 4.60 g⁄kg in sub soil. There was a close relationship between SOC content and basic soil properties, especially the bulk density of both top soil layer and sub soil layer. The distribution of SOC content was harmonized with distribution of plants. In comparative analysis, the flooded forest that composted with a high percentage of vegetation coverage (Khud Tew, Khud Chi Tao) had a significantly higher SOC content. The SOC storage varied from 2.65 kg/m^2 to 4.18 kg/m^2. Khud Chi Tao contained the maximum amount of SOC storage, whereas Kwo Chi Yai had the minimum. Limitation of flooded forest survival concerned over landscape change, particularly plant disappearance and waterlogged shortage. Therefore, vegetation and hydrology management have to be implemented practically to retain the existing organic carbon in wetlands and allow the soil to sequester additional carbon.

1. INTRODUCTION

One of the most important wetland ecosystem services is carbon sequestration. it is worth emphasizing that, in wetland landscapes, all components are continually interacting with ecosystems (Chaikumbung et al., 2019). Wetlands have mostly been recognized as the transitional zones that fall between terrestrial and aquatic ecosystems and are highly productive. They are characterized by waterlogged conditions with a low decomposition rate of organic material and impact the wetland creation on carbon stocks. Wetlands are also known to be an important component of the global carbon cycle (Moomaw et al., 2018). Although wetlands occupy only 6% of the earth's surface but is one of the most important parts of terrestrial ecosystems and the largest carbon pool (Stolarski et al., 2018). However, the complexity of the wetland carbon cycle causes difficulty in estimating the wetland carbon pool. Soil organic carbon (SOC) is one of the keystone elements in controlling soil properties. It enables soils to be resilient against extended droughts and extreme rainfall events, especially in wetlands. Generally, wetlands contain a disproportionate amount of the earth's total soil carbon which holding between 20 and 30% (Ren et al., 2020). The global soil organic carbon stock in wetlands is uncertain, ranging from 202 to 535 Pg C (Mitra et al., 2005). The SOC content in wetland soils is also affected by natural conditions and human activities (Ma et al., 2015), which play a key role in the global Carbon cycle and how much organic carbon remains in wetlands. SOC is a reservoir in the terrestrial ecosystem and it maintains soil properties such as organic matter, and it is critical in tackling climate change because of its carbon storage capacity (Lal et al., 2018). Soil properties play a key role in soil

Citation: Teartisup P, Kerdsueb P, Worakhunpiset S. Organic Carbon in Wetland Soil: Seasonal Flooded Forest, Northeastern Thailand. Environ. Nat. Resour. J. 2021;19(1):1-9. (https://doi.org/10.32526/ennrj/19/2020035)

carbon accumulation and transformation (Sims et al., 2012). During the management of wetlands, we should pay attention to the original SOC content before wetland cultivation, as well as the balance of SOC inputs and outputs during the wetland cultivation process. In addition, other soil properties, such as pH, total nitrogen, and bulk density, should be considered due to their close correlation with SOC (Xu et al., 2019). The 12th session of Conference of Parties (COP 12) aspires to increase global soil organic matter stocks as a compensation for the global emissions of greenhouse gases by SOC anthropogenic sources (Minasny et al., 2017), highlighting the extreme role that wetlands play in the carbon cycle. Therefore, carbon sequestration is an important environmental service that wetland ecosystems can provide (Marin-Muniz et al., 2014). However, information about the vertical distribution and storage of SOC in wetlands is scant.

The Chi River is located in the Chi River Basin, Northeastern of Thailand. The Chi River Basin is one of the two major sub-basins forming the lower part of the Mekong River and its estimated catchment area is 4,947,600 ha (Arunyanart et al., 2017). One of the wetland types within the Chi River is the seasonal flooded forests which are mostly influenced by water and climate conditions. Nowadays, the loss of seasonal flooded forests in the Chi River territory is considered to be the highest among the lower Mekong area over the past 60 years (Homdee et al., 2016). The seasonal flooded forests serve as a natural wetland capital or stock, yielding a sustainable flow of useful goods and services. However, increasingly intensive human activities and the vulnerability of climate change have caused severe degradation of natural wetlands, which directly threatens wetland health and causes the decline of its ecological functions. Hence, the natural wetland conditions and human activities also affect SOC content in soils and its major role in forming and stabilizing soil structure, enhancing soil physical properties, and nutrient recycling. Because of the extreme role that wetlands play in the carbon cycle, it is feasible to consider changes in wetlands, along with the SOC process, may transform them to be a carbon sink. To envision this, an explicit description of the SOC distribution and storage is needed. The overall objectives of this study were (i) to examine the relationship between some soil properties and SOC content; and (ii) to estimate the SOC storage of the wetland.

2. METHODOLOGY

2.1 The study site

The Chi Basin is located in the central part of Northeastern Thailand between the range 15.3 ºN to 17.3 ºN and 101.3 ºE to 104.3 ºE (Figure 1). The overall topography has an average elevation of 120 to 170 m.a.s.l., and its total catchment area covers approximately 49,476 km^2. Rice is the major crop in the rain-fed agricultural area, which accounts for 60% of the land use in the basin. There are mountains and high plateau ranges on the border from the North to the West making the lower part look like a flat bowl in which deciduous and evergreen forests are the main forest types covering 20% of the entire area (Homdee et al., 2016). Chi River has wetlands composed of flooded forests as follows: Khud Tew, Nong Ngow, Kang Kha, Khud Chi Tao and Kwo Chi Yai. These five seasonal flooded forests and wetlands, which cover along the river basin, are public benefit areas. These five wetlands provide important ecological services and benefits to the local communities causing continuous use and disturbance of the area. The local climate is influenced by tropical monsoons and this area usually undergoes a long period of warmth due to its inland nature and tropical latitude zone. From March-May is the summer season, the hottest period of the year, with maximum temperatures usually reaching 40ºC or higher. The following rainy season significantly reduces the temperatures from mid-May to lower than 40ºC. Then, the outbreaks of cold weather from China occasionally reduce the temperatures to fairly low values in the winter.

In the Northeast Plateau of the Chi River Basin, the average annual precipitation is approximately 1,150 mm/year and the range in precipitation varies between 900 mm and 1,700 mm. The terrain slopes downward slightly from West to East and this area has distinct geological features, characterized by sandy sedimentary rocks from mainly the Triassic period and younger with a limited area of quaternary alluvium (Department of Mineral Resources, 2013). The quaternary alluvium can be found particularly along the river valleys.

2.2 Sampling and laboratory method

The field survey was conducted from January to March in 2017. The sampling points of soils were distributed according to seasonal flooded forests and each site was assigned a set of 10 plots to collect

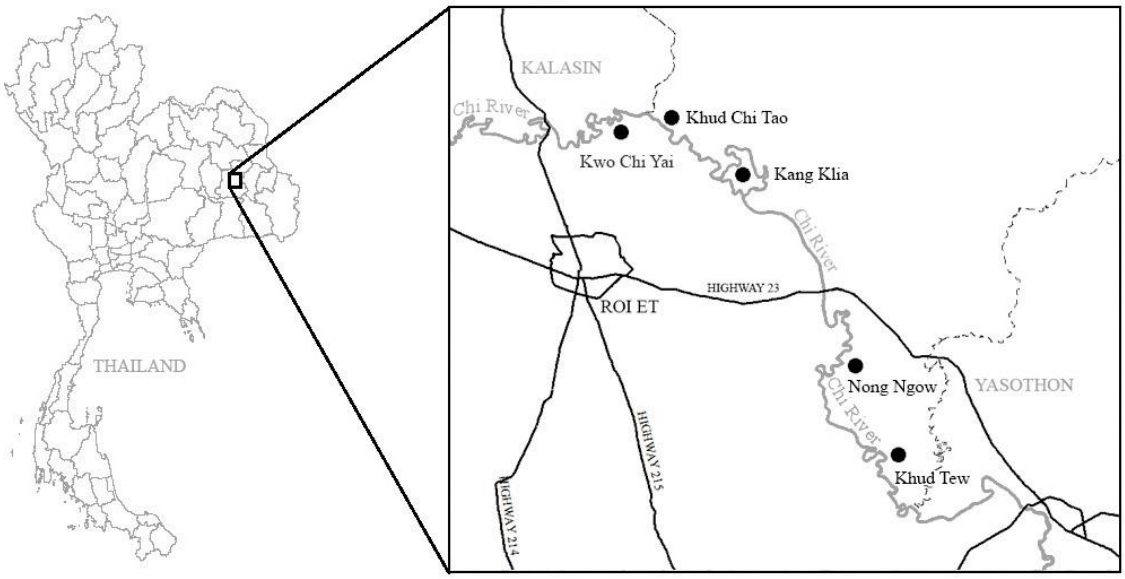

Figure 1. Location of Chi River Basin and distribution of the sampling points. Seasonal flooded forests P1 (Khud Tew); P2 (Nong Ngow); P3 (Kang Klia); P4 (Khud Chi Tao); P5 (Kwo Chi Yai).

soil samples. Samples from each plot were collected in triplicate from both the surface and subsurface soil. The soil samples were collected after the removal of plant debris and detritus. Sampling was performed using a 10 cm diameter drill in each layer at two depth ranges, 0 cm to 30 cm and 30 cm to 60 cm, to get a total of 300 soil samples that were kept in plastic bags. Using a cut ring method, two bulk density samples were collected in a stainless steel cylinder of 100 cm^3 in volume. At the laboratory, the composite soil samples were oven dried until constant weight and then weighed g for soil bulk density determination (Rayment and Higginson, 1992). The soil samples were described as air dried, then the temperature shall not be more than 30°C). The dried samples were sieved by 100 meshes. The SOC was determined by dry combustion method (Wang et al., 2016). Ammonium saturation method was used to determine cation exchange capacity (CEC) (Chesworth, 2008). Soil reaction (pH) was measured in a solution with 1 to 5 ratios between soil and water (He et al., 2012). Soil texture was determined by pipet method. Kjeldahl method determined total nitrogen (Bremner and Mulvaney, 1982). Organic matter was determined by Walkley- Black method. For general wetland surveys, we used line transect and vegetation inventory and specie identification (Table 1).

Table 1. Wetland and environment

Profile	Wetland	Coordinate	Flood duration (months/year)	Vegetation		Soil sample
				Species	Coverage	
P1	Khud Tew	103.97E 15.86N	<2	*Albizia Odoratissima, Combretum quadrangulare Kurz, Streblus asper Lour*	66%	30
P2	Nong Ngow	103.93E 15.96N	<2	*Albizia Odoratissima, Streblus asper Lour*	55%	30
P3	Kang Klia	103.82E 16.16N	<2	*Albizia Odoratissima, Combretum quadrangulare Kurz*	53%	30
P4	Khud Chi Tao	103.74E 16.22N	<2	*Albizia Odoratissima, Combretum quadrangulare Kurz, Streblus asper Lour*	78%	30
P5	Kwo Chi Yai	103.96E 16.21N	2-3	*Albizia Odoratissima, Combretum quadrangulare Kurz*	41%	30

Soil bulk density was determined by undisturbed soil sampling with stainless steel cylinder. Then the bulk density of dry matter (BD, g/cm^3) was calculated from (1).

$$BD = m(1-C_w)/V \quad (1)$$

Where; m is total weight of wet soil (g); C_w is water content (%); V is volume of cylinder (cm^3).

The soil organic carbon density of a single section is calculated by the layer thickness and weight. The difference of SOC in difference depths can help to reduce the estimation error (Zhang et al., 2018). The density of SOC (D_{soc}, kg/m^3) was calculated from (2).

$$D_{soc} = BD \times SOC \quad (2)$$

Where; BD indicates soil bulk density (g/cm^3); and SOC indicates the organic Carbon content of dry soil (g/kg).

In the other profile, the organic carbon storage was calculated from (3) (Bridhikitti, 2017).

$$TC = \sum D_{soci} \times H_i \quad (3)$$

Where; TC is the SOC storage per unit area (kg/m^2); H is the thickness of profile (m); " i" is number of layers.

2.3 Statistical analysis

The data analysis was calculated by statistical software (SPSS). Soil properties were measured in terms of average and deviation. The relationship between SOC components and partial soil properties were conducted with Pearson's correlation coefficient by proposing the related variables in the linear regression model. The differences of mean values in the soil data sets were determined between various wetlands and at different depths. The t-test method was used to determine statistical differences at a 95% level of confidence ($p<0.05$).

3. RESULTS AND DISCUSSION

3.1 Result

3.1.1 Soil physical and chemical properties

Table 2 shows the physical and chemical properties of all the soil samples. The pH values indicated that all layers were slightly acid (less than 6.5). Cation exchange capacity values were medium to moderately high (more than 10 meq 100/g). The rich exchange properties of these soils are in the clear results indicate.

The whole bulk density was 1.12 g/cm^3 to 1.51 g/cm^3. However, the areas with flood duration of 2-3 months/year showed lower bulk densities than the areas with flood duration less than 2 months/year.

The organic matter of all layers also showed a variability of contents from low to moderately high (less than 3.5%). However, the average organic matter content of soil samples with high vegetation cover (P1, P2, P3, and P4) was a little higher.

In general, the percentage nitrogen in these soils showed low values (less than 0.2%). Except that soil samples of P3, P4, P5 had high nitrogen values in the top soil, depending strongly on both organic matter and soil depth. When the organic matter values were high, the percentage nitrogen tended to be higher and certainly was more abundant in top soil layers than sub soil layers.

Table 2. Soil properties

Wetland	Depth	BD	CEC	pH	OM	N	SOC
		g/cm^3	meq 100/g		%	%	g/kg
Khud Tew (P1)	Top soil	1.23±0.02	20.52±1.84	4.64±0.29	3.34±1.55	1.83±0.19	5.81±3.30
	Sub soil	1.48±0.05	14.32±3.73	4.65±0.30	0.72±0.21	0.14±0.06	4.60±1.90
Nong Ngow (P2)	Top soil	1.21±0.02	19.28±2.81	5.04±0.38	2.00±0.58	1.96±0.08	5.33±3.02
	Sub soil	1.41±0.05	20.21±3.01	5.52±0.41	0.74±0.31	0.16±0.06	4.21±2.51
Kang Klia (P3)	Top soil	1.28±0.01	20.33±1.80	4.72±0.24	2.02±0.51	6.22±2.39	5.02±1.94
	Sub soil	1.51±0.01	15.01±4.23	5.09±0.25	0.65±0.36	0.13±0.04	4.04±1.51
Khud Chi Tao (P4)	Top soil	1.32±0.04	19.04±2.48	4.56±0.32	2.49±0.72	6.83±2.64	5.90±2.73
	Sub soil	1.50±0.06	13.49±3.42	4.94±0.46	0.74±0.27	0.13±0.06	4.01±1.92
Kwo Chi Yai (P5)	Top soil	1.12±0.01	15.14±4.05	4.88±0.23	1.12±0.13	3.77±1.21	3.52±0.91
	Sub soil	1.20±0.03	15.72±4.77	5.07±0.27	0.96±0.23	0.13±0.03	4.11±1.10

Remark: Top soil is 0 cm to 30 cm; Sub soil is 30 cm to 60 cm; ± is standard deviation

3.1.2 Distribution of the SOC content

In Figure 2, the vertical distributions of SOC are shown. Profiles P1, P2, P3 and P4 had high SOC content in the top soil layer and decreased sharply in sub soil layers. Profile P5 presented the inverse SOC content distribution pattern, showing higher SOC content in the sub soil layer. Plants in P5 had probably undergone drought circumstances or human exploitation creating abandoned plant matter on the ground. Thus, tree leave debris was found deeper than the surface layer. Variation in SOC content between top and sub soil was small, only 0.6 g/kg, while the variation between profiles was more than 1 g/kg. It has been reported that the hydrologic condition is the main factor that causes the SOC content to be uniform with depth (Zhang et al., 2016).

3.1.3 Organic carbon density and organic carbon storage

For all of soil profiles, the SOC density of top soil layer varies from 3.92 kg/m^3 to 7.79 kg/m^3, with a mean of 6.3 kg/m^3. Meanwhile, sub soil layers vary from 4.92 kg/m^3 to 6.81 kg/m^3, with a mean of 5.9 kg/m^3, reflecting a decreasing soil bulk density of P4 followed by P1, P2, P3, and P5, sequentially. Similarly, the SOC content was highest in P4 followed by P1, P2, P3, and P5.

The vertical distribution of SOC density showed two patterns along with increase of soil depth. Profiles P1, P2, P3, and P4 had higher SOC density in the top soil layer and lower SOC density in the sub soil layer. The exception to this pattern was seen in profile P5, which presented the inverse SOC density distribution pattern. The SOC density in profile P5 increased in the sub soil layer. The estimation of SOC storages showed variation in values from 2.65 kg/m^2 to 4.18 kg/m^2, with a mean of 3.68 kg/m^2. The highest was P4 followed by P1, P2, P3, and P5, sequentially.

3.1.4 Bulk density and organic carbon relationship

The correlation analysis found that SOC content in wetland is closely related to bulk density ($r=0.36$, $p<0.05$). Interestingly, as the SOC content decreased, the bulk density increased. The reasonable cause may be that plant matter, particularly the stem and leaves of plants, accumulate to become a litter layer, porous-textured high organic matter with an abundance of organic carbon inside. According to the results, SOC density showed a distribution pattern similar with the SOC content. SOC content and soil bulk density determine the SOC density. The linear correlation value between SOC density and SOC content was estimated to be highly significant ($r=0.85$, $p<0.05$) (Figure 3).

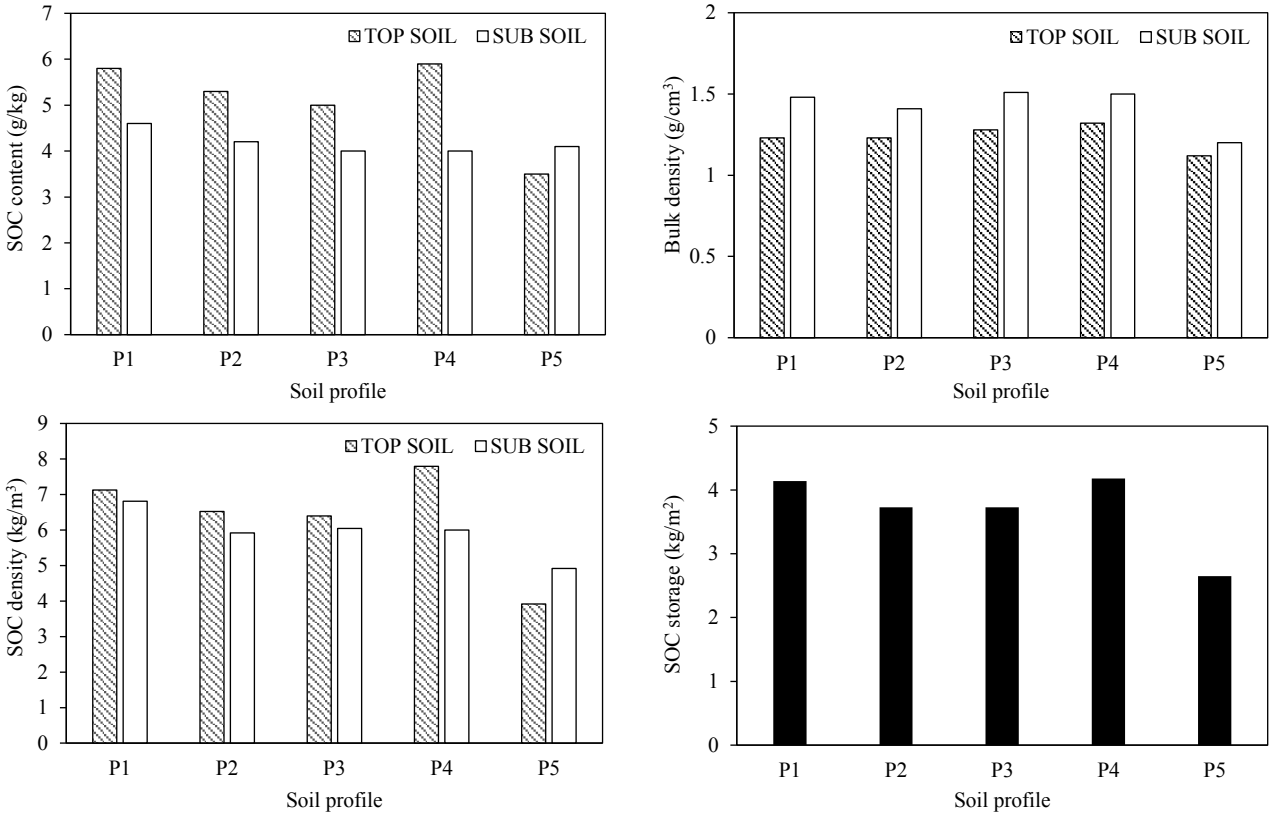

Figure 2. Distribution of SOC content, bulk density, SOC density, and SOC storage

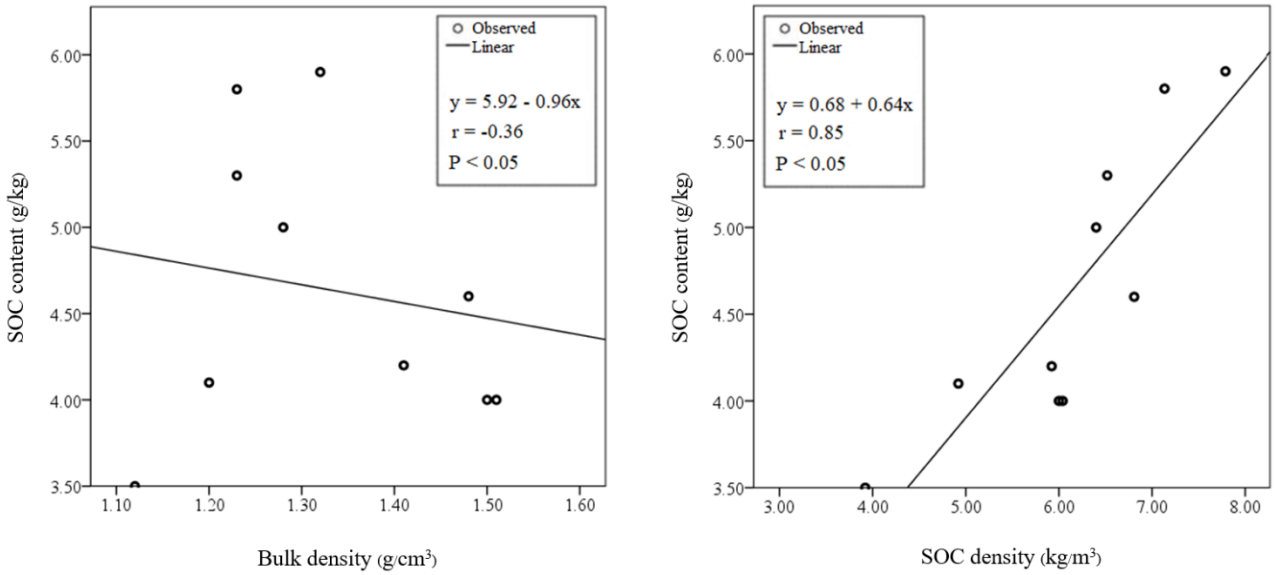

Figure 3. Scatter plot correlation in SOC content, Bulk density, and SOC density

3.1.5 Soil organic carbon content and density in vertical distribution

The vertical distribution of SOC content and SOC density normally decreased top-down to the lower depth. The wetlands (P1, P2, P3, and P4) showed high SOC content in top soil, more than 5 g/kg and then decreased significantly in sub soil, less than 5 g/kg. The results show the maximum SOC density occurred in the top soil in profile P4 (7.79 kg/m^3) and the minimum in profile P5 (3.92 kg/m^3). Conversely, the profile P5 showed higher values in sub soil. It is possible that there were previous events causing a lot of carbon input to the sub soil depth, such as logging and droughts. The vertical distribution database is found in Table 3.

Table 3. Vertical distribution of SOC content and SOC density

Profile	SOC content (g/kg)		SOC density (kg/m^3)	
	Top soil	Sub soil	Top soil	Sub soil
P1	5.81^{Aa}	4.60^{Ba}	7.13 ^{Ca}	6.80 ^{Db}
P2	5.33^{Ab}	4.21 ^{Ba}	6.51 ^{Cb}	5.92 ^{Da}
P3	5.02^{Ab}	4.04 ^{Ba}	6.40 ^{Cb}	6.04 ^{Da}
P4	5.90^{Aa}	4.01 ^{Ba}	7.78 ^{Ca}	6.00 ^{Da}
P5	3.52^{Ac}	4.11 ^{Aa}	3.92 ^{Cc}	4.82 ^{Dc}

Remark: Mean value followed by a different upper case letter indicates significant differences between the soil depths at p<0.05, mean value followed by a different lower case letter indicates significant differences between soil profiles at p<0.05.

3.2 Discussion

3.2.1 Characteristic of soil organic carbon content in wetland

A consequence of interactions among many factors affect the vertical distribution of SOC. Land use and vegetation are main factors that input organic matter directly to the soil by plant litter (roots, stems, leaves). In this study, SOC content decreased with the change in depth. SOC in the top soil was significantly higher than sub soil (Xu et al., 2016). One wetland area (P5) of this study presented SOC content that differs from the others in that the top soil SOC was 3.5 g/kg and increased to 4.1 g/kg in sub soil. This might be the effect of plants that were buried due to some previous drought, and exploitation by man, indirectly in combination with this area having the lowest percentage of vegetation of only 41%. Moreover, we suggest that the organic matter (OM) value was somewhat high (0.96%) in this sub soil. Organic matter contributes most of the organic carbon (Rennert et al., 2018). This finding is in agreement with Mayer et al. (2019), who also found high amounts of SOC in sub soil caused by alluvial sediments rich in OM that were successively buried during previous flooding

events. In addition, the study of Wang et al. (2016) that found the deeper soil contained higher SOC content than the top layer at a sampling site in a coastal wetland. This might be influenced by some previous events such as storm, drought, and human disturbances leading to the accumulation of plant material in the subsoil and a more thorough decomposition, which is affected by depth and age. Moreover, since this area has the lower amount of vegetative coverage, the downward migration of organic matter to the deep soil by water leaching combined with rainfall might be a factor of higher SOC in the deeper soil. In addition, the lower SOC in top soil might be caused by human activities leading to the loss of SOC in the top soil (Okebalama et al., 2017). Moreover, wet conditions are obviously related to biochemical processes in soil. Long duration flooding causes an anaerobic environment that restricts the degradation of organic matter (Lim et al., 2020). This balance may be altered by both natural and anthropic factors. Esteves et al. (2001) suggested that permanent waterlogging induces anaerobic conditions in which the SOC decomposes slowly while the optimal range soil proportions for the physiological performance of the plants were adequate by of air and water (Morales-Olmedo et al., 2015). Ferronato et al. (2019) found that the effect of soil waterlogging on chemical and biological reactions in wetlands depended on the rate of water flow and erosional processes.

The vegetation mainly affected the horizontal distribution of SOC content. In particular, the vegetation coverage contributed plant debris to SOC content. Our study revealed the SOC content of five wetlands ranged from 3.5 g/kg to 5.8 g/kg with an average of 5.1 g/kg in top soil. Comparatively, it was higher than paddy fields which have 2.40 g/kg (Yod-i et al., 2014). Obviously, the profile P4 had the highest SOC content followed by P1, P2, P3, and P5, sequentially which correlated with the descending order of vegetation coverage. The results also show SOC content among sites was significantly different. This is in accordance with the studies of Demenoisa et al. (2017) and Wang et al. (2016) who suggested that the highest vegetation covered areas with stable plant communities had enriched SOC content and the vegetation coverage was highly aligned with the horizontal distribution of SOC content.

This research showed the conversion of wetland into abandoned plant not only caused a breakdown of the SOC content that changed the soil structure, but also the decline of SOC. Kunlanit et al. (2019) found that the SOC contents in top soil were higher than sub soil in a forest area. This research indicated that the SOC content and distribution depended on various factors, including not only soil properties, but also the surrounding environment. Questions still remain about the influence of vegetation, particularly because of the short-time of this investigation. The change of seasonal vegetation may provide a dynamic of SOC contents caused by the variation of plant residue. Therefore, the continuous monitor in all seasons should be considered for more understanding of this accumulation process and its relationship with SOC content.

3.2.2 Organic carbon density and storage in wetland

The important measurements to estimate the SOC density is the soil bulk density and SOC content. Apparently, the SOC density showed the trends of being lower in the sub soil with little variability between locations, while top soil had a higher SOC density and more variability. Amber and Ken (2011) and Zhang et al. (2019) suggested that SOC density is not only an important role in organic carbon storage estimating but the characteristics of organic carbon storage in different ecosystem are also reflected since horizontal consideration, the difference of canopy cover had significant. Our results indicate that SOC density in profile P4 was 1.98 times of SOC density in profile P5. Obviously, a large amount of vegetation coverage was found at the area with the predominant SOC density. Wu et al. (2015) suggested that reclamation has a great influence on bringing down SOC density which might be due to reclamation not only reducing plant residue, but also changing physical factors of soil and water, such as heat condition, accumulation, and microorganism disappearance. Therefore, Sulman et al. (2009) stated that the decomposer activity and vegetation input were interrupted, as well as the SOC density was obviously conducive to decline and parallel decay of different individual compounds (Schowalter, 2017). Xu et al. (2016) mentioned that SOC content decreases with increasing depth in a corn field. Similarly, the other profiles with large vegetation coverage lead to more storage canopy of SOC as well. From this point of view, in the wetland, the primary factor that limits the storage of SOC was the condition of the vegetation. This conforms to the study of Wang et al. (2016) that suggested the significance of vegetation coverage on

SOC content, and also indicated that plant factors, as well as sedimentation rate, water content and coarse grain size of soil were considered as the key factors that have an effect on the sequestration of organic carbon. Meanwhile, Kayranli et al. (2010) stated that the relative degree of carbon input and output is the factor that controls SOC. This research found the mean of SOC storage was 3.68 kg/m^2, whereas Wu et al. (2015) observed the SOC in a wetland plateau of China was 14.6 kg/m^2, Zhang et al. (2018) observed the SOC in a wetland in Northeast China was 27.4 kg/m^2. This research found the mean of SOC storage was 3.68 kg/m^2, whereas Zhang et al. (2019) observed a site at Guizhou Province of China stored approximately 1.58 Pg of SOC and suggested that the average SOC density in the top 1.00 m of soil associated with different land uses decreased. Xu et al. (2016) indicated the existence of global patterns in carbon related to time, temperature and latitudinal gradients following afforestation. YaoMin et al. (2012) found the SOC content in wetlands is an important part of the terrestrial soil organic carbon pools, but there was a lack of data.

In comparison, this research finding was much lower than other reports with respect to SOC storage. Thus, the explanation for this finding may be that the flood duration was too short, making low sedimentation rate, limiting vegetation decomposed as well as the soil parent material was sandstone that producing somewhat coarse grain size of soil particle and soil drainage well until organic matter avoids embedding in situ. The best practice should be implemented to pause the organic carbon decline, such as zoning for plant protected areas, emphasizing understanding and wise use of wetlands by the local communities, as well as supporting permanent waterlogging by checked dam.

4. CONCLUSION

In this study, the distribution and preservation of soil organic carbon in flooded forest wetlands was examined. The results showed that SOC content of top soil was higher than sub soil. The horizontal distribution of SOC content in top soil varied much more than in sub soil. Either soil bulk density or SOC density have related with SOC content, the soil bulk density closely related SOC content in term of negative relationship ($r=-0.36$, $p<0.05$), and this suggested that The SOC density had a strong positive relationship with SOC content ($r=0.85$, $p<0.05$). Comparison of areas with different vegetation coverage and also waterlogged less than three months a year showed the SOC content had a tendency of decreasing from high to low as the percentage of vegetation coverage decreased. Apparently, Khud Chi Tao, which had the highest vegetation coverage (78%), had the maximum amount of soil storage, containing 5.90 g/kg, whereas Kwo Chi Yai, which had the lowest vegetation coverage (41%), had the minimum amount of soil storage, only 3.52 g/kg. Due to the limitation of plant coverage area took care of SOC storage depressing, as showed 4.18 kg/m^2 in highest percentage of vegetation coverage and 2.65 kg/m^2 in lowest percentage of vegetation coverage. These wetlands indicated that the soil storage had an average value of 3.68 kg/m^2. Thus, the wetland management should consider maintaining plants and moisture in the soils to permanently conserve organic carbon. Actually, this approach is rarely practical because the wetland area suffers from frequent droughts, and the local people still disturb the natural resources regularly. Therefore, in terms of sustainable management, there should be specific measures set up for land utilization, following wetland management measures at the national level and in accordance with local needs. Thus, the wetland measures taken will lead to action and the relevant sectors will be able to formulate strategies and allocate budgets to restore and reclaim flooded forest wetlands to maintain ecological value. Meanwhile, steps should also be taken to raise awareness in the local communities of the importance of flooded forest wetlands to mitigate climate change.

ACKNOWLEDGEMENTS

This study was funded by National Research Council of Thailand (NRCT). We are appreciative so much to ENVI Clinic, Faculty of Environment and Resource Studies, Mahidol University for facilities.

REFERENCES

Amber DN, Ken WB. The contribution of carbon-based payments to wetland conservation compensation on agricultural landscapes. Agricultural Systems 2011;104(1):75-81.

Arunyanart N, Limsiri C, Uchaipichat A. Flood hazards in the Chi River Basin, Thailand: Impact management of climate change. Applied Ecology and Environmental Research 2017; 15(4):841-61.

Bremner JM, Mulvaney CS. Methods of Soil Analysis. Wisconsin, USA: American Society of Agronomy and Soil Science Society of America; 1982.

Bridhikitti A. Soil and biomass carbon stocks in forest and agricultural lands in tropical climates. Songklanakarin Journal of Science and Technology 2017;39(6):697-707.

Chaikumbung M, Doucouliagos H, Scarborough H. Institutions, culture, and wetlands values. Ecological Economics 2019;157:195-204.

Chesworth W. Encyclopedia of Soil Science. Dordrecht, Netherlands: Springer; 2008.

Demenoisa J, Carricondeb F, Reyc F, Stokesd A. Tropical plant communities modify soil aggregate stability along a successional vegetation gradient on a Ferralsol. Ecological Engineering 2017;109:161-8.

Department of Mineral Resources. Geological map of Thailand (scale 1:1,000,000). Bangkok, Thailand: Ministry of Natural Resources and Environment; 2013.

Esteves FA, Enrich PA, Biesboer DD. Potential denitrification in submerged natural and impacted sediments of Lake Batata, An Amazonian Lake. Hydrobiologia 2001;444(1):111-7.

Ferronato C, Marinari S, Francioso O, Bello D, Trasar-Cepeda C, Antisari LV. Effect of waterlogging on soil biochemical properties and organic matter quality in different salt marsh systems. Geoderma 2019;338:302-12.

He Y, DeSutter T, Prunty L, Hopkins D, Jia X, Wysocki DA. Evaluation of 1:5 soil to water extract electrical conductivity methods. Geoderma 2012;185-186:12-7.

Homdee T, Pongput K, Kanae S. A comparative performance analysis of three standardized climatic drought indices in the Chi River Basin, Thailand. Agriculture and Natural Resource 2016;50(3):211-9.

Kayranli B, Scholz M, Mustafa A, Hedmark A. Carbon storage and fluxes within freshwater: A critical review. Wetlands 2010;30(1):111-24.

Kunlanit B, Butnan S, Vityakon P. Land-use changes influencing c sequestration and quality in topsoil and subsoil. Agronomy 2019;9(9):2-6.

Lal R, Smith P, Jungkunst H, Mitsch W, Lehmann J, Ramachandran N, et al. The carbon sequestration potential of terrestrial ecosystems. Journal of Soil and Water Conservation 2018;73(6):145-52.

Lim M, Patureau D, Heran M, Lesage G, Kim J. Removal of organic micropollutants in anaerobic membrane bioreactors in wastewater treatment: Critical review. Environmental Science Water Research and Technology 2020;6:1230-43.

Ma K, Liu J, Balkovic J, Skalski R, Azevedo LB, Kraxner F. Changes in soil organic carbon stocks of wetlands on China's Zoige plateau from 1980 to 2010. Ecological Modelling 2016;327:18-28.

Marin-Muniz JL, Hernandez ME, Moreno-Casasola P. Comparing soil carbon sequestration in coastal freshwater wetlands with various geomorphic features and plant communities in Veracruz, Mexico. Plant Soil 2014;378:1-15.

Mayer S, Kolbl A, Volkel J, Kogel-Knabner I. Organic matter in temperate cultivated floodplain soils: Light fractions highly contribute to subsoil organic carbon. Geoderma 2019;337: 679-90.

Minasny B, Malone BP, McBratney AB, Angers DA, Arrouays D, Chambers A, et al. Soil carbon 4 per mile. Geoderma 2017; 292:59-86.

Mitra S, Wassmann R, Vlek PL. An appraisal of global wetland area and its carbon stock. Current Science 2005;88:25-35.

Moomaw WR, Chmura GL, Davies GT, Finlayson CM, Middleton BA, Natali SM, et al. Wetlands in a changing climate: Science, policy and management. Wetlands 2018;38(2):183-205.

Morales-Olmedo M, Ortiz M, Selles G. Effects of transient soil waterlogging and its importance for rootstock selection. Chilean Journal of Agricultural Research 2015;75(1):45-56.

Okebalama CB, Igwe CA, Okolo CC. Soil organic carbon levels in soils of contrasting land uses in Southeastern Nigeria. Tropical and Subtropical Agroecosystems 2017;20(3):493-504.

Rayment GE, Higginson FR. Australian Soil and Land Survey Handbook: Volume 3, Australian Laboratory Handbook of Soil and Water Chemical Methods. Melbourne, Australia: Inkata Press; 1992.

Ren Y, Li X, Mao D, Wang Z, Jia M, Chen L. Investigating spatial and vertical patterns of wetland soil organic carbon concentrations in China's Western Songnen plain by comparing different algorithms. Sustainability 2020;12(3):2-13.

Rennert T, Georgiadis A, Ghong P, Rinklebe J. Compositional variety of soil organic matter in Mollic floodplain-soil profiles-also an indicator of pedogenesis. Geoderma 2018;311:15-24.

Schowalter TD. Insect Ecology: An Ecosystem Approach. 4th ed. London, United Kingdom: Elsevier; 2017.

Sims L, Pastor J, Lee T, Dewey B. Nitrogen, phosphorus and light effects on growth and allocation of biomass and nutrients in wild rice. Oecologia 2012;170:65-76.

Stolarski MJ, Śnieg M, Krzyżaniak M, Tworkowski J, Szczukowski S, Graban L, et al. Short rotation coppices, grasses and other herbaceous crops: Biomass properties versus 26 genotypes and harvest time. Industrial Crops and Products 2018;119:22-32.

Sulman BN, Desai AR, Cook BD, Saliendra N, Mackay DS. Contrasting carbon dioxide fluxes between a drying shrub wetland in northern Wisconsin, and nearby Forests. Biogeosciences 2009;6(6):1115-26.

Wang O, Song J, Cao L, Li X, Yuan H, Li N. Distribution and storage of soil organic carbon in a coastal wetland under the pressure of human activities. Soil Sediments 2016;17(1):11-22.

Wu Y, Wang F, Zhu S. Vertical distribution characteristics of soil organic carbon content in Caohai wetland ecosystem of Guizhou plateau, China. Journal of Forestry Research 2015;27:551-6.

Xu S, Liu X, Li X, Tian C. Soil organic carbon changes following wetland cultivation: A global meta-analysis. Geoderma 2019; 347:49-58.

Xu X, Li D, Cheng X, Ruan, H, Luo Y. Carbon: Nitrogen stoichiometry following afforestation: A global synthesis. Science Report 2016;6:19117.

YaoMin Z, ZhenGuo N, Peng G, YongJiu D, Wei S. Preliminary estimation of the organic carbon pool in China's wetlands. Chinese Science Bulletin 2012;58(6):1-9.

Yod-i G, Aumtong S, Punya T. Effect of water management and soil on permanganate oxidizable carbon and total organic carbon in paddy soil. Khon Kaen Agriculture Journal 2014;42(Special Issue):322-330. (in Thai)

Zhang Z, Zhou Y, Wang S, Huang X. Estimation of soil organic carbon storage and its fractions in a small karst watershed. Acta Geochim 2018;37:113-24.

Zhang W, Xiao H, Tong C, Su Y, Xiang W, Huang D, et al. Estimating organic carbon storage in temperate wetland profiles in northeast China. Geoderma 2008;146(1-2):311-6.

Zhang Z, Huang X, Zhou Y, Zhang J, Zhang X. Discrepancies in karst soil organic carbon in southwest China for different land use patterns: A case study of Guizhou Province. International Journal of Environmental Research and Public Health 2019;16(21):3-14.

Restoration of Water Storage Potential in a Degraded Dry Dipterocarp Forest with Enrichment Planting of Three Needle Pine (*Pinus kesiya* Royle ex Gordon), Northern Thailand

Thananiti Thichan*, Niwat Anongrak, Soontorn Khamyong, and Panida Kachina

Faculty of Agriculture, Chiang Mai University, Chiang Mai 50200, Thailand

ARTICLE INFO

Received: 2 Jun 2020
Received in revised: 17 Aug 2020
Accepted: 27 Aug 2020
Published online: 28 Oct 2020
DOI: 10.32526/ennrj/19/2020130

Keywords:
Biomass water/ Dry dipterocarp forest/ Plant biomass/ Soil water/ Water storage

*** Corresponding author:**
E-mail: thananiti61@gmail.com

ABSTRACT

The research assessed water storage in a dry dipterocarp forest (DDF) with enriched 34-year-old pine planting and the role of pine. Plant surveys were carried out using 10, 40×40 m^2 plots, and data were obtained by measuring tree stem girths and heights. Plant features, biomass, and stored water amounts were measured. Fresh plant samples of abundant species were taken one time per month from January to December 2018. Three soil pits were made in three plots, and soil samples along 100 cm depth were taken on the same days of collecting plant samples for studying fied capacity, water content and water amount. The DDF was divided into three stands based on the most dominant tree species; *Shorea obtusa*, *Dipterocarpus tuberculatus*, and *Dipterocarpus obtusifolius*. The forest was composed of 86 species with biomass at 101.62 Mg/ha and contained an average water amount of 88.01 m^3/ha. The water amount in biomass varied with sampling times from 58.74 to 111.83 m^3/ha. The average MWHC of 100 cm soil was estimated to be 5,113.74 m^3/ha. The water amount in soil also varied with sampling times from 3,651.50 to 4,481.06 m^3/ha. As a result, the total water amount in plant biomass and soil (ecosystem) of the DDF varied in a range from 3,735.0 to 4,558.67 m^3/ha. The pine contributed to 30.87 m^3/ha (35.07% of the total) and could increase by 64.92% the water storage potential of the forest, and thus these results support the concept of pine enrichment planting in the poor DDF.

1. INTRODUCTION

Deforestation in tropical counties such as Thailand has been mainly caused by forest clearing for people settlement and agriculture, and thus the present forest area of the country has decreased to 31.68% of the total in 2018 (Royal Forest Department, 2019). However, most remaining forests have suffered in part from forest concession, and illegal cutting by investors and local people. The secondary degraded forests can be observed in many areas over the country. The ecosystem function of water storage in forest biomass was different among abundant and degraded forests (Phongkhamphanh et al., 2018). Enrichment planting of selective tree species in the degraded forests is considered as an alternative method of forest restoration within a shorter period. The degraded forests have more opened canopy with big gaps, higher light intensity, fluctuating site temperature and poorer soil due to erosion as compare to the undisturbed forest. The tree species selected for enriched planting should be light demanding, fast growing, drought tolerant and have lesser nutrient requirements (Santos et al., 2020). Some enriched planting in poor natural forests has been practiced in Thailand, but very few data are published. Asanok et al. (2013) studied functional traits and the ability of tree species to reestablish in 15-year-old enriched secondary montane forest in the uplands of northern Thailand. The planted trees were native species such as *Castanopsis acuminatissima* (Blume) A. DC., *Betula alnoides* Buch. Ham. ex G. Don, *Cinnamomum iners* Reinw. ex Blume, *Diospyros glandulosa* Lace, and *Ternstroemia gymnanthera* (Wight and Arn.) Bedd. *Betula alnoides* Buch. Ham. ex G. Don could grow the

Citation: Thichan T, Anongrak N, Khamyong S, Kachina P. Restoration of water storage potential in a degraded dry dipterocarp forest with enrichment planting of three needle pine (*Pinus kesiya* Royle ex Gordon), Northern Thailand. Environ. Nat. Resour. J. 2021;19(1):10-23. (https://doi.org/10.32526/ennrj/19/2020130)

best with 12 cm stem DBH and 8.3 m height. In some counties, enrichment planting of native species in forest plantation of exotic species may be practiced as replacing the stand to avoid invasion of exotic species into natural forest. Chu et al. (2019) reported that enriched planting of native tree species in a 16-year-old *Eucalyptus* plantation in South China showed significantly reducing surface water flow, soil erosion and nutrient losses.

Forest ecosystems can store water in various components after rainfall. As the rain falls into the forest, a part is intercepted by the forest canopy and later lost into the atmosphere through evaporation, and the remains pass the canopy as through fall and stem flow to the forest floor. Organic layers on the forest floor can absorb a part of water, and the remaining amounts infiltrate into mineral soil. The water is also lost from the forest floor and soil through evaporation. Some water is retained by soil organic matter, fibrous roots and particles, particularly silt and clay which are varied with multiple soil layers along soil depth (He et al., 2019), while the excess amount percolates into the underground water table and moved out into the streams. Plants usually absorb a large amount of water as well uptake nutrients from soil solution for their physiological processes and growth. The functional role of the water cycle in forest ecosystems is important to maintain all organisms including plants, animals and microbes. Forest removal in the seasonal tropical montane forest resulted in typically increasing mean annual water yield and decreasing dry-season flows (Peña-Arancibia et al., 2019). Noywuli et al. (2019) reported that the forest-removal upstream watershed in Indonesia had a low carrying capacity condition indicated prominently by drought.

In the tropics, rainfall is only one source of water supply to watersheds and all types of ecosystem, and the forest ecosystem is considered as the most effective ecosystem in water cycle through many processes. However, different forests have variable roles on the water cycle. Typically, five forests in northern Thailand are classified: the dry dipterocarp forest, mixed deciduous forest, dry evergreen forest, pine forest (pine-dry dipterocarp forest and pine-lower montane forest) and the montane forest (Khamyong et al., 2004; Khamyong and Anongrak, 2016). Most literature studies focus on inputs of precipitation into forest ecosystems and movement of water through many processes, particularly interception-evaporation by forest canopy, through fall, stem flow, plant uptake, transpiration, water flow through vegetation, evaporation from soil, infiltration into soil, drainage and runoff, stream flow, etc. However, very few data are available for the water quantity stored in the plant biomass of forests. As for the montane forest, Khamyong et al. (2014a) provided the pioneer work on water storage in plants and soils of two community montane forests of Karen tribe in northern Thailand. Phongkhamphanh et al. (2018) compared the water storage potential of two-site DDFs. Khamyong et al. (2014b) and Sumanochitraporn et al. (2014) also evaluated the role of reforestation on watershed hydrology including 22-year-old teak and pine plantations in Chiang Rai Province, northern Thailand.

This research was conducted in the Huai Hong Khrai Royal Development Study (HHKRDS) Center established in 1982, Doi Saket District, Chiang Mai Province. It is about 27 km to the north of Chiang Mai City on the road to Chiang Rai Province. Before 1982, the two forests, mixed deciduous forest and dry dipterocarp forest, in this area were devastated to become extremely poor. Most medium and big trees were cut for timber whereas many small trees were used for fuel woods and only the small trees of 5 to 10 m heights with a scattered distribution remained (Khamyong et al., 2016). After heavy rainfall in rainy season, a lot of eroded soil transported in surface runoff was moved to the streams with dissolved red-sediment water. In dry season, all standing trees had no leaves as their deposition on the forest floor was the major fuels of annual forest fires. It was quite an extremely poor small watershed as called “Huai Hong Khrai”. The King (Rama 9) visited this area with profound understanding of the problems and established the Center as a place of study for the people in the north about integrated watershed management. Many activities of managing forest and wildlife resources, agriculture, and fishery are demonstrated in the Center for the study and extension of officers and Thai people. Foreign visitors also come here for learning.

The research paper assesses the role of enrichment planting of three needle pine (*Pinus kesiya* Royle ex Gordon) on water storage potential in plants and soil (ecosystem) of the degraded DDF, and to find out the contribution of planted pine on ecosystem water storage. The data provide useful information for forest conservation and watershed restoration.

2. METHODOLOGY

2.1 Study area

The research area, the HHKRDS Center covers an area of 1,360 ha with an altitude range between 350

and 591 m.m.s.l. (Figure 1). There are three seasons in this area: rainy season (May to September), winter (November to February), and summer (March to April). Meteorological data recorded using instruments in the Center report the following data: average annual rainfall, 1,328.9 mm; maximum and minimum air temperatures, 32.2°C and 18.9°C; and water evaporation, 1,222.6 mm/year (Khamyong et al., 2016). The two deciduous forests, the DDF and the mixed deciduous forest, distribute in most of the area. The parent rocks include sandstone, volcanic rock, shale, and limestone.

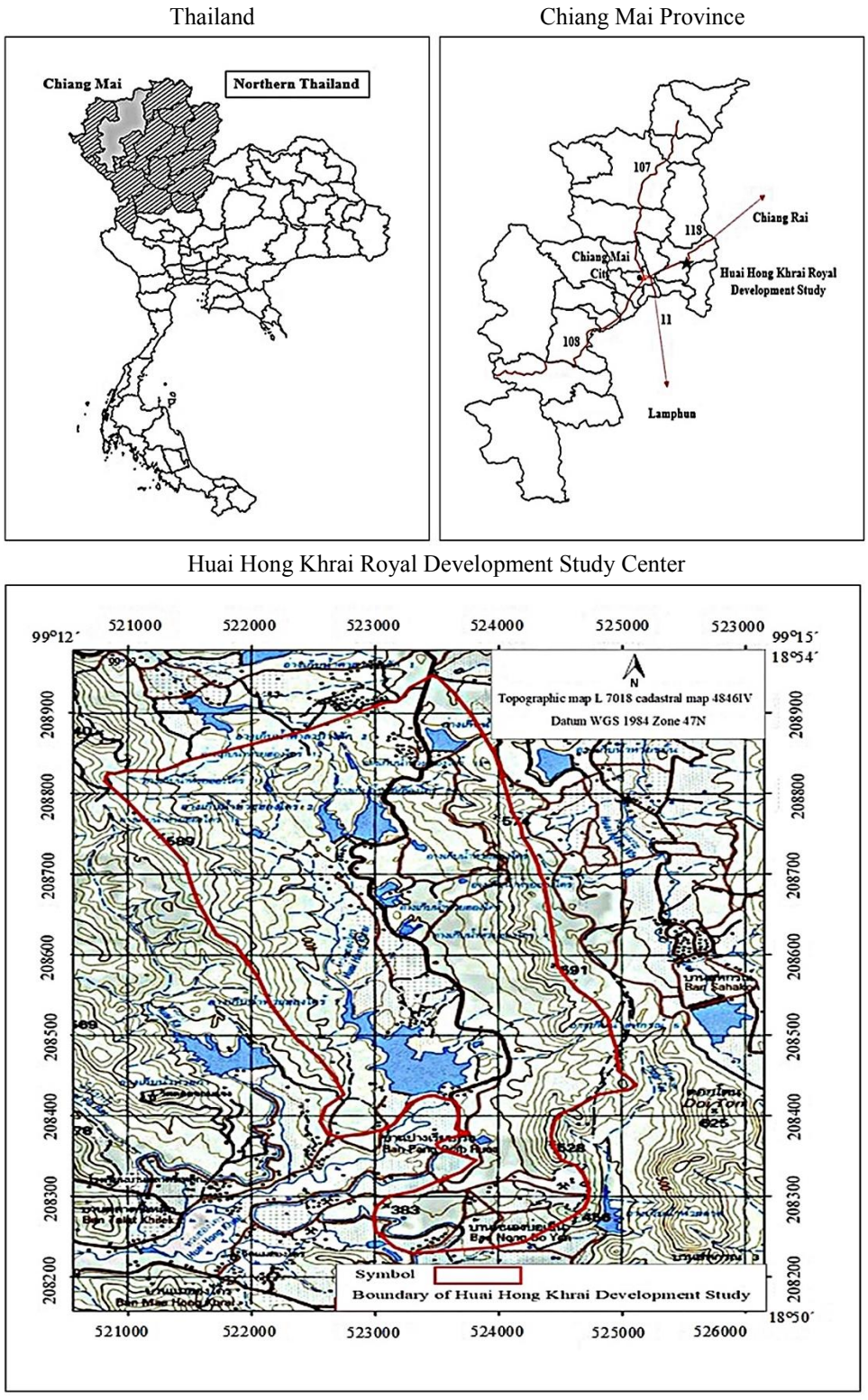

Figure 1. Location map of the study area

2.2 Plant community study

Census of plant species composition, richness, and diversity in the DDF was taken. Field vegetation survey in the forest was carried out using a method of plant community analysis. The sampling plots were 40×40 m^2 in size and ten plots were used, which were arranged randomly in the forest areas. Stem girths at breast height (gbh, 1.3 m above ground) and tree heights of all species with height over 1.5 m were measured. All plots were located using the global positioning system (GPS). The field plant data were later calculated for quantitative characteristics including frequency, density, dominance and important value index (IVI) and species diversity refer to Shannon-Wiener Index (SWI) (Krebs, 1985) and forest condition index (FCI) based on an equation studied by Seeloy-ounkeaw et al. (2014).

2.3 Standing plant biomass

The standing biomass amounts in the stem, branch, leaf, and root organs were calculated using allometric equations studied in the deciduous forests in Thailand by Ogino et al. (1967). The root biomass was calculated using an equation given by Ogawa et al. (1965).

2.4 Water storage in plants and soils

2.4.1 Water storage in plant biomass

Samples of fresh bark, stem, branch, and leaf on the standing trees of ten abundant species in the DDF were taken 12 times (each per month) from January to December 2018. Four stem-gbh classes of <25 cm, 26-50 cm, 51-75 cm, and >76 cm were divided for big tree species, and applied two or three gbh classes for the medium-sized and small tree/shrub species. Three tree individuals of each species were used as the sample trees for each gbh class. The fresh plant samples of 10 to 30 g were oven dried at 75°C until constant weights were achieved, and later quantified for their water content. The water content in the root used average values of the water content in the stem and branch because of having woody tissues as root. The water amount in biomass of each species was calculated by multiplying its biomass with the water content (by dry weight) of each gbh class. The average contents of these species were used for calculating the water amounts in biomass of the other species.

2.4.2 Water storage in soils

The soil derived from the volcanic rock in the DDF was studied by making three pits, 1.5 m × 1 m × 1 m in size, in selected three plots, and soil samples were collected along the depth using a 100 cm^3 corer in 12 months (each per month) as the same days of collecting fresh plant samples from eight soil depths with three replications: 0-5, 5-10, 10-20, 20-30, 30-40, 40-60, 60-80, and 80-100 cm. Some physical properties, organic matter (OM) by Walkley and Black Titration (Nelson and Sommers, 1996), field capacity (FC), maximum water holding capacity (MWHC), and water content on the sampling days were later analyzed in a laboratory (Brady and Weil, 2010). The MWHC was determined from the field capacity (FC). Water was added into the soil sample with the 100 cm^3 corer until the soil sample was completely saturated with water, and the water allowed to drain out of the macro pores. Then, the soil samples were oven dried at 105°C within a few days or until they achieved constant weights, and later, their moisture contents were determined by volume as field capacity (FC). Finally, the amount of water storage per unit area in each soil layer was determined and the total amount within the soil depth per unit area was calculated.

3. RESULTS AND DISCUSSION

3.1 Results

The results of this study include findings on plant community structures, amounts of standing plant biomass, values of water content, and water storage in plant biomass and soil within three seasons of the DDF with pine enriched planting.

3.1.1 Assessment of plant community structures, diversity, and forest conditions

Based on Smitinand (2014), the woody plants sampled within 10 sampling plots, each of size 40×40 m^2, were identified to be a total of 83 species, 69 genera, and 36 families (Table 1). These included 15 big trees, 24 medium-sized trees, 21 small trees, 16 shrubs, 3 climbers, and 3 unknown species. The forest was divided into three stands based on the dominant tree species: seven plots of *Dipterocarpus tuberculatus*, two plots of *Dipterocarpus obtusifolius* and one plot of *Shorea obtusa*. The species richness of these stands varied between 22 and 45 species per plot and tree densities varied from 1,688 to 3,606 trees/ha. The pine density contributed to only 5.53% of the total density.

The quantitative characteristics of plant species in the forest were investigated. Twelve species had the highest frequency value (100%); *Pinus kesiya, Dipterocarpus tuberculatus, Shorea obtusa, Aporosa villosa, Wendlandia tinctoria, Pterocarpus*

macrocarpus, Strychnos nux-vomica, Canarium subulatum, Syzygium cumini, Dalbergia oliverli, Bridelia retusa, and *Quercus kerrii*. The dipterocarps species of *Dipterocarpus obtusifolius* and *Shorea siamensis* had the values as 70% and 10%, respectively.

Average density of all species was 2,729 trees/ha. The species with the highest density was *Dipterocarpus tuberculatus* (473 trees/ha), followed by *Shorea obtusa* (291), *Aporosa villosa* (266), *Dipterocarpus obtusifolius* (201), *Wendlandia tinctoria* (151), *Pinus kesiya* (146), *Gluta usitata* (143), *Symplocos recemosa* (76), *Strychnos nux-vomica* (71), *Canarium subulatum* (60), *Dalbergia cultrata* (54), and *Pterocarpus macrocarpus* (52). These 12 species accounted for 72.70% of the total density.

The dominance of tree species was calculated from the stem basal area by measurement of stem girths at the breast height. *Pinus kesiya* had the highest dominance (31.81%), followed by *Dipterocarpus tuberculatus* (16.79), *Shorea obtusa* (12.06), *Dipterocarpus obtusifolius* (11.87), *Gluta usitata* (6.34), *Aporosa villosa* (3.52), *Pterocarpus macrocarpus* (2.03), *Semecarpus ancardium* (1.78), *Dalbergia cultrata* (1.54), *Strychnos nux-vomica* (1.27), and *Wendlandia tinctoria* (1.22). These 11 species accounted for 90.23% of the total dominance.

Table 1. A species list of tree species in the DDF with planted pine

Family	Scientific name	Growth form
1. Acanthaceae	1. *Justica modesta* (Bremek.) V.A.W. Graham	shrub
2. Anacardiaceae	2. *Buchanania lanzan* Spreng.	big tree
	3. *Gluta usitata* (Wall.) Ding Hou	big tree
	4. *Lannea coromandelica* (Houtt.) Merr.	big tree
	5. *Semecarpus anacardium* Linn.f.	medium tree
3. Apocynaceae	6. *Aganosma marginata* (Roxb.) G.Don	climber
4. Bignoniaceae	7. *Markhamia stipulata* (Wall.) Seem. var. *pierrei* (Dop) Santisuk & Vidal	medium tree
	8. *Heteropanax sulfureum* Kurz.	small tree
	9. *Stereospermum cylindricum* Pierre ex Dop.	medium tree
	10. *Stereospermum neuranthum* Kurz	medium tree
5. Burseraceae	11. *Canarium subulatum* Guillaumin	big tree
6. Celastraceae	12. *Celastrus paniculata* Willd.	climber
7. Clusiaceae	13. *Garcinia cowa* Roxb. ex Choisy	small tree
8. Combretaceae	14. *Terminalia alata* Heyne ex Roth	big tree
	15. *Terminalia chebula* Retz. var. *chebula*	medium tree
9. Chrysobalanaceae	16. *Parinari anamensis* Hance	medium tree
10. Dilleniaceae	17. *Dillenia obovata* (Blume) Hoogland	small tree
11. Dipterocarpaceae	18. *Dipterocarpus obtusifolius* Teijsm. ex Miq.	big tree
	19. *Dipterocarpus tuberculatus* Roxb.	big tree
	20. *Shorea siamensis* Miq.	big tree
	21. *Shorea obtusa* Wall. ex Blume	big tree
12. Ebenaceae	22. *Diospiros ehretioides* Wall. ex G. Don	small tree
13. Ericaceae	23. *Craibiodendron stellatum* (Pierre) W.W. Sm.	small tree
14. Fabaceae	24. *Acacia catechu* (L.f.) Willd.	medium tree
	25. *Albizia odoratissima* (L.f.) Benth.	medium tree
	26. *Albizia chinensis* (Osbeak) Merr.	big tree
	27. *Butea superba* Roxb.	climber
	28. *Dalbergia cultrata* Graham ex Benth	big tree
	29. *Dalbergia dongnaiensis* Pierre	medium tree
	30. *Dalbergia oliveri* Gamble	medium tree
	31. *Dalbergia velutina* Benth.	climber
	32. *Indigofera sootepensis* Craib	shrub
	33. *Leucaena leucocephala* (Lam.) de Wit	small tree
	34. *Millettia xylocarpa* Miq.	medium tree
	35. *Millettia extensa* (Benth.) Baker	medium tree

Table 1. A species list of tree species in the DDF with planted pine (cont.)

Family	Scientific name	Growth form
	36. *Peltophorum pterocarpum* (DC.) Backer ex K.	medium tree
	37. *Pterocarpus macrocarpus* Kurz	big tree
	38. *Spatholobus parviflorus* (DC.) Kuntze	climber
	39. *Xylia xylocarpa* Taub. Var. *kerrii* Nielsen	big tree
15. Fagaceae	40. *Quercus kerrii* Craib.	medium tree
	41. *Lithocarpus elegans* (Blume) Hatus. ex Soepadmo	medium tree
16. Hypericaceae	42. *Cratoxylum formosum* Byer	small tree
17. Irvingiaceae	43. *Irvingia malayana* Oliv. ex A. W. Benn.	big tree
18. Lamiaceae	44. *Vitex peduncularis* Wall. ex Schauer	medium tree
19. Lauraceae	45. *Litsea glutinosa* (Lour.) C.B. Rob.	medium tree
	46. *Phoebe lanceolata* (Nees) Nees	medium tree
20. Malvaceae	47. *Colona flagrocarpa* (C.B. Clarke)	small tree
	48. *Decaschistia siamensis* Craib	shrub
	49. *Sterculia balanghas* L.	shrub
21.Melastomataceae	50. *Memecylon plebejum* Kurz var. *plebejum*	shrub
22. Meliaceae	51. *Chukrasia tabularis* A. Juss.	medium tree
23. Moraceae	52. *Ficus* sp.	medium tree
24. Myrtaceae	53. *Eucalyptus camaldulensis* Dehnh.	medium tree
	54. *Syzygium albiflorum* (Duthie & Kurz) Bahadur & R.C. Gaur	medium tree
	55. *Syzygium cumini* (L.) Skeels	small tree
25. Ochnaceae	56. *Ochna intergerrima* (Lour.) Merr.	small tree
26. Oleaceae	57. *Chionanthus ramiflorus* Roxb.	small tree
	58. *Olea salicifolia* Wall. Ex G. Don	small tree
27. Opiliaceae	59. *Meilentha suavis* Pierre	small tree
28. Pentaphylacaceae	60. *Anneslea fragrans* Wall.	small tree
29. Phyllanthaceae	61. *Antidesma acidum* Retz.	shrub
	62. *Antidesma ghaesembilla* Gaertn.	shrub
	63. *Antidesma sootepene* Craib	shrub
	64. *Aporosa villosa* (Wall. ex Lindl.) Baill.	shrub
	65. *Bridelia retusa* (L.) A. Juss.	medium tree
	66. *Glochidion zeylanicum* (Gaaertn.) A. Juss.	shrub
	67. *Phyllanthus emblica* L.	small tree
30. Pinaceae	68. *Pinus kesiya* Royle ex Gordon	big tree
31. Rhamnaceae	69. *Zizyphus rugosa* Ram.	climber
32. Rubiaceae	71. *Catunaregam spathulifolia* Tirveng.	shrub
	72. *Gardenia sootepensis* Hutch	small tree
	73. *Gardenia obtusifolia* Roxb. ex Gordon	shrub
	74. *Haldina cordifolia* Ridsd.	medium tree
	75. *Ixora cibdela* Craib	shrub
	76. *Morinda coreia* Ham.	small tree
	77. *Pavetta indica* RL.	shrub
	78. *Wendlandia tinctoria* (Roxb.) DC.	small tree
	79. *Vangueria pubescens* DC.	shrub
33. Saliciaceae	80. *Casearis gallifera* Tathana	small tree
34. Symplocaceae	81. *Symplocos recemosa* Roxb.	small tree
35. Strychnaceae	82. *Strychnos nux-vomica* L.	shrub
36. Ulmaceae	83.*Ulmus lancaefolia* Roxb. ex Wall.	small tree
Unknown	84-86. Climber -1, 2, 3	climber

The importance value index combines three factors of the relative frequency, relative density and relative dominance into a measure that can be used to imply the ecological influence of each species in the DDF. The species with the highest IVI was *Pinus kesiya* (13.32% of all species), followed by *Dipterocarpus tuberculatus* (12.31%), *Shorea obtusa* (8.51%), *Dipterocarpus obtusifolius* (7.07%), *Aporosa villosa* (5.36%), *Gluta usitata* (4.70%), *Wendlandia tinctoria* (3.19%), *Pterocarpus macrocarpus* (2.25%), *Strychnos nux-vomica* (2.23%), *Symplocos recemosa* (2.03%), *Dalbergia cultrata* (1.93%), and *Canarium subulatum* (1.79%). These 12 species accounted for 64.69% of the total value.

As shown in Table 2, the values of the SWI as indicating plant species diversity were different among plots, 3.49 to 4.31 (3.87±0.24 on average), while the forest condition index values were measured to be a range of 1.03 to 10.98 (6.18±3.24 on average). If the pine was not planted in the forest, the values would decrease to 3.79±0.25 for the SWI, and 2.70±2.24 for the FCI.

Table 2. Plant communities within 10 sampling plots in the DDF

Plot	Dominant	Species	Density	Pine density		SWI		FCI	
No.	Species	richness	(ha)	(ha)	%	A	B	A	B
1	*D. tuberculatus*	45	3,356	175	5.21	4.31	4.24	7.72	3.79
2	*D. tuberculatus*	34	3,606	106	2.94	3.66	3.58	10.98	2.45
3	*D. tuberculatus*	30	1,788	56	3.14	3.90	3.81	6.74	1.52
4	*D. tuberculatus*	22	1,688	69	4.07	3.49	3.38	3.23	0.51
5	*S. obtusa*	40	3,594	219	6.08	4.04	3.96	9.53	6.17
6	*D. obtusifolius*	40	3,231	163	5.02	3.71	3.60	9.49	6.82
7	*D. tuberculatus*	31	1,856	263	14.14	3.86	3.82	5.12	2.47
8	*D. obtusifolius*	37	2,813	69	2.44	3.89	3.82	1.03	0.78
9	*D. tuberculatus*	38	2,817	256	9.09	4.12	4.06	3.56	0.74
10	*D. tuberculatus*	38	2,538	81	3.20	3.77	3.68	4.39	1.75
Mean		36	2,729	146	5.53	3.87	3.79	6.18	2.70
S.D.		7	741	80	3.61	0.24	0.25	3.24	2.24

Remark: A=DDF with planted pine, B=DDF without planted pine

3.1.2 Growth and population of pine

Within 10 plots, a total of 233 individuals of pine were found. The biggest pine had the stem-gbh of 129.5 cm with 25.5 m height, while the values of 10.9 cm and 4.1 m belonged to the smallest tree. The number of trees in the gbh classes of <25, 26-50, 51-75, and >75 cm were 5, 26, 97, and 105 trees, respectively, whereas the height classes of <5, 6-10, 11-15, 16-20, and >20 m consisted of 2, 19, 96, 89, and 27 trees. The average values of gbh and height were 72±22.02 cm and 15.1±3.97 m, respectively. The seedlings of pine were not observed in the forest. Thus, the annual growth rates (annual ring width) of pine varied from 0.5 to 6 mm (3.4 mm on average). The variable growth might be caused by competition with other tree species and the influences of site factors (Pornleesangsuwan, 2012).

3.1.3 Amount of standing plant biomass

Table 3 shows the amounts of plant biomass within 10 plots in the DDF with planted pine, and the average amount was measured as 101.62 Mg/ha, divided into bark, stem, branch, leaf, and root organs at 1.72 (1.69%), 64.07 (63.04%), 17.89 (17.60%), 2.34 (2.30%), and 15.59 (15.37%) Mg/ha, respectively. The biomass amounts in these stands varied in a range of 58.73 to 148.43 Mg/ha.

Among 86 species, the pine biomass was the highest, 36.79 Mg/ha (36.20% of the total). The tree species having the lower amounts were in the following order: *Dipterocarpus tuberculatus* (15.97 Mg/ha), *Dipterocarpus obtusifolius* (12.47 Mg/ha), *Shorea obtusa* (12.19 Mg/ha), *Gluta usitata* (6.59 Mg/ha), *Ptercarpus macrocarpus* (2.45 Mg/ha), *Aporosa villosa* (1.89 Mg/ha), *Semecarpus anacardium* (1.51 Mg/ha), *Dalbergia cultrata* (1.40 Mg/ha), *Irvingia malayana* (1.08 Mg/ha), etc. These 10 species accounted to 92.34 Mg/ha (90.87% of the total biomass). Therefore, the enriched planting of this pine could increase a large amount of biomass in the degraded DDF.

Table 3. Amounts of standing plant biomass of tree species in the DDF with planted pine

No.	Name	Biomass (Mg/ha)					
		Bark	Stem	Branch	Leaf	Root	Total
1	*P. kesiya*	0.24	23.90	4.50	0.95	7.20	36.79
2	*D. tuberculatus*	0.37	9.83	3.40	0.34	2.03	15.97
3	*D. obtusifolius*	0.18	7.85	2.69	0.23	1.52	12.47
4	*S. obtusa*	0.40	7.42	2.60	0.24	1.53	12.19
5	*G. usitata*	0.11	4.08	1.54	0.10	0.76	6.59
6	*P. macocarpus*	0.04	1.51	0.58	0.04	0.28	2.45
7	*A. villosa*	0.03	1.20	0.27	0.07	0.32	1.89
8	*S. anacardium*	0.03	0.94	0.30	0.03	0.20	1.51
9	*D. cultrata*	0.03	0.87	0.27	0.03	0.19	1.40
10	*I. malayana*	0.02	0.67	0.23	0.02	0.13	1.08
11	Species 11 to 86	0.26	5.79	1.51	0.30	1.44	9.29
Total		1.72	64.07	17.89	2.34	15.59	101.62

3.1.4 Water storage in plants and soil of DDF with planted pine

(1) Amount of water stored in plant biomass

Data regarding the water contents (percentage by fresh weight) in different organs of ten dominant tree species in the DDF were studied. The water contents of these species varied greatly among species, sampling times and stem-gbh classes.

Four gbh classes were used for the three species. The average values of water content in bark, stem, branch, leaf and root were measured as the following order: *Dipterocarpus obtusifolius*: 49.76%, 40.16%, 58.10%, 55.46%, 41.96%, *Dipterocarpus tuberculatus*; 61.11%, 42.16%, 62.83%, 65.76%, 54.43%, and *Irvingia malayana*; 54.87%, 35.93%, 48.06%, 54.85%, 46.90%. Three gbh classes were used for *Shorea obtusa*. Their averages were 45.72%, 37.89%, 48.04%, 54.95%, 43.31%, respectively. Two gbh classes were used for the six species. The average values of water content in these organs were calculated as the following order: *Pinus kesiya*; 56.86%, 40.39%, 55.57%, 59.93%, 45.04%, *Aporosa villosa*; 41.63%, 47.86%, 59.47%, 68.88%, 44.91%, *Wendlandia tinctoria*; 52.77%, 46.65%, 53.66%, 62.83%, 49.65%, *Symplocos racemosa*; 46.36%, 50.36%, 59.06%, 64.80%, 48.23%, *Syzygium cumini*; 55.25%, 42.55%, 49.01%, 55.34%, 46.14%. One gbh class was applied for *Memecylon plebejum* and the averages were 38.04%, 42.14%, 57.52% and 38.04%, respectively.

The water amount of all stands (10 plots) during January to December varied from 58.74 to 111.83 m^3/ha (88.01±12.61 m^3/ha on average). The percentages of water amount in the bark, stem, branch, leaf, and root were calculated as the following order: 2.40%, 50.51%, 26.69%, 4.20%, and 16.19%. The average water amounts stored in plant biomass of the DDF for 12 months varied from 58.74 to 111.83 m^3/ha (88.01±12.61 m^3/ha on average). It was the highest in July (rainy season) and the lowest in October (end of rain season). The amount was not the lowest in dry season. It is supposed that leaf fall might reduce lose through transpiration.

As shown in Table 4, the average water amount in pine biomass (sp.1) was the highest among 86 species, 30.87 m^3/ha or 35.07% of the total. The species with lower amounts were in the following order: *Dipterocarpus tuberculatus* (sp.2, 16.68 m^3/ha), *Dipterocarpus obtusifolius* (sp.3, 10.36), *Shorea obtusa* (sp.4, 8.77), *Gluta usitata* (sp.5, 5.53), *Ptercarpus macrocarpus* (sp.6, 2.07), *Aporosa villosa* (sp.7, 1.99), *Semecarpus anacardium* (sp.8, 1.31), *Dalbergia cultrata* (sp.9, 1.21), *Strychnos nux-vomica* (sp.10, 0.87), etc. These 10 species accounted to 79.67 m^3/ha or 90.52% of the total.

(2) Water storage in soils

The soil derived from volcanic rock in the DDF dominated mainly by *Diterocarpus tuberculatus* was very deep, more than 2 m, and classified into the more developed soil of Order Oxisols. It is the reddish soil containing the high content of iron oxides. In general, the physical properties of the soil, particularly depth, gravel content, bulk density, texture, and organic matter content, have an influence on water movement and retention throughout the soil profile (Brady and Weil, 2010). The data on the soil physical properties in the DDF are given in Table 5. The bulk density (BD) was almost moderately high throughout soil

depth. The organic matter was high only at the soil surface and decreased to low and very low to subsoil while the gravel content was almost very low. Except for the intermediate content of sand at the soil surface, this soil contained the low content of sand and silt, but the clay content was relatively high throughout the soil profile.

Table 4. Amounts of water stored in biomass of tree species in the DDF with planted pine

Month	Water in plant biomass (m^3/ha)											Total
	Species number											
	sp.1	sp.2	sp.3	sp.4	sp.5	sp.6	sp.7	sp.8	sp.9	sp.10	11-86	
Jan	28.56	16.89	11.14	8.73	5.49	2.06	1.99	1.30	1.20	0.87	8.27	86.51
Feb	29.79	15.91	9.58	8.44	5.31	1.98	1.72	1.23	1.13	0.78	7.61	83.49
Mar	29.36	18.35	9.84	9.07	5.37	2.03	1.74	1.27	1.18	0.84	7.90	86.94
Apr	25.61	15.45	9.99	9.34	5.31	2.00	2.18	1.27	1.17	0.85	8.11	81.29
May	35.63	18.45	10.93	10.09	5.87	2.22	2.35	1.44	1.33	0.99	9.25	98.56
Jun	29.49	16.39	10.89	9.29	5.47	2.06	1.99	1.32	1.21	0.88	8.41	87.41
Jul	40.44	21.10	12.59	11.21	6.95	2.59	2.32	1.63	1.51	1.09	10.40	111.83
Aug	40.32	16.17	10.69	8.31	5.91	2.20	2.31	1.37	1.27	0.89	8.62	98.07
Sep	29.85	17.84	10.38	8.62	5.66	2.13	2.12	1.35	1.26	0.92	8.79	88.92
Oct	17.71	12.05	6.88	5.58	3.94	1.48	1.43	1.01	0.90	0.70	7.07	58.74
Nov	35.78	15.49	11.19	7.91	5.90	2.17	1.90	1.32	1.22	0.82	8.10	91.81
Dec	27.90	16.06	10.24	8.66	5.21	1.96	1.75	1.23	1.13	0.80	7.66	82.61
Mean	30.87	16.68	10.36	8.77	5.53	2.07	1.99	1.31	1.21	0.87	8.35	88.01
S.D.	6.39	2.19	1.35	1.34	0.69	0.25	0.29	0.14	0.14	0.10	0.87	12.61

Table 5. Physical properties of 100 cm soil under the DDF with planted pine

Depth	OM	BD	Gravel	Particle distribution (%)			Texture	FC	MWHC
(cm)	(%)	Mg/m^3	%	Sand	Silt	Clay		(%)	m^3/ha
Pedon 1									
0-5	4.34	1.64	33.60	65.4	12.0	22.6	SCL	44.85	277.06
5-10	2.06	1.66	31.91	46.4	9.0	44.6	SC	37.17	273.55
10-20	1.24	1.67	32.06	33.4	6.0	60.6	C	37.53	554.39
20-30	0.84	1.65	35.29	48.0	8.0	44.0	SC	39.50	533.81
30-40	0.61	1.74	29.28	34.5	6.5	59.0	C	39.36	555.21
40-60	0.46	1.69	28.98	32.7	5.2	62.1	C	41.23	1,095.07
60-80	0.44	1.74	30.45	34.5	6.0	59.5	C	41.63	1,092.76
80-100	0.44	1.71	30.96	29.6	6.0	64.4	C	43.50	1,124.35
Total									5,506.19
Pedon 2									
0-5	4.34	1.62	36.48	24.2	40.2	35.6	CL	41.73	239.20
5-10	1.65	1.83	35.75	25.5	36.5	38.0	CL	36.47	216.05
10-20	0.72	1.81	32.69	15.2	30.2	54.6	C	35.85	514.84
20-30	0.45	1.82	34.86	16.5	26.6	56.9	C	33.90	442.70
30-40	0.44	1.72	32.98	17.1	24.4	58.5	C	38.42	484.31
40-60	0.22	1.79	28.53	13.2	24.6	62.2	C	38.60	1,055.12
60-80	0.15	1.85	32.30	15.5	20.3	64.2	C	39.72	885.88
80-100	0.13	1.77	29.56	14.4	20.1	65.5	C	39.85	991.18
Total									4,829.29

Remarks: SCL=Sandy Clay Loam; SC=Sandy Clay; C=Clay; CL=Clay Loam

Table 5. Physical properties of 100 cm soil under the DDF with planted pine (cont.)

Depth (cm)	OM (%)	BD Mg/m^3	Gravel %	Particle distribution (%)			Texture	FC (%)	MWHC m^3/ha
				Sand	Silt	Clay			
Pedon 3									
0-5	4.20	1.67	32.26	60.6	14.9	24.5	SCL	41.76	250.96
5-10	1.85	1.69	31.36	40.4	23.2	36.4	CL	41.85	248.08
10-20	0.88	1.71	28.56	48.4	5.0	46.6	SC	42.73	555.75
20-30	0.60	1.69	31.14	33.5	7.5	59.0	C	41.92	513.43
30-40	0.44	1.68	33.42	33.7	6.3	60.0	C	46.47	490.80
40-60	0.44	1.70	33.96	30.7	5.2	64.1	C	46.92	965.23
60-80	0.38	1.72	38.38	30.5	5.0	64.5	C	47.87	967.07
80-100	0.20	1.65	34.90	30.6	6.0	63.4	C	46.53	1,014.42
Total									5,005.74

Remarks: SCL=Sandy Clay Loam; SC=Sandy Clay; C=Clay; CL=Clay Loam

The soil study on water storage was carried out 12 times (January to December 2018). The field capacities of water (% by weight) in three soil pits (pedons) varied along soil depths: 33.90 to 47.87%. The water contents in different soil depth of the three pedons varied greatly with sampling times with the values lower than the field capacity. The values were low in dry season (mid-February to April), increased in rainy season especially September, and decreased in winter (November to mid-February). These caused the variations of water amount in 100 cm soil during a year. The maximum water holding capacity which was calculated from the field capacity varied with soil depth and three pedons, and the total amount within 100 cm depth varied from 4,829.29 to 5,506.19 m^3/ha (5,113.74 m^3/ha on average). This capacity could store the maximum rainfall amount of 514 mm. The amount of soil water was the lowest in February (3,651.50 m^3/ha, 71.40% of MWHC) and the highest in October (4,481.06 m^3/ha, 87.62%).

(3) Water storage in the DDF ecosystem (plants and soils) with planted pine

Figure 2 shows the amounts of water stored in the DDF ecosystem (plant biomass and soil system) during January and December 2018. Generally, the amounts of water stored in plant biomass and soil can vary day by day, month by month, and year by year. However, the results of this study show that the amount varied from the lowest (3,651.50 m^3/ha in February) to the highest (4,481.06 m^3/ha in October). The difference was only 829.56 m^3/ha. It could be concluded that the soil (100 cm depth) in the DDF ecosystem could store the largest water amount at 97.86% and the remainder (2.14%) belonged to the plant biomass. The movement of water between soil and plants is due to water uptake by roots as influenced by transpiration to the atmosphere (Landberg and Gower, 1997).

3.2. Discussion

3.2.1 Contribution of planted pine to community structures, species diversity and forest condition

The enrichment planting of three needle pine in the degraded DDF could increase species composition, number of species (species richness) as well as species diversity indicated by SWI of species diversity. The SWI was calculated from the equation derived from species richness and relative population abundance of each species in the plot. One species of pine with the average density of 146±80 trees/ha contributed to community structure in the DDF, and resulted in the small increase of SWI value from 3.79±0.25 to 3.87±0.24 whereas the forest condition index (FCI) was raised from 2.70±2.24 to 6.18±3.24. These data implied that the enrichment planting could increase species diversity and improve forest condition of the forest after planting for 34 years. This pine occurs naturally in dry areas from 1,000 to 1,900 m altitude in the transition zone (ecotone) between the DDF and lower montane forest of northern Thailand (Seramethakun, 2012; Marod et al., 2019), and is recognized as a fast-growing tree species. Thus, the pine could reduce the time of plant succession and forest development of the degraded DDF (Pornleesangsuwan, 2012). Seeloy-ounkeaw (2014) reported that the utilization community forest (UF) was distributed in areas of 1,000 to 1,250 m altitude. Within 50 sampling plots, three needle pine had 98% frequency value with the density of 153 trees/ha. Its dominance and IVI were measured to be 25.82% and 11.97%, respectively. In the conservation community

forest as the watershed covered the areas of 1,100 to 1,800 m, this pine had the lower frequency value (58%) with the density of 94 trees/ha. However, it had the highest values of dominance and IVI among 236 species within 50 plots: 15.77% and 6.51%, respectively. This pine has the high potential to plant in the opened dry areas of degraded forests.

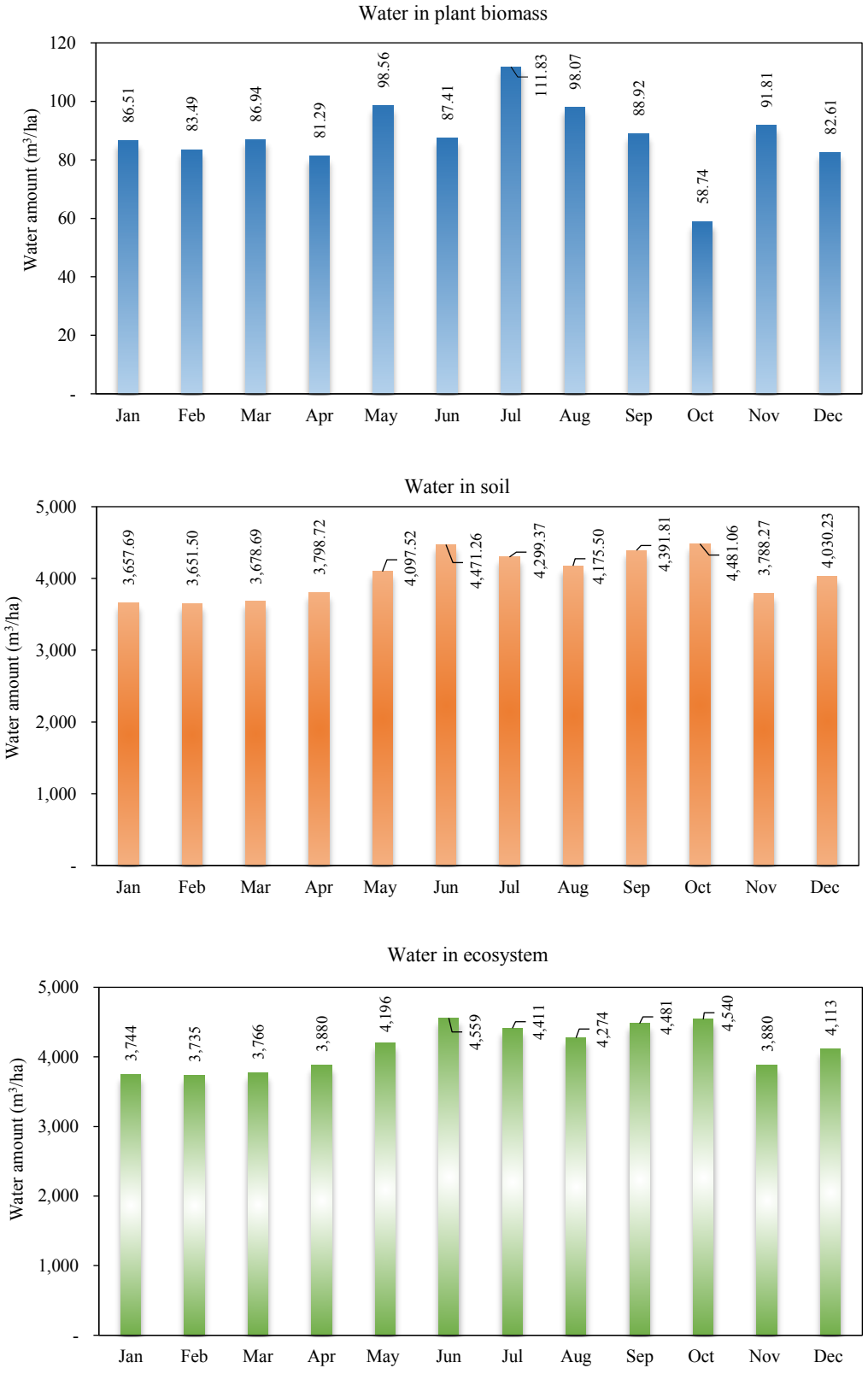

Figure 2. The water amounts stored in plant biomass, soil and ecosystem of the DDF during January to December 2018

3.2.2 Contribution of planted pine to plant biomass and water storage

The enrichment planting of three needle pine in the degraded DDF could increase also plant biomass as well as the water storage potential. The pine produced the amount of plant biomass at 36.79 Mg/ha (32.20% of the total) within 34 years, and increased the biomass from 64.83 to 101.62 Mg/ha. This pine species could store the amount of water at 28.57 m^3/ha (32.46% of the total) and restore the water storage potential in plant biomass in the forest from 59.44 to 88.01 m^3/ha. Therefore, the enrichment planting of this pine could increase 48.07% (1.41 m^3/ha/yr) of the total water storage potential in the DDF (without planted pine). Sutthawan et al. (2016) found that the DDF on sandstone in adjacent area has the annual increment of plant biomass as 1.38 Mg/ha or 1.77 m^3/ha of water. Seramethakun (2012) reported that the natural pine-DDF dominated by *Shorea obtusa* at Kanlaya Ni Wattana District in Chiang Mai could produce the amount of biomass at 84.96 Mg/ha, and the pine had the contribution to the biomass at 31.12 Mg/ha (36.62% of the total). As for the degraded lower montane forest which had the amount of biomass at 79.48 Mg/ha, the contribution of pine to the biomass was high as 67.94% of the total.

Khamyong et al. (2014a) studied water storage in the lower montane forest in northern Thailand. The community forest of Karen village was divided into the conservation forest (CF) and the utilization forest (UF). Selective tree cutting for house construction and fuelwood was permitted by village regulations only in the UF. The CF was protected for the watershed and become a recovery forest. The amount of standing plant biomass in the CF (252.4±72.5 Mg/ha) was higher than that in the UF (139.7±36.3 Mg/ha). The amounts of water in the plant biomass varied between seasons. The amounts of water in the CF varied between 208.2±68.9 and 231.2±70.7 m^3/ha, whereas the amounts of water in the UF varied in the range from 107.1±29.7 to 129.0±33.3 m^3/ha. Thus, the lower montane forest had higher amounts of water stored in plant biomass than the DDF with planted pine as present study (88.01 m^3/ha).

Different soils have the variable capacity of water storage depending upon soil depth, organic matter, gravel content, bulk density and textures (sand silt and clay content). The soil in this study was a very deep reddish soil, and classified into Order Oxisols. The bulk density, gravel content and organic matter were almost low throughout the 100 cm depth, but the clay content was very high. The soil with the high clay content usually has the high retention of water, but the clay of the Oxisols is aggregated to a strong grade of fine and very fine granular structure which causes it has the rapid permeability after rainfall (Soil Survey Staff, 1999), and the water storage by this soil maybe not be as high as predicted as other soils with the high clay content. Within 100 cm soil, this soil had the MWHC of 5,113.74 m^3/ha. This value was nearly the same to the deep soil of Order Ultisols in the lower montane forest, 4,956 m^3/ha (Khamyong et al., 2014a). Sumanochitraporn et al. (2014) found that the deep soil (the Ultisols) in a 22-year-old teak plantation could store the lower amount of water at 3,617.60 m^3/ha while the Ultisols under the 22-year-old three needle pine had the higher value of 5,632.87 m^3/ha (Khamyong et al., 2014b).

Very few researches have investigated directly on pine restoration causing dehydration in the rehabilitation area. However, some assumptions can be considered by the fact that the pine is an evergreen species with transpiration throughout a year. However, the transpiration of pine is normally lower than other species (Urban et al., 2019). The second is mycorrhizal fungi in the root system can absorb more water from soil into the pine root as commonly occurred in most forest tree species (Barea et al., 2011; Leski et al., 2019; Rożek et al., 2020). These leads to movement of soil water into the tree roots. A part is stored in different organs and the rest is lost into atmosphere through transpiration.

3.2.3 Suggestion for further research

Various aspects of further research are considered. Enrichment planting of pine increased tree density as well as biomass in the forest. The air temperature beneath its canopy can reduce light intensity throughout a year because it is an evergreen species. The water stored in its biomass could absorb solar radiation and released the heat through transpiration, and then soil water can be assimilated by roots into the tree. This can cool the forest environment and give a specific microclimate such as soil temperature. Thus, the research on effects of pine enrichment planting on changing microclimate is considerably important. Also, since there are other evergreen and deciduous tree species used in enrichment planting worldwide, the different effects among species will be the interacting research topic. Different tree species have variable transpiration. Urban et al. (2019) found that the annual transpiration

of two stands with the same age (49 years old) was different. *Pinus sylvestris* had 20% lower than *Larix sibirica* transpiration in central Siberia. Therefore, the study on different transpiration among enrichment planting species is also a significant aspect.

4. CONCLUSION

Enrichment planting of tree species in the xeric degraded forest in the tropic is usually difficult. The selected species must have tolerance to drought, forest fire, extremely high surface air temperature and poor soil. Three needle pine (*Pinus kesiya*) has been used for reforestation in highland watershed in Thailand according to these tolerant natures. After 34 years, pine enrichment planting in the degraded DDF covered on the deep soil of Order Oxisols in northern Thailand could increase plant species diversity, improve forest condition, forest biomass as well as water storage since this pine species is a fast-growing evergreen tree species, and exists in some sites of the natural DDF as called the pine-DDF. The improved forest condition by its rapid growth resulted in increasing number or population of big tree individuals in the forest. This 34-year-old pine could increase the plant biomass and water storage potential in the forest at 56.75% and 48.07% of the total, respectively.

ACKNOWLEDGEMENTS

This research received financial support from National Research Council of Thailand (NRCT) in 2017, and a fund from Graduate School of Chiang Mai University. The authors would like to thank the head and officers of the HHKRDS Center for permission to conduct research in the forest, and for all facilities provided during field data collection.

REFERENCES

Asanok L, Marod D, Duengkae P, Pranmongkol U, Kurokawa H, Aiba M, et al. Relationships between functional traits and the ability of forest tree species to reestablish in secondary forest and enrichment plantations in the uplands of northern Thailand. Forest Ecology and Management 2013;296:9-23.

Barea JM, Palenzuela J, Cornejo P, Sánchez-Castro I, Navarro-Fernández C, Lopéz-García A, et al. Ecological and functional roles of mycorrhizas in semi-arid ecosystems of Southeast Spain. Journal of Arid Environments 2011;75:1292-301.

Brady NC, Weil RR. Elements of the Nature and Properties of Soils. New Jersey, USA: Pearson Education International; 2010.

Chu S, Ouyang J, Liao D, Zhou Y, Liu S, Shen D, et al. Effects of enriched planting of native tree species on surface water flow, sediment, and nutrient losses in a Eucalyptus plantation forest in southern China. Science of the Total Environment 2019;675:224-34.

He ZB, Zhao MM, Zhu X, Du J, Chen LF, Lin J. Temporal stability of soil water storage in multiple soil layers in high elevation forests. Journal of Hydrology 2019;569:532-45.

Khamyong S, Lykke AM, Seramethakun D, Barfod A. Species composition and vegetation structure of an upper montane forest at the summit of Mt. Doi Inthanon, Thailand. Nordic Journal of Botany 2004;23:83-97.

Khamyong S, Seeloy-ounkeaw T, Anongrak N, Sri-ngernyuang K. Water storages in plants and soils in two community forests of Karen tribe, northern Thailand. Tropics 2014a;23(3):111-25.

Khamyong S, Sumanochitraporn S, Anongrak N. Roles of a pine (*Pinus kesiya*) plantation on water storages in the Doi Tung Reforestation Royal Project, Chiang Rai Province, northern Thailand. Thai Journals of Forestry 2014b;33(3):75-87.

Khamyong S, Anongrak N. Carbon and nutrient storages in an upper montane forest at Mt. Inthanon summit, northern Thailand. Environment and Natural Resources Journal 2016;14(1):26-38.

Khamyong S, Sutthawan P, Paramee S, Anongrak N. Dry dipterocarp forest on sandstone of the Huai Hong Khrai Royal Development Study Center, Chiang Mai Province: I. Assessment of plant species diversity and carbon storage. Thai Journals of Forestry 2016;35(3):42-55.

Krebs CJ. Ecology: The Experimental Analysis of Distribution and Abundance. New York, USA: Harper and Row Publishers; 1985.

Landsberg JJ, Gower ST. Application of Physiological Ecology to Forest Management. California, USA: Academic Press; 1997.

Leskia T, Rudawskaa M, Kujawskaa M, Stasińskab M, Janowskia D, Karlińskia L, et al. Both forest reserves and managed forests help maintain ectomycorrhizal fungal diversity. Biological Conservation 2019;238:Article ID 108206.

Marod D, Hermhuk S, Sungkaew S. Species composition and spatial distribution of dominant trees in the forest ecotone of a mountain ecosystem, northern Thailand. Environment and Natural Resources Journal 2019;17(3):40-9.

Nelson DW, Sommers LE. Total carbon, organic carbon, and organic matter. In: Bigham JM, editor. Method of Soil Analysis Part 3: Chemical Methods No.5. Madison: Soil Science Society of America: American Society of Agronomy; 1996. p. 961-1010.

Noywuli N, Sapei A, Pandjaitan NH, Eriyatno. Assessment of watershed carrying capacity for the aesesa flores watershed management, East Nusa Tenggara province of Indonesia. Environment and Natural Resources Journal 2019;17(3): 29-39.

Ogawa H, Yoda K, Ogino K, Kira K. Comparative ecological study on three main types of forest vegetation in Thailand II. Plant Biomass. Nature and Life in Southeast Asia 1965;4: 49-80.

Ogino K, Ratanawongs D, Tsutsumi T, Shidei T. The primary production of tropical forest in Thailand. Southeast Asian Studies 1967;5:122-54.

Peña-Arancibia JL, Bruijnzeel LA, Mulligan M, Van Dijk AIJM. Forests as 'sponges' and 'pumps': Assessing the I mpact of deforestation on dry season flows across the tropics. Journal of Hydrology 2019;574:946-63.

Phongkhamphanh T, Khamyong S, Anongrak N. Water storage potential of two different dry dipterocarp forest sites in

northern Thailand. Journal of Tropical Forest Research 2018;2(1):1-18.

Pornleesangsuwan A. Pine Growth, Soil Properties and Succession in *Pinus kesiya* Plantations, and Influence of Fragmented Forests on Reforestation in Boakaew Highland Watershed, Chiang Mai Province [dissertation]. Chiang Mai, Thailand: Chiang Mai University; 2012.

Royal Forest Department. Forest areas in Thailand (1973-2018) [Internet]. 2019 [cited 2019 Aug 22]. Available from: https://forestinfo.Forest.go.th/55/Content.aspx?id=72.

Rożeka K, Rolaa K, Błaszkowskib J, Leskic T, Zubeka S. How do monocultures of fourteen forest tree species affect arbuscular mycorrhizal fungi abundance and species richness and composition in soil. Forest Ecology and Management 2020;465:Article ID 118091.

Santos VAHF, Ferreira MJ. Initial establishment of commercial tree species under enrichment planting in a Central Amazon secondary forest: Effects of silvicultural treatments. Forest Ecology and Management 2020;460: Article ID 117822

Seeloy-ounkeaw T. Plant Species Diversity and Storages of Carbon, Nutrients and Water in Fragmented Montane Forest Ecosystems Nearby Doi Inthanon, Chiang Mai Province [dissertation]. Chiang Mai, Thailand: Chiang Mai University; 2014.

Seeloy-ounkeaw T, Khamyong S, Sri-ngernyuang K. Variations of plant species diversity along altitude gradient in conservation and utilization community forests at Nong Tao Village, Mae Wang District, Chiang Mai Province. Thai Journals of Forestry 2014;33(2):1-18.

Seramethakun T. Plant Species Diversity, Soil Characteristics and Carbon Stocks in Subtype Communities of Natural Pine Forest, Kunlaya Ni Wattana District, Chiang Mai Province [dissertation]. Chiang Mai, Thailand: Chiang Mai University; 2012.

Smitinand, T. Thai Plant Names. Bangkok, Thailand: Office of the Forest Herbarium, Department of National Parks, Wildlife and Plant Conservation; 2014.

Soil Survey Staff. Soil Taxonomy. In: A Basis System of Soil Classification for Making and Interpreting Soil Surveys. Washington, D.C., USA: Government Printing Office; 1999.

Sumanochitraporn S, Khamyong S, Anongrak N. Ecosystem water storage in a teak plantation under the Doi Tung Reforestation Royal Project, Chiang Rai Province, northern Thailand. Thai Journals of Forestry 2014;33(3):11-22.

Sutthawan P, Khamyong S, Paramee S, Anongrak N. Dry dipterocarp forest on sandstone of the Huai Hong Khrai royal development study center, Chiang Mai Province II. Monitoring plant diversity and carbon storage. Thai Journal of Forestry 2016;35(3):56-71.

Urban J, Rubtsov AV, Urban AV, Shashkin AV. Canopy transpiration of a *Larix sibirica* and *Pinus sylvestris* forest in Central Siberia. Agricultural and Forest Meteorology 2019;271:64-72.

Efficiency of Glutinous Rice Straw Extracts (RD-Six) and Water Hyacinth in Inhibiting Algal Growth and Reducing Nutrients from a Hyper-eutrophic Pond

Wipawan Intasan[1], Ratcha Chaichana[1,2*], and Patana Anurakpongsatorn[1]

[1]Department of Environmental Technology and Management, Faculty of Environment, Kasetsart University, Bangkok 10900, Thailand
[2]Research Group: Natural Environment in Forest and Freshwater Ecosystems, Faculty of Environment, Kasetsart University, Bangkok 10900, Thailand

ARTICLE INFO

Received: 14 Jul 2020
Received in revised: 8 Sep 2020
Accepted: 15 Sep 2020
Published online: 28 Oct 2020
DOI: 10.32526/ennrj/19/2020148

Keywords:
Allelochemical/ Eutrophication/ Phenolic compound/ Phytoplankton/ Restoration/ Thailand/ Water quality

*** Corresponding author:**
E-mail: fscircc@ku.ac.th

ABSTRACT

Eutrophication is one of the main water pollution problems, which occurs throughout Thailand. This research focused on the use of glutinous rice straw (RD-Six) extract and water hyacinth to reduce nutrients and to inhibit phytoplankton growth in hypereutrophic water. In this research, we used (1) control without glutinous rice straw extract and water hyacinth; and (2) experimental treatment with glutinous rice straw extract and water hyacinth. Experiments were set up for eight days in ten concrete circle pit blocks (0.80 m in diameter and 0.40 m in height) in year 2020 (five replicates for each control and experimental treatment). Water quality was analyzed physically, chemically and biologically, and the effect of glutinous rice straw extract on phytoplankton and the growth rate of water hyacinth were also determined. The result showed that values of water quality parameters (turbidity, DO, BOD, SS, TKN, NH_3-N, NO_2, TP, SRP, TN, and Chlorophyll a) were improved. The values of water quality were significantly lower ($p<0.05$) in experimental treatments than in controls. Glutinous rice straw extract had no effect on water hyacinth growth. The study of phytoplankton composition demonstrated that, prior to the experiment, Cyanophyta was the dominant group in both control and experimental treatments. After the experiment, Cyanophyta became less abundant in experimental treatments. Reduction of Cyanophyta could be caused by the direct effect of allelochemicals (phenolic compounds) from glutinous rice straw extract. Therefore, this combined method has displayed their effectiveness in reducing nutrients and inhibiting phytoplankton growth in eutrophic water.

1. INTRODUCTION

Human activities from rapid expansion of intense agricultural areas, industry and urban settlement have led to environmental problems and degradation. In particular, nutrient pollution, coming from both point sources and non-point sources is regarded as a serious environmental problem, especially in Thailand. Addition of excessive nutrients into lakes and rivers can cause a rapid algae bloom or eutrophication (Rodrigo et al., 2018). This problem can lead to water quality deterioration, reduction in diversity of flora and fauna, and human health problems posed by harmful algae blooms (HABs) of the cyanobacteria group (Usharani and Keerthi, 2020).

There are several physical and chemical methods that can be used to inhibit algal growth and to solve eutrophication problems. These methods include, for example, the use of chemical substances (e.g., copper sulphate, aluminium sulphate, Phoslock) (Jančula and Maršálek, 2011; Umphres et al., 2012) or ultrasonic treatment (Broekman et al., 2010). However, operation of these methods is often costly and may result in long-lasting chemical residues in the environment (Umphres et al., 2012). In recent years, rice straw extract has received considerable attention as an algaecide (Ella et al., 2007) and has been used in many countries. This method is environmentally friendly, effective, and low in operational cost. Most

Citation: Intasan W, Chaichana R, Anurakpongsatorn P. Efficiency of glutinous rice straw extracts (RD-Six) and water hyacinth in inhibiting algal growth and reducing nutrients from a hyper-eutrophic pond. Environ. Nat. Resour. J. 2021;19(1):24-33. (https://doi.org/10.32526/ennrj/19/2020148)

rice straw extracts are a group of phenolic compounds (coumaric, vanillic, ferulic, hydroxy benzoic, salicylic, syringic, and benzoic acids), which can inhibit phytoplankton growth and can cause abnormalities against photosynthesis processes of phytoplankton (Ferrier et al., 2005; Park et al., 2006). In particular, phenolic compounds selectively affect blue-green algae (e.g., *Microcystis aeruginosa*) (Hua et al., 2018) and phytoplankton communities then can shift from cyanobacteria to other groups such as diatoms (Islami and Filizadeh, 2011). Reduction of cyanobacteria, especially *Microcystis*, is beneficial since *Microcystis* produces microcystin that can cause toxicity to the liver and skin irritation in animals and humans.

Water hyacinth (*Eichhornia crassipes*), belonging to the Family Pontederiaceae, is a floating plant with large and thick leaves. Its roots are underwater, but the stems and leaves float above the water surface. It grows well in hot and humid climates with the optimum temperature between 25-35°C. Water hyacinth is propagated quickly and can be found everywhere in water bodies. It is more durable and grows better in deteriorated water than other plants. There are several research experiments that used water hyacinth such as; removal of heavy metals (Jayaweera et al., 2008; Mishra and Tripathi, 2009), reduction of concentrations of dyestuffs (Ekambaran and Perumal, 2017), and absorption of nutrients (Yi et al., 2009). From research, water hyacinth was highly effective in treating 89.4% nitrogen and 84.0% phosphorus (Lu et al., 2018) in eutrophic water restoration due to its strong nutrient absorption capacity (Gong et al., 2018; Rezania et al., 2015; Wang et al., 2012). The structure of its roots has a large surface area, which is suitable for the growth of different types of microbes that can decompose organic matter in wastewater into inorganic substances. It also enables the tracing of the elements that plants use to grow from the uptake which passed through its porous membranes and accumulates in leaves and roots (Chunkao et al., 2012; Gopal, 1987).

In Thailand, glutinous rice straw is one of the highest amount agricultural waste products as Thai people consume rice as a staple food. Farmers eliminate remaining glutinous rice straw by burning, and this can cause serious air pollution problems that are harmful to human health (Chen et al., 2017). Water hyacinth, an invasive alien species, was introduced to Thailand in 1901. It flourishes and is widespread in tropical countries and should be used for the benefit of society. The use of glutinous rice straw extract (Eladel et al., 2019; Kang et al., 2017; Iredale et al., 2012; Islami and Filizadeh, 2011) and water hyacinth should be an interesting option to control algal blooms. This combined technique is uncomplicated, has a low cost of operation and reduces the use of chemicals, and therefore is safe for humans, animals and the environment. The objectives of this study were to investigate the efficacy of glutinous rice straw extract application and water hyacinths to control phytoplankton growth and to improve eutrophic water quality, and to determine the impact of glutinous rice straw extracts on phytoplankton composition and assemblages. The data of this study may apply well in treating eutrophic waters in Thailand.

2. METHODOLOGY

2.1 Study site

This research was conducted at Lumpini Park (13.729932 N, 100.541309 E), which is a large public park located at the center of Bangkok, Thailand. Lumpini Park covers an area of 360 rai or approximately 57.6 ha. This park has a large pond (water surface area of 111,000 m^2, volume of 222,000 m^3 and average depth of 2 m) and a network of small ponds. A variety of fish and aquatic animals exists in the area (invertebrates, water birds, and water monitors). The park's pond has poor water circulation and receives public artificial bird and fish feeding. Therefore Lumpini Park represents eutrophic unban ponds that have severely suffered from frequent rapid growth of phytoplankton and should be urgently managed for a better ecological condition.

2.2 Experimental design and setup

In this study, ten concrete circle pit blocks (0.80 m in diameter and 0.40 m in height) were used (Figure 1) because they are available in the market, affordable and are heavy enough to be placed in the water without drifting. Moreover, concrete circle pit blocks are stronger and more durable in the water than other materials. 120 L of water were pumped into each concrete circle pit block from a large pond by an electrical pump. The experiments were divided into two sets; (1) control (five concrete circle pit blocks as replicates) without glutinous rice straw extract and water hyacinth, and (2) experimental treatment (five concrete circle pit blocks as replicates) with extracts of glutinous rice straw and water hyacinth (Figure 1).

Figure 1. Setup of experiment; (a) concrete circle pit blocks, (b) experimental treatment, and (c) control

In this study, RD-Six extracts from glutinous rice straw were used due to its high phenolic contents (146.92±6.12 mg/L) and our preliminary study revealed that rice straw extract at a concentration of 3.0 g/L showed high effect and resulted in the decline of chlorophyll a up to 81%. Extracts were prepared by cutting dried glutinous rice straw into small pieces (approximately two cm in length). Then, pieces of glutinous rice straw (30 g) were placed in a 1-L beaker with reverse osmosis water and were incubated at room temperature for five days. After five days, the aqueous extract was filtered with GF/C paper to get extracts at a concentration of 30 g/L. 12 L of aqueous extracts from glutinous rice straw were then applied into each concrete circle pit block of experimental treatments (about 10% by volume of the concrete circle pit block). The water level in each concrete circle pit block was about 30 cm. Young water hyacinths were selected and used in experimental treatment (approximate length of leaves: 15 cm). Fresh water hyacinths were weighed on digital scales prior to the experiment (by holding the water hyacinth in the air for 15 min until without water droplets) (Lu et al., 2018). After that, water hyacinths were put into a series of experimental concrete circle pit blocks (five replications), covering approximately 80% of the water surface.

Water samples were collected from all concrete circle pit blocks for physical and chemical water quality analysis prior to experiment. After water collection, glutinous rice straw extract and water hyacinth were applied to the concrete circle pit blocks. Water samples were collected daily for eight days in February, 2020, between 09.00-10.00 am. Water samples were stored in 1.5 L plastic bottles and preserved under the method of APHA et al. (1998).

Water quality parameters were measured on site (temperature (°C), salinity (g/L), and conductivity (µs/cm) using the YSI 30 handheld meter). Other water quality parameters were measured in the laboratory, including pH (by pH meter (HACH, HQ411D)), turbidity (NTU, by turbidimeter (HACH, 2100AN)), dissolved oxygen (DO) (mg/L, by azide modification of the Winkler method), biological oxygen demand (BOD_5) (mg/L, by incubation), total suspended solid (SS) (mg/L, by dried at 103-105°C), total Kjeldahl nitrogen (TKN) (mg/L, by Semi-Micro-Kjeldahl (Velp,DKL)), ammonia nitrogen (NH_3-N) (mg/L, by titrimetric method (Velp, UDK139)), nitrate nitrogen, (NO_3-N) (mg/L, by Ultraviolet spectrophotometric method), nitrite (NO_2-N) (mg/L, by colorimetric-method (HACH, DR6000)), total phosphorus (TP), and soluble reactive phosphorus (SRP) (mg/L, by ascorbic acid-spectrophotometric method (HACH, DR6000), total nitrogen (TN as sum of TKN, NO_3-N, NO_2-N) (mg/L), and chlorophyll a (µg/L, by acetone extraction method).

The effects of glutinous rice straw extract on the density and composition of phytoplankton species was

determined by filtering 10 L of water through a plankton net (mesh size: 20 µm). Samples of phytoplankton were preserved by adding 70% ethyl alcohol. Phytoplankton samples were then classified up to species level and counted in a Sedgewick Rafter counting chamber under a compound microscope. The growth rate of water hyacinths was also determined by comparing the weight at the beginning and the end of the experiment.

2.3 Statistical analysis

Mean±standard deviation is presented throughout this article, except algal composition that is presented as percentage. Independent samples T-test was used to examine the differences of physical, chemical and biological parameters between control and experimental treatment. Statistical significance was accepted at a level of $p<0.05$. Statistical analysis was performed by statistical analysis SPSS software version 23 (trial).

3. RESULTS

3.1 Water quality

The result of water quality is presented in Table 1. Overall, nutrient concentrations in both control and experimental treatment were exceptionally high. Trophic state can be classified as hypereutrophic condition as indicated by high TN and TP values. When comparing water quality values between control and experimental treatment, the results showed that temperature, pH, conductivity, salinity, NO_3-N, and SRP were not significantly different ($p>0.05$). In contrast, turbidity, SS, DO, BOD, TKN, NH_3-N, NO_2-N, TN, TP, and chlorophyll a were significantly different ($p<0.05$) between control and experimental treatment. At the end of the experiment, most values of nutrients and chlorophyll a were relatively lower in the experimental treatment than in control.

Table 1. Comparison of water quality parameters between control and experimental treatment at the end of experiment.

Parameters	Control	Experimental treatment
Temperature (°C)	29±0[a]	29±0[a]
pH	7.3±0.1[a]	7.3±0.0[a]
Conductivity (µs/cm)	1707±15[a]	1715±8[a]
Salinity (g/L)	0.9±0.1[a]	0.9±0.0[a]
Turbidity (NTU)	28±1[a]	15±2[b]
SS (mg/L)	38±4[a]	15±2[b]
DO (mg/L)	6.0±0.3[a]	3.4±0.2[b]
BOD (mg/L)	12±0[a]	7±1[b]
TKN (mg/L)	5.04±0.00[a]	3.02±0.31[b]
NH_3-N (mg/L)	1.12±0.00[a]	0.73±0.15[b]
NO_3-N (mg/L)	1.10±0.07[a]	1.03±0.01[a]
NO_2-N (mg/L)	0.06±0.02[a]	0.02±0.01[b]
TN (mg/L)	6.20±0.07[a]	4.07±0.29[b]
TP (mg/L)	0.30±0.02[a]	0.16±0.01[b]
SRP (mg/L)	0.02±0.01[a]	0.01±0.00[a]
Chlorophyll a (µg/L)	306.93±48.71[a]	91.56±10.18[b]

Remark: Values are mean±SD, different superscript letters in the same row indicates values with significant difference ($p<0.05$).

Table 2 shows removal efficiency of water quality parameters between control and experimental treatment. Overall, removal efficiency of water quality in experimental treatment was much higher than in control. In particular, removal efficiency of chlorophyll a in experimental treatment was up to 81.5% compared with that in control, of which the efficiency was only approximately 27.4%.

Table 2. Removal efficiency between control and experimental treatment

Parameters	Control			Experimental treatment		
	Day 0	Day 7	Removal rate (%)	Day 0	Day 7	Removal rate (%)
Turbidity	66±8.00	28±1.00	57.6	64±4.00	15±2.00	76.6
SS	60±6.00	38±4.00	36.7	55±5.00	15±2.00	72.7
BOD	19±3.00	12±0.00	39.2	19±1.00	7±1.00	63.5
TKN	5.82±0.31	5.04±0.00	13.4	5.15±0.47	3.02±0.31	41.4
NH_3-N	1.01±0.15	1.12±0.00	-10.9	0.95±0.15	0.73±0.15	23.2
NO_3-N	1.14±0.03	1.10±0.07	3.5	1.15±0.05	1.03±0.01	10.4
NO_2-N	0.03±0.01	0.06±0.02	-100	0.03±0.01	0.02±0.01	33.3
TN	6.99±0.33	6.20±0.07	11.3	6.33±0.48	4.07±0.29	35.7
TP	0.32±0.07	0.30±0.02	6.3	0.31±0.07	0.16±0.01	48.4
SRP	0.02±0.01	0.02±0.01	0.0	0.02±0.01	0.01±0.00	50.0
Chlorophyll a	422.82±63.28	306.93±48.71	27.4	494.96±69.29	91.56±10.18	81.5

Figure 2 shows the tendency of water quality values between the control and experimental treatments. Values of turbidity and SS showed a tendency to decrease from the beginning toward the end of the experiment. In the experimental treatment, BOD increased after application of glutinous rice straw extract and then started to decline toward the end of the experiment. In contrast, DO dropped after the addition of glutinous rice straw extract and subsequently increased and remained constant until the end of experiment.

Figure 3 shows the tendency of nutrient concentrations between the control and experimental treatments. In the experimental treatment, nitrogen contents (ammonia, nitrate, and TN) appeared to increase right after application of glutinous rice straw extract. Then, concentrations of nitrogen contents started to decline toward the end of experiment. TP and SRP values in experimental treatment were relatively lower than in control and gradually declined until the end of experiment.

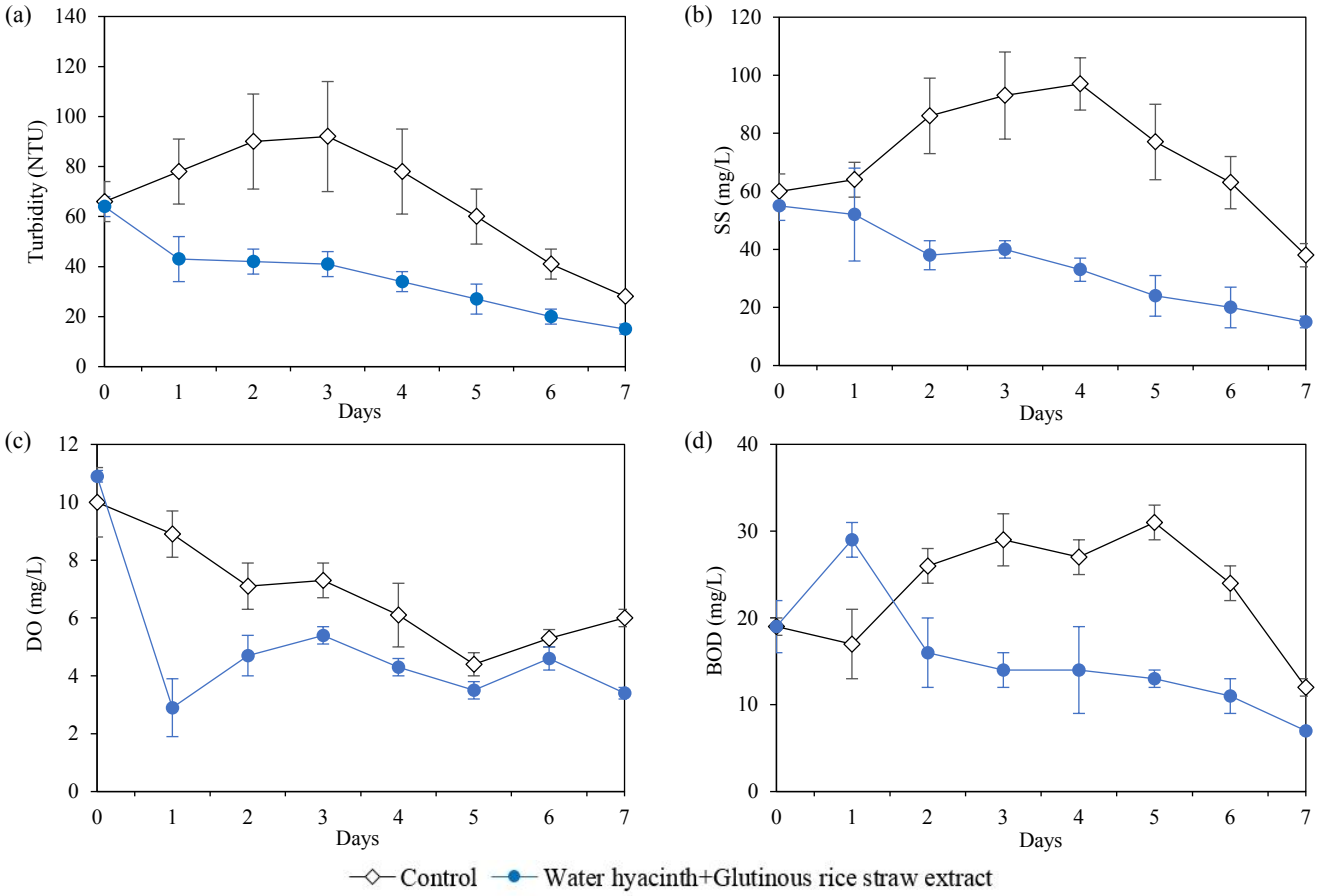

Figure 2. Physical-chemical parameters variation between control and experimental treatments (a) turbidity, (b) SS (c) DO, and (d) BOD

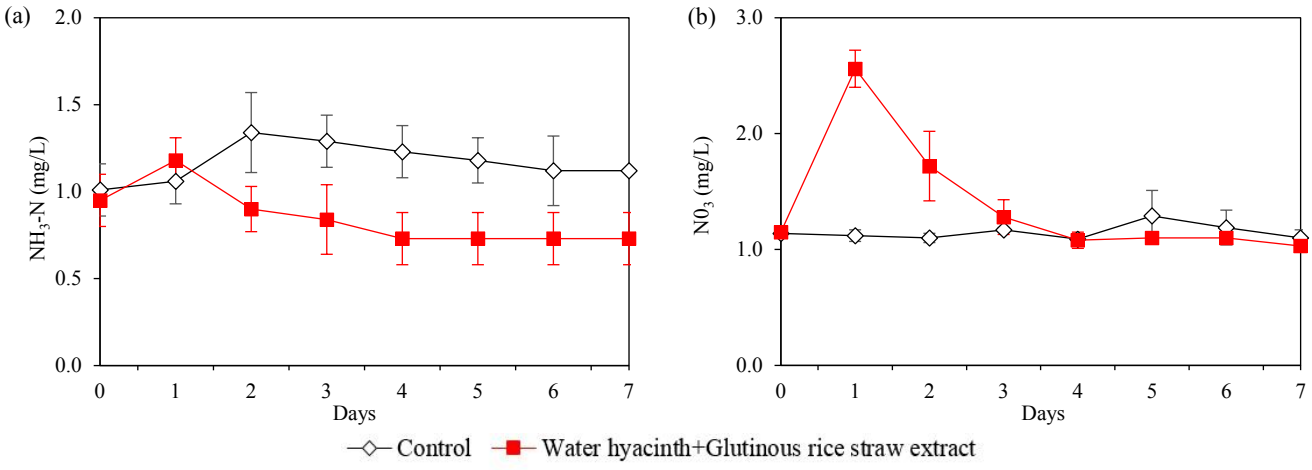

Figure 3. Comparison of nutrient concentration between control and experimental treatment; (a) NH_3-N, (b) NO_3, (c) TN, (d) TP, and (e) SRP.

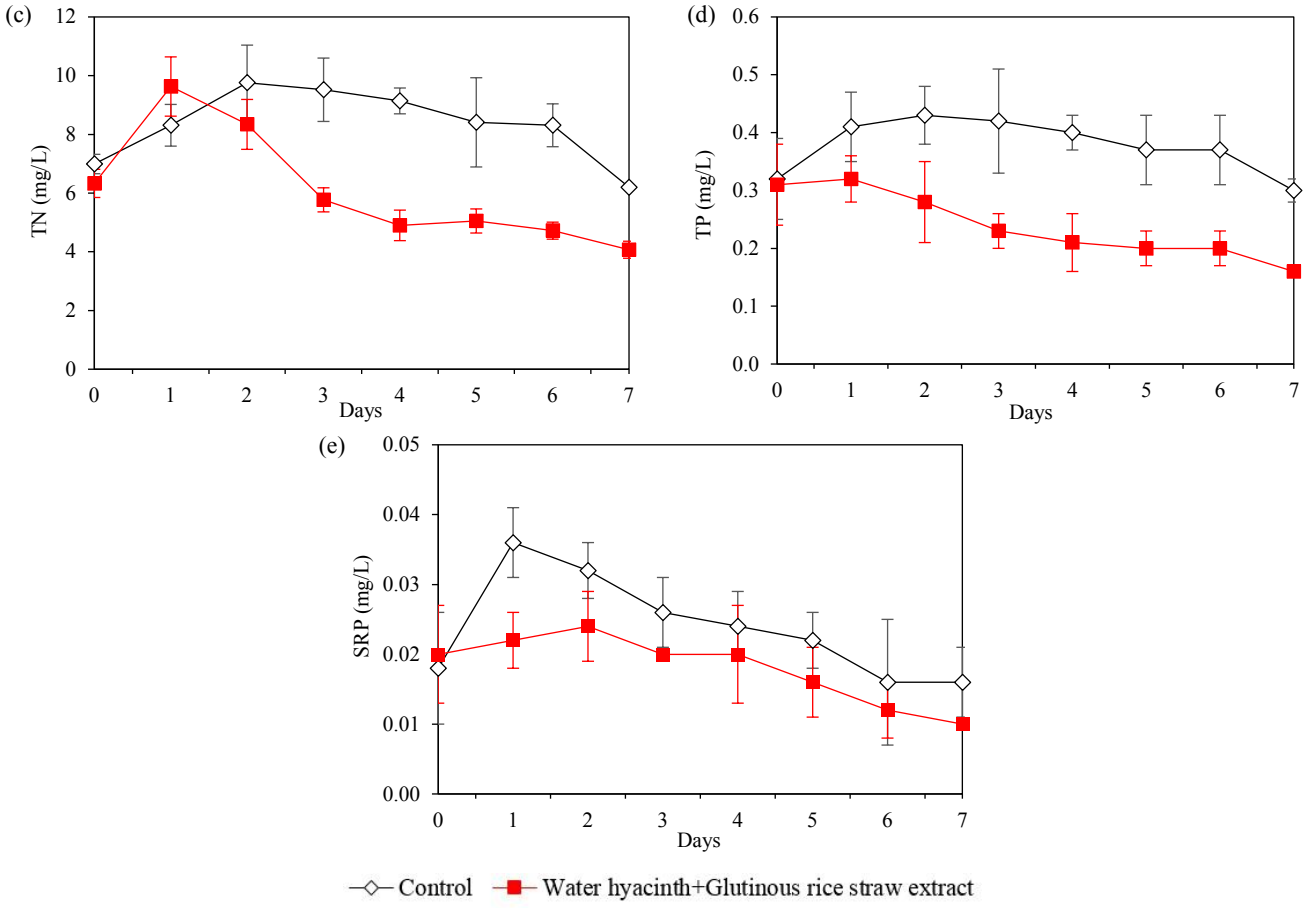

Figure 3. Comparison of nutrient concentration between control and experimental treatment; (a) NH_3-N, (b) NO_3, (c) TN, (d) TP, and (e) SRP (cont.).

3.2 Effect of glutinous rice straw extract on phytoplankton

This study investigated the effect of glutinous rice straw extract on chlorophyll a. It was revealed that, in the control, chlorophyll a concentration increased in the middle of the study and was relatively higher than in experimental treatment (Figure 4). In contrast, chlorophyll a concentration in the experimental treatment started to decrease from day one until the end of the experiment.

The result of phytoplankton composition showed that there were three divisions of phytoplankton belonging to; (1) Cyanophyta, (2) Chlorophyta, and (3) Chromophyta. In total, there were 34 species of phytoplankton (Table 3). *Cylindrospermopsis raciborskii* was the dominant species in both control and experimental treatment. At the beginning of the experiment, Cyanophyta was the most abundant group (69.8%) in the control, followed by Chromophyta (23.2%) and Chlorophyta (7.0%) respectively. In the experimental treatment, Cyanophyta was also the main phytoplankton group (88.8%), followed by Chromophyta (8.0%) and Chlorophyta (3.2%).

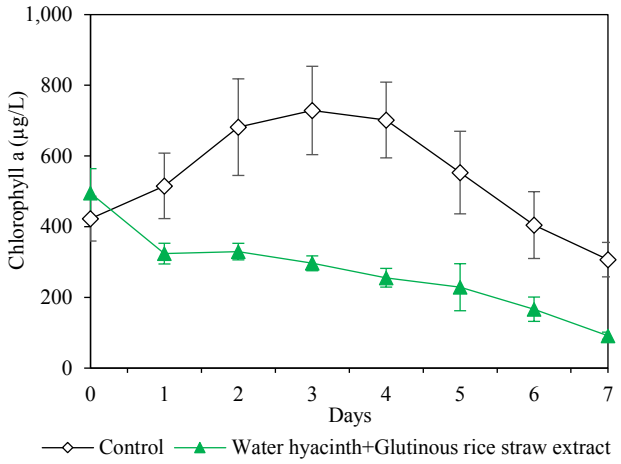

Figure 4. Tendency of chlorophyll a content between control and experimental treatment.

At the end of the experiment, the most common phytoplankton in the control was still Cyanophyta (83.3%), followed by Chromophyta (12.3%) and Chlorophyta (4.3%), respectively. In contrast, the abundance of phytoplankton groups in the experimental treatment shifted to Cyanophyta (45.7%), Chromophyta (45.2%), and Chlorophyta (9.0%), respectively.

Table 3. Impact of glutinous rice straw extract and water hyacinth on algal composition in treatments.

	Control		Treatment	
	Before	After	Before	After
Cyanophyta				
Chroococcus sp.	11,134	-	7,524	-
Cylindrospermopsis raciborskii	2,672,552	4,099,762	7,302,232	335,502
Merismopedia minima	102,988	147,552	121,076	14,341
Oscillatoria sp. (1)	67,412	24,680	30,164	7,676
Oscillatoria sp. (2)	16,720	-	-	-
Spirulina sp.	6,853	19,141	2,886	-
%	69.8	83.3	88.8	45.7
Chlorophyta				
Closteriopsis sp.	-	19,051	11,742	3,952
Coelastrum microsporum	7,258	7,271	3,762	5,181
Crucigeniella sp.	3,382	9,912	9,595	3,762
Monoraphidium contortum	72,816	75,703	32,179	14,051
Monoraphidium sp.	22,255	14,089	9,746	-
Pediastrum duplex	3,838	-	3,762	3,838
Pediastrum angulosum	-	-	3,914	-
Scenedesmus armatus	37,962	23,780	30,874	11,993
Scenedesmus acuminatus	34,899	28,733	9,428	7,879
Scenedesmus sp.	6,688	-	-	-
Selenastrum quadricanda	48,317	11,102	96,525	3,965
Tetraedron trigonum	-	7,448	-	3,800
Tetraedron gracile	3,838	-	3,762	-
Euglena sp.	24,746	22,630	40,050	3,927
Euglena acus	-	3,601	-	4,180
Phacus acuminatus	-	-	15,656	-
Phacus helikoides	-	-	-	4,180
Phacus ranula	3,838	-	-	-
Lepocinclis sp.	20,064	-	-	-
%	7.0	4.3	3.2	9.0
Chromophyta				
Aulacoseira granulata	-	-	1,955	-
Cocconesis sp.	5,035	7,448	-	4,180
Cyclotella sp.	815,108	424,149	565,007	283,845
Fragilaria sp.	3,382	-	-	-
Navicula sp.	10,526	10,602	7,091	10,298
Nitzschia sp.	115,657	171,920	93,518	49,157
Nitzschia closterium	5,976	14,610	2,083	6,061
Surirella sp.	-	-	186	-
Peridinium sp. (1)	-	5,504	3,724	-
%	23.2	12.3	8.0	45.2

3.3 Effect of glutinous rice straw extract on water hyacinth

During the experiment, water hyacinths grew well and produced new sprouts. At the end of the experiment, leaf size increased, and stems and roots were also longer and larger. Figure 5 shows fresh weight of water hyacinths before (552.54±1.93 g) and after (1,362.38±77.38 g) the experiment. The growth rate of water hyacinth was at 59.4%.

4. DISCUSSION

4.1 Water quality

The results of water quality analysis showed that the values of most parameters in the experimental

treatment were lower than in the control, with significant differences ($p<0.05$). Water quality from the lake indicated that the lake was hypereutrophic with algal blooms. Treatment of eutrophic water by glutinous rice straw extract and water hyacinth showed remarkable results. Turbidity and suspended solids content decreased in the experimental treatment. This may be linked to filtration done by the roots of water hyacinths. Some of the suspended solid content may be adsorbed by the surface of the roots, and then slowly settled down (Lu et al., 2018) at the bottom of the concrete circle pit blocks. Leaves and stems of the water hyacinth may also help reduce the wind speed, thereby reducing the diffusion of sediment in the water. The decrease of dissolved oxygen in the experimental treatment is possibly due to the decrease of phytoplankton. Water hyacinth obstructed sunlight, causing the decrease of oxygen produced by the photosynthesis process of phytoplankton (Di Luca et al., 2019).

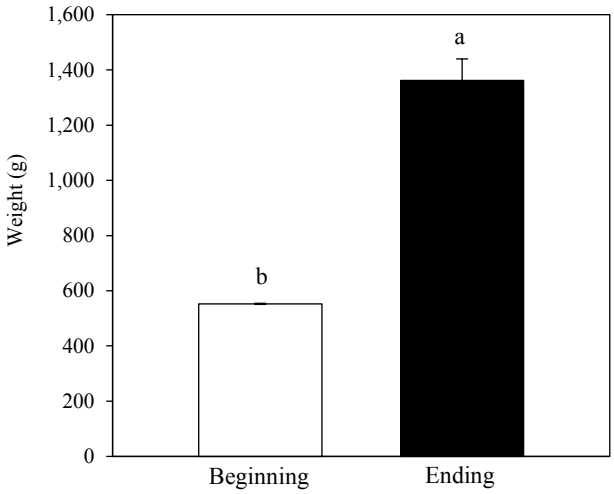

Figure 5. Comparison of wet weight (g) between the beginning and the end of experiment. Different letters on bars indicate significant difference of water hyacinth weight ($p<0.05$).

Nitrogen contents at the beginning of the experimental treatment were high after addition of glutinous rice straw extract (Duan et al., 2017; Eladel et al., 2019). Toward the end of experiment, nitrogen slightly declined, which may be explained by microbes living around the roots of the water hyacinth that transformed organic into inorganic substances and absorbed them through the root cells (Gopal, 1987). BOD value in the control remained higher than in the experimental treatment. This might attribute to the fact that in the absence of plant rhizomes, the rate of impurity elimination by microbes became slower (Valipour et al., 2015). In contrast, BOD reduction in the experimental treatment was faster and could result from decomposition by microbes associated with water hyacinth. Water quality results showed that water hyacinth was effective in reducing the amount of nitrogen and phosphorus in the water through plant absorption (Lu et al., 2018).

4.2 Effect of glutinous rice straw extract on phytoplankton

The use of glutinous rice straw extract, together with water hyacinth, effectively reduced the amount of phytoplankton. The experimental treatment, with the addition of glutinous rice straw extract, had lower levels of chlorophyll a than in the control with significant differences statistically ($p<0.05$). Glutinous rice straw extract inhibited the growth of phytoplankton as its phenolic compounds caused the abnormalities against photosynthesis and cell processes of the algae (Hua et al., 2018). This study is consistent with the study in a fish pond (*Oreochromis niloticus*) as it showed that content of chlorophyll a in the pond containing extracts from rice straws were 50% less than those without addition of rice straw extract (Eladel et al., 2019). Shading from water hyacinth may have also limited the growth rates of phytoplankton in experimental treatment.

In addition, glutinous rice straw extract affected the composition of phytoplankton. Phytoplankton composition shifted from Cyanobacteria to Chromophyta in the experimental treatment. It is believed that phenolic compounds released from glutinous rice straw selectively influenced Cyanobacteria more than other phytoplankton groups (Ridge and Pillinger, 1996). The results of this study corresponded with Islami and Filizadeh (2011) who used rice straw to control algal species in water. Rice straw extract is effective in controlling algae, especially cyanobacterial phytoplankton (*Microcystis aeruginosa, Scenedesmus subspicatus,* and *Anabaena flos-aquae*), without inhibiting diatom species (*Hydrodictyon reticulatum* and *Oscillatoria tenuis*) (Islami and Filizadeh, 2011). Further research is still needed to understand mechanisms of glutinous rice straw extracts involved in cyanobacteria growth inhibition. Photosynthetic activities, maximum quantum yield (Fv/Fm) and growth inhibition efficiency of cyanobacteria should be further compared and investigated.

4.3 Effect of glutinous rice straw extract on water hyacinth

This study also evaluated the effect of glutinous rice straw extract on growth rate of water hyacinths in the experimental treatment. The results showed that water hyacinth grew well in the concrete circle pit blocks with glutinous rice straw extract. The weight of water hyacinth increased by 59.3% compared to its weight prior to the experiment. Phenolic compounds released from glutinous rice straw seem to have no effect on water hyacinth but have negative effects only on phytoplankton (Eladel et al., 2019). The growth of water hyacinth in the experiment may also be linked to various environmental factors such as high nutrient contents in the water, optimum water temperature (27-30^{o}C), pH (7.2-7.5) and salinity (0.8-0.9 g/L). These environmental factors are consistent with the previous studies showing that water hyacinth is resistant to a wide range of environment. Water hyacinth can grow in water with temperature between 10-40^{o}C and pH 6-8 (Rezania et al., 2015).

5. CONCLUSION

Glutinous rice straw extracts and water hyacinth proved an effective control method for nuisance algal blooms and high nutrient contents in a fresh-water environment. Glutinous rice straw extract application reduced phytoplankton and shifted species composition, especially Cyanophyta. Phenolic compounds released directly from glutinous rice straw extract, appeared to be the main inhibitory effect on phytoplankton. However, the extracts from glutinous rice straw did not affect the growth of water hyacinth. Water hyacinth plays a synergistic role to compete for nutrients with phytoplankton. Water hyacinth, along with other microorganisms associated to it, significantly reduced the level of organic and inorganic substances. Therefore, this combined method, which is simple, uncomplicated and environmentally friendly, should be promoted.

ACKNOWLEDGEMENTS

We would like to thank Department of Environmental Technology and Management, and Faculty of Environment, Kasetsart University for financial support in this research project. We also received partial research fund from Research Group: Natural Environment in Forest and Freshwater Ecosystems, Faculty of Environment, Kasetsart University. Lastly, we are thankful to the Analytical Laboratory at the Department of Drainage and Sewerage, Bangkok, for supporting water quality analysis.

REFERENCES

American Public Health Association (APHA), American Water Works Association (AWWA), and Water Environment Federation (WEF). Standard Methods for the Examination of Water and Wastewater. 20th ed. Washington D.C., USA: American Public Health Association; 1998.

Broekman S, Pohlmann O, Beardwood ES, De Meulenaer EC. Ultrasonic treatment for microbiological control of water systems. Ultrasonics Sonochemistry 2010;17(6):1041-8.

Chen J, Li C, Ristovski Z, Milic A, Gu Y, Islam MS, et al. A review of biomass burning: Emissions and impacts on air quality, health and climate in China. Science of the Total Environment 2017;579:1000-34.

Chunkao K, Nimpee C, Duangmal K. The King's initiatives using water hyacinth to remove heavy metals and plant nutrients from wastewater through Bueng Makkasan in Bangkok, Thailand. Ecological Engineering 2012;39:40-52.

Di Luca GA, Mufarrege MM, Hadad HR, Maine MA. Nitrogen and phosphorus removal and *Typha domingensis* tolerance in a floating treatment wetland. Science of the Total Environment 2019;650:233-40.

Duan J, He S, Feng Y, Yu Y, Xue L, Yang L. Floating ryegrass mat for the treatment of low-pollution wastewater. Ecological Engineering 2017;108:172-8.

Ekambaran SP, Perumal SS. Water hyacinth (*Eichhornia crassipes*): An efficient and economic adsorbent for textile effluent treatment: A review. Arabian Journal of Chemistry 2017;10:3548-58.

Eladel H, Abd-Elhay R, Anees D. Effect of rice straw application on water quality and microalgal flora in fish ponds. Egyptain Journal of Botany 2019;59(1):171-84.

Ella SM, Hosny MM, Bakry MF. Growth inhibition of bloom-forming using rice straw in water courses (case study). Proceedings of the Eleventh International Water Technology Conference: 2007 Mar 15-16; Sharm El-Sheikh, Egypt; 2007.

Ferrier MD, Butler BR, Terlizzi DE, Lacouture RV. The effects of barley straw (*Hordeum vulgare*) on the growth of freshwater algae. Bioresource Technology 2005;96(16):1788-95.

Gong Y, Zhou X, Ma X, Chen J. Sustainable removal of formaldehyde using controllable water hyacinth. Journal of Cleaner Production 2018;181:1-7.

Gopal B. Water Hyacinth. Amsterdam, Netherlands: Elsevier Science; 1987.

Hua Q, Liu Y, Yan Z, Zeng G, Liu S, Wang W, et al. Allelopathic effect of the rice straw aqueous extract on the growth of *Microcystis aeruginosa*. Ecotoxicology and Environmental Safety 2018;148:953-9.

Iredale RS, McDonald AT, Adams DG. A series of experiments aimed at clarifying the mode of action of barley straw in cyanobacterial growth control. Water Research 2012;46(18): 6095-103.

Islami HR, Filizadeh Y. Use of barley straw to control nuisance freshwater algae. Journal American Water Works Association 2011;103(5):111-8.

Jančula D, Maršálek B. Critical review of actually available chemical compounds for prevention and management of cyanobacterial blooms. Chemosphere 2011;85(9):1415-22.

Jayaweera MW, Kasturiarachchi JC, Kularatne R, Wijeyekoon S. Contribution of water hyacinth (*Eichhornia crass*ipes (Mart.) Solms) grown under different nutrient conditions to Fe-removal mechanisms in constructed wetlands. Journal of Environmental Management 2008;87(3):450-60.

Kang P, Kim B, Mitchell MJ. Effects of rice and rye straw extracts on the growth of a cyanobacterium, *Microcystis aeruginosa*. Paddy Water Environment 2017;15:617-23.

Lu B, Xu Z, Li J, Chai X. Removal of water nutrients by different aquatic plant species: An alternative way to remediate polluted rural rivers. Ecological Engineering 2018;110:18-26.

Mishra VK, Tripathi BD. Accumulation of chromium and zinc from aqueous solutions using water hyacinth (*Eichhornia crassipes*). Journal of Hazardous Materials 2009;164(2): 1059-63.

Park M, Han M, Ahn C, Kim H, Yoon B, Oh H. Growth inhibition of bloom-forming cyanobacterium *Microcystis aeruginosa* by rice straw extract. Letters in Applied Microbiology 2006;43(3):307-12.

Rezania S, Ponraj M, Talaiekhozani A, Mohamad SE, Din MFM, Taib SM, et al. Perspectives of phytoremediation using water hyacinth for removal of heavy metals, organic and inorganic pollutants in wastewater. Journal of Environmental Management 2015;163:125-33.

Ridge I, Pillinger JM. Towards understanding the nature of algal inhibitors from barley straw. Hydrobiologia 1996;340:301-5.

Rodrigo MA, Valentin A, Claros J, Moreno L, Segura M, Lassalle M, et al. Assessing the effect of emergent vegetation in a surface-flow constructed wetland on eutrophication reversion and biodiversity enhancement. Ecological Engineering 2018;113:74-87.

Umphres GD, Roelke DL, Netherland MD. A chemical approach for the mitigation of *Prymnesium parvum* blooms. Toxicon 2012;60(7):1235-44.

Usharani K, Keerthi KV. Nitrate bioremoval by phytotechnology using *Utricularia aurea* collected from eutrophic lake of Theerthamkara, Kerala, India. Pollution 2020;6(1):149-57.

Valipour A, Kalyanraman V, Ahn Y. Effectiveness of domestic wastewater treatment using a bio-hedge water hyacinth wetland system. Water 2015;7(1):329-47.

Wang Z, Zhang Z, Zhang J, Zhang Y, Liu H, Yan S. Large-scale utilization of water hyacinth for nutrient removal in lake Dianchi in China: The effects on the water quality, macrozoobenthos and zooplankton. Chemosphere 2012; 89(10):1255-61.

Yi Q, Hur C, Kim Y. Modeling nitrogen removal in water hyacinth ponds receiving effluent from waste stabilization ponds. Ecological Engineering 2009;35(1):75-84.

In Vitro and *In Vivo* Inhibition of *Cylindrocladium reteaudii* by Essential Oils of *Acorus calamus* Rhizomes

Phanin Sintawarak[1], Suwimon Uthairatsamee[2], and Tharnrat Keawgrajang[2*]

[1]Department of National Parks, Wildlife and Plant Conservation, Chatuchak, Bangkok 10900, Thailand
[2]Department of Forest Biology, Faculty of Forestry, Kasetsart University, Bangkok 10900, Thailand

ARTICLE INFO

Received: 29 Apr 2020
Received in revised: 23 Aug 2020
Accepted: 23 Sep 2020
Published online: 5 Nov 2020
DOI: 10.32526/ennrj/19/2020076

Keywords:
Acorus calamus/ Leaf blight/ Biocontrol/ *Eucalyptus*/ Antifungal activity

*** Corresponding author:**
E-mail: ffortrk@ku.ac.th

ABSTRACT

Cylindrocladium reteaudii (Bugnic.) Boesew. is a severe pathogen which can cause leaf blight disease in *Eucalyptus* seedlings in tropical countries. This study investigated the antifungal activity of essential oils extracted from *Acorus calamus* L. rhizomes in inhibiting the growth of *C. reteaudii*, both in *in vitro* and *in vivo* experiments. The extraction of essential oils from rhizomes was carried out by hydro-distillation technique and the *in vitro* antifungal testing was done by using the poisoned food technique. The results indicated that an essential oil concentration of 2,000 ppm can completely inhibit the fungal growth with a 50% inhibitory concentration value of 54.76 ppm. For the *in vivo* experiment, it was found that an essential oil concentration of 500 ppm and Captan® of 1,000 ppm were not significantly different in inhibiting the growth of *C. reteaudii*. However, these two treatments significantly inhibited the fungal growth ($p<0.05$) when compared with the control treatments. Physiological and anatomical characteristics were investigated to check for the antifungal activity after the application of essential oils. Results showed that essential oil spraying had no effect on the leaf transpiration rate and temperature of the *Eucalyptus* seedlings, but the incident disease ratio was high when an essential oil concentration of more than 1,500 ppm was applied. Therefore, it can be inferred that the essential oils from *A. calamus* rhizomes at an optimum concentration can be an efficient antifungal compound with a potential to control leaf and shoot blight diseases in *Eucalyptus* seedlings in a nursery.

1. INTRODUCTION

Owing to a growing demand for forest products and environmental services, the area under planted forests is likely to increase continuously all the world (FAO, 2016). *Acacia* and *Eucalyptus* are short rotation cycle trees which constitute the main planted species in forests around the South and Southeast Asia. Such planted forests are distributed in approximately 7 million ha in these regions (Harwood and Nambiar, 2014). The area under *Eucalyptus* plantations worldwide is about 20 million ha, out of which 0.5 million ha is located in Thailand (Manavakun, 2014). As the plantation area is increasing dramatically every year, so is the threat from pests and pathogens.

Leaf and shoot blight caused by *Cylindrocladium* - an amorph of *Calonectria* species, is one of the most severe fungal diseases in regions experiencing high precipitation in Southeast Asia and South America and is a particularly serious problem in *Eucalyptus* plantations and nurseries (Kang et al., 2001; Crous, 2002; Rodas et al., 2005; Thu et al., 2010; Devi, 2011). Previous reports indicate that the mortality rate in *Eucalyptus* plantations were between 60-100% in Vietnam (Old et al., 2003). Resulting from this fungal pathogen, hybrid clonal *Eucalyptus* cutting production in commercial forest nurseries in China decreased drastically (Zhou et al., 2008). Pongpanich (1998) reported that *Cylindrocladium reteaudii* causes leaf blight and damping-off disease in *Eucalyptus* seedlings in Thailand with frequent outbreaks in nurseries. Consequently, this fungus has become a serious disease, especially plaguing the commercial *Eucalyptus* nurseries (Pongpanich et al., 2010). However, this fungus affects a broad range of host

Citation: Sintawarak P, Uthairatsamee S, Keawgrajang T. *In Vitro* and *In Vivo* inhibition of *Cylindrocladium reteaudii* by essential oils of *Acorus calamus* Rhizomes. Environ. Nat. Resour. J. 2021;19(1):34-42. (https://doi.org/10.32526/ennrj/19/2020076)

plants and is an important pathogen found in agricultural and forest plants (Kang et al., 2001; Crous, 2002; Old et al., 2003; Lombard et al., 2010a). Recently, subtropical and tropical regions became a hot spot for *Calonectria* (=*Cylindrocladium*), with several new species having been reported (Lombard et al., 2010a; Lombard et al., 2010b; Alfenas et al., 2015; Lombard et al., 2015; Lombard et al., 2016; Liu and Chen, 2017; Pham et al., 2019; Wang et al., 2019). However, the disease control and management of these fungi is still poorly understood.

Many fungicides, like carbendazim, benomyl, and captafol, have been used to control the extent and severity of the disease in nurseries (Mohanan, 2014). However, such fungicides can have negative impacts on people's health and the surrounding environment (Rouabhi, 2010). Recently, biological control has been used instead of chemical control for disease management. Biocontrol agents have been used to control this disease which is plaguing *Eucalyptus* plantations, especially by *Cylindrocladium* spp., in which *Trichoderma hazianum* can be used as a biocontrol agent to inhibit the growth of *C. quinqueseptatum*, which is responsible for the damping-off disease (Mohanan, 2007). The rhizobacterium *Pseudomonas fulva* has been effective in inhibiting the growth of *C. candelabrum* while promoting rooting and growth of *Eucalyptus* (Mafia et al., 2009). Moreover, *Streptomyces ramulosus* has been considered as a potential biocontrol agent in controlling *Eucalyptus* leaf and shoot blight caused by *Cylindrocladium* sp. (Himaman et al., 2016).

Essential oils, like *Cinnamomum verum*, *Curcuma longa*, *Cymbopogon martini*, *Pimpinella anisum*, *Vetiveria zizanioides*, and *Acorus calamus*, are plant extracts, and can be another form of biological agents effective against fungi causing such diseases (Bansod and Rai, 2008; Sharma et al., 2009). Tabassum and Vidyasagar (2013) and Uma et al. (2017) reported that essential oils have a comparable efficiency to fungicides but have no side effects on the users. *Acorus calamus* (Acoraceae), commonly known as sweet flag, is a semi-aquatic plant. It is a perennial monocot with a creeping and highly branched aromatic rhizome (Kamil et al., 2017). The rhizome of *A. calamus* and its essential oils are widely use in the flavoring industry. In addition, it was found that the essential oils extracted from *A. calamus* are efficient in combating many plant fungal pathogens such as *Curvularia lunata*, *Rhizoctonia bataticola*, *Sclerotium roftsii*, and *Uromyces* spp. (Radušienė and Pečiulytė, 2008; Sharma et al., 2009; Kithan and Daiho, 2014; Rita et al., 2017; Roy and Yonzune, 2018). The essential oil extracted from the rhizome of *A. calamus* contains β-asarone and α-asarone, which are the dominant antimicrobial components in *A. calamus* (Phongpaichit et al., 2005; Devi and Ganjewala, 2009). However, the knowledge about the antifungal activity of *A. calamus* against *C. reteaudii* is still limited. Moreover, most of previous studies have reported on the efficacy under laboratory conditions. Therefore, this study aimed to evaluate the efficiency of essential oils extracted from the rhizome of *A. calamus* to inhibit the growth of *C. reteaudii*, when used in both the *in vitro* and *in vivo* techniques. This study also compared the physiological effects of using rhizome extracted essential oils with an efficient and widely used commercial fungicide to the *Eucalyptus*.

2. METHODOLOGY

2.1 Essential oil extraction

One year old rhizomes of *A. calamus* were collected from the Bang Bua Thong District, Nonthaburi Province, central Thailand (13°58'22.8"N 100°22'10.2"E). They were air dried to a constant weight. The dried rhizomes were then extracted for their essential oils through hydro-distillation for 3 h. The distillated oils were dried by adding anhydrous sodium sulfate to remove water and kept in sealed glass tubes at 4°C. Finally, the essential oils were obtained at a concentration between 3.67-5.00 (%v/w).

2.2 Fungal isolation and the preparation of fungal pure culture

Eucalyptus leaf samples, affected by blight disease, were collected at the nursery managed by the Siam forestry Co. Ltd, Kanchanaburi Province, western Thailand (14°15'25.9"N 99°44'56.0"E). *C. reteaudii* was isolated by using the tissue transplanting method on Potato Dextrose Agar (PDA) media and sub cultured on PDA to obtain a pure culture. They were then identified at the species level according to the procedure outlined in Crous (2002). Additionally, the pure culture of *C. reteaudii* was checked for its pathogenicity according to Koch's postulates.

2.3 *In vitro* antifungal activity of the essential oils

The efficiency of *A. calamus* essential oil in inhibiting the growth of *C. reteaudii* was examined by the poisoned food technique (Sharma et al., 2009). Cultured media were prepared by dissolving *A. calamus* essential oil in a 2% dimethyl sulfoxide

(DMSO) solution. Different concentrations of essential oil were used, viz. 31.25, 62.5, 125, 250, 500, 1,000, and 2,000 parts per million (ppm). PDA medium and 2% DMSO incorporated PDA medium were used as control treatments. Mycelium plugs having 8 mm diameter were obtained from four day old cultures and were placed at the center of the plate. Five replications were maintained for each simulation. The cultures were incubated at room temperature (30±2°C). When the *C. reteaudii* colony on control treatments (only PDA and 2% DMSO) grew to the size of a Petri-dish, the colony diameter was measured and the percent inhibition was calculated according to the formula:

$$\% \text{ Inhibition} = [(A - B) / A] \times 100$$

Where; A is the growth of colony fungus (cm) in the PDA medium and B is the growth of the colony fungus (cm) in treatment media.

The percent inhibition was compared by a one-way ANOVA and the means were compared using the Duncan's new multiple range test (DMRT) at a confidence level of 95%.

2.4 *In vivo* antifungal activity of the essential oils

2.4.1 Plant material

Shoots of *Eucalyptus* hybrid clone H4 (*Eucalyptus camaldulensis* x *E. urophylla*), of 10 cm length, were cut and shoots with two mature leaves, leaf and branch skin, without any lesions caused by diseases and insects, were selected. The bottom 1 cm of the selected shoots was cut and dipped in 500 ppm of Indole-3-butyric acid (IBA) and talcum powder. Each shoot was then placed in a seedling pot containing sterilized coconut fiber and osmocote fertilizer. The seedling pots were placed in the nursery and a constant humidity (air humidity about 80-90%) was maintained by spraying water three times a day until the *Eucalyptus* cuttings were two months old. Subsequently, the antifungal activity of the derived essential oils was examined.

2.4.2 Experimental design and data measurement

The experimental setup was a completely randomized design (CRD) consisting of eight treatments: sterile water, 2% DMSO, Captan® 1,000 ppm (fungicide) and essential oil at 50 ppm, 500 ppm, 1,000 ppm, 1,500 ppm, 2,000 ppm. Three replicates were used for each treatment.

Before the experiment was conducted, each simulation was covered with a polypropylene bag to protect any cross-contamination from other replicates. In each seedling, photos of *Eucalyptus* leaves were taken by a digital camera (Cannon EOS 5D Mark III) and the leaf surface area was determined by the Image J software (Aboukarima et al., 2017). Ten mL of *C. reteaudii* spore suspension (5×10^5 spore/mL) was then sprayed onto the seedling. After an incubation time of 24 h, each treatment was sprayed with 30 mL of different solutions according to the experimental design at 7 p.m. and was sprayed every 3 days and continuously sprayed 3 times. The total duration was 11 days since the spore suspension of *C. reteaudii* was sprayed. After the last spray, the leaf surface area of the *Eucalyptus* seedling was measured again and the disease ratio calculated as per the formula below:

$$\text{Disease ratio} = \text{diseased leaf area / total leaf area } (cm^2)$$

Finally, the disease ratio determined during each treatment was analyzed by One-way ANOVA and means were compared by DMRT at a significance level of 95%.

2.5 Physiological and anatomical characteristics of *Eucalyptus* seedlings

The transpiration rate and mean leaf surface temperature of the *Eucalyptus* seedlings were investigated to check for the antifungal activity after the application of essential oils. To measure the transpiration rate, water was added to each potted seedling until saturation was reached and was then wrapped with polythene. Pots containing seedlings were weighed at 6.00 a.m. and 6.00 p.m. After determining the loss in weight, an amount equal to the water used during the day was added. The transpiration rate was calculated following the formula below:

$$\text{Transpiration rate} = (Ws - Wd) / LSA,$$

Where; Ws is the weight of the pots at 6.00 a.m., Wd is weight of the pots at 6.00 p.m. and LSA is leaf surface area. To determine the average leaf temperature, three leaves were randomly selected to measure the temperature by using a Testo 830-T1 infrared thermometer at 6:00 a.m., 9:00 a.m., noon (12:00), 3:00 p.m., and 6:00 p.m. Individual leaf temperatures measured each day were used to obtain an averaged leaf temperature. All the data were

analyzed by a One-way ANOVA and the means were compared using DMRT at a significance level of 95%.

2.6 Anatomical investigation of leaf characters

The effect of essential oils on the anatomy of *Eucalyptus* leaf was also conducted. Three leaf specimens of each treatment were randomly selected from three treatment groups, i.e., sterile water, 500 ppm, and 2,000 ppm. Thus, nine leave were prepared in total. The cross section of leaves was prepared by using a freezing microtome. The thin cross-section leaf was selected under stereo microscope (Zeiss Stemi 508) for preparing the semi-permanent slide. The observation of leaf anatomical characteristic was done under the compound microscope (Zeiss Axioskop 40).

3. RESULTS

3.1 *In vitro* antifungal activity of the essential oils

All concentrations of essential oils derived from *A. calamus* were able to inhibit the growth of *C. reteaudii in vitro* (Table 1). When the concentration of essential oil was high, the percentage of growth inhibition increased (Table 1). However, at 2,000 ppm, the growth of *C. reteaudii* was completely inhibited with the corresponding IC_{50} value (50% inhibition concentration) being 54.76 ppm.

Table 1. Percentage growth inhibition of *C. reteaudii* and 50% inhibition concentration (IC_{50}) by *A. calamus* essential oils at various concentrations

Treatment		Percentage of growth inhibition (mean±SD)
A. calamus essential oil	31.25 ppm	36.44^{g}±2.14
	62.50 ppm	50.22^{f}±0.50
	125 ppm	52.22^{e}±0.79
	250 ppm	56.00^{d}±2.02
	500 ppm	76.56^{c}±3.25
	1,000 ppm	79.22^{b}±1.01
	2,000 ppm	100.00^{a}±0.00
Control	Only PDA	0.00^{h}±0.00
	2% DMSO	0.00^{h}±0.00
IC_{50} (ppm)		54.76

Note: SD=standard deviation; means in the column with similar letters are not statistically significant from each other at p>0.05.

Figure 1. *In vivo* evaluation of the essential oil extracted from *A. calamus* rhizomes against *C. reteaudii*, *Eucalyptus* leaf and shoot blight pathogen. (A=sterile water, B=2% DMSO, C=50 ppm, D=500 ppm, E=1,000 ppm, F=1,500 ppm, G=2,000 ppm, H=Captan® 1,000 ppm)

3.2 *In vivo* antifungal activity of the essential oils

The disease ratio was significantly different among treatments (p<0.05, Table 2). Spraying essential oil at 500 ppm was not significantly different in inhibiting the growth of *C. reteaudii* when compared to spraying Captan® at 1,000 ppm. These two treatments had a leaf disease ratio which was less than the control treatments. In addition, the results showed that spraying the essential oil at a concentration of 1,500 and 2,000 ppm increased the *C. reteaudii* diseases in the *Eucalyptus* seedlings, with a disease ratio 0.40 and 0.41, respectively (Figure 1).

Table 2. Disease ratio of *Eucalyptus* seedlings of various concentrations of essential oil

Treatments		Disease ratio (mean±SD)
A. calamus essential oils	50 ppm	0.24^{b}±0.01
	500 ppm	0.11^{a}±0.06
	1,000 ppm	0.25^{b}±0.07
	1,500 ppm	0.40^{c}±0.01
	2,000 ppm	0.41^{c}±0.01
Chemical	Captan® 1,000 ppm	0.11^{a}±0.02
Control	Sterile water	0.22^{b}±0.01
	2% DMSO	0.26^{b}±0.09

Note: SD=standard deviation; means in the column with similar letters are not statistically significant from each other at p>0.05.

3.3 Effect of *A. calamus* essential oil on the physiological and anatomical characteristics of *Eucalyptus* seedlings

The results indicated that the transpiration rate per leaf surface area and the mean leaf temperature were not significantly different across treatments (p>0.05, Table 3). Although spraying essential oil at a concentration of 1,000 and 1,500 ppm resulted in increasing the disease ratio, the two concentrations had no effect on the transpiration rates and leaf temperatures of the seedlings. Our results showed that spraying the essential oil at a concentration of 2,000 ppm affected the structure of mesophyll layer. The cellular shrinkage in the mesophyll layer of the leaf had lost the intercellular space (Figure 2).

Table 3. Comparison the transpiration rate and leaf daily temperature of *Eucalyptus* seedlings between before and after the application in different treatments

Treatments		Transpiration rate (mg/cm^2)		Leave daily temperature (ºC)	
		Before	After	Before	After
A. calamus essential oil	50 ppm	55.57	26.13	27.47	28.80
	500 ppm	56.13	27.65	27.54	28.51
	1,000 ppm	58.87	36.26	27.53	28.85
	1,500 ppm	48.76	33.17	27.62	28.35
	2,000 ppm	53.71	33.16	27.48	28.59
Chemical	Captan® 1,000 ppm	50.81	27.60	27.71	28.47
Control	Sterile water	59.98	28.64	27.51	28.65
	2% DMSO	51.22	24.09	27.70	28.27
		ns	ns	ns	ns

Note: Means (n=3) in column are not statistically significant at p>0.05.

4. DISCUSSION

Cylindrocladium (=*Calonectria*) is one of the most severe leaf and shoot blight pathogens affecting *Eucalyptus* trees in South and Southeast Asia (Kang et al., 2001; Crous, 2002; Old et al., 2003; Lombard et al., 2010a). Owing to suitable environmental conditions, several new *Cylindrocladium* taxa were reported in these regions (Liu and Chen, 2017; Pham et al., 2019; Wang et al., 2019). Moreover, these fungi have a wide range of hosts, including agricultural and forest plants. Consequently, disease control of these fungi becomes even more difficult. With regards to *C. reteaudii*, it is one of the most virulent fungal diseases affecting *Eucalyptus* trees (Pongpanich et al., 2010; Devi, 2011; Filho et al., 2018). However, disease management of this pathogen is still poorly understood, particularly after the application of biological agents. Several previous studies have indicated that the essential oils of *A. calamus* are effective in inhibiting fungal pathogens, both in humans and plants (Radušienė and Pečiulytė, 2008; Sharma et al., 2009; Yami and Shukla, 2016; Rita et al., 2017). Accordingly, our results indicated that *A. calamus* essential oil inhibited the growth of *C. reteaudii*, which causes leaf and shoot blight in *Eucalyptus*. This study is the first of its kind to report the growth inhibition of *C. reteaudii* using essential oils of *A. calamus*, as indicated by a IC_{50} value of 54.76 ppm. Phongpaichit et al. (2005) previously found that hyphae and conidia shrank and collapsed when treated with the levels of β-asarone from *A. calamus* extracts. Essential oils have a highly complex chemical composition with apparently different mechanisms to inhibit fungal growth.

Generally, the inhibitory activity of *A. calamus* extract against several fungal pathogens in laboratory bioassays have been reported previously (Kithan and Daiho, 2014; Rita et al., 2017; Roy and Yonzune, 2018). Contrastingly, the inhibitory activity in nursery bioassay (*in vivo*), where environmental conditions

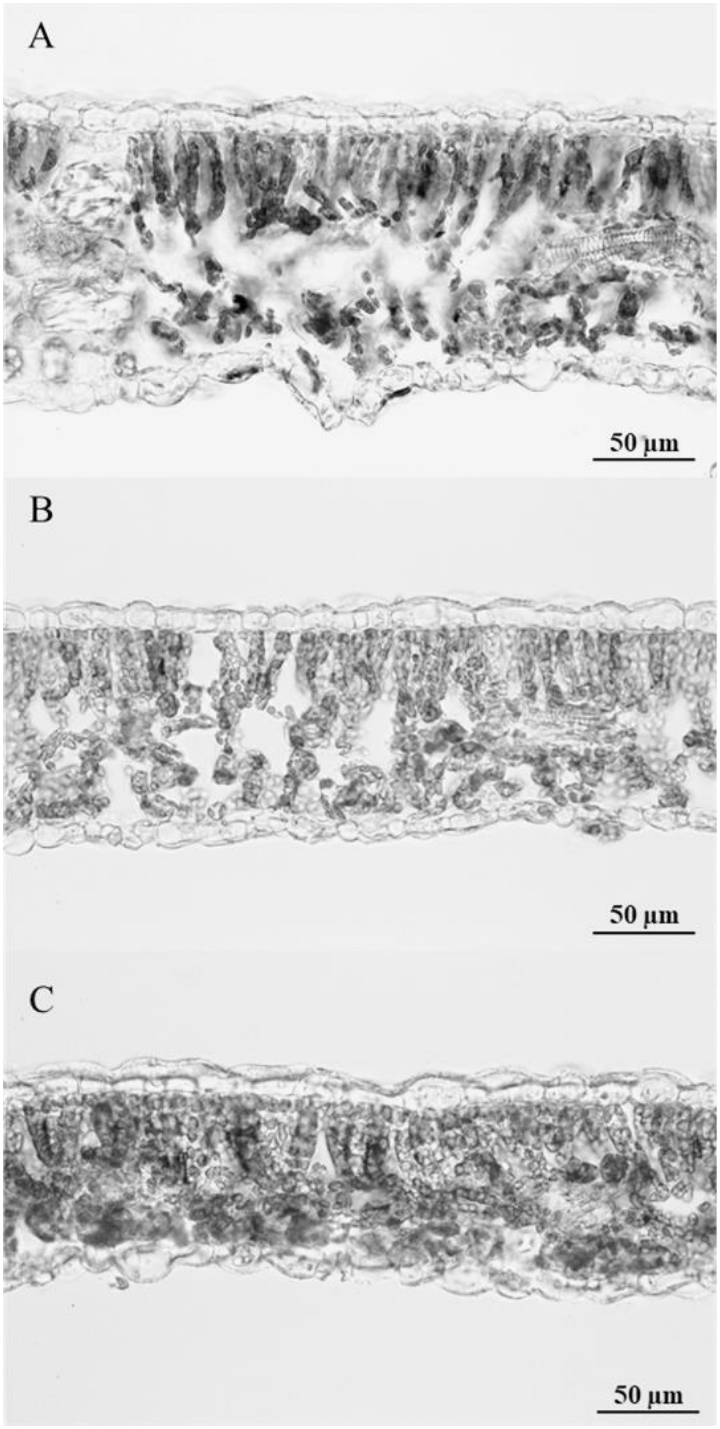

Figure 2. Cross section of *Eucalyptus* leaf under different treatments (A=sterile water, B=essential oil at 500 ppm, and C=essential oil at 2,000 ppm).

are controlled, is still limited. This study firstly concluded that a concentration of 500 ppm essential oil, obtained from *A. calamus* rhizomes, is efficient in inhibiting the leaf blight disease caused by *C. reteaudii* in *Eucalyptus* seedlings. Moreover, this concentration of essential oils was found as effective as double the concentration of Captan® (1,000 ppm) and can be used as an alternative to it. Captan® is one of the most efficient fungicides and is widely used for controlling *Eucalyptus* diseases in commercial nurseries, especially in Thailand. However, Captan® has many ill-effects on human health and the environment (Gordon, 2010; Rouabhi, 2010). Therefore, the essential oil of *A. calamus* extract can be used as an alternative to control the disease in *Eucalyptus* seedlings without compromising the safety of humans and the environment. Furthermore, the pathogens find it hard to build sufficient resistance

against essential oils, and thus it has a potential as an environmentally friendly biofungicide (Derbalah et al., 2012).

Several beneficial activities of essential oils from plant extract have been reported, with the potential in controlling various fungal disease species being one of the most intensively published in literature. However, there are few studies focusing on toxicity of the essential oil on the plant, particularly from the *A. calamus* essential oil. According to previous reports, the transpiration rate and photosynthesis of plants is affected when essential oils are applied (Baker, 1970; Frender, 2017). Our results indicated that the seedlings had a high disease ratio after the application of essential oils at concentrations above 1,500 ppm. Moreover, we found that the mesophyll layer of *Eucalyptus* leaves was collapsed in intercellular spaces (Figure 2), which is an important structure for exchanging gases during photosynthesis, and respiration of the plant. Furthermore, the essential oils can cause electrolyte leakage, which can disrupt the cell membrane and result in loss of integrity (Kaur et al., 2010; Poonpaiboonpipat et al., 2013). Baker (1970) reported that plant processes, including photosynthesis, respiration, and transpiration, are disturbed when high concentrations of oils are applied. Therefore, our results indicated that the seedlings might be susceptible to fungal infections causing diseases when applying high concentrations of the essential oil. Moreover, burnt leaf and twig of *Eucalyptus* seedlings was observed 24 h after the foliage was sprayed with *A. calamus* essential oil at a concentration >2,000 ppm (data not published). The essential oils from some plant species have phytotoxicity, which can effect germination and growth of several monocots and dicots (Poonpaiboonpipat et al., 2013; Ibáñez and Blázquez, 2018; Yoshida et al., 2018; Smeriglio et al., 2019). The essential oil of *A. calamus* has been previously shown to inhibit seed germination and growth of seedlings of *Lactuca sativa* and *Lolium perenne* (Satyal et al., 2013). These previous works, however, did not provide information regarding susceptibility to plant disease.

This study indicates the potential use of essential oil from rhizome of *A. calamus* as an effective biocontrol agent, showing strong inhibitory effects on the growth of *C. reteaudii* both in laboratory and nursery bioassays. In laboratory bioassay, the recommended concentration of the *A. calamus* essential oil was 2,000 ppm for inhibiting growth of *C. reteaudii in vitro*. While, 500 ppm of the *A. calamus* essential oil was recommended to control the leaf blight disease caused by *C. reteaudii* in *Eucalyptus* seedlings, the essential oil should be used at recommended concentration every three days and continuously sprayed three times. However, the optimum concentration of essential oil should be determined carefully as a high concentration (more than 1,500 ppm) might damage the leaves making them more prone to the fungal disease. This finding warrants further research on the fungicidal effects of *A. calamus* against other *Cylindrocladium* species and phytotoxicity of the essential oil from *A. calamus* on the growth and physiological process of *Eucalyptus*.

5. CONCLUSION

The potential of *A. calamus* essential oil as a biocontrol agent was conducted both in laboratory and nursery conditions. Our results confirmed the fungicidal effects of *A. calamus* prevent *C. reteaudii* from causing leaf and shoot blight in *Eucalyptus.* However, an essential oil concentration of 500 ppm applied every three days and continuously sprayed three times is recommended to control the growth of *C. reteaudii* under nursery conditions. Contrastingly, more than 1,500 ppm of essential oil could damage the seedlings increasing disease incidence.

ACKNOWLEDGEMENTS

This work was funded by the National Research Council of Thailand (Year 2018). A young researcher scholarship for graduate student was awarded to the first author. We would like to sincerely thank the Siam forestry Co. Ltd, Kanchanaburi Province, western Thailand for all the kind support. We thank the two referees for their invaluable comments and suggestions which helped in improving our manuscript substantially. The manuscript has been thoroughly reviewed with the kind help of Dr. Tushar Andriyas, Center for Material Sciences, Institute of Interdisciplinary Studies, and University of Allahabad, India.

REFERENCES

Aboukarima AM, Zayed MF, Minyawi M, Elsoury HA, Tarabye HHH. Image analysis-based system for estimating cotton leaf area. Asian Research Journal of Agriculture 2017;5(1):1-8.

Alfenas RF, Lombard L, Pereira OL, Alfenas AC, Crous PW. Diversity and potential impact of *Calonectria* species in *Eucalyptus* plantations in Brazil. Studies in Mycology 2015;80:89-130.

Baker JM. The effects of oils on plants. Environmental Pollution 1970;1:27-44.

Bansod S, Rai M. Antifungal activity of essential oils from indian medicinal plants against human pathogenic *Aspergillus fumigatus* and *A. niger*. World Journal of Medical Sciences 2008;3(2):81-8.

Crous PW. Taxonomy and Pathology of *Cylindrocladium* (*Calonectria*) and Allied Genera. St. Paul, USA: American Phytopathological Society Press; 2002.

Derbalah AS, Derwir YH, El-Sayed AENB. Antifungal activity of some plant extracts against sugar beet damping-off caused by *Sclerotium rolfsii*. Annals of Microbiology 2012;62:1021-9.

Devi S. *Cylindrocladium quinqueseptatum* leaf and twig blight disease of *Eucalyptus* species. International Referred Research Journal 2011;2:49-51.

Food and Agriculture Organization (FAO). Global forest resources assessment 2015 [Internet]. 2016 [cited 2020 Apr 10]. Available from: https://www.fao.org/resources/infographics/infographics-details/en/c/325836/.

Frender K. The relationship between leaf surface temperature and lighting spectrum [Internet]. 2017 [cited 2019 Dec 1]. Available from: https://www.maximumyield.com/the-relationship-between-leaf-surface-temperature-and-lighting-spectrum/2/3226.

Filho MRC, Martins I, Peixoto GHS, Muniz PHPC, Carvalho DDC, Mello SCM. Biological control of leaf spot and growth promotion of Eucalyptus plants by *Trichoderma* spp. Journal of Agricultural Science 2018;10(9):459-67.

Gordon EB. Captan and folpet. In: Krieger RI, editor. Hayes' Handbook of Pesticide Toxicology. 3rd ed. USA: Elsevier; 2010. p. 1711-42.

Harwood CE, Nambiar EKS. Productivity of acacia and eucalypt plantations in Southeast Asia. 2. trends and variations. International Forestry Review 2014;16(2):249-59.

Himaman W, Thamchaipenet A, Pathom-aree W, Duangmal K. Actinomycetes from *Eucalyptus* and their biological activities for controlling *Eucalyptus* leaf and shoot blight. Microbiological Research 2016;188:42-52.

Ibáñez MD, Blázquez MA. Phytotoxicity of essential oils on selected weeds: Potential hazard on food cops. Plants 2018; 7(79):1-15.

Kang JC, Crous PW, Old KM, Dudzinski MJ. Non-conspecificity of *Cylindrocladium quinqueseptatum* and *Calonectria quinqueseptata* based on a β-tubulin gene phylogeny and morphology. Canadian Journal of Botany 2001;79:1241-7.

Kamil SS, Hameed IH, Hamza LF. *Acorus calamus*: Parts used, insecticidal, anti-fungal, antitumour and anti-inflammatory activity: A review. International Journal of Pharmaceutical Quality Assurance 2017;8(3):153-7.

Kithan C, Daiho L. *In Vitro* evaluation of botanicals, bio-Agents and fungicides against leaf blight of *Etlingera linguiformis* caused by *Curvularia lunata* var. *aeria*. Journal of Plant Pathology and Microbiology 2014;5(3):1-6.

Kaur S, Singh HP, Mittal S, Batish DR, Kohli RK. Phytotoxic effects of volatile oil from *Artemisia scoparia* against weeds and its possible use as a bioherbicide. Industrial Crops and Products 2010;32:54-61.

Liu QL, Chen SF. Two novel species of *Calonectria* isolated from soil in a natural forest in China. MycoKeys 2017;26:25-60.

Lombard L, Crous PW, Wingfield BD, Wingfield MJ. Species concepts in *Calonectria* (*Cylindrocladium*). Studies in Mycology 2010a;66:1-14.

Lombard L, Zhou XD, Crous PW, Wingfield BD, Wingfield MJ. *Calonectria* species associated with cutting rot of *Eucalyptus*. Persoonia 2010b;24:1-11.

Lombard L, Chen SF, Mou X, Zhou XD, Crous PW, Wingfield MJ. New species, hyperdiversity and potential importance of *Calonectria* spp. from *Eucalyptus* in South China. Studies in Mycology 2015;80:151-88.

Lombard L, Wingfield MJ, Alfenas AC, Crous PW. The forgotten *Calonectria* collection: Pouring old wine into new bags. Studies in Mycology 2016;85:159-98.

Mafia RG, Alfenas AC, Maffia LA, Ferreira EM, Binoti DHB, Mafia GMV. Plant growth promoting rhizobacteria as agents in the biocontrol of eucalyptus mini-cutting rot. Tropical Plant Pathology 2009;34(1):10-7.

Manavakun N. Harvesting Operations in Eucalyptus Plantations in Thailand [dissertation]. Helsinki, University of Helsinki; 2014.

Mohanan C. Biological control of seedling disease in forest nurseries in Kerala. Journal of Biological Control 2007; 21(2):189-95.

Mohanan C. Diseases in Eucalypts: status and management. In: Bhojvaid PP, editor. Eucalypts in India. India: ENVIS Centre on Forestry, National Forest Library and Information Centre, Forest Research Institute; 2014. p. 281-314.

Old KM, Wingfield MJ, Yuan ZQ. A Manual of Diseases of Eucalypts in South-East Asia. Jakarta, Indonesia: Center for International Forestry Research; 2003.

Pham NQ, Barnes I, Chen S, Liu F, Dang QN, Pham TQ, et al. Ten new species of *Calonectria* from Indonesia and Vietnam. Mycologia 2019;111(1):1-25.

Pongpanich K. Diseases of Eucalyptus in Thailand and Options for Reducing their Impact. Proceedings of the IUFRO/FAO Workshop on "Pests Management in Tropical Forest Plantations"; 1998 May 25-29; Chanthaburi: Thailand; 1998.

Pongpanich K, Ayawong C, Himaman W, Duengkae K, Sakolrak B. Eucalyptus Disease in Thailand. Bangkok, Thailand: The Agricultural Cooperative Federation of Thailand; 2010.

Poonpaiboonpipat T, Pangnakorn U, Suvunnamek U, Teerarak M, Charoenying P, Laosinwattana C. Phytotoxic effects of essential oil from *Cymbopogon citratus* and its physiological mechanisms on barnyardgrass (*Echinochloa crus-galli*). Industrial Crops and Products 2013;41:403-7.

Phongpaichit S, Pujenjob N, Rukachaisirikul V, Ongsakul M. Antimicrobial activities of the crude methanol extract of *Acorus calamus* Linn. Songklanakarin Journal of Science and Technology 2005;27(2):517-23.

Radušienė J, Pečiulytė D. Volatile Constituents of *Acorus calamus* and their antimicrobial activity. Acta Horticulturae 2008; 765:35-42.

Rita WS, Kawuri R, Swantara IMD. The essential oil contents of Jeringau (*Acorus calamus* L.) Rhizomes and their antifungal activity against *Candida albicans*. Journal of Health Sciences and Medicine 2017;1(1):33-8.

Rodas CA, Lombard L, Gryzenhoinf M, Slippers B, Wingfield MJ. *Cylindrocladium* blight of *Eucalyptus grandis* in Colombia. Australasian Plant Pathology 2005;34:143-9.

Rouabhi R. Introduction and toxicology of fungicides. In: Carisse O, editor. Fungicides. London, UK: Intech Open; 2010. p 363-82.

Roy S, Yonzone R. Effect of abiotic factors on the incidence of rust disease in *Acorus calamus* L. under Terai zone of west Bengal, India. International Journal of Current Microbiology and Applied Sciences 2018;7(1):1194-200.

Satyal P, Paudela P, Poudelb A, Dosokyc NS, Moriarityc DM, Voglera B, et al. Chemical compositions, phytotoxicity, and biological activities of *Acorus calamus* essential oils from Nepal. Natural Product Communications 2013;8(8):1179-81.

Sharma PK, Raina AP, Dureja P. Evaluation of the antifungal and phytotoxic effects of various essential oils against *Sclerotium rolfsii* (Sacc) and *Rhizoctonia bataticola* (Taub). Journal Archives of Phytopathology and Plant Protection 2009; 42(1):65-72.

Smeriglio A, Trombetta D, Cornara L, Valussi M, Feo V, Caputo L. Characterization and phytotoxicity assessment of essential oils from plant byproducts. Molecules 2019;24:1-16.

Tabassum N, Vidyasagar GM. Antifungal investigations on plant essential oils: A review. International Journal of Pharmacy and Pharmaceutical Sciences 2013;5(2):19-28.

Thu PQ, Griffiths M, Pegg G, McDonald J, Wylie R, King J, et al. Healthy plantations: A field guide to pests and pathogens of *Acacia*, *Eucalyptus* and *Pinus* in Vietnam. Queensland, Australia: Department of Employment, Economic Development and Innovation; 2010.

Uma K, Xin H, Kumar BA. Antifungal effect of plant extract and essential oil. Chinese Journal of Integrative Medicine 2017;23(3):233-9.

Wang Q, Liu Q, Chen S. Novel species of *Calonectria* isolated from soil near *Eucalyptus* plantations in southern China. Mycologia 2019;111(6):1028-40.

Yami H, Shukla AK. Antifungal activity of essential oils derived from some plants against phytopathogenic fungi. Annals of Plant Sciences 2016;5(7):1374-80.

Yoshida NC, Saffran FP, Lima WG, Freire TV, Siqueira JM, Garcez WS. Chemical characterization and bioherbicidal potential of the essential oil from the leaves of *Unonopsis guatterioides* (A.DC.) R.E.Fr. (Annonaceae). Natural Product Research 2018;33:3312-6.

Zhou XD, Xie YJ, Chen SF, Wingfield MJ. Diseases of eucalypt plantations in China: Challenges and opportunities. Fungal Diversity 2008;32:1-7.

Potential of Passive Sampling and Plant Absorption to Quantify Inhalation Exposure to Volatile Organic Compounds

Veerapas Na Roi-et[1] and Supawat Chaikasem[2*]

[1]Faculty of Public Health, Thammasat University, Hangchat, Lampang 52190, Thailand
[2]Faculty of International Maritime Studies, Kasetsart University, Sri Racha, Chonburi 20230, Thailand

ARTICLE INFO

Received: 14 Jun 2020
Received in revised: 11 Sep 2020
Accepted: 1 Oct 2020
Published online: 6 Nov 2020
DOI: 10.32526/ennrj/19/2020110

Keywords:
Volatile organic compounds/ Passive samplers/ Inhalation exposure/ Health risk assessment/ Plant absorption

*** Corresponding author:**
E-mail: supawat.ch@ku.th

ABSTRACT

Emission of volatile organic compounds (VOCs) from photocopiers was investigated to assess the potential health impacts on inhalation exposure to VOCs. VOCs samples were collected during working hours using SKC VOCs 575 series passive sample. Twenty-one quantified VOCs were measured and analyzed by GC-MS/MS. The results showed that the total VOCs concentration emitted in the photocopy centers A and B were 2.29×10^4 and 2.32×10^4 µg/m^3, respectively. The highest detected chemical was trans-1,2-Dichloroethene at about 2.18×10^4) photocopy center A (and 2.15×10^4 µg/m^3) photocopy center B (The results reveal that the non-carcinogenic risk for inhalation exposure to m-Xylene, p-Xylene, and trans-1,2-Dichloroethene were in the range 0.94-1.53 and 1.19-1.79 and 51.54-52.23, respectively, resulting in the hazard index (HI) of non-carcinogenic VOCs in total being greater than 1.0. This indicated that the cumulative effects of inhalation exposure to VOCs at low concentrations should be of concern, even though it does not exceed the occupational exposure limits and Threshold Limit Values-Time Weighted Average for the mixtures (TLV-TWA$_{mix}$). Plants display a greener solution to reduce indoor air pollution. The bio-concentration levels of total VOCs in *Epipremnum aureum* were noted as 74.71 to 174.42, signifying that *E. aureum* is effective for removal of VOCs naturally and sustainably.

1. INTRODUCTION

Volatile organic compounds (VOCs) are a ubiquitous group of harmful air pollutants that currently are the most common air pollutants existing in both indoor and outdoor air (Ari, 2020). The regulatory definition of VOCs used by the United States Environmental Protection Agency (U.S. EPA) is any compound of carbon, excluding carbon monoxide, carbon dioxide, carbonic acid, metallic carbides or carbonates, and ammonium carbonate, which participate in atmospheric photochemical reactions (Srivastava and Majumdar, 2011). In the field of Indoor Air Quality (IAQ), U.S. EPA (2020a) clarifies that the term "volatile organic compounds" denotes any of thousands of organic (carbon-containing) chemicals that are present mostly as gases at room temperature. Inorganic carbon-containing gases such as carbon dioxide and carbon monoxide are excluded from this definition. VOCs are chemical compounds that arise by man-made or natural events. They include a very wide variety of types of molecules that can be categorized in many ways, such as by the types of chemical bonds (alkanes, alkenes, alkynes, saturated, unsaturated), by structure (e.g., straight-chained, branched, ring structures), by the function of specific parts of the molecules (e.g., aldehydes, ketones, alcohols, etc.), or by specific elements included (e.g., chlorinated hydrocarbons that contain chlorine, hydrogen, and carbon).

Hazardous air pollutants (HAPs) are air pollutants that are carcinogenic or have serious health effects, such as the cause of disability of a newborn baby or have a serious impact on the environment and ecosystem. Many VOCs are dangerous to human health (Kim et al., 2008; Na Roi-et et al., 2017) and are collectively named as hazardous VOCs. Short-term and long-term exposure to HAPs, even in low concentrations can cause harmful effects on human

Citation: Na Roi-et V, Chaikasem S. Potential of passive sampling and plant absorption to quantify inhalation exposure to volatile organic compounds. Environ. Nat. Resour. J. 2021;19(1):43-56. (https://doi.org/10.32526/ennrj/19/2020110)

health (i.e., cancerous illnesses, neurological disorders, central nervous system damage, respiratory irritation, and symptoms such as headaches, dizziness, fatigue, confusion, and nausea) (Durmusoglu et al., 2010; Na Roi-et et al., 2017; Saikomol et al., 2019; Sakai et al., 2017; Shrubsole et al., 2019; Xing et al., 2018; Zhang et al., 2019). The Clean Air Act amendments of 1990 identified 187 substances as HAPs published by the U.S. EPA for regulation of the emissions of HAPs. The important members of hazardous VOCs were benzene, dichloromethane, formaldehyde, chloroform, etc. (U.S. EPA, 2020b).

The presence of volatile organic compounds (VOCs) and the associated health risks in residential and public buildings are well reported (Delgado-Saborit et al., 2011; Hoskins, 2003; Shrubsole et al., 2019; Weschler, 2009). The Pollution Control Department (PCD) of Thailand notified the limit values of VOCs at 24 h in the atmosphere to limit harm to human health as Acetaldehyde <860 µg/m^3, Acrolein <0.55 µg/m^3, Acrolonitrile <10 µg/m^3, Benzene <7.6 µg/m^3, Benzyl chloride <12 µg/m^3, 1,3-Butadiene <5.3 µg/m^3, Bromomethane <190 µg/m^3, Carbon tetrachloride <150 µg/m^3, Chloroform <57 µg/m^3, 1,2-Dibromoethane <370 µg/m^3, 1,4-Dichloroethane <1,100 µg/m^3, 1,2-Dichloroethane <48 µg/m^3, Dichloromethane <210 µg/m^3, 1,2-Dichloropropane <82 µg/m^3, 1,4-Dioxane <860 µg/m^3, Tetrachloroethylene <400 µg/m^3, 1,1,2,2-Tetrachloroethane <83 µg/m^3, Trichloroethylene <130 µg/m^3, Vinyl chloride <20 µg/m^3 (PCD, 2009), respectively. However, VOC concentration in indoor air is generally higher than the outdoor air by about 5-10 times (Dales et al., 2008). The concentration of VOCs of benzene, toluene, m,p-xylene, and aromatic hydrocarbons have the highest indoor air pollutant concentration (Wetzel and Doucette, 2015). Although individual VOC are observed even in low concentrations, the mixture can produce additive and probably synergistic effects (Orwell et al., 2004). WHO (2013) reported that the additive effects were considered as a significant mechanism driving the health impacts from combined or multiple exposures of VOCs. In this regard, it becomes an emerging threat to human health associated with chronic exposure to multiple VOCs. There is growing concern about potentially harmful pollutants that may be released from office productivity devices. Photocopiers and laser printers are important sources of VOCs, which derive from toners and printed circuit boards during the printing process (Tang et al., 2012). The VOCs emissions from photocopiers are much higher than other office equipment (Destaillats et al., 2008). As a result, photocopiers are major sources of exposure to VOCs and can lead to potential health impacts due to their proximity.

Photocopiers and laser printers are generally used as office equipment. Exposure of VOCs released during operation and maintenance of photocopiers and laser printers have been associated with the effects on human health. Furthermore, other sources of VOCs can be plastic materials and electronic components of photocopiers and laser printers (Destaillats et al., 2008; Kowalska et al., 2015). However, some VOC species may not only be an immediate hazard but also leading to long-term effects on human health. According to this regard, it is a necessity to understand the VOC species released to find the appropriate way to control the emissions.

The monitoring techniques of VOCs are generally composed of sampling, pretreatment, separation, and detection processes. Passive sampling techniques have been successfully applied to monitor VOC concentrations due to their simplicity, low cost, compactness, light weight, portability, and easy to implement (Sakurai et al., 2013). The early applications were for examining pollution in industrial sites, but over the past several years there has been significant progress in using passive sorbent samplers for measuring VOCs at the lower concentrations needed to assess human health risk onsite. Passive samplers have been shown to yield results equivalent to other established methods for many VOCs (Cocheo et al., 2009; Healy et al., 2018). The sampling protocols are simple and have several advantages over more traditional indoor air sampling techniques, for instance, U.S. EPA Methods TO-15 and TO-17 (U.S. EPA, 2009a). Passive samplers are small and lightweight compared with the canisters used in Method TO-15, and less expensive. This method provides accurate results for a large range of sampling durations, from daily to quarterly sampling periods for certain compounds (U.S. EPA, 2012). The ability to collect time-weighted average samples over longer durations than the 8 to 96 hours offered by the more traditional methods is an advantage because these longer periods can provide data that are more representative of the long-term average. Preferably, badge type passive samplers have greater adsorption rates than tube type passive samplers due to shorter diffusion length and larger surface area (Strandberg et

al., 2005). A passive sampler is particularly employed for the determination of time- weighted average (TWA) concentrations (Novic et al., 2017).

Plants used as a tool of environmental monitoring have many advantages over other systems: they are cheap, sensitive, and easy to sample. An indoor plant is often proposed as a passive approach for indoor air pollution mitigation. The use of the indoor plant to reduce potentially harmful pollutants such as VOCs has been studied for decades (Fukushi et al., 2005; Moya et al., 2019; Orwell et al., 2004; Wolverton et al., 1989). *Epipremnum aureum* (*E. aureum*) is widely used as an indoor plant because of its air pollution removal capacity, and tolerance to heat, humidity, and pests (Fukushi et al., 2005; Na Roi-et et al., 2017; Orwell et al., 2004). It can also grow in a water-filled container without any added nutrients and soil (Meshram and Srivastava, 2015). Gong et al. (2019) evaluated the benzene removal rate of four ornamental plants, namely *Epipremnum aureum*, *Chlorophytum comosum*, *Hedera helix*, and *Echinopsis tubiflovra*, and they reported that the highest benzene removal rate was observed in *E. aureum* of about 1.10 μg/m^3 cm^2. Yang et al. (2009) investigated twenty-eight indoor plant species for their ability to remove volatile organic pollutants and found that the total VOC removal efficiency of *E. aureum* was 6.71 μg/m^3 m^2 h. In addition, *E. aureum* is a popular houseplant and native to tropical areas such as Thailand (Moya et al., 2019; Na Roi-et et al., 2017). Therefore, it was selected as a passive approach for pollutant removal of VOCs from office equipment.

To investigate the potential of using *E. aureum* to reduce VOC concentrations of indoor air pollutants, this study performed lab experiments with the aim to evaluate VOC species and concentrations released inside two different photocopy centers to further interpret the health impacts of VOCs exposure. Also, the appropriate mitigation measure to decrease potential health impacts by the use of *E. aureum* as a passive approach to remove VOCs was discussed.

2. METHODOLOGY

2.1 Determination of VOCs with a passive approach

The indoor air quality of two photocopy centers was investigated for a broad range of VOCs utilizing passive samplers and plants for four times in February, 2020. The photocopy center was located at an educational institution, which is visited by approximately 50-200 people per working day. Each photocopy center consists of three employees and four photocopiers with similar manufacturer's brands. The area of photocopy centers A and B was 9.39 m^2, 9.92 m^2, respectively. Both of them included one glass door for the entrance and four glass windows around the building to supply natural ventilation.

This study was a cross-sectional study to assess the risk of total VOC exposure. VOCs were collected using SKC passive sampling model 575, containing 350 mg of charcoal. The samples were collected during a 10 h working period from 07.30 a.m. to 05.30 p.m. using badge type passive samplers in both photocopy centers. Martin et al. (2017) reported that the workers in photocopy centers rarely spend their entire day at a single workstation, and they conduct a varying number of tasks, such as walking to and from the service counter to the copier to retrieve completed print jobs, light copier maintenance (e.g., replacing spent toner cartridges, refilling paper bins, and staples), and other tasks away from their workstation and copiers, such as document finishing (e.g., binding) and shipping. Hence, the passive samplers in our study were placed in the middle of the room at a distance of 1 m from the photocopiers which were laid out along the room walls. The passive sampler was hanging at a height of 1.5 m measured from the floor, which is the average breathing height.

The *E. aureum* or Golden Pothos were seedlings from local breeder stores. They were cultured inside compacted clean coconut husk in 10 cm diameter pots under clean conditions. At 30 days of age, a set of 25 healthy *E. aureum* with heights of 15-20 cm and average leaf areas of 2,600±141 cm^2 was used in the experiment. *E. aureum* was used as a passive approach. The absorption by plant leaf was collected from the photocopy centers A and B for 24 h. A pot of *E. aureum* was placed inside of the rooms to collected indoor air samples, with 1.5 m distance from the entrance, in a setting between the photocopiers which was least influenced by the outdoor environment, and in order not to obstruct the operation.

At each photocopy center, air samples were collected to represent the inhalation exposure from photocopiers and plant leaves were analysed to evaluate the potential of plant leaves as passive samplers for VOCs in the indoor environment. The schematic diagram of the position of *E. aureum*, photocopy machines (A and B), and passive samplers point is illustrated in Figure 1. After the end of the sampling, passive samplers and plant leaves were stored in an icebox and transferred to keep in a

refrigerator at 4°C before the extraction process. Then, the samples were examined by GC-MS/MS after the extraction process.

2.2 Samples preparation and extraction

The SKC passive samplers (SKC 575-001, Lot 2000, containing 350 mg of charcoal) were used as passive samplers for VOCs determination. VOCs adsorbed on samplers were extracted using 5 mL carbon disulfide (AR grade, 99.9% CS_2, MW.76.13, Kemaus).

E. aureum leaves without visible injury were randomly collected from the same plant using a gloved hand and ethanol-cleaned scissors. Three to five leaves were then cleaned with distilled water and dried with tissue paper. The plant leave samples were placed into a petri dish and cut into smaller pieces. The small pieces of *E. aureum* leaves were then mixed to obtain 5 g of a final leaf sample weight. Methanol is commonly used as the extraction solvent of plant samples (Atawodi et al., 2010; Chaikasem and Na Roi-et, 2020; Geethangili and Ding, 2018; Larson et al., 2014; Parekh et al., 2005). Five milliliters of methanol (HPLC grade, ≥99.9% CH_3OH, MW.32.04, Sigma-Aldrich) were gently poured over the cut leaf for VOC extraction. After standing for 30 min, the extracted samples were collected.

All extracted samples were filtered through 0.2 µm PTFE syringe filters into amber glass vials with polyspring inserts and then analyzed for VOCs determination using gas chromatograph-mass spectrometer/mass spectrometer (GC-MS/MS).

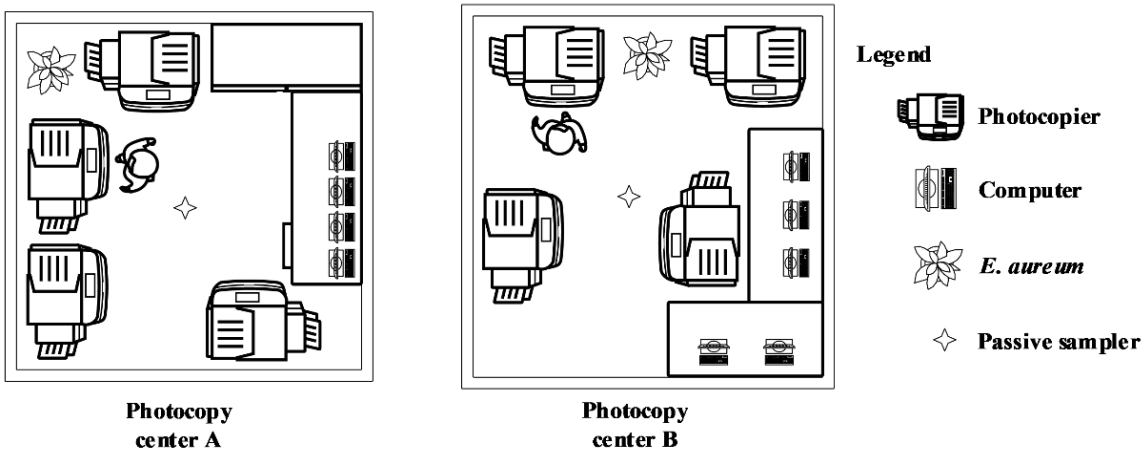

Figure 1. The schematic diagram of the position of *E. aureum* and photocopiers (A and B).

2.3 Analysis apparatus

The Thermo Scientific gas chromatography triple quadrupole mass spectrometry (TSQ 8000 Evo Triple Quadrupole GC-MS/MS, Thermo Scientific, USA) was employed for sample analysis. Analytes were separated on a DB-5MS Ultra Inert capillary gas chromatographic column (30 m × 0.25 mm × 0.25 µm), and the carrier gas was helium at a flow velocity of 1.0 mL/min. The GC-MS/MS conditions were as follows: The PTV (Programmed Temperature Vaporization) injector temperature was 290°C, the injection volume was 2 µL. The GC oven temperature was initially kept at 60°C for 0.5 min, then raised at a rate of 15°C/min to 300°C and held for 2 min.

The mass selective detector was operated using positive electron ionization (+EI) in the selected ion monitoring (SIM) mode. The collision gas (Argon) pressure was 1.5 mTorr. The value of the electron emission current was 50 µA. The ion source and transfer line temperatures were 250°C and 290°C, respectively.

The regression analysis, correlation coefficient (R^2), limit of detection (LOD), and limit of quantification (LOQ) of a calibration curve for VOCs covered the determination of 21 VOC species as presented in Table 1. A six-point calibration was carried out to quantify individual VOC species. Linear correlation between individual VOC concentrations and peak area was checked with correlation coefficients resulting from the six-point calibration curve. The correlation coefficient was greater than 0.99, indicating good linearity for the quantification of individual VOC species. The LOD and LOQ were calculated following the method described by Miller and Miller (2010).

Table 1. Regression analysis, correlation coefficient, LOD, and LOQ of calibration curves for all VOCs species

Compounds	Calibration curve	R^2	LOD (μg/m^3)	LOQ (μg/m^3)
Tetrachloroethene	Y = 356614 + 2299.35X	0.9944	0.25	0.83
Styrene	Y = 1.82362 ×10^6+15696X	0.9901	0.21	0.69
Methylene chloride	Y = 7.04441×10^6+6975.05X	0.9912	48.73	162.43
1,2-Dichloroethane	Y = 6.04807×10^7+19616.2X	0.9958	0.18	0.59
1,1,1-Trichloroethane	Y = 968965×5062.85X	0.9989	0.09	0.29
cis-1,2-Dichloroethene	Y = 6.10499×10^6+1503.48X	0.9970	0.22	0.72
trans-1,2-Dichloroethene	Y = 729647+575.304X	0.9963	0.73	2.44
Carbon tetrachloride	Y = 1.38908×10^8+15651.1X	0.9957	4.48	14.94
Toluene	Y = 1.85655×10^6+39080.9X	0.9979	70.75	235.84
Ethylbenzene	Y = 85522.1+17287.8X	0.9945	0.01	0.02
1,1-Dichloroethene	Y = 5.65658×10^6+1661.65X	0.9993	0.18	0.61
Benzo(a)pyrene	Y = 980471+11399.7X	0.9938	0.09	0.30
1,3-Dichloropropane	Y = 9.30625×10^6+1373.73X	0.9972	2.90	9.66
1,2-Dichloropropane	Y = 9.63784×10^6+1177.48X	0.9949	4.14	13.81
1,3-Dichloropropene	Y = 1.81483×10^6+4147.92X	0.9988	0.69	2.29
Vinyl chloride	Y = 1.02388×10^7+9413.95X	0.9953	2.64	8.80
Trichloroethene	Y = 1.21394×10^6+5908.96X	0.9950	0.05	0.16
Benzene	Y = 2.2215×10^6+12135.9X	0.9902	0.31	1.02
o-Xylene	Y = 126643+3414.45X	0.9961	0.11	0.38
m-Xylene	Y = 4.65885×10^6+17399X	0.9993	0.23	0.76
p-Xylene	Y = 4.65885×10^6+17399X	0.9993	0.23	0.76

2.4 Quantitative risk assessment

Before evaluating potential health impacts from inhalation exposures to VOCs, the concentration of individual VOC species was compared to occupational exposure limits. Also, VOCs are one component of air pollution containing a mixture of hundreds of carbon-containing gaseous pollutants. Therefore, the most common method for evaluating Threshold Limit Values-Time Weighted Average for mixtures (TLV-TWAmix) is to assume additive effects among the VOC mixtures. The TLV-TWA$_{mix}$ was calculated as follows (Watts, 1997):

$$\text{TLV} - \text{TWA}_{\text{mix}} = \frac{\sum_{i=1}^{n} C_i}{\sum_{i=1}^{n} \frac{C_i}{\text{TLV-TWA}}}$$

Where n is the number of VOCs; C_i is VOCs concentration, and Threshold Limit Values-Time Weighted Average (TLV-TWA) is the American Conference of Governmental Industrial Hygienists Threshold Limit Values (ACGIH TLV). The Risk Assessment Guidance for Superfund (RAGS): Part F was recommended for quantitative risk assessment to estimate the level of inhalation exposure to VOCs. Adjusted inhalation exposure to VOC concentrations (EC_i) was proposed as a continuous exposure concentration for each person to calculate health risk based on U.S. EPA guidelines. The EC_i are time-weighted average concentrations derived from measured VOC concentrations and then adjusted based on the exposure scenario characteristics being evaluated (U.S. EPA, 2009b). The EC_i was calculated in μg/m^3 as follows:

$$\text{EC}_i = \frac{c_m \times \text{ET} \times \text{EF} \times \text{ED}}{\text{AT}}$$

In this expression, C_m is the measured VOCs concentrations (μg/m^3); ET is the exposure time (10 h/day); EF is the exposure frequency (168 days/year); ED is the exposure duration (5 years); AT is the averaging time (hours). For the hazard assessments of non-carcinogenic risk and carcinogenic risk, the averaged time (ED × 365 days/year × 24 h) and expected lifetime (70 years × 365 days/year × 24 h) are substituted for AT, respectively.

The inhalation exposure to non-carcinogenic and carcinogenic VOCs has followed the conventional approaches proposed by U.S. EPA (U.S. EPA, 2009b) and previous studies (Al-Zboon and Forton, 2019; Ari et al., 2020; El-Hashemy and Ali, 2018; Kitwattanavong et al., 2013; Loonsamrong et al., 2015; Xing et al., 2018). Health risk assessment

associated with non-carcinogenic and carcinogenic risk caused by inhalation exposure to VOCs were estimated by combining EC_i with the Reference Concentration for Inhalation Exposure (RfC) and Inhalation Unit Risk (IUR) obtained from the Integrated Risk Information System (IRIS) (U.S. EPA, 2016a), Department of Toxic Substances Control (DTSC) (DTSC, 2019), Office of Environmental Health Hazard Assessment (OEHHA) (OEHHA, 2011).

Non-carcinogenic risk assessment for the mixture of VOCs species was determined as the Hazard Index (HI), which is defined as follows:

$$HI = \sum_{i=1}^{i=n} HQ_i$$

Where HI is the hazard index of multiple VOC species, which is used to estimate potential health risk. The HI was acquired from the summing of Hazard Quotient (HQ_i) for inhalation exposure to VOCs. The HQ_i can be calculated by dividing the adjusted inhalation exposure to VOCs concentrations (EC_i) by inhalation reference concentration (RfC_i) expressed in $\mu g/m^3$:

$$HQ_i = \frac{EC_i}{RfC_i}$$

The HQ_i greater than 1.0 would indicate the possibility of a non-carcinogenic effect from inhalation exposure. The HQ_i lower than 1.0 provides acceptable risk; however, the cumulative acceptable risk for each VOC species must also be less than 1.0.

Carcinogenic risk assessment was estimated using the following equation:

$$R_i = EC_i \times IUR_i$$

Where R_i is the estimated inhalation carcinogenic risk; EC_i is the adjusted inhalation exposure to VOC concentrations, and IUR_i is the inhalation unit risk ($m^3/\mu g$) of carcinogenic compounds as a result of the continuous exposure concentration to that contaminants at 1.0 $\mu g/m^3$ (assuming 70 kg body weight and inhalation rate of 20 m^3/d over 70 year lifetimes). The acceptable value of cancer risk is less than 1.0×10^{-6}. This indicates no potential carcinogenic risk resulting from exposure to carcinogenic substances. Likewise, the total risk was determined by summing individual cancer risk. The total carcinogenic risk of inhalation exposure to VOCs lower than 1.0×10^{-6} represents an acceptable level.

3. RESULTS AND DISCUSSION

3.1 VOCs concentrations

During the printing process, VOC emissions can result from heating the drum and toner to temperature levels observed inside printing equipment to compress the toner on paper. The VOC emissions by the use of printers and copiers were caused by circuit boards, toners and inks, paper, and plastic construction materials. Kowalska et al. (2015) studied the characteristic of VOCs emitted from seven office devices (office printers and copying devices) and found that all of them release VOCs with a difference in individual VOCs species and concentrations. The dominant VOC species related to the printing process were chlorinated VOCs, styrene, xylenes, ethylbenzene, acetophenone, benzaldehyde, and many other benzene derivatives (El-Hashemy and Ali, 2018; Henschel et al., 2001; Kowalska et al., 2015).

VOCs were grouped into two categories according to their chemical structure characteristics namely; non-halogenated hydrocarbons and halogenated hydrocarbons. Concentrations of halogenated hydrocarbons were the dominant components of the detected VOCs. The non-halogenated hydrocarbon and halogenated hydrocarbon concentrations were 1.11×10^3, 2.18×10^4 and 1.73×10^3, 2.15×10^4 $\mu g/m^3$ in photocopy centers A and B, respectively.

The total VOCs concentrations were 2.29×10^4 and 2.32×10^4 $\mu g/m^3$ for photocopy centers A and B, respectively. Figure 2(a), (b) illustrated the concentration distributions of detected VOC in the photocopy centers. Of these, halogenated hydrocarbons were the dominant component of detected VOCs, contributing 95.16% and 92.54% of total VOCs. Among the halogenated hydrocarbons, tran-1,2-Dichloroethene was the most prevalent VOC in emissions from printing equipment. Additionally, the highest concentrations of m-Xylene, p-Xylene, and trans-1,2-Dichloroethene observed in photocopy center A were 4.89×10^2, 6.20×10^2, and 2.18×10^4 $\mu g/m^3$, and the highest concentration of m-Xylene, p-Xylene, and trans-1,2-Dichloroethene in photocopy center B were determined as 7.97×10^2, 9.36×10^2, and 2.15×10^4 $\mu g/m^3$, respectively. The mean indoor air concentrations for the total VOCs detected at photocopy center B were greater than photocopy center A. These findings suggest that the number of works at photocopy center B was greater than A. Wang et al. (2011) proved that while the copier and laser printer are printing, there will b e an i ncrease in

the amount of m-Xylene, p-Xylene, and trans-1,2-Dichloroethene concentrations. The increase of the total VOC concentration of toner is caused by the VOCs released by the heated fuser (El-Hashemy and Ali, 2018). The highest concentration of VOC found in this study was trans-1,2-Dichloroethene, which is largely used in the industrial sector, for example as a solvent of polymer products, chemical spills, burning vinyl objects, chemicals transformations, etc. The sources of trans-1,2-Dichloroethene in photocopy centers may be released from toner, typewriter fluid, document protectors, file folders, PVC furniture, insulation of power cables, etc. (Kowalska and Gierczak, 2013).

VOCs are classified as HAPs due to their malodorous and hazardous properties (Durmusoglu et al., 2010). Exposure to HAPs can cause potential short-term and long-term adverse effects on human health. In this study, 21 species of VOCs were analyzed using GC-MS/MS. The summary lists for the 21 species of VOCs and total VOC concentrations are presented in Table 2. However, only three of the 21 total VOCs were quantified and identified because the concentrations of the remaining 18 VOCs were below LOD values.

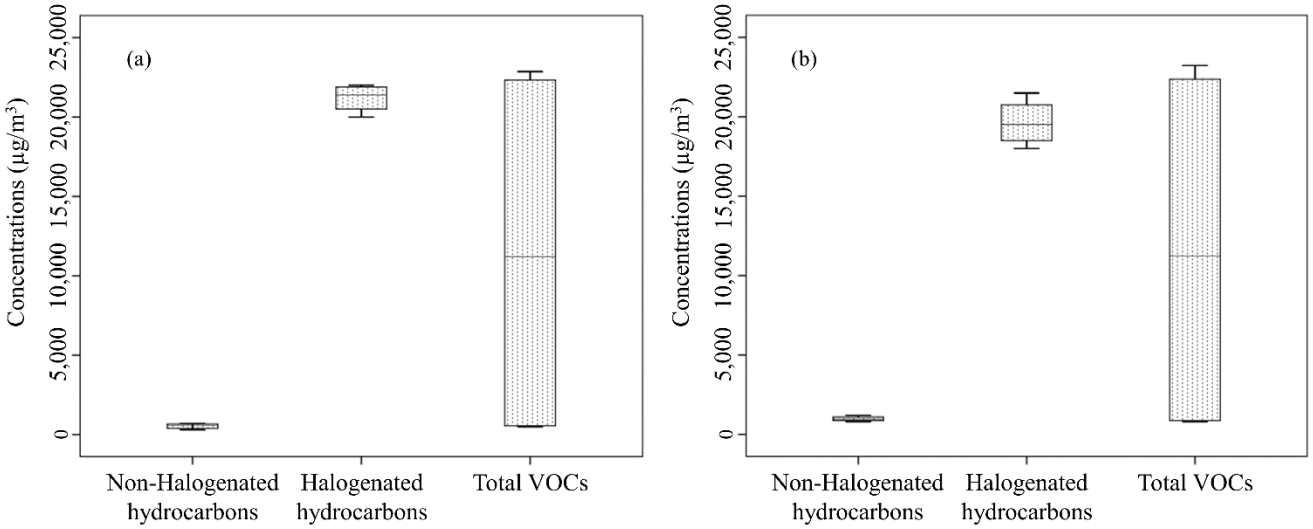

Figure 2 . The characteristics and distributions of detected VOCs groups: (a) Photocopy center A; (b) Photocopy center B.

Table 2. The summary lists for the 21 species of VOCs and total VOCs concentration

Compounds	Photocopy center (µg/m^3)		Occupational exposure limits (µg/m^3)			
	A	B	ACGIH[a] TLV	NIOSH[b] REL	OSHA[c] PEL	DLPW[d]
Non-Halogenated hydrocarbons						
Styrene	<0.21	<0.21	8.52×10^4	2.15×10^5	4.26×10^5	4.26×10^5
Toluene	<70.75	<70.75	7.54×10^4	3.75×10^5	7.54×10^5	7.54×10^5
Ethylbenzene	<0.01	<0.01	8.68×10^4	4.35×10^5	4.35×10^5	4.35×10^5
Benzo(a) pyrene	<0.09	<0.09	-	-	2.00×10^2	-
Benzene	<0.31	<0.31	1.60×10^3	3.19×10^2	3.19×10^3	3.19×10^3
o-Xylene	<0.11	<0.11	4.35×10^5	4.35×10^5	4.35×10^5	4.35×10^5
m-Xylene	<0.23-4.89×10^2	<0.23-7.97×10^2	4.35×10^5	4.35×10^5	4.35×10^5	4.35×10^5
p-Xylene	<0.23-6.20×10^2	<0.23-9.36×10^2	4.35×10^5	4.35×10^5	4.35×10^5	4.35×10^5
Halogenated hydrocarbons						
Tetrachloroethene	<0.25	<0.25	1.70×10^5	-	6.78×10^5	6.78×10^5
Methylene chloride	<48.73	<48.73	1.74×10^5	-	8.68×10^4	8.68×10^4
1,2-Dichloroethane	<0.18	<0.18	4.05×10^4	4.00×10^3	2.02×10^5	2.02×10^5
1,1,1-Trichloroethane	<0.09	<0.09	1.90×10^6	1.90×10^6	1.90×10^6	1.90×10^6
cis-1,2-Dichloroethene	<0.22	<0.22	7.90×10^5	7.90×10^5	7.90×10^5	7.90×10^5
trans-1,2-Dichloroethene	<0.73-2.18×10^4	<0.73-2.15×10^4	7.90×10^5	7.90×10^5	7.90×10^5	7.90×10^5

Table 2. The summary lists for the 21 species of VOCs and total VOCs concentration (cont.)

Compounds	Photocopy center (µg/m^3)		Occupational exposure limits (µg/m^3)			
	A	B	ACGIH[a] TLV	NIOSH[b] REL	OSHA[c] PEL	DLPW[d]
Carbon tetrachloride	<4.48	<4.48	3.15×10^4	1.26×10^4	6.29×10^4	6.29×10^4
1,1-Dichloroethene	<0.18	<0.18	1.98×10^4	-	4.0×10^3	1.98×10^4
1,3-Dichloropropane	<2.90	<2.90	-	-	-	-
1,2-Dichloropropane	<4.14	<4.14	4.62×10^4	-	3.50×10^5	-
1,3-Dichloropropene	<0.69	<0.69	4.54×10^3	5.0×10^3	-	-
Vinyl chloride	<2.64	<2.64	2.56×10^3	-	2.56×10^3	2.56×10^3
Trichloroethene	<0.05	<0.05	5.37×10^4	-	5.37×10^5	5.37×10^5
Total VOCs	2.29×10^4	2.32×10^4	-	-	-	-

Note: [a]ACGIH TLV: American Conference of Governmental Industrial Hygienists-Threshold Limit Values; [b]NIOSH REL: National Institute for Occupational Safety and Health-Recommended Exposure Limits; [c]OSHA PEL: Occupational Safety and Health Administration-Permissible Exposure Limits; [d]DLPW: Department of Labour Protection and Welfare (Source: ACGIH (2019); DLPW (2017); NIOSH (2019); OSHA (2019))

According to Table 2, the individual VOC species concentrations measured in this study were lower than the occupational exposure limits set by ACGIH (ACGIH, 2019), NIOSH (NIOSH, 2019), OSHA (OSHA, 2019), and DLPW (DLPW, 2017). Although the concentration of individual VOC species was below the limits of their respective standard of 8-hour time-weighted average (TWA), their potential health effects on workers cannot be disqualified. The major pathway of exposure from VOCs in the environment occurs by inhalation. Although the concentrations are very low (in µg/m^3 level), they are still toxic to a worker in office due to their chronic exposure to the low level of VOCs. In this regard, risk assessment was employed to evaluate the potential effects on human health of the concentrations of individual and cumulative VOC exposures via inhalation for workers.

3.2 Inhalation exposure risks to VOCs

The concentration of individual VOC species was measured in photocopy centers by passive sampling at the worker's breathing zone for the whole workday. The TLV-TWA$_{mix}$ was computed using all of the detectable VOCs: 4.89×10^2 µg/m^3 m-Xylene, 6.20×10^2 µg/m^3 p-Xylene, 2.18×10^4 µg/m^3 trans-1,2-Dichloroethene and 7.97×10^2 µg/m^3 m-Xylene, 9.36×10^2 µg/m^3 p-Xylene, 2.15×10^4 µg/m^3 trans-1,2-Dichloroethene in photocopy centers A and B, respectively. The results indicated that 7.62×10^5 and 7.47×10^5 µg/m^3 of TLV-TWA$_{mix}$ were observed in photocopy centers A and B, respectively. The inhalation exposure to total VOCs concentrations of 2.29×10^4 and 2.32×10^4 µg/m^3 is lower than TLV-TWA$_{mix}$ of 7.62×10^5 and 7.47×10^5 µg/m^3. This means that inhalation exposure to total VOC concentrations in both photocopy centers is not harmful to human health based on TLV-WA$_{mix}$. However, chronic toxicity is often incurred by long-term exposure to low concentrations of VOCs. Therefore, there is a need to investigate the effects on health by prolonged exposure to low concentrations of VOCs.

As aforementioned, the occupational exposure of VOC species concentration was present in low concentrations under the exposure limits and TLV-TWA$_{mix}$. However, VOC mixtures can produce additive effects. Therefore, there is a need to investigate the health risk assessment of inhalation exposure to VOCs. Considering the twenty one components of standards VOCs, three VOCs species were detected at both photocopy centers (m-Xylene, p-Xylene, and trans-1,2-Dichloroethene) and were used to assess the risk of inhalation exposure to VOCs. Table 3 illustrated the available toxicological data associated with target health-related VOCs used in this study and their source.

Table 3. Toxicity values associated with target health-related VOCs

Compounds	CAS Number	IARC Group	RfC (µg/m^3)		IUR (m^3/µg)	
			Values	Source	Values	Source
Tetrachloroethene	127-18-4	2A	40	IRIS	2.6×10^{-7}	IRIS
Styrene	100-42-5	2B	1,000	IRIS	-	-
Methylene chloride	75-09-2	2B	600	IRIS	1.0×10^{-6}	OEHHA

Table 3. Toxicity values associated with target health-related VOCs (cont.)

Compounds	CAS Number	IARC Group	RfC (µg/m^3)		IUR (m^3/µg)	
			Values	Source	Values	Source
1,2-Dichloroethane	107-06-2	2B	-	-	2.6×10^{-5}	IRIS
1,1,1-Trichloroethane	71-55-6	3	5,000	IRIS	-	-
cis-1,2-Dichloroethene	159-59-2	3	8	DTSC	-	-
trans-1,2-Dichloroethene	156-60-5	3	80	DTSC	-	-
Carbon tetrachloride	56-23-5	2B	100	IRIS	6.0×10^{-6}	IRIS
Toluene	108-88-3	3	5,000	IRIS	-	-
Ethylbenzene	100-41-4	2B	1,000	IRIS	2.5×10^{-6}	OEHHA
1,1-Dichloroethene	75-35-4	3	200	IRIS	-	-
Benzo(a)pyrene	50-32-8	2A	0.002	IRIS	1.1×10^{-3}	OEHHA
1,3-Dichloropropane	142-28-9	-	80	DTSC	-	-
1,2-Dichloropropane	78-87-5	1	4	IRIS	1.0×10^{-5}	OEHHA
1,3-Dichloropropene	542-75-6	2B	20	IRIS	-	-
Vinyl chloride	75-01-4	1	100	IRIS	7.8×10^{-5}	OEHHA
Trichloroethene	79-01-6	1	2	IRIS	4.1×10^{-6}	IRIS
Benzene	71-43-2	1	30	IRIS	2.2×10^{-6}	IRIS
o-Xylene	95-47-6	3	100	IRIS	-	-
m-Xylene	108-38-3	3	100	IRIS	-	-
p-Xylene	106-42-3	3	100	IRIS	-	-

Note: IARC: Group 1-Carcinogenic to humans; Group 2A-Probably carcinogenic to humans; Group 2B-Possibly carcinogenic to humans; Group 3-Not classifiable as to its carcinogenicity to humans; Group 4-Probably not carcinogenic to humans (Source: DTSC (2019); OEHHA (2009); OEHHA (2011); U.S. EPA (2016a))

The detectable VOCs with available toxicological data characterizing their risk are provided in Table 4. Only RfC values are reported, because there were no published IUR values for m-Xylene, p-Xylene, and trans-1,2-Dichloroethene. Therefore, cancer risks as a result of lifetime inhalation exposure to detected VOCs were not determined.

Table 4. The non-carcinogenic and carcinogenic risk of inhalation exposure to VOCs

Risk characterization	Compounds	Photocopy center A			Photocopy center B		
		EC (µg/m^3)	RfC (µg/m^3)	HQ	EC (µg/m^3)	RfC (µg/m^3)	HQ
Non-cancer risk	m-Xylene	9.37×10^{1}	100	0.94	1.53×10^{2}	100	1.53
	p-Xylene	1.19×10^{2}	100	1.19	1.79×10^{2}	100	1.79
	trans-1,2-Dichloroethene	4.18×10^{3}	80	52.23	4.12×10^{3}	80	51.54
Hazard Index (HI)				54.36			54.86
		EC (µg/m^3)	IUR (m^3/µg)	R ($\times10^{-6}$)	EC (µg/m^3)	IUR (m^3/µg)	R ($\times10^{-6}$)
Cancer risk	m-Xylene	6.70	-	-	1.09×10^{1}	-	-
	p-Xylene	8.49	-	-	1.28×10^{1}	-	-
	trans-1,2-Dichloroethene	2.98×10^{2}	-	-	2.94×10^{2}	-	-
Total Risk (R)				-			-

Source: DTSC (2019); OEHHA (2011); U.S. EPA (2016a)

In addition, the non-carcinogenic risk assessment of inhalation exposure to VOCs is presented in Table 4 and Figure 3(a) and (b). The results reveal that the HQ of m-Xylene, p-Xylene, and trans-1,2-Dichloroethene were 0.94, 1.19, and 52.23, respectively. Regarding the HI of total VOCs, it reached 54.36, thus exceeding the threshold (HI>1.0) in photocopy center A. Likewise, the calculated HQ of photocopy center B was 1.53, 1.79, and 51.54 for m-Xylene, p-Xylene, and trans-1,2-Dichloroethene,

respectively, resulting in the HI of total VOCs reaching 54.86, thus exceeding the acceptable value of 1.0. This indicated that the risk of non-carcinogenic effects may occur and it's probably higher as HI value increases. Figure 3(a) and (b) also shows the distribution of each HQ to HI value. The HQ to HI value of trans-1,2- Dichloroethene (96.09% and 93.94%) was the dominant contributor, followed by p-Xylene (2.19% and 3.27%), and m-Xylene (1.72% and 2.79%) in photocopy centers A and B, respectively. This finding implies that the measures to decrease the inhalation exposure to VOCs should be taken into account options such as an indoor plant for passive removal for VOCs.

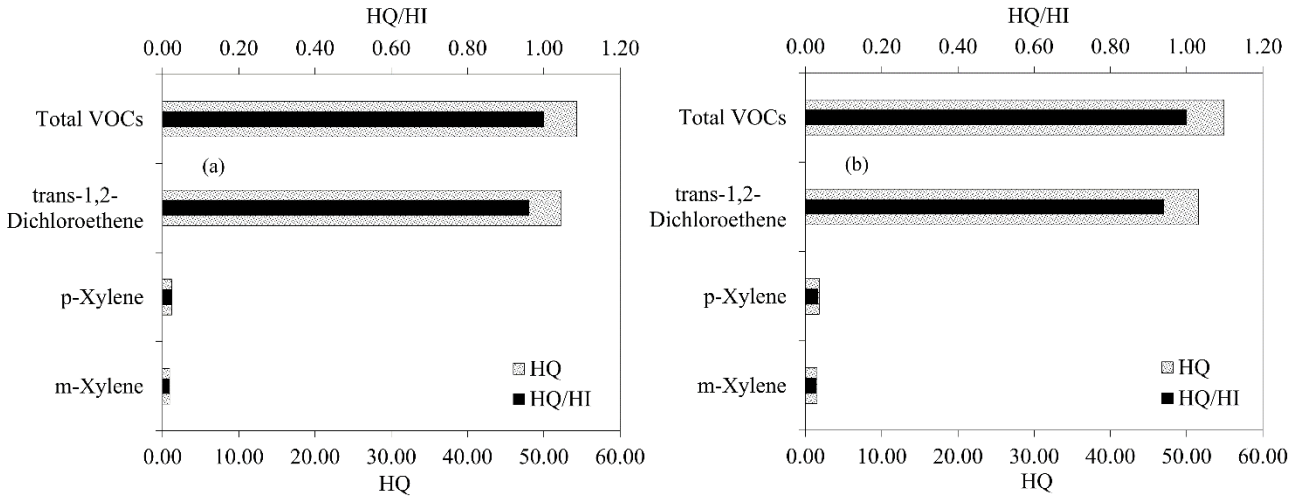

Figure 3. The distributions of non-carcinogenic risk estimates for inhalation exposure to VOCs: (a) Photocopy center A; (b) Photocopy center B.

3.3 Potential of *E. aureum* for passive removal of VOCs

The main point on phytoremediation mechanisms of air pollutions is the plant's aerial parts such as the cuticle and stomata. The most explicit route is the mechanical collection of deposits on plant parts like flowers, stems, leaves, etc. (Agarwal et al., 2019). The major absorbtion of the lipophilic semi-volatile compounds are obtained through the cuticle by leaf surface adsorption (Gawronski et al., 2017). When the volatiles are absorbed by the plant tissue within the stomatal cavity, a concentration gradient occurs and subsequently gravitates into the leaf by diffusion. *E. aureum* were studied for their possibility of absorbing VOCs during exposure for 24 h. The *E. aureum* was placed in the photocopy center to mitigate the amount of VOCs.

The results showed the differences in the absorption of individual VOC species between the tested and controlled *E. aureum*. The concentrations of chlorinated hydrocarbons as trans-1,2-Dichloroethene and Tetrachloroethene observed in photocopy center A were an average of 9.47×10^3 µg/m^3. In the photocopy center B, the average was determined as 5.07×10^3 µg/m^3. The analysis of total VOCs in leaf specimens is shown in Figure 4. At time 0 h, the result presented the plant contaminated with VOCs before the study. Meanwhile, results at 24 h show that the plants could absorb more VOCs in their leaves. According to Mishra and Pandey (2019), the bio-concentration factor (BCF) was calculated to describe the ability of plants for elemental accumulation from total VOCs using the following equation:

$$\text{BCF} = \frac{\text{Total VOCs}_{24}}{\text{Total VOCs}_{0}}$$

Where; BCF is the bio-concentration factor of total VOCs in the plant's leaves. Total VOCs_{24} represents the amount of total VOCs found in the plant's leaves at 24 h. Total VOCs_0 is the amount of total VOCs observed in the plant's leaves at 0 h. The concentrations in the plant leaves were determined on a dry-weight basis and made equivalent to volume by assuming the density as 1.0 (1 g leaves dry-weight=1 mL).

The removal of VOCs involves a combination of biotransformation and absorption mechanisms which may be achieved by different plant parts. Both the stomata and cuticles participate in the VOC removal process. Benzene penetrates more easily through the cuticle, while formaldehyde, a hydrophilic VOC, enters more easily through stomatal openings.

The ease of penetration through the stomata depends on stomatal openings and associated factors, while the molecular size of VOCs is more important in the case of entry through the cuticle (Gawronski et al., 2017; Gong et al., 2019). The bio-concentration levels of total volatile organic compounds in *E. aureum* were noted from high to low as 174.42-74.71. Their ability was detected with a relatively good correlation coefficient (R^2=0.723) that represents the relationship between the level of VOCs observed in the air and the plant's leaves. The correlation is significant at 0.01 (two-tailed). The relation showed that the types and levels of VOCs as trans-1,2-Dichloroethene detected in the passive samplers were consistent with levels discovered within the *E. aureum*. The ability of the plant to absorb VOCs is related to the exposure time.The passive sampler and plant absorption can potentially be used to monitor low concentration VOCs. When compared to other species for the bio-concentration level of m-Xylene, p-Xylene, and Tetrachloroethene, *E. aureum* had the same range of accumulation as holly or *Ilex aquifolium* (U.S. EPA, 2016b). Furthermore, the higher bio-concentration of VOCs in leaves indicate their infiltration into tissues by air pollution uptake (Agarwal et al., 2019). *E. aureum* is effective for removing VOCs, especially in indoor areas by adsorbing particulates on their leaves.

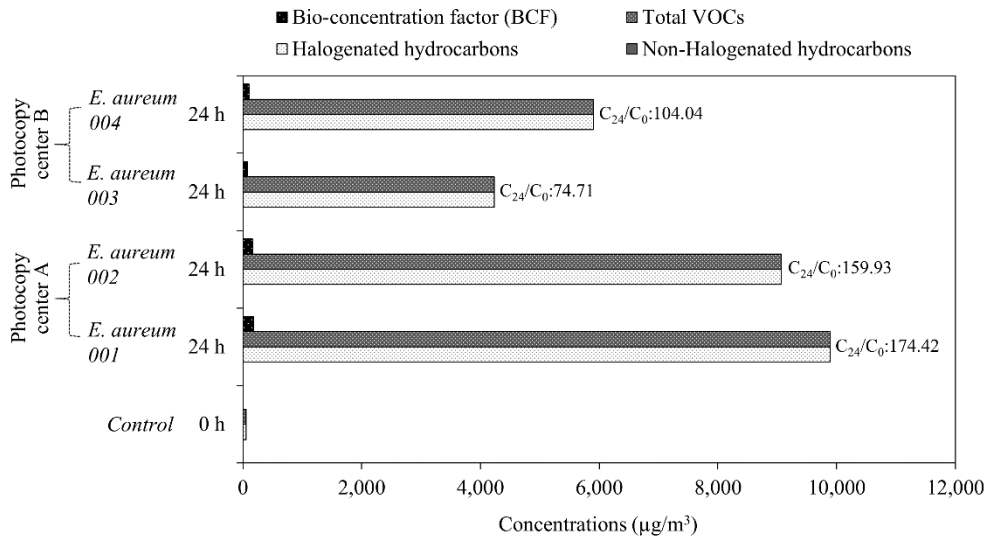

Figure 4. Bio-concentration factor of *E. aureum* for passive removal of VOCs.

The photocopy centers should be designed with sufficient ventilation and engineering controls ought to be implemented to mitigate emissions at the source. The air conditioner is adjusted to guidance temperature to reduce the amount of volatile organic compounds released in the event of high heat. Try to choose ink cartridges that are natural inks to reduce the impact on operators and customers. Furthermore, employees should be informed of the potential hazards and guidelines of such emissions. Workers should protect themselves by wearing suitable protective gloves and masks to avoid direct and indirect contact with VOCs. Indoor plant cultivation has the potential to improve air quality by removing specific air pollutants.

4. CONCLUSION

This study investigated the VOC characteristics and risk assessment associated with emissions from photocopy centers. The obtained results indicate that the total VOCs concentrations were 2.29×10^4 and 2.32×10^4 µg/m^3 which include three substances (m-Xylene, p-Xylene, and trans-1,2-Dichloroethene) in photocopy centers A and B, respectively. The trans-1,2-Dichloroethene was the most abundant among VOC profiles. It was observed that VOC species concentrations were lower than recommended limit values set by ACGIH, NIOSH, OSHA, and DLPW. Long-term exposure to VOCs even at lower concentrations than its limit value poses a potential health risk. The non-carcinogenic and carcinogenic risks due to inhalation exposure were also determined. However, the toxicity values associated with observed VOCs were not reported. Therefore only the risk of non- carcinogenic VOCs was determined. The non-cancer risk associated with non-carcinogenic VOCs as indicated by HI exceeded the acceptable limit value in both photocopy centers, indicating that exposed VOCs

posed a probable health threat of non-carcinogenic effects to workers. Hence, *E. aureum* or Golden Pothos for the passive VOCs removal at the photocopy center further reduces VOCs concentrations and provides risk abatement resulting in reduced exposure to VOCs of workers.

ACKNOWLEDGEMENTS

The authors wish to thank the owner of the photocopy center for their valuable time, effort, and contribution to this study.

REFERENCES

Agarwal P, Sarkar M, Chakraborty B, Banerjee T. Phytoremediation of air pollutants: Prospects and challenges. In: Pandey VC, Bauddh K, editors. Phytomanagement of Polluted Sites. Amsterdam: Elsevier; 2019. p. 221-41.

Al-Zboon KK, Forton OT. Indoor air quality in steel rolling industries and possible health effects. Environment and Natural Resources Journal 2019;17(4);20-9.

American Conference of Governmental Industrial Hygienists (ACGIH). 2019 TLVs and BEIs. Cincinnati, OH, USA: ACGIH Signature Publications; 2019.

Ari A. A comprehensive study on gas and particle emissions from laser printers: Chemical composition and health risk assessment. Atmospheric Pollution Research 2020;11(2):269-82.

Ari A, Ari PE, Yenïsoy- Karakaş S, Gaga EO. Source characterization and risk assessment of occupational exposure to volatile organic compounds (VOCs) in a barbecue restaurant. Building and Environment 2020;174:106791.

Atawodi SE, Atawodi JC, Idakwo GA, Pfundstein B, Haubner R, Wurtele G, et al. Evaluation of the polyphenol content and antioxidant properties of methanol extracts of the leaves, stem, and root barks of *Moringa oleifera* Lam. Journal of Medicinal Food 2010;13(3):710-6.

Chaikasem S, Na Roi-et V. Health risk assessment of pesticide residues in vegetables from river basin area. Applied Environmental Research 2020;42(2):46-61.

Cocheo C, Boaretto C, Pagani D, Quaglio F, Sacco P, Zaratin L, et al. Field evaluation of thermal and chemical desorption BTEX radial diffusive sampler radiello compared with active (pumped) samplers for ambient air measurements. Journal of Environmental Monitoring 2009;11(2):297-306.

Dales R, Liu L, Wheeler AJ, Gilbert NL. Quality of indoor residential air and health. Canadian Medical Association Journal 2008;179(2):147-52.

Delgado-Saborit JM, Aquilina NJ, Meddings C, Baker S, Harrison RM. Relationship of personal exposure to volatile organic compounds to home, work and fixed site outdoor concentrations. Science of the Total Environment 2011;409(3):478-88.

Department of Labour Protection and Welfare (DLPW). Notification of the department of labour protection and welfare title, "Concentration limits of hazardous chemicals" [Internet]. 2017 [cited 2020 Apr 28]. Available from: http://www.ratchakitcha.soc.go.th/DATA/PDF/2560/E/198/34.PDF.

Department of Toxic Substances Control (DTSC). Human Health Risk Assessment Note Number 10: Toxicity Criteria. California, USA: Human and Ecological Risk Office; 2019.

Destaillats H, Maddalena RL, Singer BC, Hodgson AT, McKone TE. Indoor pollutants emitted by office equipment: A review of reported data and information needs. Atmospheric Environment 2008;42(7):1371-88.

Durmusoglu E, Taspinar F, Karademir A. Health risk assessment of BTEX emissions in the landfill environment. Journal of Hazardous Materials 2010;176(1-3):870-7.

El- Hashemy MA, Ali HM. Characterization of BTEX group of VOCs and inhalation risks in indoor microenvironments at small enterprises. Science of the Total Environment 2018; 645:974-83.

Fukushi K, Sriussadaporn C, Shimazaki D, Yamamoto K. Assessment of roadside air quality in the Tokyo metropolitan area by a novel biomonitoring method. WIT Transactions on Ecology and the Environment 2005;82:563-76.

Gawronski SW, Gawronska H, Lomnicki S, Sæbo A, Vangronsveld J. Plants in air phytoremediation. In: Cuypers A, Vangronsveld J, editors. Advances in Botanical Research. London: Academic Press; 2017. p. 319-46.

Geethangili M, Ding S-T. A review of the phytochemistry and pharmacology of *Phyllanthus urinaria* L. Frontiers in Pharmacology 2018;9:1109.

Gong Y, Zhou T, Wang P, Lin Y, Zheng R, Zhao Y, et al. Fundamentals of ornamental plants in removing benzene in indoor air. Atmosphere 2019;10:221.

Healy RM, Bennett J, Wang JM, Karellas NS, Wong C, Todd A, et al. Evaluation of a passive sampling method for long-term continuous monitoring of volatile organic compounds in urban environments. Environmental Science and Technology 2018; 52(18):10580-9.

Henschel DB, Fortmann RC, Roache NF, Liu X. Variations in the emissions of volatile organic compounds from the toner for a specific photocopier. Journal of the Air and Waste Management Association 2001;51(5):708-17.

Hoskins JA. Health effects due to indoor air pollution. Indoor and Built Environment 2003;12(6):427-33.

Kim K-H, Shon Z-H, Kim M-Y, Sunwoo Y, Jeon E-C, Hong J-H. Major aromatic VOC in the ambient air in the proximity of an urban landfill facility. Journal of Hazardous Materials 2008; 150(3):754-64.

Kitwattanavong M, Prueksasit T, Morknoy D, Tunsaringkarn T, Siriwong W. Health risk assessment of petrol station workers in the inner city of Bangkok, Thailand, to the exposure to BTEX and carbonyl compounds by inhalation. Human and Ecological Risk Assessment 2013;19(6):1424-39.

Kowalska J, Gierczak T. Qualitative and quantitative analyses of the halogenated volatile organic compounds emitted from the office equipment items. Indoor and Built Environment 2013;22(6):920-31.

Kowalska J, Szewczyńska M, Pośniak M. Measurements of chlorinated volatile organic compounds emitted from office printers and photocopiers. Environmental Science and Pollution Research 2015;22(7):5241-52.

Larson EC, Hathaway LB, Lamb JG, Pond CD, Rai PP, Matainaho TK, et al. Interactions of Papua New Guinea medicinal plant extracts with antiretroviral therapy. Journal of Ethnopharmacology 2014;155(3):1433-40.

Loonsamrong W, Taneepanichskul N, Puangthongthub S, Tungsaringkarn T. Health risk assessment and BTEX exposure among car park workers at a parking structure in Bangkok, Thailand. Journal of Health Research 2015;29(4):285-92.

Martin J, Demokritou P, Woskie S, Bello D. Indoor air quality in photocopy centers, nanoparticle exposures at photocopy workstations, and the need for exposure controls. Annals of Work Exposures and Health 2017;61(1):110-22.

Meshram A, Srivastava N. *Epipremnum aureum* (Jade Pothos): A multipurpose plant with its medicinal and pharmacological properties. Journal of Critical Reviews 2015;2(2):21-5.

Miller JN, Miller JC. Statistics and Chemometrics for Analytical Chemistry. 6th ed. Gosport, UK: Ashford Colour Press Ltd; 2010.

Mishra T, Pandey VC. Phytoremediation of red mud deposits through natural succession. In: Pandey VC, Bauddh K, editors. Phytomanagement of Polluted Sites. Amterdam: Elsevier; 2019. p. 409-24.

Moya TA, Dobbelsteen A, Ottelé M, Bluyssen PM. A review of green systems within the indoor environment. Indoor and Built Environment 2019;28(3):298-309.

Na Roi-et V, Chiemchaisri W, Chiemchaisri C. Genotoxicity assessment of volatile organic compounds in landfill gas emission using comet assay in higher terrestrial plant. Bulletin of Environmental Contamination and Toxicology 2017; 98:283-9.

National Institute for Occupational Safety and Health (NIOSH). Index of chemical names, synonyms and trade names [Internet]. 2019 [cited 2020 Apr 29]. Available from: https://www.cdc.gov/niosh/npg/npgsyn-d.html.

Novic AJ, O'Brien DS, Kaserzon SL, Hawker DW, Lewis SE, Mueller JF. Monitoring herbicide concentrations and loads during a flood event: A comparison of grab sampling with passive sampling. Environmental Science and Technology 2017;51(7):3880-91.

Occupational Safety and Health Administration (OSHA). Permissible exposure limits-Annotated tables [Internet]. 2019 [cited 2020 Apr 28]. Available from: https://www.osha.gov/dsg/annotated-pels/index.html.

Office of Environmental Health Hazard Assessment (OEHHA). International Agency for Research on Cancer and U.S. Environmental Protection Agency Carcinogen Classifications: Appendix E. California, USA: Office of Environmental Health Hazard Assessment; 2009.

Office of Environmental Health Hazard Assessment (OEHHA). Chemical-specific Summaries of the Information Used to Derive Unit Risk and Cancer Potency Values: Appendix B. California, USA: Office of Environmental Health Hazard Assessment; 2011.

Orwell RL, Wood RL, Tarran J, Torpy F, Burchett MD. Removal of benzene by the indoor plant/substrate microcosm and implications for air quality. Water, Air, and Soil Pollution 2004;157:193-207.

Parekh J, Jadeja D, Chanda S. Efficacy of aqueous and methanol extracts of some medicinal plants for potential antibacterial activity. Turkish Journal of Biology 2005;29:203-10.

Pollution Control Department (PCD). Development of Environmental and Emission Standards of Volatile Organic Compounds (VOCs) in Thailand: PCD 03-101. Bangkok, Thailand: Air Quality and Noise Management Bureau; 2009.

Saikomol S, Thepanondh S, Laowagul W. Emission losses and dispersion of volatile organic compounds from tank farm of petroleum refinery complex. Journal of Environmental Health Science and Engineering 2019;17:561-70.

Sakai N, Yamamoto S, Matsui Y, Khan MF, Latif MT, Mohd MA, et al. Characterization and source profiling of volatile organic compounds in indoor air of private residences in Selangor State, Malaysia. Science of the Total Environment 2017; 586:1279-86.

Sakurai K, Miyake Y, Amagai T. Reliable passive-sampling method for determining outdoor 1,3-butadiene concentrations in air. Atmospheric Environment 2013;80:198-203.

Shrubsole C, Dimitroulopoulou S, Foxall K, Gadeberg B, Doutsi A. IAQ guidelines for selected volatile organic compounds (VOCs) in the UK. Building and Environment 2019; 165:106382.

Srivastava A, Majumdar D. Monitoring and reporting VOCs in ambient air. In: Mazzeo N, editor. Air Quality Monitoring, Assessment and Management. London: Intech; 2011. p. 137-48.

Strandberg B, Sunesson A-L, Olsson K, Levin J-O, Ljungqvist G, Sundgren M, et al. Evaluation of two types of diffusive samplers and adsorbents for measuring 1,3-butadiene and benzene in air. Atmospheric Environment 2005;39(22):4101-10.

Tang T, Hurraß J, Gminski R, Mersch-Sundermann V. Fine and ultrafine particles emitted from laser printers as indoor air contaminants in German offices. Environmental Science and Pollution Research 2012;19(9):3840-9.

United States Environmental Protection Agency (U.S. EPA). Standard Operating Procedure for Measurement of Volatile Organic Compounds Using Canisters with Passive Air Sampling Kits: Toxics in Schools, VOC SOP. Georgia, USA: U.S. EPA Region 4, Science and Ecosystem Support Division; 2009a.

United States Environmental Protection Agency (U.S. EPA). Risk Assessment Guidance for Superfund Volume I: Human Health Evaluation Manual (Part F: Supplemental Guidance for Inhalation Risk Assessment). Washington, DC, USA: Office of Superfund Remediation and Technology Innovation; 2009b.

United States Environmental Protection Agency (U.S. EPA). Fluctuation of Indoor Radon and VOC Concentrations Due to Seasonal Variations: EPA/600/R-12/673. Las Vegas, NV, USA: National Exposure Research Laboratory; 2012.

United States Environmental Protection Agency (U.S. EPA). Integrated risk information system (IRIS) [Internet]. 2016a [cited 2020 Apr 28]. Available from: https://cfpub.epa.gov/ncea/iris/search/index.cfm.

United States Environmental Protection Agency (U.S. EPA). Bioconcentration factors for volatile organic compounds in vegetation [Internet]. 2016b [cited 2020 Jun 12]. Available from: https://archive.epa.gov/esd/archive-vacuum/web/html/bio2.html.

United States Environmental Protection Agency (U.S. EPA). Volatile organic compounds' impact on indoor air quality [Internet]. 2020a [cited 2020 Aug 23]. Available from: https://www.epa.gov/indoor-air-quality-iaq/volatile-organic-compounds-impact-indoor-air quality.

United States Environmental Protection Agency (U.S. EPA). Initial list of hazardous air pollutants with modifications [Internet]. 2020b [cited 2020 Aug 23]. Available from: https://www.epa.gov/haps/initial-list-hazardous-air-pollutants-modifications.

Wang Z-M, Wagner J, Wall S. Characterization of laser printer nanoparticle and VOC emissions, formation mechanisms, and strategies to reduce airborne exposures. Aerosol Science and Technology 2011;45(9):1060-8.

Watts RJ. Hazardous Wastes: Sources, Pathways, Receptors. NY, USA: John Wiley and Sons, Inc; 1997.

Weschler CJ. Changes in indoor pollutants since the 1950s. Atmospheric Environment 2009;43(1):153-69.

Wetzel TA, Doucette WJ. Plant leaves as indoor air passive samplers for volatile organic compounds (VOCs). Chemosphere 2015;122:32-7.

Wolverton BC, Johnson A, Bounds K. Interior Landscape Plants for Indoor Air Pollution Abatement: Final Report. NASA Stennis Space Center, MS, USA: NASA John C. Stennis Space Center Science and Technology Laboratory; 1989.

World Health Organization (WHO). Combined or Multiple Exposure to Health Stressors in Indoor Built Environments. Copenhagen, Denmark: WHO Regional Office for Europe; 2013.

Xing L, Wang L, Zhang R. Characteristics and health risk assessment of volatile organic compounds emitted from interior materials in vehicles: A case study from Nanjing, China. Environmental Science and Pollution Research 2018;25:14789-98.

Yang DS, Pennisi SV, Son K-C, Kays SJ. Screening indoor plants for volatile organic pollutant removal efficiency. HortScience 2009;44(5):1377-81.

Zhang D-C, Liu J-J, Jia L-Z, Wang P, Han X. Speciation of VOCs in the cooking fumes from five edible oils and their corresponding health risk assessments. Atmospheric Environment 2019;211:6-17.

Occurrence and Polymer Types of Microplastics from Surface Sediments of Molawin Watershed of the Makiling Forest Reserve, Los Baños, Laguna, Philippines

Jomel S. Limbago[1,2,3*], Marion Michael A. Bacabac[2,3], Dawn Rosarie M. Fajardo[2,3], Camille Rose T. Mueda[2,3], Arselene U. Bitara[2,4], Karla Louise P. Ceguerra[2,3], Maria Riza C. Lopez[2,4], Gabrielle Ann V. Posa[2,3], and Hildie Maria E. Nacorda[4]

[1]Fisheries and Marine Science Department, Cavite State University - Naic Campus, Cavite, Philippines
[2]Graduate School, University of the Philippines Los Baños, Laguna, Philippines
[3]Institute of Biological Sciences, College of Arts and Sciences, University of the Philippines Los Baños, Laguna, Philippines
[4]School of Environmental Science and Management, University of the Philippines Los Baños, Laguna, Philippines

ARTICLE INFO

Received: 2 Jun 2020
Received in revised: 11 Sep 2020
Accepted: 5 Oct 2020
Published online: 9 Nov 2020
DOI: 10.32526/ennrj/19/2020114

Keywords:
Microplastics/ Molawin Creek/ Surface sediments/ Fourier-transform infrared spectroscopy

*** Corresponding author:**
E-mail: jlimbago@up.edu.ph

ABSTRACT

Microplastic pollution is an emerging topic in environmental science. However, information about its prevalence in the freshwater ecosystems is still scarce. This study quantified and identified microplastic form and polymer types from surface sediments of the Molawin River. Sediment samples were collected from the upstream, midstream, and downstream stations of the river. Isolation of microplastics was performed through a modified granulometric approach, density separation, and filtration. Stereoscopic microscopy and Fourier-transform infrared spectroscopy (FTIR) were conducted to quantify and describe microplastics and identify the polymer types based on the infrared spectrum of absorption, respectively. The highest concentration of microplastics was found in the downstream station, with an average number of 97±12 items/100 g and 47.33±11.39 items/100 g sediment dry weight in the bank and channel, respectively. The isolated microplastics were dominated by ≥100 to ≤200 µm size range. Based on stereoscopic microscopy, microfragments and microfibers were the most common microplastic type, while polyethylene (PE) and polypropylene (PP) were the polymer types identified based on FTIR analyses. This study revealed the presence of microplastics and confirmed the microplastics polymers present in the Molawin Watershed of Makiling Forest Reserve.

1. INTRODUCTION

Microplastic pollution is an emerging contaminant, and it is considered as one of the most discussed topics in the field of environmental science (Wagner et al., 2014; Eerkes-Medrano et al., 2015; Anderson et al., 2017). These micropollutants are divided into two categories: primary and secondary. Primary microplastics are manufactured raw "minute" plastic materials and move directly into water bodies (Browne et al., 2007; Andrady, 2011). Secondary microplastics are derived from various types of materials (meso- and macro-plastics) that degrade into smaller particles which are not readily detected (Thompson et al., 2004; Browne et al., 2007; Andrady, 2011). Generally, less than 5 mm plastics are considered microplastics (GESAMP, 2015). While some other authors used other size classifications. Blair et al. (2017) divides the size class into large microplastics, small microplastics, microdebris, and microplastic. Large microplastics are microplastics ranging from 1-5 mm (Faure et al., 2012), small microplastics (<1 mm) (Vianello et al., 2013), microdebris (<2 mm) (Lechner et al., 2014), small microplastics (<1 mm) and microplastics (<0.5 mm) (Thompson et al., 2004; Fendall et al., 2009; Sanchez et al., 2014; Corcoran, 2015). At present, however, there is no standard definition of microplastics in terms of size range (Hidalgo-Ruz et al., 2012).

Although there is no standard microplastics size classifications, the study of Lehtiniemi et al. (2018) showed that fish and mysid shrimp uptake <200 µm size microplastics. Moreover, the smaller sizes of microplastic could be a great concern because it could be ingested by planktonic organisms and entrained by

Citation: Limbago JS et al. Occurrence and polymer types of microplastics from surface sediments of Molawin Watershed of the Makiling Forest Reserve, Los Baños, Laguna, Philippines. Environ. Nat. Resour. J. 2021;19(1):57-67. (https://doi.org/10.32526/ennrj/19/2020114)

settling detritus (Cole et al., 2013; Botterell et al., 2019; Ballent et al., 2013). The entry of smaller size microplastics and nanoplastics in the planktonic food web could lead to further bioaccumulation and biomagnification in higher vertebrates (Saley et al., 2019; Akhbarizadeh et al., 2019). Hence, microplastics size are crucial nominators on determining the impact of microplastics on environment fauna. On top of that, microplastics are also vectors of highly hydrophobic contaminants and endocrine-disrupting chemicals such as polyaromatic hydrocarbon, polychlorinated biphenyls, and polybrominated diphenyl ethers (Chen et al., 2018; Chen et al., 2019). This emerging concern has brought the microplastic research on the international spotlight since widespread plastic littering is a pronounced issue, however, degradation and its possible entry into the food web has long not been taken into account.

The increasing prevalence of microplastics in our aquatic ecosystems can be attributed to the continuous production and patronage of synthetic plastics coupled with poor solid waste management (Ang and Sy-Changco, 2007; Magalang, 2014). Recent literature has brought to light the abundance of microplastics in freshwater systems that are comparable to that of coastal and marine environments (Anderson et al., 2017; Blettler et al., 2017; Peng et al., 2018). For example, the studies of Sadri and Thompson (2014), Gallagher et al. (2016), and Vendel et al. (2017) reported acute microplastic pollution in estuaries indicating river input to coastal litters. Despite terrestrial water being considered as a significant transport vector of microplastics towards coastal environments, studies on its prevalence in freshwater ecosystems are still lacking to date-highlighting the need to focus on investigating its presence and distribution in the freshwater ecosystem (Wagner et al., 2014; Li et al., 2020).

Molawin Creek is one of the watersheds of the Makiling Forest Reserves under the administration of the University of the Philippines-Los Baños and a minor tributary of Laguna de bay (Liongson et al., 2005). The watersheds of the reserve is habitat to diverse and abundant freshwater fish populations, including one endemic fish species *Leiopotherapon plumbeus*, and diminutive fish species such as *Glossogobius celebius* and *Hippichthys heptagonus* which are prone to extinction (Paller et al., 2011). Towards protecting its fauna and flora, Molawin has been declared as Biopark in 2010 (Casila et al., 2019). However, despite being a forest reserve and declared as a Biopark, anthropogenic micropollutants from university facilities, commercial, and residential communities that may affect the aquatic organisms have received limited attention, considering biological sustainability is highly dependent on the physical, chemical, and biological viability of a particular habitat. On top of that, damaging biological diversity will eventually affect the ecological services that a watershed provides. Hence, from an ecological standpoint, there is a need to obtain a baseline study that will fill the data gap identified.

The objectives of this work were to (i) identify and characterize microplastics from surface sediments of Molawin Creek; (ii) determine the distribution of microplastics from surface sediments of different stations of the Molawin Creek; and (iii) identify the microplastics polymers isolated from surface sediments of Molawin Creek. The hypotheses that were defined to validate the objectives of the study are as follows: (i) the number of microplastics is higher in the downstream station of the Molawin Creek than in the midstream, and upstream stations; (ii) fibers and fragments are the most abundant type of microplastics present in Molawin Creek; and (iii) polyethylene is the most abundant type microplastic polymer in Molawin Creek. The result of this study will reveal the occurrence and will confirm the polymer types of microplastics in Molawin Watershed of the Makiling Forest Reserve. And eventually will contribute to the international data gap of the presence of microplastic prevalence in a freshwater body.

2. METHODOLOGY

2.1 Description of the study site

Three sampling stations within the river system of Molawin Creek, one of the major watersheds of the Makiling Forest Reserve at Los Baños, Laguna, Philippines, were identified in the study-upstream, midstream, and downstream stations (Figure 1). The upstream station located in Flat Rocks (14.147700°N, 121.229260°E) is inside the University of the Philippines Los Baños campus along the Mt. Makiling trail. The general area of the upstream station is not adjacent to any built-up infrastructure nor human settlement and is heavily forested. The midstream station designated at Molawin Biopark (14.162320°N, 121.244440°E), also inside the campus, is primarily surrounded by University establishments. On the other hand, the downstream station is in Barangay Bayog (14.189360°N, 121.259830°E) and is mostly surrounded by built-up areas, particularly residential

areas along the riverbank, and annual crops, forms a confluence with Maahas Creek. These sampling stations were selected to compare the concentration of microplastics in different depositional environments and varying anthropogenic activities. Banks and channels were considered as a substation in the study.

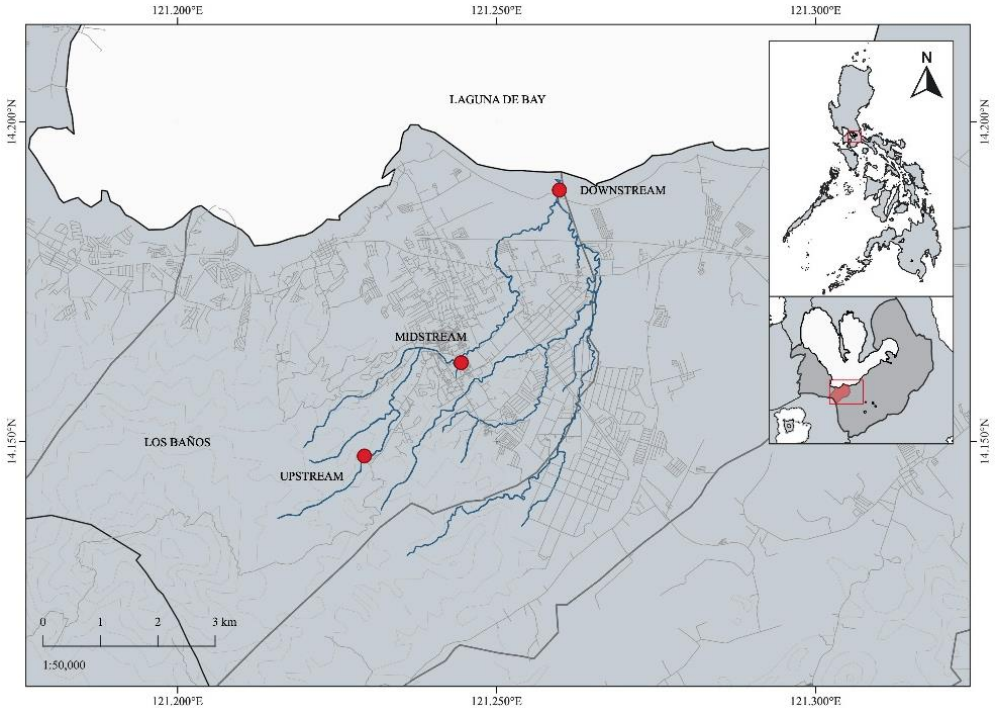

Figure 1. Land use map of the general study site with three sampling stations. The red points indicate upstream (Flat Rocks), midstream (Molawin Biopark), and downstream (Bayog) stations along Molawin Creek, Los Baños, Laguna, Philippines.

2.2 Sediment sampling

One day field sampling was conducted in October 2018. The collection of sediment samples from three stations, with two substations, was carried out along the Molawin Creek. Along the banks of each substation, a 50 m transect line was laid down haphazardly. While in channels of each substation, the transect line was laid down to areas satisfying these criteria: (i) should be in a straight reach of 50 m; and (i) should not be adjacent to hydraulic structures. Then three replicates were randomly collected along the transect line following the bank and the channel of the creek. Surface sediments (0-5 cm) were collected in a modified 15 cm × 15 cm quadrat laid on the substrate using a metal trowel with gradations. However, a different sample collection method was employed in the channel of the downstream station. In the downstream station's channel, a box corer (15 cm × 15 cm) was used to collect the sediments. Samples were placed in glass containersand then sealed to avoid contamination during transport. All obtained samples were stored at 4°C for subsequent laboratory analysis.

2.3 Processing of sediment samples and microplastic isolation

The isolation of microplastics was conducted according to the methods prescribed by the National Oceanic and Atmospheric Administration (NOAA) and a modified granulometric approach (Masura et al., 2015; Thompson et al., 2004; Kedzierski et al., 2016; Whitmire et al., 2017). Briefly, sediment samples were weighed (~1000 g wet weight) and were oven-dried at 60°C for 48 h. Dried samples were sifted through a nested set of standardized sieves with progressively smaller openings (2 mm - 0.63 μm) (López, 2017).

Sediments with less than 0.5 mm size were then weighed. Because of differences in sediment dry weight, a standardized aliquot of 100 g dry weight of sediments was used in subsequent analysis (Peng et al., 2017). Samples were poured with 500 mL of concentrated saline solution (200 NaCl g/L) in 1,000 mL glass jars (Thompson et al., 2004). After settling the samples overnight, the supernatants were sifted through Whatman filter No. 2 with the aid of a vacuum pump. The tube of vacuum pumps was then rinsed

with Milli Q water to minimize cross-contamination between samples. Samples were then placed in Petri plates and were oven-dried at 60°C for an hour.

2.4 Stereoscopic microscopy and microplastic quantification

Samples of microplastics in filter paper were photographed and documented using a stereomicroscope at 40X magnification. Isolated particles were counted, measured for maximum length (relative to a 5 mm scale bar), and classified based on its general form-microfibers, microfragments, microfilms, and microbeads. Microplastics size of <0.5 mm as early defined and used by some authors (Thompson et al., 2004; Fendall et al., 2009; Sanchez et al., 2014; Corcoran, 2015) was considered in this study because this size has higher ingestibility by aquatic organisms and were entrained by settling detritus (Lehtiniemi et al., 2018; Cole et al., 2013; Botterell et al., 2019; Ballent et al., 2013). Suspected microplastic particles were submitted for Fourier-transform infrared spectroscopy (FTIR) analyses for validation and identification of plastic polymer types.

2.5 Fourier-transform infrared spectroscopy

Polymer types of microplastics were determined separately using the FTIR spectrometer (Bruker, United States). Wave numbers were recorded in transmission mode with 4,000-6,000/cm range and a spectral resolution of 4/cm. A total of 24 scans were co-added for every spectrum. The background measurements were conducted with the same settings: against air for samples that have not adhered to the filter paper, and against the filter paper for adhering samples. The FTIR instrument was administered by OPS IR software V7.5. Post-processing of the spectra was also implemented using the same software.

2.6 Data analyses

Results were expressed as mean±standard errors (SE) from three sample replicates. Data analyses were performed using MS Office Excel 365, and histogram of microplastics size distribution were plotted using Paleontological Statistics (PAST) software version 2.17.

3. RESULTS

3.1 Microplastic quantity

The results of the study showed that microplastics were present in all sampling stations (Figure 2). The highest number of microplastics was found in downstream sampling stations (47.33±11.39 items and 97.00±12.34 items/100 g sediment dry weight in channel and bank, respectively), followed by midstream stations (1.33±0.88 items and 6.33±1.20 items/100 g sediment dry weight in channel and bank, respectively) and the least number of microplastics were isolated from upstream stations (1.00±0.58 items/100 g sediment dry weight in both substations).

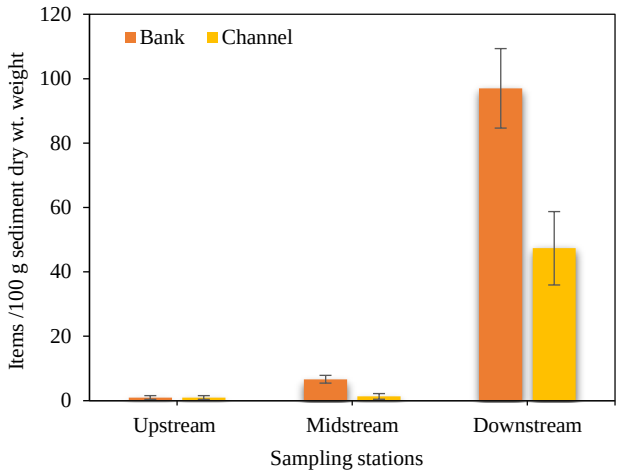

Figure 2. Mean number±standard error (n=3 per substation) of microplastics identified from surface sediments of three sampling stations of the Molawin Creek (bank and channel).

3.2 Microplastic types

All types of microplastics were isolated and identified from the Molawin Creek continuum (Figure 3). As shown in Table 1, the most collected microplastics type was microfragments in all stations with the exception for the midstream channel substation (Table 1). As shown in Table 1, the highest number of microfragments was isolated from the bank (71.33 items/100 g sediment dry weight) and in the channel (30 items/100 g sediment dry weight) of the downstream station. Microfibers isolated from the bank (20 items/100 g sediment dry weight) is higher than the microfibers identified from the channel (5 items/100 g sediment dry weight) of the downstream station. In contrast, microfilm (11.67 items/100 g sediment dry weight) in the channel is higher than microfilms identified from the bank (5 items/100 g sediment dry weight) of the downstream station. On the other hand, only microfragment in the channel of midstream station has a notable number (4 items/100 g sediment dry weight). Microbeads are the least identified microplastic from the Molawin Creek continuum. In terms of size range, microplastics with ≥100 to ≤200 µm length dominated the isolated particles (Figure 4).

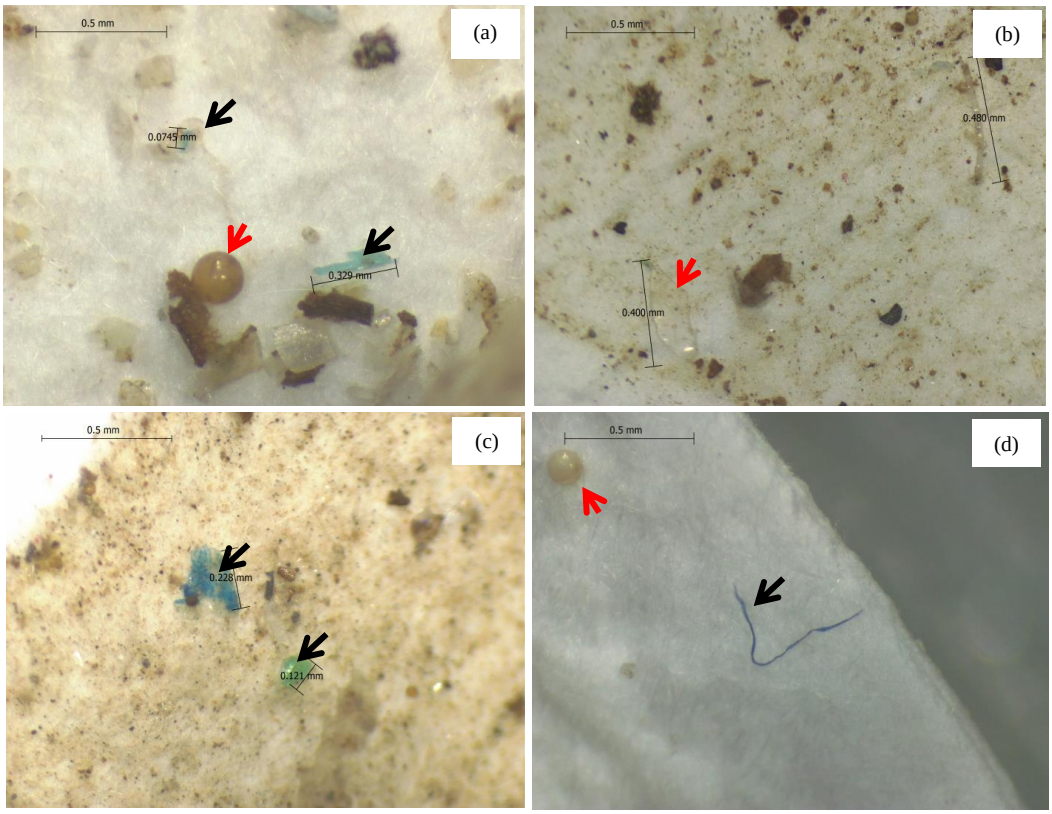

Figure 3. Microplastic types identified from Molawin Creek continuum: (a) black arrows - microfragments; red arrow - microbeads; (b) black arrow - microfiber; red arrow - microfilm; (c) microfragments; (d) black arrow - microfiber; red arrow - microbeads. Scale bar=0.5 mm.

Table 1. The average number of microplastic types obtained from sediment samples of bank and channel of Molawin Creek, Los Baños, Laguna, Philippines.

Station	Average number of microplastics types				
	Fragment	Beads	Films	Fiber	Total
Upstream channel	1.00	0.00	0.00	0.00	1.00
Upstream bank	0.67	0.00	0.00	0.33	1.00
Midstream channel	0.33	0.00	0.00	1.00	1.33
Midstream bank	4.00	0.67	1.00	0.67	6.33
Downstream channel	30.00	0.67	11.67	5.00	47.33
Downstream bank	71.33	0.67	5.00	20.00	97.00

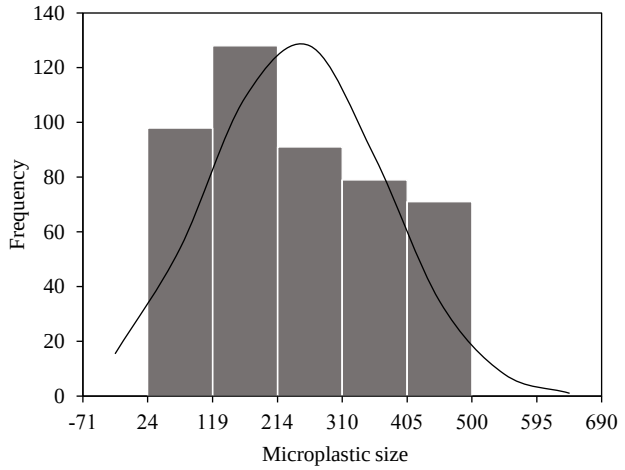

Figure 4. Microplastic size distribution along Molawin Creek continuum.

3.3 Sediment granulometry

Sediment grain size distribution in the Molawin Creek is shown in Figure 5. It is observed that upstream and midstream sampling stations are composed of course sediments. In terms of larger grain size (≥2 mm), upstream substations are composed of 70.56% (bank) and 76.04% (channel), midstream substations are composed of 63.79% (bank) and 46.01% (channel) while downstream substations are composed only of 26.78% (bank) and 20.15% (channel). Grain sizes of downstream stations are typically composed of smaller grains and moderately sorted according to grain sizes in comparison to upstream and midstream stations.

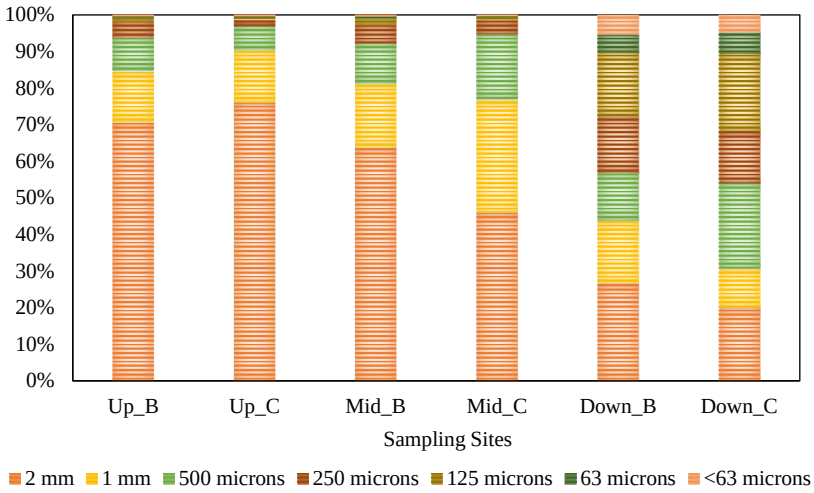

Figure 5. Sediment grain sizes distribution of Molawin Creek. Upstream-Bank (Up_B); Upstream-Channel (Up_C); Midstream-Bank (Mid_B); Midstream-Channel (Mid_C); Downstream-Bank (Down_B) and Downstream-Channel (Down_C).

3.4 Fourier-transform infrared spectroscopy (FTIR)

Previous studies on polymers using FTIR analyses have established the absorption bands used for the identification of high-density polyethylene (HDPE), low-density polyethylene (LDPE), and polypropylene (PP) spectra. The stretching of vibration bands of CH_2 in polyethylene and CH_2/CH_3 in polypropylene was observed within the range of 3,000-2,800/cm, while the bending vibrations of CH_2 and CH_3 groups fall in the range of 1,500-1,350/cm, and CH_2 rocking vibration between 1,200-700/cm (Käppler et al., 2015). Fourier-transform infrared spectroscopy (FTIR) analysis (Bruker, United States) presented the spectra of microplastic samples that were obtained from three stations in the Molawin Creek. The samples from the bank and channel of the downstream station exhibited peaks within the range of 3,000-2,800/cm (Figures 6(a) and (b)). In the midstream station, only samples collected from the bank registered peaks with a similar range (Figure 7(b)). No significant peaks were observed in the samples acquired in the channel of midstream station (Figure 7(a)). Furthermore, results from the spectra of microplastics in the upstream station for both bank and channel substations were negligible (Figures 8(a) and (b)). Polypropylene (PP) particles were identified for both samples obtained in the bank and channel of the downstream station. Polyethylene (PE) polymers were the only samples that were determined from the bank of the midstream station. Lastly, no microplastic polymers were recorded in the channel of midstream station, and for both the bank and channel of the upstream station.

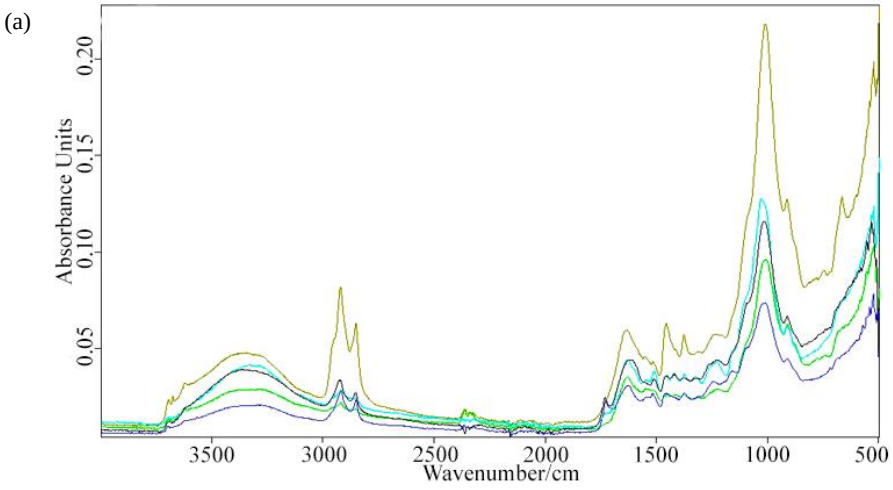

Figure 6. Fourier-transform infrared spectroscopy (FTIR) spectra of microplastic samples obtained from surface sediments of the downstream stations of Molawin Creek. (a) channel; (b) bank.

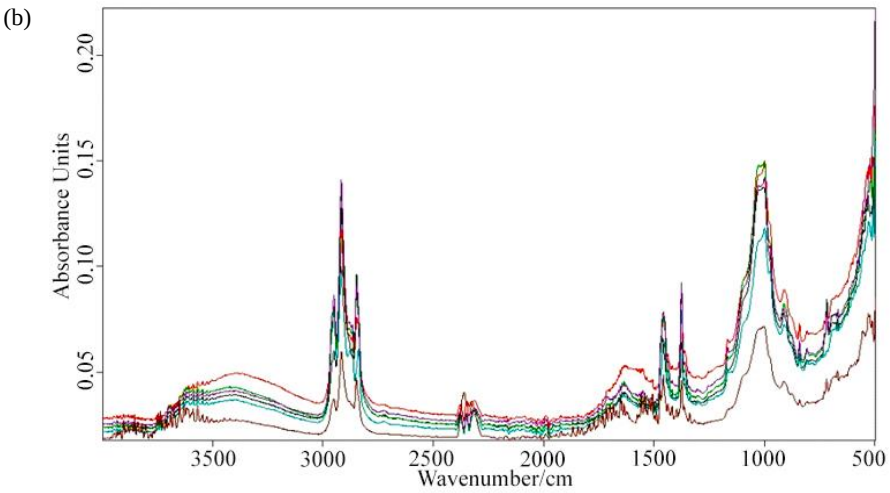

Figure 6. Fourier-transform infrared spectroscopy (FTIR) spectra of microplastic samples obtained from surface sediments of the downstream stations of Molawin Creek. (a) channel; (b) bank (cont.).

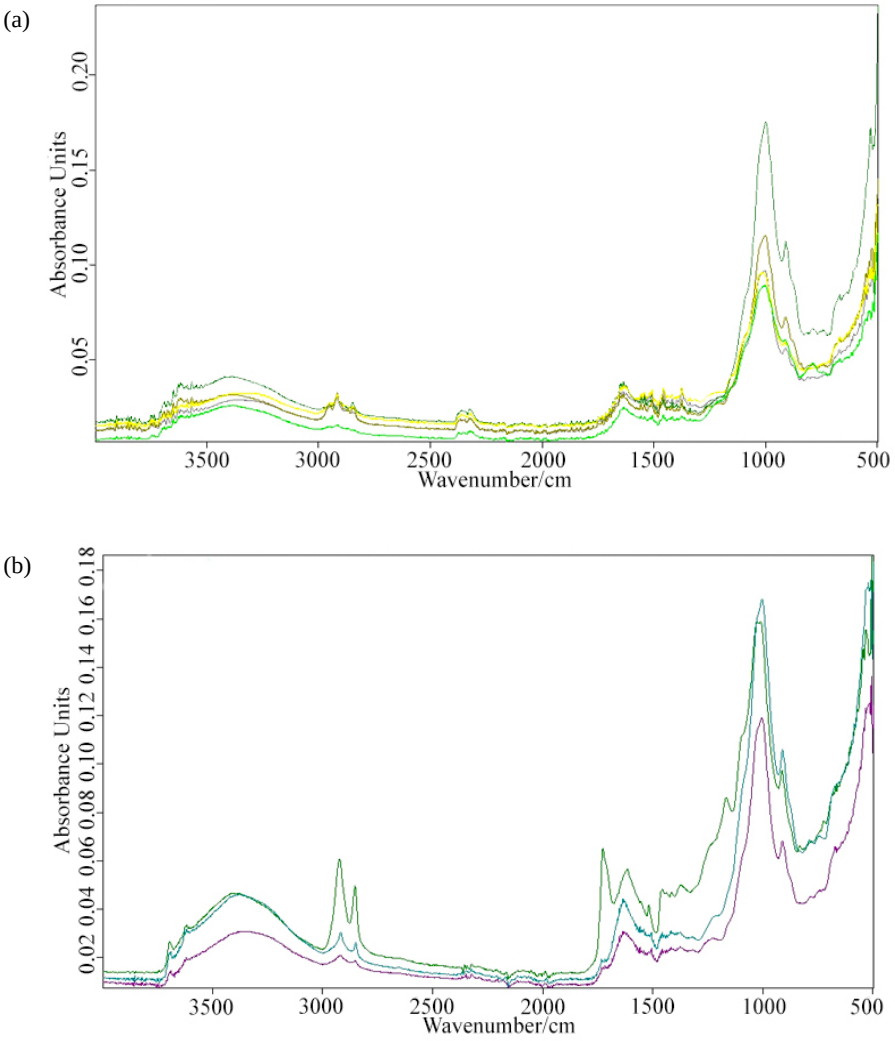

Figure 7. Fourier-transform infrared spectroscopy (FTIR) spectra of microplastic samples obtained from surface sediments of the midstream stations of Molawin Creek. (a) channel; (b) bank.

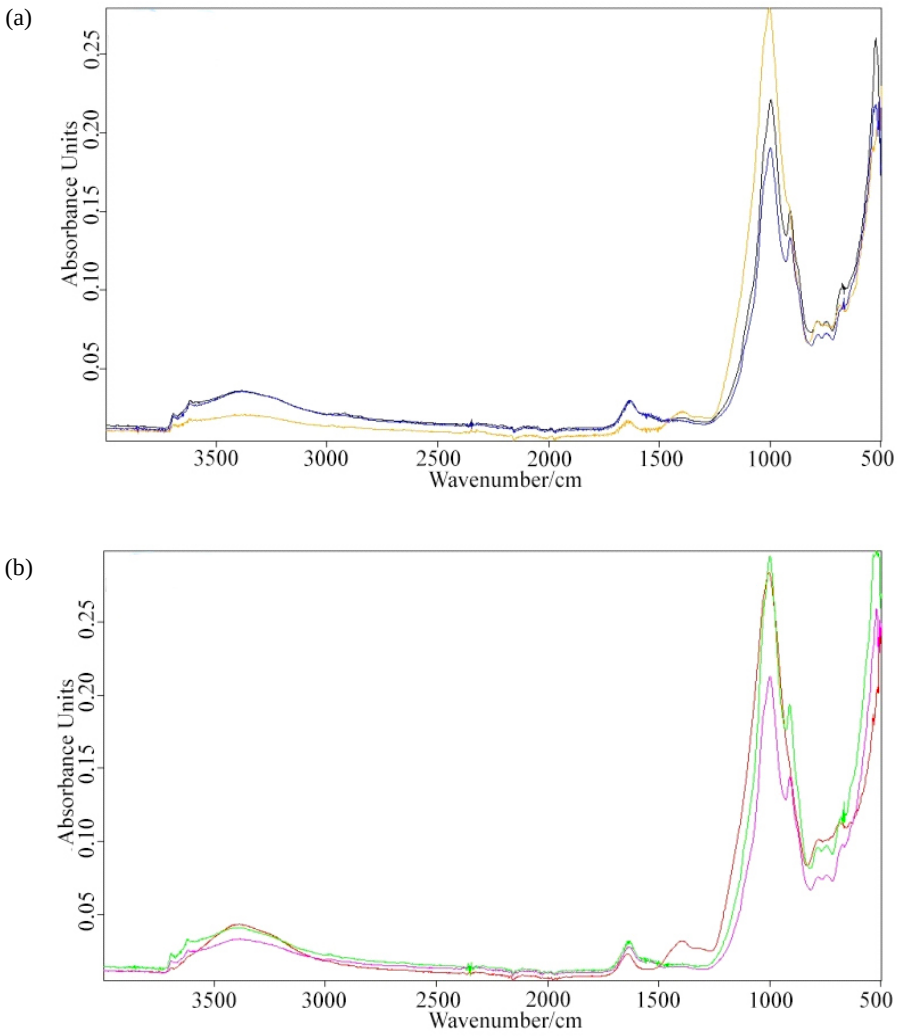

Figure 8. Fourier-transform infrared spectroscopy (FTIR) spectra of microplastic samples obtained from surface sediments of the upstream stations of Molawin Creek. (a) channel; (b) bank.

4. DISCUSSION

Environmental scientists, globally, have put increasing attention on microplastics research (Guzzetti et al., 2018). The issue raises concern since microplastics are considered vectors of endocrine-disrupting compounds (EDCs) in the aquatic environment (Chen et al., 2018; Chen et al., 2019). However, the focus seemed limited to the marine ecosystem, where microplastic prevalence in the freshwater ecosystem has an immense data gap (Wagner et al., 2014; Li et al., 2020). In this study, we assessed the occurrence of microplastics in the Molawin Creek continuum using a modified granulometric approach. Microplastic physical and polymer types were further identified using light microscopy and Fourier-transform infrared spectroscopy (FTIR).

The results were consistent with the first hypothesis of the study, which followed a decreasing trend of microplastic abundance from the upstream to downstream stations. Microplastics were prevalent in sediment samples from both the bank and channel of the Molawin Creek downstream station, where a confluence with the Maahas Creek is formed (Liongson et al., 2005). Through stereoscopic identification, only one microplastic type has been isolated from the upstream stations and in the channel of the midstream station. Additionally, six microplastic types were isolated from the bank of the midstream station. The isolated microplastics were dominated by ≥100 to ≤200 μm in terms of size. Differences in sizes of microplastics may provide insights into their sources and unknown weathering transport effects. On the other hand, minimal anthropogenic activities in the upstream and midstream could be attributed to low microplastic counts, contrary to downstream stations where residential areas are located along the riverbanks. The

presence of microplastic in Molawin Biopark, which is inside the University Campus, is an indicator that waste from the University are drained in the watershed, eventually affecting the habitat.

Population density is not a sole factor affecting the microplastics abundance in the freshwater ecosystem (Klein et al., 2015; Tibbetts et al., 2018). Other factors that could affect the abundance of microplastics in sediments include microplastic polymer density, river hydrodynamics, weather conditions, and heteroaggregation of microplastics rendering higher riverbed retention (Corcoran, 2015; Kowalski et al., 2016; Hurley et al., 2018; Nizzetto et al., 2016; Besseling et al., 2017). The downstream station of the Molawin Creek has fine-grained sediments as compared to upstream and midstream stations. The lower velocities in the downstream station of rivers are known to be sinks for fine-grained sediments. Fine-grained sediments have higher retention, which provides an explanation to the microplastics abundance variation within upstream, midstream, and downstream stations (Nizzetto et al., 2016). Hence, the potential for microplastic settlement is higher (Corcoran, 2015; Vaughan et al., 2017; Botterell et al., 2019). The river hydrodynamics could also explain the greater abundance of microplastics in banks than in channels. This result is in accordance with the study of Tibbetts et al. (2018) where the abundance of microplastics in low velocity environments was recorded. Results of this study, moreover, implies that low velocity environments like banks, floodplains, lakes, meander cut-offs are areas for accumulation of microplastics.

In congruence with the studies of Deocaris et al. (2019), Mani et al. (2015), and Tibbetts et al. (2018) microfragments are the predominant microplastic type in Molawin Creek. Fragmentation or abrasion and degradation of larger plastic items result in microplastic fragments and fibers (Wagner et al., 2014). This suggests that microplastic pollution from the Molawin Creek is from the degradation of larger plastic material and is derived from land-based litters. However, the results did not conform with the second hypothesis of the study, where fibers and fragments were hypothesized to be the dominant microplastic type in the Molawin Creek. Presently, there is no adequate literature explaining the prevalence of fibers over fragments or vice versa. Some authors that published reports on the dominance of fibers over fragments are studies of Horton et al. (2017) and Vermaire et al. (2017).

Interestingly, polyethylene (PE) and polypropylene (PP) were detected using the FTIR spectra, consistent with the third hypothesis of the study. The FTIR spectra also confirm that microplastic is more abundant in banks than in channels. PE and PP were detected from the bank and channel of the downstream station and only PE polymers from the bank of midstream station. The presence of PE could be attributed to the widely used PE-based plastic bags (Yurtsever and Yurtsever, 2017). The current use of oxo-biodegradable type PE plastic bags also contributes to the abundance of microfragments since these materials are easily degraded by UV radiation or heat into smaller fragments (Eyheraguibel et al., 2018). While there are microplastics that were determined in physical identification and microscopy, polymer types were not detected in FTIR analyses. This underscores the importance of the chemical-based identification techniques such as FTIR, and Raman spectroscopy (Jung et al., 2018; Simon et al., 2018; Song et al., 2015; Lenz et al., 2015). Physical identification would lead to the misidentification of microplastics since there is no standard method for physical identification and quantification (Hidalgo-Ruz et al., 2012; Shim et al., 2017; Song et al., 2015). However, it should be noted that the approximate density of 200 g NaCl/L water will only allow recovery of polystyrene, polypropylene, high-density polypropylene, and nylon (Gray et al., 2018). Denser polymers were possibly not recovered by the protocol and methodology of this study.

While this study is one of the few attempts to record the presence of microplastics in the Philippine freshwater bodies, several limitations should be acknowledged. The protocol followed was designed for marine sediments, and density separation procedures could not separate denser microplastic particles. This study, hence, likely underestimated the microplastic counts in the Molawin Creek continuum. Moreover, there is no standard, manual for microplastic visual identification rendering errors in isolation and quantification. Further studies should be implemented to establish a more standardized technique for quantifying and identifying microplastics in the freshwater ecosystem.

5. CONCLUSION

The present study revealed four primary results: (i) microplastics are present in Molawin Watershed of the Makiling Forest Reserve; (ii) microplastics in Molawin Creek were dominated by ≥100 to ≤200 μm

size range; (iii) microplastic is more prevalent in the downstream station of the creek compared to upstream and midstream stations; and (iv) polyethylene and polypropylene microplastic polymers are present in Molawin Creek. These data indicate that downstream station is an accumulation zone of microplastics and highlights the need to study its impact on aquatic fauna and flora of Molawin Watershed and pollution contribution on Laguna de bay.

ACKNOWLEDGEMENTS

We would like to acknowledge the Department of Science and Technology-Accelerated Science and Technology Human Resource Development Program (DOST-ASTHRDP) of Republic of the Philippines for scholarships grants and financial supports.

REFERENCES

Akhbarizadeh R, Moore F, Keshavarzi B. Investigating microplastics bioaccumulation and biomagnification in seafood from the Persian Gulf: A threat to human health? Food Additives and Contaminants: Part A 2019;36(11):1696-708.

Anderson PJ, Warrack S, Langen V, Challis JK, Hanson ML, Rennie MD. Microplastics contamination in Lake Winnipeg, Canada. Environmental Pollution 2017;225:223-31.

Andrady Al. Microplastics in the marine environment. Marine Pollution Bulletin 2011;62(8): 1596-605.

Ang RP, Sy-Changco JA. The phenomenon of sachet marketing: Lessons to be learned from the Philippines. Proceeding of the Marketing Association Conference Proceedings; 2007 Aug 3-6; Washington DC, USA; 2007.

Ballent A, Pando S, Purser A, Juliano MF, Thomsen L. Modelled transport of benthic marine microplastic pollution in the Nazaré Canyon. Biogeosciences 2013;10(12):7957-70.

Besseling E, Quik JTK, Sun M, Koelmans AA. Fate of nano- and microplastic in freshwater systems: A modeling study. Environmental Pollution 2017;220:540-8.

Blair RM, Waldron S, Phoenix V, Gauchotte-Lindsay C. Micro- and nanoplastic pollution of freshwater and wastewater treatment systems. Springer Science Reviews 2017;5:19-30.

Blettler MC, Ulla MA, Rabuffetti AP, Garello N. Plastic pollution in freshwater ecosystems: macro-, meso-, and microplastic debris in a floodplain lake. Environmental Monitoring and Assessment 2017;189(11):581.

Botterell ZLR, Beaumont N, Dorrington T, Steinke M, Thompson RC, Lindeque PK. Bioavailability and effects of microplastics on marine zooplankton: A review. Environmental Pollution 2019;245:98-110.

Browne MA, Galloway T, Thompson R. Microplastic-an emerging contaminant of potential concern? Integrated Environmental Assessment and Management 2007;3(4):559-61.

Casila JC, Duka M, Reyes RDL, Ureta JC. Potential of the Molawin creek for micro hydro power generation: An assessment. Sustainable Energy Technologies and Assessments 2019; 32:111-20.

Chen Q, Allgeier A, Yin D, Hollert H. Leaching of endocrine disrupting chemicals from marine microplastics and mesoplastics under common life stress conditions. Environment International 2019;130:1-2.

Chen Q, Reisser J, Cunsolo S, Kwadijk C, Kotterman M, Proeitti M, et al. Pollutants in Plastics within the North Pacific Subtropical Gyre. Environmental Science and Technology 2018;52(2):446-56.

Cole M, Lindeque P, Fileman E, Halsband C, Goodhead R, Moger J, et al. Microplastic Ingestion by Zooplankton. Environmental Science and Technology 2013;47(12):6646-55

Corcoran PL. Benthic plastic debris in marine and freshwater environments. Environmental Science: Processes and Impacts 2015;17(8):1363-69.

Deocaris CC, Allosada JO, Ardiente LT, Bitang LLG, Dulohan CL, Lapuz JKI, et al. Occurrence of microplastic fragments in the Pasig River. H_2Open Journal 2019;2(1):92-100.

Eerkes-Medrano D, Thompson R, Aldridge DC. Microplastics in freshwater systems: A review of the emerging threats, identification of knowledge gaps and prioritization of research needs. Water Research 2015;75:63-82.

Eyheraguibel B, Leremboure M, Traikia M, Sancelme M, Bonhomme S, Fromageot D, et al. Environmental scenarii for the degradation of oxo-polymers. Chemosphere 2018;198: 182-90.

Faure F, Corbaz M, Baecher H, de Alencastro L. Pollution due to plastics and microplastics in Lake Geneva and in the Mediterranean Sea. Archives des Sciences 2012;65:157-64.

Fendall LS, Sewell MA. Contributing to marine pollution by washing your face: Microplastics in facial cleansers. Marine Pollution Bulletin 2009;58:1225-8.

Gallagher A, Rees A, Rowe R, Stevens J, Wright P. Microplastics in the Solent estuarine complex, UK: An initial assessment. Marine Pollution Bulletin 2016;102(2):243-9.

Joint Group of Experts on the Scientific Aspects of Marine Environmental Protection (GESAMP). Sources, Fate and Effects of Microplastics in the Marine Environment: A Global Assessment. London England, United Kingdom: International Maritime Organization; 2015.

Gray AD, Wertz H, Leads RR, Weinstein JE. Microplastic in two South Carolina Estuaries: Occurrence, distribution, and composition. Marine Pollution Bulletin 2018;128:223-33.

Guzzetti E, Sureda A, Tejada A, Faggio C. Microplastic in marine organism: Environmental and toxicological effects. Environmental Toxicology and Pharmacology 2018;64:164-71.

Hidalgo-Ruz V, Gutow L, Thompson RC, Thiel M. Microplastics in the marine environment: A review of the methods used for identification and quantification. Environmental Science and Technology 2012;46(6):3060-75.

Horton AA, Svendsen C, Williams RJ, Spurgeon DJ, Lahive E. Large microplastic particles in sediments of tributaries of the River Thames, UK - Abundance, sources and methods for effective quantification. Marine Pollution Bulletin 2017; 114(1):218-26.

Hurley R, Woodward J, Rothwell JJ. Microplastic contamination of riverbeds significantly reduced by catchment-wide flooding. Nature Geoscience 2018;11:251-7.

Jung MR, Horgen FD, Orski SV, Rodriguez VC, Beers KL, Balazs GH, et al. Validation of ATR FT-IR to identify polymers of plastic marine debris, including those ingested by marine organisms. Marine Pollution Bulletin 2018;127:704-16.

Käppler A, Windrich F, Löder MGJ, Malanin M, Fischer D, Labrenz M, et al. Identification of microplastics by FTIR and

Raman microscopy: A novel silicon filter substrate opens the important spectral range below 1300 cm^{-1} for FTIR transmission measurements. Analytical and Bioanalytical Chemistry 2015;407:6791-801.

Kedzierski M, Tilly VL, Bourseau P, Bellegou H, César G, Sire O, et al. Microplastics elutriation from sandy sediments: A granulometric approach. Marine Pollution Bulletin 2016; 107(1):315-23.

Klein S, Worch E, Knepper TP. Occurrence and spatial distribution of microplastics in river shore sediments of the Rhine-Main area in Germany. Environmental Science and Technology 2015;49(10):6070-6.

Kowalski N, Reichardt AM, Waniek JJ. Sinking rates of microplastics and potential implications of their alteration by physical, biological, and chemical factors. Marine Pollution Bulletin 2016;109(1):310-9.

Lechner A, Keckeis H, Lumesberger-Loisl F, Zens B, Krusch R, Tritthart M, et al. The Danube so colourful: A potpourri of plastic litter outnumbers fish larvae in Europe's second largest river. Environmental Pollution 2014;188:177-81

Lenz R, Enders K, Stedmon CA, Mackenzie DMA, Nielsen TG. A critical assessment of visual identification of marine microplastic using Raman spectroscopy for analysis improvement. Marine Pollution Bulletin 2015;100(1):82-91.

Lehtiniemi M, Hartikainen S, Näkki P, Engström-Öst J, Koistinen A, Setälä, O. Size matters more than shape: Ingestion of primary and secondary microplastics by small predators. Food Webs 2018;17:1-6.

Li C, Busquets R, Campos LC. Assessment of microplastics in freshwater systems: A review. Science of the Total Environment 2020;707:1-12.

Liongson LQ, Tabios GQ, Daño AM. Laguna Lake's Tributary River Watersheds. In: Lasco RD, Espaldon MVO, editors. Ecosystems and People: The Philippine Millennium Ecosystem Assessment (MA) Subglobal Assessment. Environmental Forestry Programme, College of Forestry and Natural Resources, University of the Philippines Los Baños; 2005. p. 53-62.

López GI. Grain size analysis. In: Allan SG, editor. Encyclopedia of Geoarchaeology. 1st ed. Netherlands: Springer; 2017. p. 341-8.

Magalang AA. Municipal solid waste management in the Philippines. In: Pariatamby A, Tanaka M, editors. Municipal Solid Waste Management in Asia and the Pacific Islands. Singapore: Springer; 2014. p. 281-98.

Mani T, Hauk A, Walter U, Burkhardt-Holm P. Microplastics profile along the Rhine River. Scientific Reports 2015;5(1):1-7.

Masura J, Baker J, Foster G, Arthur C, Herring C. Laboratory Methods for the Analysis of Microplastics in the Marine Environment: Recommendations for Quantifying Synthetic Particles in Waters and Sediments. Maryland, USA: NOAA Marine Debris Division; 2015.

Nizzetto L, Bussi G, Futter MN, Butterfield D, Whitehead PG. A theoretical assessment of microplastic transport in river catchments and their retention by soils and river sediments. Environmental Science: Processes and Impacts 2016; 18(8):1050-9.

Paller VGV, Labatos BV, Lontoc BM, Matalog OE, Ocampo PP. Freshwater fish fauna in watersheds of Mt. Makiling Forest Reserve, Laguna, Philippines. Philippine Journal of Science 2011;140(2):195-206.

Peng G, Xu P, Zhu B, Bai M, Li D. Microplastics in freshwater river sediments in Shanghai, China: A case study of risk assessment in mega-cities. Environmental Pollution 2018; 234:448-56.

Peng G, Zhu B, Yang D, Su L, Shi H, Li D. Microplastics in sediments of the Changjiang Estuary, China. Environmental Pollution 2017;225:283-90.

Sadri SS, Thompson RC. On the quantity and composition of floating plastic debris entering and leaving the Tamar Estuary, Southwest England. Marine Pollution Bulletin 2014;81(1): 55-60.

Saley AM, Smart AC, Bezerra MF, Burnhum TLU, Capece LR, Lima LFO, et al. Microplastic accumulation and biomagnification in a coastal marine reserve situated in a sparsely populated area. Marine Pollution Bulletin 2019;146:54-9.

Sanchez W, Bender C, Porcher JM. Wild gudgeons (*Gobio gobio*) from French rivers are contaminated by microplastics: Preliminary study and first evidence. Environmental Research 2014;128:98-100.

Shim WJ, Hong SH, Eo SE. Identification methods in microplastic analysis: A review. Analytical Methods 2017;9(9):1384-91.

Simon M, van Alst N, Vollertsen J. Quantification of microplastic mass and removal rates at wastewater treatment plants applying Focal Plane Array (FPA)-based Fourier Transform Infrared (FT-IR) imaging. Water Research 2018;142:1-9.

Song YK, Hong SH, Jang M, Han GM, Rani M, Lee J, et al. A comparison of microscopic and spectroscopic identification methods for analysis of microplastics in environmental samples. Marine Pollution Bulletin 2015;93(1-2):202-9.

Thompson RC, Olsen Y, Mitchell RP, Davis A, Rowland SJ, John AWG, et al. Lost at sea: Where is all the plastic? Science 2004;304(5672):838.

Tibbetts J, Krause S, Lynch I, Sambrook SG. Abundance, distribution, and drivers of microplastic contamination in urban river environments. Water 2018;10(11):1597-611.

Wagner M, Scherer C, Alvarez-Muñoz D, Brennholt N, Bourrain X, Buchinger S, et al. Microplastics in freshwater ecosystems: What we know and what we need to know. Environmental Sciences Europe 2014;26:12.

Whitmire SL, van Bloem SJ, Toline CA. Quantification of Microplastics on National Park Beaches. NOAA Marine Debris Program; 2017.

Vaughan R, Turner SD, Rose NL. Microplastics in the sediments of a UK urban lake. Environmental Pollution 2017;229:10-8.

Vendel AL, Bessa F, Alves VEN, Amorim ALA, Patricio J, Palma ART. Widespread microplastic ingestion by fish assemblages in tropical estuaries subjected to anthropogenic pressures. Marine Pollution Bulletin 2017;117(1-2):448-55.

Vermaire JC, Pomeroy C, Herczegh SM, Haggart O, Murphy M. Microplastic abundance and distribution in the open water and sediment of the Ottawa River, Canada, and its tributaries. FACETS 2017;2:301-14.

Vianello A, Boldrin A, Guerriero P, Moschino V, Rella R, Sturaro A, et al. Microplastic particles in sediments of Lagoon of Venice, Italy: First observations on occurrence, spatial patterns and identification. Estuarine, Coastal and Shelf Science 2013;130:54-61.

Yurtsever M, Yurtsever U. Commonly used disposable plastic bags as a source of microplastic in environment. Proceedings of the International Conference on Microplastic Pollution in the Mediterranean Sea; 2017 Sept 26-29; Capri: Italy; 2017.

Hydrogeochemical Analysis of Phewa Lake: A Lesser Himalayan Lake in the Pokhara Valley, Nepal

Udhab Raj Khadka[1,2*] and AL. Ramanathan[2]

[1]Central Department of Environmental Science, Tribhuvan University, Kathmandu, Nepal
[2]School of Environmental Sciences, Jawaharlal Nehru University, New Delhi 110067, India

ARTICLE INFO

Received: 20 May 2020
Received in revised: 11 Sep 2020
Accepted: 5 Oct 2020
Published online: 24 Nov 2020
DOI: 10.32526/ennrj/19/2020083

Keywords:
Eutrophication/ Lake characteristics/ Major ion/ Trophic status/ Weathering

*** Corresponding author:**
E-mail: ukhadka@cdes.edu.np

ABSTRACT

Phewa Lake in Nepal is a lake of international importance providing crucial ecological and economic services. However, increased urbanization, population growth and anthropogenic activities have resulted in degradation of the lake. Thus, understanding the lake hydro-geochemistry is crucial for identifying sources of elements. Preceding studies have mostly covered limnological and physico-chemical assessments which are not sufficient to explain the lake catchment characteristics. This study has assessed the major ions in relation to their hydro-geochemical processes in the catchment. To evaluate monsoonal impact, the rainwater was also analyzed. The major ions were determined by using standard methods. The results revealed significant seasonal variations in temperature, pH, TDS, EC, and most of the major ions. There was domination of the total anions (Tz^-) over the total cations (Tz^+) indicating possible ionic contribution through decomposition of organic compounds. The domination of Ca^{2+}, Mg^{2+} and HCO_3^- elucidates influence of carbonate weathering. The high (>1) equivalent ratio for $(Ca^{2+}+Mg^{2+})/(Na^++K^+)$, and $(Ca^{2+}+Mg^{2+})/(Tz^+)$ ratio ≈1 also suggest abundance of $(Ca^{2+}+Mg^{2+})$ and prevalence of carbonate weathering. The low (<0.5) $(Na^++K^+)/Tz^+$ ratio suggests lesser contribution of cations via alumino-silicate weathering. The positive correlation between Ca^{2+} and Mg^{2+}, and SO_4^{2-} and Ca^{2+} indicate their common sources. Although the major ions were within the acceptable limits for irrigation, fish farming and recreation purposes, the increased trophic status of the lake suggests possibility of other processes making the limiting nutrients available for algal and macrophytes growth. Further studies incorporating sediment-water interaction is anticipated for the better management of the lake.

1. INTRODUCTION

Lakes and reservoirs play a vital role in the cycling of elements. However, the present increased urbanization and anthropogenic pressure has hastened the transport of lithogenic and anthropogenic elements to the lakes altering the lake characteristics (Das et al., 1995). The elements brought to the lake are not primarily fixed on the sediment, and can be released back to the water-column with the change in environmental conditions (Forstner and Wittmann, 1983; Håkanson, 2004; Singh et al., 2005). Hence, knowing lake water chemistry is important for determining its use in domestic, recreational, irrigational and industrial purposes and understanding the nature of the catchment lithology, soil erosion, precipitation and anthropogenic activity. Additionally, it is important for determining the source of elements to the lake and understanding seasonal changes (Anshumali and Ramanathan, 2007; Das and Kaur, 2001).

The lakes in the Pokhara Valley are threatened by siltation, urbanization, land-use change and agricultural activity in the catchment and degradation of water quality (Rai, 2000a; Ross and Gilbert, 1999). As the high altitude lakes react faster to the changes in their environment; these lakes are vulnerable (Vreca and Muri, 2006). The Pokhara Valley has nine lakes playing a key role in maintaining regional hydrological cycle by recharging water, controlling flood and trapping sediment along with their

Citation: Khadka UR, Ramanathan AL. Hydrogeochemical analysis of Phewa Lake: a lesser Himalayan Lake in the Pokhara Valley, Nepal. Environ. Nat. Resour. J. 2021;19(1):68-83. (https://doi.org/10.32526/ennrj/19/2020083)

contribution in economy, tourism and biodiversity. Thus, the Lake Cluster of Pokhara Valley has been recognized as the Ramsar Site on 2nd February, 2016 (Ramsar, 2016). Phewa Lake is the largest lake of the cluster and second largest of Nepal with biologically rich watershed (Oli, 1997; Shrestha and Janauer, 2001). Giri and Chalise (2008) reported 39 species of water-birds including 15 winter visitors, 10 resident, 10 occasional visitors, and 4 rare winter visitors. Besides, this is a multipurpose lake used for irrigation, commercial fish farming and fishery research, cultural sites, and recreation. Thousands of people depend on the lake for their livelihood and income generation from tourism, fisheries, irrigation, power generation and water supply (Ramsar, 2016). According to CSUWN (2011), the lake catchment area provides annual economic benefits worth USD 43.6 million through various ecosystem services. The study has also reported the lake as one of the attractive tourist destinations accounting 203,527 international and 200,000 domestic tourist visitors in the fiscal year 2008/2009. MoFE (2018) and Poudyal et al. (2016) have enlisted 23 ecosystem services of the local, regional and global importance provided by Phewa Lake Watershed. Moreover, as a Ramsar site, Phewa Lake provides habitats for various aquatic lives including endemic and migratory water fowls. The lake watershed is mostly covered by forest (47%) followed by agriculture (39.6%), water body and wetland (4.9%), built-up land (4.8%), waste land (2.7%) and bush/scrub and grass (1%) (Regmi et al., 2017). The settlement in the catchment includes six villages of Pokhara Metropolitan City. The urban land includes a large number of hotels and restaurants on the north-eastern shore. The growing population and urbanization in the catchment are causing municipal discharge, discharge from hotels/restaurants and sub-surface flow from septic tanks leading to sedimentation and siltation, and water quality deterioration (Rai, 2000a; Ross and Gilbert, 1999). Based on the rate of areal decline and sediment influx, 80% storage capacity of Phewa Lake has been reported to be lost by the next 110-347 years (Watson et al., 2019).

Phewa Lake is one of the better-studied lakes in the Pokhara Valley (Adhikari and Khadka, 2017; Ferro and Swar, 1978; Gurung et al., 2006; Gurung et al., 2010; Hickel, 1973; Jones et al., 1989; Kato and Hayashi, 1982; Pradhan and Kim, 2017; Rai, 2000a; Rai, 2000b; Regmi et al., 2017; Ross and Gilbert, 1999; Rowbotham and Dudycha, 1998; Swar and Fernando, 1979a; Swar and Fernando, 1979b; Swar and Fernando, 1980; Watson et al., 2019). However, the preceding works have mostly covered limnology, land-use studies, slope stability assessment, morphological changes and geological studies indicating very scarce hydro-geochemical studies. Thus, the present study has attempted to assess the hydro-geochemical characteristics of Phewa Lake. Besides, the study has also focused on examining the monsoon rain water for understanding impact of monsoon on the lake water. Findings of the study could be useful in future sustainable management of the Phewa Lake as well as other lakes in the region.

2. METHODOLOGY

2.1 Study area

The Pokhara Valley is characterized by the presence of Annapurna Himalaya, many lakes, and turbulent Seti River with a deep gorge (Figure 1). Phewa Lake lies in Pokhara Metropolitan City, the provincial capital of Gandaki Province and the second tourist destination after Kathmandu. The lake watershed occupies about 123 km^2 areas at 28°11'39" N to 28°17'25" N latitudes, and 83°47'51" E to 83°59'17" E longitudes within an elevation range from 789 m.a.s.l. to 2,508 m.a.s.l. (Regmi et al., 2017). The main inflows are perennial spring-fed streams, Harpan River with several small seasonal streams mostly draining during the monsoon. The lake has an area of 4.43 km^2 with maximum depth of 23.5 m and an average depth of 8.6 m (Gurung et al., 2006; Gurung et al., 2010) and a single outflow towards the southeast (Figure 1).

Geologically, the Pokhara Valley is an intermontane fluvial basin spread around the midstream of Seti River filled by a large volume of layered clastic deposits brought from the Annapurna Mountain (Yamanaka et al., 1982). The lake watershed constitutes weak, low-medium grade Pre-cambrian to early Cambrian grey phyllitic schists, talc-rich red phyllite schists (Ross and Gilbert, 1999; Rowbotham and Dudycha, 1998), quartzite schists inter-bedded with grey phyllite schists, carbonaceous conglomerate (Impat, 1980), and gneiss, granite, quartzite and schist (Gautam et al., 2000).

Climatically, the watershed is humid subtropical to temperate type with maximum monthly temperature ranging from 21.9±1.5°C (January) to 32.0±1.5°C (April); and minimum temperature ranging from 8.4±1.9°C (January) to 22.9±0.9°C (July) accounting more than 80% annual rainfall during June to September with humidity variation from 66.04±11.74% (April) to 94.06±2.43% (January) (Table 1).

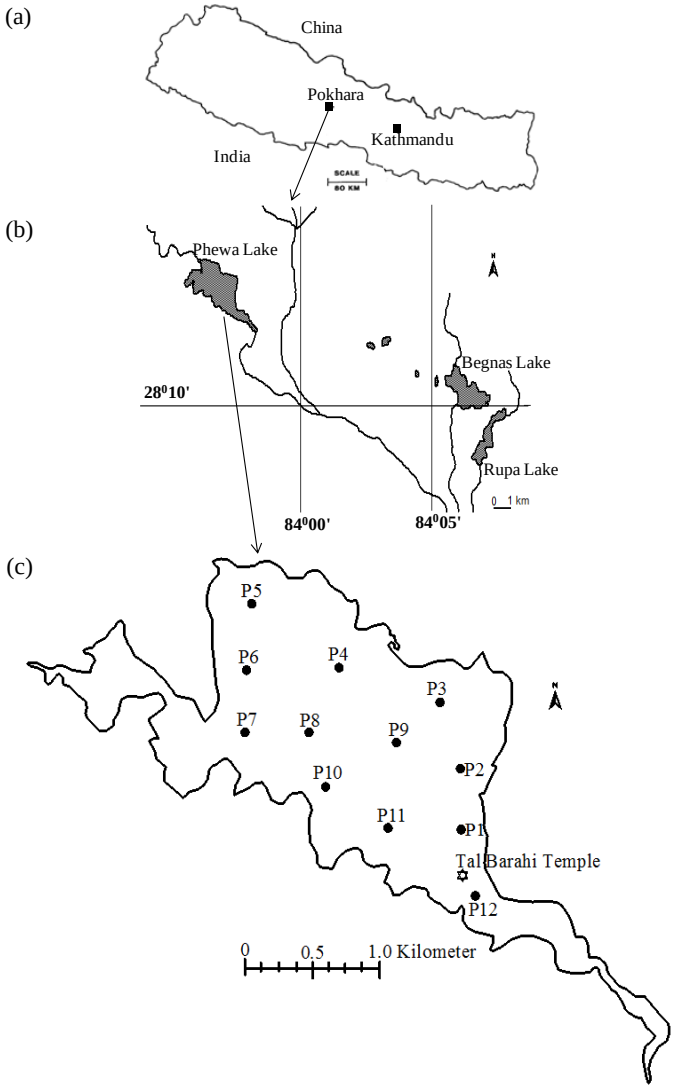

Figure 1. Location of the study area (a) showing distribution of lakes in the valley; (b) and sampling locations in Phewa Lake; (c) (Modified Hickel, 1973)

Table 1. The climatic condition of the study area during study period (2008-2009). Units: temperature in °C, humidity in %, and rainfall in mm

Season	Months	Max. Temp	Min. Temp	Humidity*	Humidity**	Rainfall
Post-monsoon	Oct	28.35±1.08	15.79±1.63	85.27±5.37	67.65±6.05	102.8
	Nov	25.37±1.52	11.95±1.75	86.89±5.83	60.75±8.03	-
	Dec	22.33±1.59	9.52±1.43	93.34±4.17	65.04±6.28	-
	Jan	21.89±1.49	8.42±1.86	94.06±2.43	57.96±6.51	-
Pre-monsoon	Feb	25.71±1.65	10.62±1.15	84.92±6.45	41.53±8.22	-
	Mar	28.65±1.78	12.62±1.45	69.09±7.50	41.74±9.52	25.3
	Apr	32.00±1.51	17.37±2.19	66.04±11.74	39.53±15.60	45.6
	May	30.78±2.10	19.14±1.56	75.91±11.98	58.30±14.87	260.2
Monsoon	Jun	31.52±2.01	21.43±1.53	81.30±10.79	68.50±11.53	609.3
	Jul	31.13±2.33	22.85±0.92	90.46±5.69	73.40±9.85	762.7
	Aug	30.51±1.98	22.57±1.01	91.41±3.88	78.03±9.38	1026.2
	Sept	30.28±1.72	21.03±0.88	86.82±6.02	73.71±7.54	302.5

Data source: Department of Hydrology and Meteorology, Government of Nepal (***** Humidity at 8:45 am and ** at 5:45 pm)

2.2 Sample collection and analysis

The 12 surficial water samples from Phewa Lake were collected during November 2008 (post-monsoon), April 2009 (pre-monsoon), and August 2009 (monsoon) from 12 locations, here referred as P1, P2, P3……P12 (Figure 1(c)), ensuring representation of the total lake area, traversing on a rowboat. The subsequent season's samples were carefully collected from the same locations. Two sets of water samples were collected for cation and anion analyses. For cation analysis, samples were preserved in nitric acid (HNO_3) to avoid precipitation or adsorption (APHA, 2005). All the samples were stored in properly cleaned plastic bottles, soaked overnight in HNO_3 (5% v/v), and rinsed with MilliQ water. The bottles were pre-washed with the water sample to be collected. Three rain water samples were collected from city area of Pokhara in a single rain event in August 2009 in properly cleaned and pre-washed plastic bags.

Water parameters like hydrogen ion concentration (pH), electrical conductivity (EC), bicarbonate (HCO_3^-), total dissolved solids (TDS) and dissolved oxygen (DO) were measured on-site using respective portable electrodes for pH, EC and TDS; acid titration method for HCO_3^- and Winkler's method for DO (APHA, 2005). The water samples were filtered through 0.45 µm cellulose filter paper and transported in an ice box and analyzed at the hydro-geochemistry laboratory of School of Environment Sciences, Jawaharlal Nehru University, New Delhi, India. Dissolved Cl^- was determined by colorimetric method, SO_4^{2-} by turbidimetric method, PO_4^{3-} by ascorbic acid method (APHA, 2005), NO_3^- by nitration of salicylic acid (Diatloff and Rengel, 2001) and dissolved H_4SiO_4 by molybdosilicate blue method (Strickland and Parsons, 1968). The major cations like Na^+, K^+, Mg^{2+}, and Ca^{2+} were determined by the Atomic Absorption Spectrophotometer (AAS-Thermo Scientific M Series). The high grade reagents and MilliQ water (Model Milli-Q, Biocell) were used during the analyses. In every analysis, controls were performed on appropriate blank solutions and precision was maintained by running known standard after every ten samples. The analytical precision was within ±10%. The data acquired were analyzed using Statistical Package for Social Sciences (SPSS) version 17.0.

3. RESULTS AND DISCUSSION

3.1 Physico-chemical characteristics of the lake water

The physico-chemical characteristics of the lake water show spatial and seasonal variations. Temperature is an important parameter regulating lake stratification. In Phewa Lake, the surface water temperature followed the pattern of the ambient temperature (Table 1) showing higher values during the monsoon (27.9±0.9°C) compared to pre-monsoon (26.3±0.5°C) and post-monsoon (23.5±0.8°C) with significant ($p<0.05$) seasonal variation (Table 2).

The pH is an important parameter controlling weathering patterns and availability of the dissolved solids in lakes. In Phewa Lake, pH ranged from slightly acidic (6.5) to alkaline (8.0) during post-monsoon, neutral (7.0) to alkaline (9.1) during pre-monsoon and alkaline (7.5-7.9) during monsoon with significant variation ($p<0.05$) between post-monsoon and pre-monsoon, and pre-monsoon and monsoon (Table 2). Rai (2000a) observed pH variation from 6.3 (August-September) to 9.7 (May). The increase in pH during pre-monsoon can be attributed to the increased rate of photosynthesis by primary producers (Das et al., 2009). The peak value of phytoplankton cell numbers and abundance of phytoplankton species during pre-monsoon (Gurung et al., 2006) indicates the role of productivity in regulating the lake water pH.

The TDS is the sum of all the ions in aqueous solution which reflects magnitude of chemical weathering in the catchment (Singh and Hasnain, 1999). In Phewa Lake, TDS ranged from 54.2 to 97.73 mg/L with highest value during post-monsoon and lowest during monsoon with significant variation ($p<0.05$) between the seasons (Table 2). Likewise, EC is the ionic strength of solution that depends on concentration, volume and movement rate of ionic species (Das and Kaur, 2001). In Phewa Lake, EC showed a similar pattern as the TDS (Table 2). The lower TDS and EC during monsoon may be due to the dilution effect (Ross, 1998) and uptake of calcium by phytoplankton (Ross and Gilbert, 1999). Ross and Gilbert (1999) even observed increase in conductivity with the increase in distance from the river mouth, probably due to cumulative effect of dissolution of carbonaceous conglomerates, the input of contaminated runoff from the city and diversion of water to the lake through the Seti Canal, relatively carbonate-rich watershed of the Seti River.

Table 2. Physico-chemical composition of the surface water in Phewa Lake. Units: Temperature in °C, pH, EC in µS/cm, TDS, ions and ionic compounds in mg/L, and Tz^+ and Tz^- in µeq/L

Parameter	Post-monsoon		Pre-monsoon		Monsoon	
	Range	Average±SD	Range	Average±SD	Range	Average±SD
Temperature	22.5-25.0	23.54 ± 0.81^a	26.0-27.0	26.25 ± 0.45^b	26.75-29.0	27.92 ± 0.89^c
pH	6.5-8.0	7.5 ± 0.50^a	7.0-9.1	8.6 ± 0.6^b	7.5-7.9	7.7 ± 0.1^a
EC	116.92-125.69	120.48 ± 2.52^a	66.67-86.38	80.64 ± 4.93^b	52.16-65.73	58.23 ± 4.04^c
TDS	94.12-102.7	97.73 ± 2.97^a	63.41-77.18	72.76 ± 3.73^b	50.38-58.51	54.18 ± 2.8^c
DO	7.0-11.0	8.42 ± 1.0^a	10.0- 10.8	10.25 ± 0.24^b	12.0-13.2	12.52 ± 0.39^c
HCO_3^-	38.77-42.51	40.91 ± 1.02^a	20.14-33.88	26.95 ± 4.27^b	11.86-18.43	16.88 ± 1.79^c
Cl^-	0.76-2.5	1.29 ± 0.47^a	1.46-8.51	2.74 ± 1.88^b	0.33-2.21	0.69 ± 0.60^a
SO_4^{2-}	8.32-10.57	9.12 ± 0.67^a	6.97-8.6	7.62 ± 0.51^b	8.73-13.54	10.75 ± 1.46^c
PO_4^{3-}	0.0-0.14	0.09 ± 0.04^a	0.07-0.3	0.13 ± 0.06^a	0.01-0.07	0.03 ± 0.02^b
NO_3^-	3.26-5.38	4.32 ± 0.87^a	4.41-14.09	7.74 ± 2.99^b	3.23-4.36	3.82 ± 0.4^a
H_4SiO_4	9.47-15.34	11.02 ± 2.21^a	8.13-9.06	8.68 ± 0.27^b	7.48-8.42	7.89 ± 0.26^b
Na^+	1.76-3.62	2.82 ± 0.61^a	3.37-3.49	3.44 ± 0.03^b	3.26-4.36	3.72 ± 0.35^b
K^+	0.52-4.37	1.28±1.02	1.15-2.48	1.39±0.36	1.08-1.87	1.54±0.25
Mg^{2+}	2.15-2.44	2.29 ± 0.08^a	1.49-1.61	1.54 ± 0.04^b	1.12-2.67	1.7 ± 0.38^b
Ca^{2+}	14.0-17.87	16.7 ± 1.07^a	6.24-7.63	6.92 ± 0.40^b	2.08-2.75	2.44 ± 0.19^c
Tz^+	1,159-1,229	$1,193\pm20.4^a$	627.2-706.8	665.5 ± 23.4^b	425.3-537	473.4 ± 33.06^c
Tz^-	950.4-999.1	969.3 ± 14.0^a	666.7-863.8	806.4 ± 49.3^b	521.6-657.3	582.3 ± 40.4^c

Different alphabets in superscript indicate significant difference in the mean values ($p<0.05$)

The DO reflects the organic pollution state of the water. In Phewa Lake, DO ranged from 8.4 to 12.5 mg/L with significant variation ($p<0.05$) between the seasons (Table 2). The higher DO during the monsoon indicates that water is well oxygenated and lower DO during post-monsoon is attributed to the beginning of water circulation due to change in temperature (Gurung et al., 2006; Rai, 2000a). The higher Biological Oxygen Demand during post-monsoon (January and December) (PSMC, 2007) suggests the high discharge and decomposition of organic matter which is also evident from low DO (Rai, 2000a; Gurung et al., 2006).

Among the major ions, HCO_3^-, PO_4^{3-}, H_4SiO_4, Mg^{2+}, Ca^{2+}, and both total cations (Tz^+) and total anions (Tz^-) are higher in the post-monsoon; Cl^-, NO_3^-, and Na^+ are higher in the pre-monsoon and SO_4^{2-} is higher in the monsoon season. Among the anions, HCO_3^- is mainly contributed from weathering and decomposition of organic matter in the catchment (Chakrapani et al., 2009; Jha et al., 2009). In Phewa Lake, HCO_3^- was the dominant anion which ranged from 16.9 to 40.9 mg/L (Table 2). The HCO_3^- dominance suggests intense chemical weathering. Chloride is a conservative anion generally originating either from sea spray via monsoon or from anthropogenic sources (Meybeck, 1983). In Phewa Lake, Cl^- varied from 0.69 to 2.74 mg/L (Table 2). The lower value of HCO_3^- and Cl^- during monsoon could be attributed to the dilution effect of the monsoon (Table 3).

Sulfur is a widespread element in the earth and is among the ten most abundant elements in the biological system. Thus, it is an essential element for organisms. In lakes, it is usually derived from oxidative weathering of sulfide bearing minerals, atmospheric deposition, dissolution of gypsum ($CaSO_4{\cdot}2H_2O$), pyrite (FeS_2) rocks and/or by mineralization of organic sulfur in humus present in the bottom soil and sediments at the interface between aerobic and anaerobic environment. Such processes are common at the surface of reduced sediment which is covered by oxygenated water (Anshumali and Ramanathan, 2007; Jones, 1982). In Phewa Lake, SO_4^{2-} ranged from 7.6 to 10.8 mg/L with significant variation between the seasons (Table 2). The higher value during post-monsoon and monsoon may be due to the monsoonal runoff from agriculture and/or due to the combined effect of weathering and mineralization of autochthonous or allochthonous organic humus brought by the monsoonal runoff from agriculture. The results show SO_4^{2-} is substantially higher than the background value, 0.2 mg/L (Jones et al., 1989) demonstrating considerable increase over the period.

Table 3. Characteristics of rainwater collected from the Pokhara City. Units: Temperature in °C, pH, EC in µS/cm, TDS, ions and ionic compounds in mg/L

Parameter	Monsoon Rainwater	
	Range	Average±SD
Temperature	21.5-23.0	22.25±0.69
pH	6.7-6.8	6.73±0.1
EC	26.13-29.1	27.64±2.58
TDS	21.38-24.0	22.65±0.96
DO	11.5-13.46	12.75±1.35
HCO_3^-	10.41-11.86	11.35±0.57
Cl^-	<0.25	<0.25
SO_4^{2-}	3.2-4.5	3.67±0.58
PO_4^{3-}	0.01-0.01	0.01±0.0
NO_3^-	3.0-4.36	3.81±0.64
H_4SiO_4	0.19-0.23	0.22±0.01
Na^+	0.15-0.88	0.52±0.4
K^+	0.09-0.33	0.21±0.13
Mg^{2+}	0.04-0.04	0.04±0.0
Ca^{2+}	0.53-0.88	0.70±0.19

Phosphorus is one of the most important limiting elements, thus its abundance is the major reason for lakes eutrophication. In Phewa Lake, PO_4^{3-} ranged from 0.03 to 0.13 mg/L showing significant variation ($p<0.05$) between post-monsoon and monsoon, and pre-monsoon and monsoon (Table 2). The higher value during the pre-monsoon may be due to evaporation effect. The distribution map reveals that during post-monsoon PO_4^{3-} concentrated towards the western, eastern, northern and south-eastern parts (Figure 2(a)) which is associated with agriculture, settlement and urban land-uses. During the pre-monsoon, PO_4^{3-} concentrated mostly towards the east (near temple) indicating anthropogenic contribution (Figure 2(b)), and during monsoon, it concentrated towards the eastern part (Figure 2(c)) which is mainly associated with urban activities. The PO_4^{3-} values of >0.05 mg/L during pre-monsoon and post-monsoon indicate anthropogenic input (Subramanian, 1984). Rai (2000a) reported PO_4^{3-} concentration up to 0.06 mg/L suggesting increase in PO_4^{3-} over the years.

The total nitrate nitrogen in water is derived either from atmospheric precipitation, biological conversion or anthropogenic inputs. In Phewa Lake, NO_3^- varied from 3.8 to 7.7 mg/L with significant variation between the post-monsoon and pre-monsoon, and pre-monsoon and monsoon (Table 2). The higher value during pre-monsoon may be due to the combined effect of evaporation and mineralization of N-containing compounds by microorganisms (Anshumali and Ramanathan, 2007; Håkanson, 1984). The NO_3^- in the monsoon possibly indicates the influence of leaching of fertilizers from agriculture. With respect to its spatial distribution, during post-monsoon, NO_3^- concentrated towards the north-western and south-western parts (Figure 2(d)) which is associated with settlement, agriculture and urban land-uses; during pre-monsoon, it concentrated towards the south-western part (Figure 2(e)) which is associated with anthropogenic inputs, and during monsoon, it spread towards the north-western, north-eastern and eastern parts (Figure 2(f)) which is associated with agriculture, settlement and urban land-uses. Rai (2000a) reported (NO_2^-+NO_3^-)-nitrogen upto 0.45 mg/L indicating increase in NO_3^- over the time.

Silicon is the second most abundant element in the earth's crust and is essential for life. In lakes, it is available for phytoplankton and algae as H_4SiO_4. In Phewa Lake, H_4SiO_4 ranged from 7.9 to 11.0 mg/L with significant variation between post-monsoon and pre-monsoon, and post-monsoon and monsoon (Table 2). The higher value during the post-monsoon might be due to the mixing which develops a vertical gradient of temperature that promotes death and decomposition of diatoms, besides weathering of the silicate minerals (Anshumali and Ramanathan, 2007; Håkanson, 1984). This is also supported by the high H_4SiO_4/Na^++K^+ ratio (Table 4). Similar finding has been reported by Anshumali and Ramanathan (2007) in Pandoh Lake of India. The dissolved silica in the pre-monsoon (8.68±0.27 mg/L) and monsoon (7.89±0.26 mg/L) are comparable to the Indian Himalayan River average, 9.6 mg/L; however the post-monsoon concentration (11.02±2.21 mg/L) is comparable to the world average, 12.0 mg/L (Subramanian, 1979). The present results show H_4SiO_4 value is substantially higher than the findings of Jones et al. (1989) (<1 mg/L SiO_2). The lower value of silica in Phewa Lake compared to the global average indicates silicate minerals are resistant to the prevailing weathering conditions. The silica may also be contributed by the dissolution of concrete in streets and sidewalks (Ravindra and Garg, 2007). The low pH supports a lower rate of silicate weathering which is evident from the positive correlation between H_4SiO_4 and pH during post-monsoon and pre-monsoon periods (Table 5 and Table 6). The negative correlation between silica, and bicarbonate and nitrate indicates their different sources (Table 7).

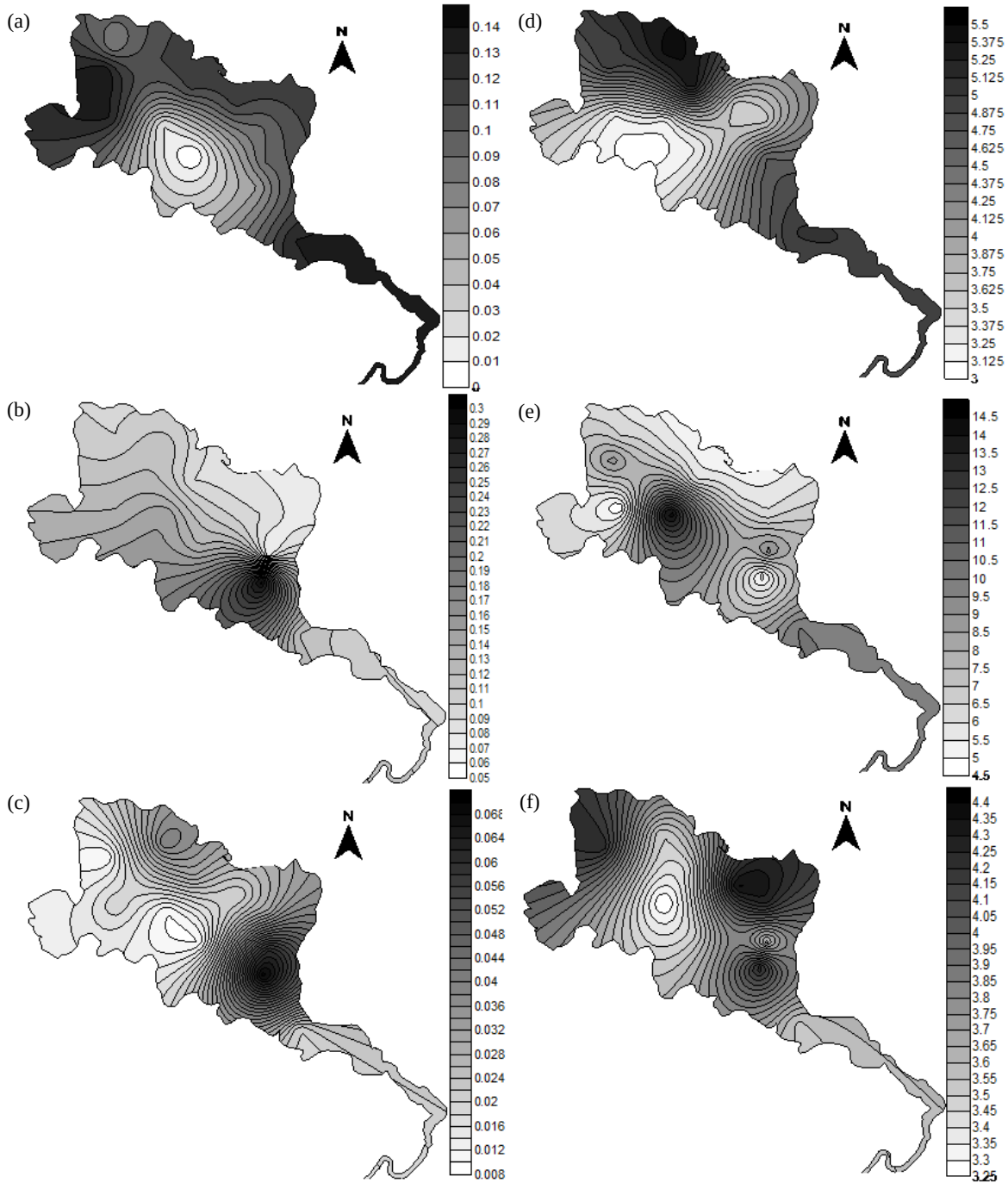

Figure 2. Isoline map showing surficial distribution of PO_4^{3-} (a=post-monsoon, b=pre-monsoon, c=monsoon) and NO_3^- (d=post-monsoon, e=pre-monsoon, f=monsoon)

Among the cations, Na^+ varied from 2.8 to 3.7 mg/L with significant variation between the post-monsoon and pre-monsoon, and post-monsoon and monsoon (Table 2). The higher value during monsoon could be due to rock weathering and continental runoff. Likewise, K^+ varied from 1.2 to 1.5 mg/L showing no significant variation between the seasons (Table 2). The higher value during monsoon may be due to silicate weathering. The surficial Mg^{2+} varied from 1.5 to 2.3 mg/L with significant variation between the post-monsoon and pre-monsoon, and post-monsoon and monsoon (Table 2). The surficial Ca^{2+} ranged from 2.4 to 16.7 mg/L with significant variation ($p<0.05$) between the seasons (Table 2). The lower Ca^{2+} during monsoon could be attributed to the dilution effect and uptake of Ca^{2+} by phytoplankton (Ross and Gilbert, 1999). The higher Ca^{2+} during post-monsoon is attributed to the release of additional Ca^{2+} by the decaying phytoplankton (Ross, 1998), in addition to the weathering processes. This is supported

Table 4. Ionic ratios of Phewa Lake in different seasons

Parameters	Post-monsoon		Pre-monsoon		Monsoon	
	Min-Max	Average±SD	Min-Max	Average±SD	Min-Max	Average±SD
$(Ca^{2+}+Mg^{2+})/(Tz^{+})$	0.77-0.9	0.86±0.04	0.69-0.72	0.71±0.01	0.46-0.65	0.55±0.05
$(Na^{+}+K^{+})/(Tz^{+})$	0.09-0.22	0.13±0.04	0.27-0.3	0.28±0.01	0.002-0.004	0.003±0.0
$H_4SiO_4/(Na^{+}+K^{+})$	0.4-1.48	0.8±0.33	0.4-0.52	0.49±0.03	0.34-0.47	0.41±0.041
$(Ca^{2+}+Mg^{2+})/(Na^{+}+K^{+})$	3.58-10.26	7.04±2.04	2.3-2.7	2.55±0.13	0.91-1.96	1.32±0.27
$HCO_3^{-}/(Ca^{2+}+Mg^{2+})$	0.59-0.76	0.66±0.04	0.68-1.16	0.93±0.14	0.8-1.35	1.07±0.14
$HCO_3^{-}/HCO_3^{-}+SO_4^{2-}$	0.75-0.8	0.78±0.01	0.69-0.79	0.73±0.03	0.41-0.61	0.55±0.05
$HCO_3^{-}/(Tz^{-})$	0.66-0.72	0.69±0.02	0.41-0.67	0.55±0.08	0.36-0.51	0.47±0.04

Table 5. Correlation matrix for the post-monsoon

Parameters	pH	TDS	EC	DO	HCO_3^{-}	Cl^{-}	SO_4^{2-}	PO_4^{3-}	NO_3^{-}	H_4SiO_4	Na^{+}	K^{+}	Mg^{2+}	Ca^{2+}
pH	1.00													
TDS	0.74**	1.00												
EC	0.45	0.46	1.00											
DO	-0.31	-0.03	-0.13	1.00										
HCO_3^{-}	0.36	0.75*	0.38	0.07	1.00									
Cl^{-}	0.09	-0.41	-0.02	-0.18	-0.77**	1.00								
SO_4^{2-}	0.13	0.30	0.37	-0.23	0.01	0.29	1.00							
PO_4^{3-}	-0.33	-0.49	-0.01	-0.07	-0.42	0.23	-0.14	1.00						
NO_3^{-}	-0.34	-0.27	-0.07	0.40	-0.11	-0.29	-0.66*	0.48	1.00					
H_4SiO_4	0.62*	0.88**	0.44	-0.02	0.63*	-0.45	0.19	-0.65*	-0.38	1.00				
Na^{+}	-0.26	-0.22	0.01	-0.04	0.25	-0.39	-0.39	0.63*	0.58*	-0.46	1.00			
K^{+}	0.24	0.00	0.20	-0.14	0.09	0.14	-0.25	-0.22	0.03	-0.21	0.18	1.00		
Mg^{2+}	-0.30	-0.54	-0.41	0.47	-0.29	0.17	-0.54	0.18	0.26	-0.42	0.13	0.17	1.00	
Ca^{2+}	0.12	0.32	0.17	0.04	-0.11	0.17	0.66*	-0.11	-0.39	0.43	-0.63*	-0.76*	-0.46	1.00

* Correlation significant at $p<0.05$ (2 tailed)

** Correlation significant at $p<0.01$ (2 tailed)

Table 6. Correlation matrix for the pre-monsoon

Parameters	pH	TDS	EC	DO	HCO_3^-	Cl^-	SO_4^{2-}	PO_4^{3-}	NO_3^-	H_4SiO_4	Na^+	K^+	Mg^{2+}	Ca^{2+}
pH	1.00													
TDS	0.30	1.00												
EC	0.04	0.95**	1.00											
DO	0.30	0.28	0.17	1.00										
HCO_3^-	0.45	0.63*	0.46	0.40	1.00									
Cl^-	-0.85**	-0.25	0.06	-0.33	-0.57	1.00								
SO_4^{2-}	0.17	0.16	0.07	0.22	0.21	-0.38	1.00							
PO_4^{3-}	-0.63*	-0.24	0.05	-0.24	-0.50	0.91**	-0.56	1.00						
NO_3^-	0.32	0.30	0.27	-0.08	-0.37	-0.16	-0.01	-0.14	1.00					
H_4SiO_4	0.63*	0.34	0.12	0.56	0.38	-0.60*	0.37	-0.48	0.18	1.00				
Na^+	0.62*	-0.08	-0.24	0.41	0.13	-0.39	0.01	-0.27	0.01	0.50	1.00			
K^+	-0.94**	-0.29	0.01	-0.42	-0.51	0.96**	-0.36	0.81**	-0.26	-0.70*	-0.52	1.00		
Mg^{2+}	0.13	0.05	0.12	-0.05	-0.07	0.10	-0.09	0.34	0.13	0.09	-0.11	-0.08	1.00	
Ca^{2+}	-0.23	0.73**	0.82**	0.09	0.34	0.29	-0.07	0.17	0.03	-0.07	-0.10	0.26	-0.17	1.00

* Correlation significant at p<0.05 (2 tailed)
** Correlation significant at p<0.01 (2 tailed)

Table 7. Correlation matrix for the monsoon

Parameters	pH	TDS	EC	DO	HCO_3^-	Cl^-	SO_4^{2-}	PO_4^{3-}	NO_3^-	H_4SiO_4	Na^+	K^+	Mg^{2+}	Ca^{2+}
pH	1.00													
TDS	0.12	1.00												
EC	0.13	0.98**	1.00											
DO	-0.26	0.27	0.17	1.00										
HCO_3^-	0.31	0.72**	0.66*	0.06	1.00									
Cl^-	0.54	0.27	0.41	-0.59*	0.22	1.00								
SO_4^{2-}	-0.52	0.33	0.33	0.47	-0.36	-0.29	1.00							
PO_4^{3-}	0.41	0.20	0.35	-0.63*	0.27	0.90**	-0.35	1.00						
NO_3^-	0.34	0.62*	0.60*	0.21	0.69*	0.23	-0.21	0.14	1.00					
H_4SiO_4	-0.09	-0.32	-0.29	-0.10	-0.70*	0.02	0.41	-0.09	-0.62*	1.00				
Na^+	-0.36	0.25	0.15	0.32	-0.02	-0.45	0.51	-0.62*	-0.15	0.06	1.00			
K^+	0.18	0.14	-0.03	0.58*	0.37	-0.62*	-0.08	-0.60*	0.19	-0.38	0.41	1.00		
Mg^{2+}	0.22	0.77**	0.87**	-0.03	0.48	0.68*	0.20	0.65*	0.50	-0.17	-0.27	-0.39	1.00	
Ca^{2+}	0.22	0.39	0.42	-0.13	0.45	0.36	-0.22	0.43	0.58*	-0.15	-0.56	-0.21	0.48	1.00

* Correlation significant at p<0.05 (2 tailed)
** Correlation significant at p<0.01 (2 tailed)

by a remarkable decrease in phytoplankton numbers and primary productivity during the post-monsoon (Gurung et al., 2006). Besides, the increase in Ca^{2+} could also be due to contribution from the dissolution of concrete in streets and sidewalks (Ravindra and Garg, 2007).

The surficial Tz^- (total anions) ranged from 582 to 969 µeq/L and the Tz^+ (total cations) ranged from 473 to 1193 µeq/L with significant ($p<0.05$) seasonal variations (Table 2). The higher Tz^- values during pre-monsoon and monsoon indicates possible contribution through decomposition of organic compounds (Dalai et al., 2002). The major ions composition of the lake water is within the range of the National Drinking Water Quality Standards and Directive 2005, thus lake water quality is acceptable for irrigation, fish farming and recreation (MoPPW, 2005). However, increasing trophic state of the lake over the period of time, as evident from massive growth of algae and water hyacinth, indicates possibility of other autochthonous processes making limiting nutrients available for the growth of algae and macrophytes. This suggests possibility of nutrients release from the lake sediments. Thus, in order to evaluate the possible internal source of nutrients, further studies incorporating sediment-water interaction need to be carried out.

3.2. Source of the major dissolved ions

The major dissolved ions are assessed to evaluate their sources and illustrate their relation to the regional geology and weathering processes. In Phewa Lake, among the cations, Ca^{2+} and Mg^{2+} were dominant over Na^+ and K^+ suggesting the dominant role of carbonate weathering (Table 2). The positive correlation between Ca^{2+} and Mg^{2+} ($r^2=0.48$) during monsoon suggests their common sources (Table 7). Likewise, the positive correlation between SO_4^{2-} and Ca^{2+} ($r^2=0.66$) during post-monsoon (Table 5) suggests their common origin like gypsum, oxidation of pyrite, dissolution of sulphate minerals and oxidation of sulfur compounds in the bottom sediment at the transition zone between aerobic and anaerobic environment (Ansumali and Ramanathan, 2007; Singh et al., 2016).

The ratios between different ions were modeled to explain their sources. In Phewa Lake, $(Ca^{2+}+Mg^{2+})/(Na^++K^+)$ ratio varied between 7.04±2.04 during post-monsoon, 2.55±0.13 during pre-monsoon, and 1.32±0.27 during monsoon, further supporting dominance of carbonate weathering (Table 4) corresponding with many Indian mountain lakes (Anshumali and Ramanathan, 2007; Das and Kaur, 2001; Jeelani and Shah, 2006; Singh et al. 2012; Singh et al., 2014; Singh et al., 2015a; Singh et al., 2015b; Singh et al., 2016). The $(Ca^{2+}+Mg^{2+})/(Tz^+)$ ratio varied from 0.77 to 0.90 during post-monsoon, 0.69 to 0.72 during pre-monsoon and 0.46 to 0.65 during monsoon suggesting domination of $Ca^{2+}+Mg^{2+}$ (Table 4). The $Ca^{2+}+Mg^{2+}$ vs. Tz^+ scatter plot (Figure 3) shows linear spread a little below the 1:1 line reflecting an increasing contribution of sodium and potassium with increase in TDS. This result suggests the major contribution of $Ca^{2+}+Mg^{2+}$ with a certain contribution of alkali derived possibly from silicate weathering (Das and Kaur, 2001). A similar trend has been reported by Bartarya (1993) in the Lesser Himalayan River Basin of Kumaun, India.

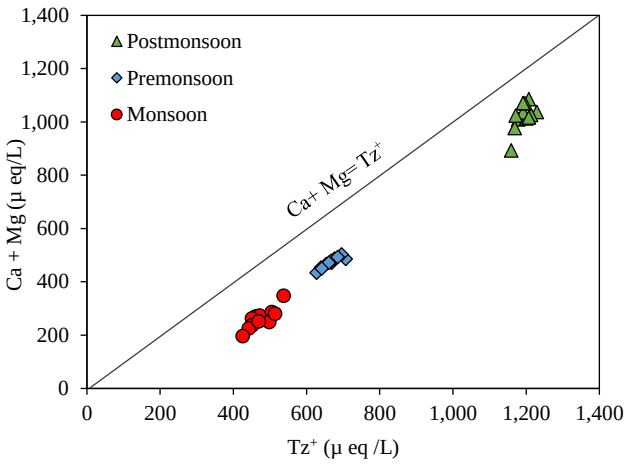

Figure 3. Scatter diagram of $Ca^{2+}+Mg^{2+}$ versus total cations (Tz^+) for Phewa Lake

The $(Na^++K^+)/(Tz^+)$ ratio is an index used for assessing contribution of cations via silicate weathering (Stallard and Edmund, 1983). In Phewa Lake, $(Na^++K^+)/Tz^+$ ratio varied between 0.13±0.04 during post-monsoon, 0.28±0.01 during pre-monsoon and 0.003±0.0 during monsoon indicating shortage of Na^+ and K^+ (Table 4). The low $(Na^++K^+)/Tz^+$ ratio suggests lower contribution of cations via alumino-silicate weathering compared to carbonate weathering. The Na^++K^+ vs. Tz^+ plot (Figure 4) further indicates that water is relatively deficient in Na^+ and K^+.

The scatter plot of $Ca^{2+}+Mg^{2+}$ vs. HCO_3^- (Figure 5) shows that pre-monsoon and monsoon samples mostly fall on or near 1:1 equiline suggesting HCO_3^- is balanced by Ca^{2+} and Mg^{2+}. However, the post-monsoon samples fall above the equiline requiring other anions to balance. The scatter plot of

$Ca^{2+}+Mg^{2+}$ vs. $HCO_3^-+SO_4^{2-}$ (Figure 6) shows the pre-monsoon and monsoon samples mostly fall below 1:1 equiline requiring a portion of HCO_3^- and SO_4^{2-} to be balanced by Na^++K^+ from silicate weathering. However, during post-monsoon, $Ca^{2+}+Mg^{2+}$ is still above the equiline requiring more neutralizing anions other than HCO_3^- and SO_4^{2-}.

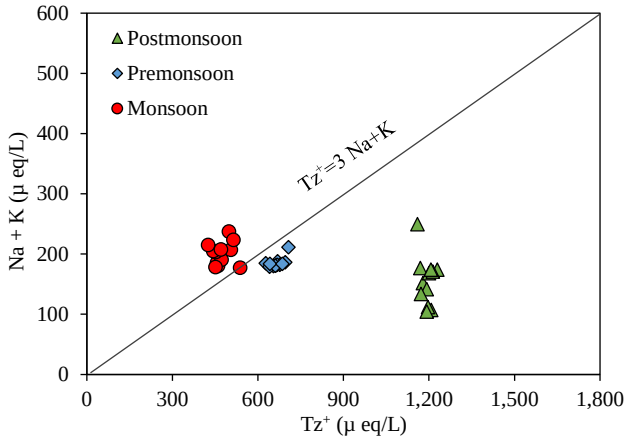

Figure 4. Scatter diagram of Na^++K^+ versus total cations (Tz^+) for Phewa Lake

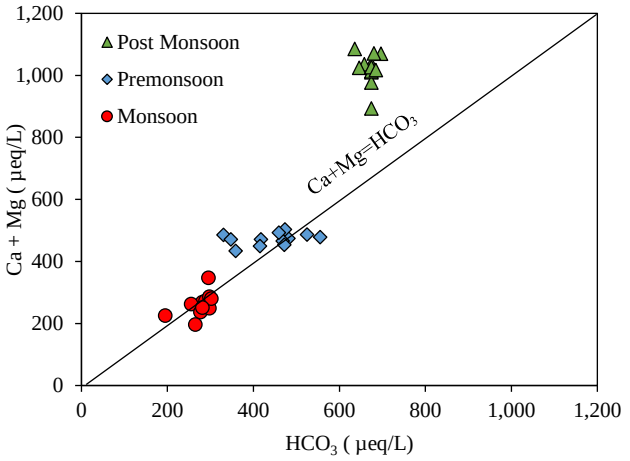

Figure 5. Scatter diagram of $Ca^{2+}+Mg^{2+}$ versus HCO_3^- for Phewa Lake

For the weathering of carbonate rocks, proton sources are required. In order to evaluate the sources of proton whether from carbonation or oxidation of sulfides, the C-ratio ($HCO_3^-/HCO_3^-+SO_4^{2-}$) is used (Brown et al., 1996). In Phewa Lake, the C-ratio varied between 0.78±0.01 during post-monsoon, 0.73±0.03 during pre-monsoon and 0.55±0.05 during monsoon seasons suggesting coupled reactions involving carbonate dissolution and proton derived primarily from oxidation of sulfide (Table 4).

The main source of the major elements and ions (Ca^{2+}, Mg^{2+}, Na^+, K^+, HCO_3^-, SO_4^{2-}, Cl^-, and Si) to the lake is weathering of the drainage basin lithology. A simple plot of TDS vs. weight ratio of $Na^+/(Na^++Ca^{2+})$ (Gibbs diagram) provides information about the relative importance of the major natural mechanisms controlling the surface water chemistry are whether from atmospheric precipitation, rock weathering or evaporation and fractional crystallization (Gibbs, 1970). The dashed 'boomerang' line represents composition of most of the world's surface water (Figure 7). The elliptical area within boomerang represents Indian rainwater average (Das and Kaur, 2001). In Phewa Lake, the Gibbs diagram demonstrates that weathering of rock primarily controls the major ion chemistry (Figure 7) as in many other high altitude lakes- Nainital, Bhimtal, Sattal, Naukuchiatal Lakes of Kumaun Himalaya (Das, 2005), Mansar Lake of Jammu, India (Al-Mikhlafi et al., 2003), Lake Pumayum Co, Southern Tibet (Zhu et al., 2010) and Begnas Lake of Nepal (Khadka and Ramanathan, 2013).

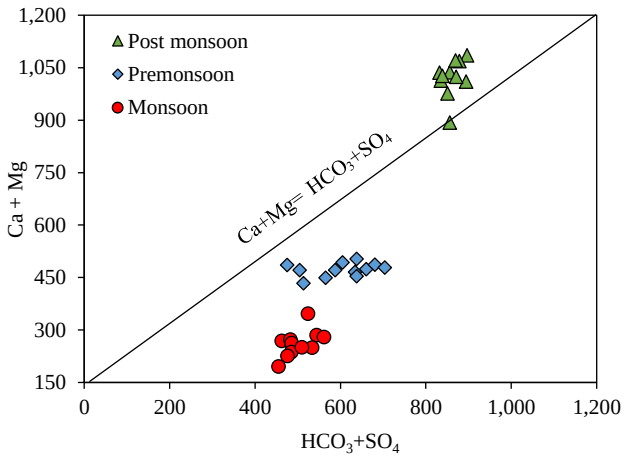

Figure 6. Scatter diagram of $Ca^{2+}+Mg^{2+}$ versus $HCO_3^-+SO_4^{2-}$ for Phewa Lake

The main water types are identified by plotting the major ion on a Piper trilinear diagram (Piper, 1944; Figure 8). The Piper diagram of Phewa Lake shows that $Ca^{2+}+Mg^{2+}$ are the dominant cations and HCO_3^- is the dominant anion defining the water to be Ca-HCO_3 type (Figure 8). The Piper plotting pattern shows that the lake water is dominated by alkaline earth (Ca^{2+}, Mg^{2+}) and weak acids (HCO_3^-). This is also evident from the major ion compositions and ionic ratios (Tables 2 and Table 4). This finding is in agreement with the Manasbal Lake of Kashmir Himalaya (Sarah et al., 2011) and Begnas Lake of Nepal (Khadka and Ramanathan, 2013). However, the seasonal variations in hydrochemical facies in Phewa Lake indicate that

water chemistry is also influenced by factors other than natural lithogenic processes.

3.3 Hydro-geochemical analysis of the Himalayan Lakes

The comparative analysis of the major ions of Phewa Lake and the other Himalayan Lakes show that many Lesser Himalayan Lakes are alkaline (Table 8). Among the Himalayan Lakes, Phewa Lake shows lower HCO_3^-, except for Begnas Lake (Khadka and Ramanathan, 2013). In Phewa Lake, SO_4^{2-} is higher than Renuka, Pandoh and Begnas Lakes, while other major cations and anions are lower than Renuka Lake (Das and Kaur, 2001), and Nainital, Bhimtal, Sattal and Naukuchiatal Lakes (Das, 2005). However, most of these values are comparable with Pandoh Lake (Anshumali and Ramanathan, 2007) and Begnas Lake (Khadka and Ramanathan, 2013). Furthermore, $(Ca^{2+}+Mg^{2+})/(Tz^+)$ ratio in Phewa Lake (0.71) is comparable with Pandoh Lake (0.79) and Begnas Lake (0.61). Similarly, $(Na^++K^+)/(Tz^+)$ ratio accounting 0.14, 0.18, and 0.22 for Phewa, Begnas and Pandoh Lakes, respectively, depicts deficiency of Na^++K^+ over the total cations. Likewise, $(Ca^{2+}+Mg^{2+})/(Tz^+)$ ratio >0.6 indicates dominance of $Ca^{2+}+Mg^{2+}$ (Table 8). These ratios suggest a dominant contribution of carbonate rock weathering in the Himalayan Lakes.

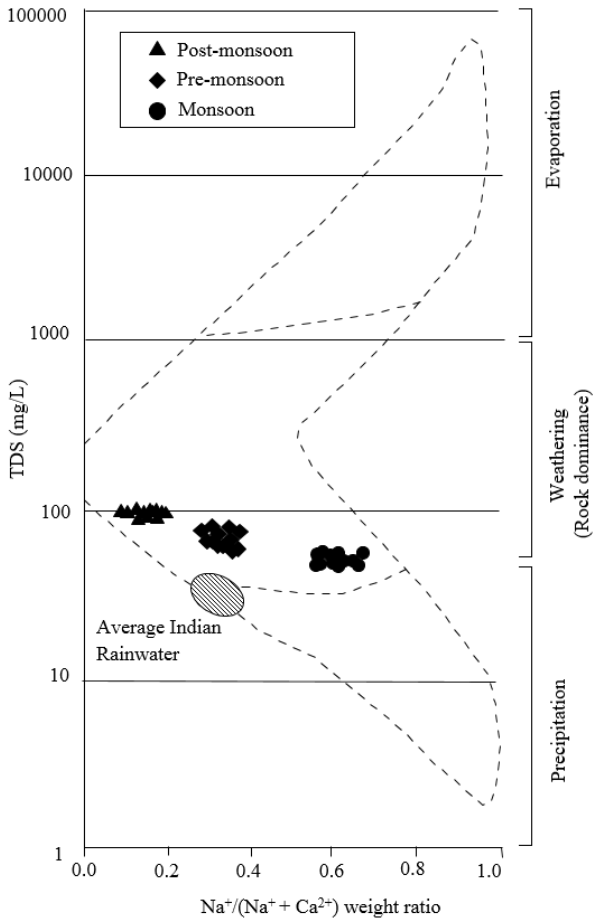

Figure 7. Gibbs diagram showing the major ions source of Phewa Lake in different seasons

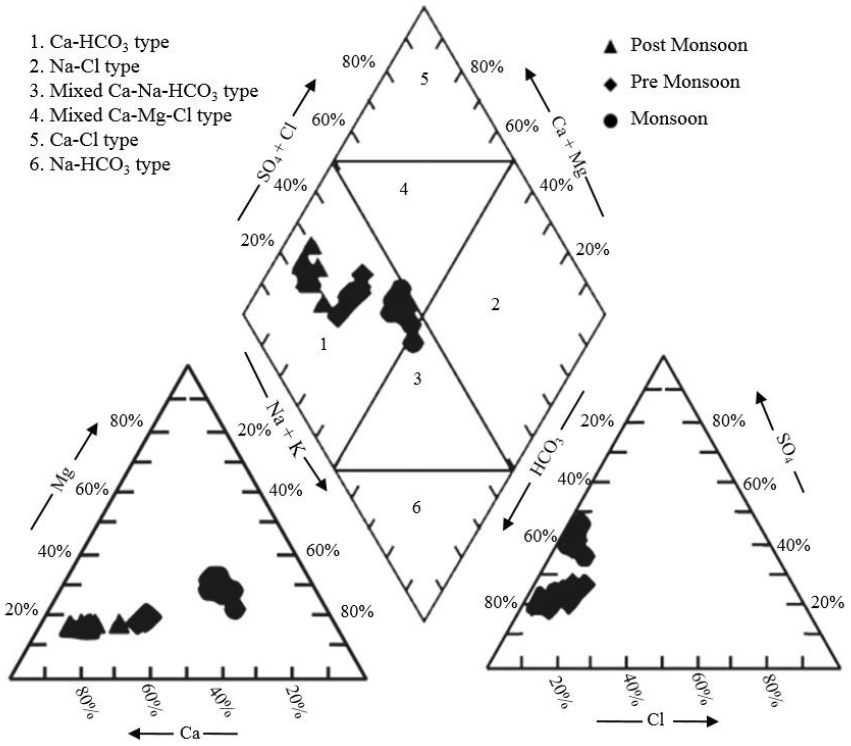

Figure 8. Piper trillinear diagram of the major ions in Phewa Lake

Table 8. Average chemical composition of water in the Lesser Himalayan Lakes (Units: ions and ionic compounds in mg/L, pH, EC in µS/cm, and ionic ratios in equivalent)

Parameters	Das and Kaur (2001)	Das (2005)				Anshumali and Ramanathan (2007)	Khadka and Ramanathan (2013)	Present Study
	Renuka Lake	Nainital	Bhimtal	Sattal	Naukuchiyatal	Pandoh Lake	Begnas Lake	Phewa Lake
pH	8.38	8.67	8.9	9.66	9.4	7.13	7.27	7.94
EC	590.25	706	180.9	119.2	147.55	80.8	90.51	86.45
DO	8.25	-	-	-	-	8.19	8.82	10.41
HCO_3^-	146.42	350.6	91.1	54.0	73.91	49.17	25.31	28.25
Cl^-	11.92	15.3	6.39	7.33	6.6	2.37	2.57	1.57
SO_4^{2-}	6.41	97.75	37.02	19.44	14.04	2.74	7.26	9.16
PO_4^{3-}	6.40	0.124	< 0.01	<0.01	<0.01	1.28	0.09	0.08
NO_3^-	-	-	-	-	-	10.33	5.34	5.29
Na^+	8.33	13.14	4.37	2.69	4.28	3.82	3.89	3.33
K^+	2.02	3.67	2.07	0.72	1.21	2.06	1.42	1.40
Mg^{2+}	38.30	59.3	6.69	5.41	5.49	3.31	1.97	1.84
Ca^{2+}	57.74	32.73	19.80	11.13	14.64	17.96	7.03	8.69
$(Ca^{2+}+Mg^{2+})/(Tz^+)$	-	-	-	-	-	0.79	0.61	0.71
$(Na^++K^+)/(Tz^+)$	-	-	-	-	-	0.22	0.18	0.14

4. CONCLUSION

The Phewa Lake is a fresh-water lake having both national and international importance. The lake is susceptible to the regional phenomena of chemical weathering**,** atmospheric precipitation and anthropogenic inputs. The surface water temperature of the lake is influenced by the ambient temperature. The lake water pH fluctuates from slightly acidic to alkaline with higher value during pre-monsoon. The EC and TDS value was minimum during monsoon and maximum during post-monsoon. The DO was minimum during post-monsoon and maximum during monsoon period. The overall physico-chemical parameters like temperature, pH, TDS, EC, DO, and major ions (Cl^-, SO_4^{2-}, PO_4^{3-}, HCO_3^-, NO_3^-, Na^+, K^+, Ca^{2+}, and Mg^{2+}) in the surficial water fluctuate with the seasons but remain within acceptable limits for fisheries and recreation. The increasing concentrations of dissolved phosphate, nitrate and sulphate over the period of time demonstrate the contribution of these nutrients from anthropogenic sources. The contribution of Ca^{2+}+Mg^{2+} to the total cations (Tz^+) was higher indicating dissolution of calcareous materials as the major sources. The dominance of total anions (Tz^-) over the total cations (Tz^+) indicates their possible contribution from decomposition of organic compounds further suggesting increased organic load in the lake. This information will be useful for the better management of the lake by controlling anthropogenic activities contributing organic load.

Moreover, although the major ions concentrations are within tolerable limits, the increasing trophic status of the lake, as manifested by massive growth of macrophytes, indicates that, along with external input, internal processes like internal loading of nutrient elements may be contributing to enhance the trophic status of the lake. Therefore, for understanding the autochthonous process releasing limiting element like phosphorus and for sustainable management and conservation of the lake, further studies on sediment-water interaction is anticipated.

ACKNOWLEDGEMENTS

The authors are grateful to the School of Environmental Sciences, Jawaharlal Nehru University, New Delhi for providing the laboratory facilities. The first author expresses sincere gratitude to the Institute of Science and Technology, Tribhuvan University, and University Grants Commission-Nepal for granting study leave and partial financial support, respectively. The authors are also thankful to the Fisheries Research Station, Pokhara, Nepal for their support during the field study.

REFERENCES

Adhikari S, Khadka UR. Phosphorous distribution in bed-sedimnents of Phewa Lake of Pokhara Valley Nepal. Curriculum Development Journal 2017;27(41):101-13.

Al-Mikhlafi AS, Das BK, Kaur P. Water chemistry of Mansar Lake (India): An indication of source area weathering and seasonal variability. Environmental Geology 2003;44:645-53.

Anshumali, Ramanathan AL. Seasonal variation in the major ion chemistry of Pandoh Lake, Mandi District, Himachal Pradesh, India. Applied Geochemistry 2007;22:1736-47.

American Public Health Association (APHA). Standard methods for the examination of water and waste water. 21st ed. Washington DC, USA: American Public Health Association, American Water Works Association, and Water Environment Federation; 2005.

Bartarya SK. Hydrochemistry and rock weathering in a sub-tropical Lesser Himalayan River Basin in Kumaun, India. Journal of Hydrology 1993;146:149-74.

Brown GH, Sharp M, Tranter M. Sub-glacial chemical erosion: Seasonal variations in solute provenance, Haut Glacier d' Arolla, Vala, Switzerland. Annals of Glaciology 1996;22:25-31.

Chakrapani GJ, Saini RK, Yadav SK. Chemical weathering rates in the Alaknanda-Bhagirathi River Basins in Himalayas, India. Journal of Asian Earth Sciences 2009;34:347-62.

Conservation and Sustainable Use of Wetlands in Nepal (CSUWN). Application of economic valuation tool: Case studies from Nepal. Kathmandu, Nepal: Ministry of Forests and Soil Conservation; 2011.

Dalai TK, Krishnaswami S, Sarin MM. Major ion chemistry in the headwater of the Yamuna River system: Chemical weathering, its temperature dependence and CO_2 consumption in the Himalaya. Geochimica et Cosmochimica Acta 2002;66:3397-416.

Das BK, Singh M, Grieken RV. The elemental chemistry of sediments in the Nainital Lake, Kumaun Himalaya, India. Science of the Total Environment 1995;168:85-90.

Das BK, Kaur P. Major ion chemistry of Renuka Lake and weathering processes, Simaur District, Himachal Pradesh, India. Environmental Geology 2001;40:908-17.

Das BK. Environmental pollution impact on water and sediments of Kumaun lakes, Lesser Himalaya, India: A comparative study. Environmental Geology 2005;49:230-9.

Das SK, Routh J, Roychoudhury AN, Klump JV, Ranjan RK. Phosphorus dynamics in shallow eutrophic lakes: An example from Zeekoevlei, South Africa. Hydrobiologia 2009;619:55-66.

Diatloff E, Rengel Z. Compilation of simple spectrophotometric techniques for the determination of element in nutrient solutions. Journal of Plant Nutrition 2001;24:75-86.

Ferro W, Swar DB. Bathymetric maps from three lakes in the Pokhara Valley (Nepal). Journal of Institute of Science and Technology 1978;1:177-88.

Forstner U, Wittmann GTW. Metal Pollution in the Aquatic Environment. 2nd ed. Verlag, Berlin: Springer; 1983.

Gautam P, Pant PR, Ando H. Mapping of subsurface karst structure with gamma ray and electrical resistivity profiles: A case study from Pokhara Valley, Central Nepal. Journal of Applied Geophysics 2000;45:97-110.

Gibbs RJ. Mechanism controlling world water chemistry. Science 1970;170:1088-90.

Giri B, Chalise M. Seasonal diversity and population status of waterbirds in Phewa Lake, Pokhara, Nepal. Journal of Wetlands Ecology 2008;1(1-2):3-7.

Gurung TB, Dhakal RP, Bista JD. Phytoplankton primary production, chlorophyll-a, and nutrient concentration in the water column of mountainous Lake Phewa, Nepal. Lakes and Reservoirs: Research and Management 2006;11:141-8.

Gurung TB, Dhakal RP, Husen Md A, Jones JR. Abundance and nutrient limiting growth rate of heterotrophic bacterio-plankton in Himalayan foot hill Lake Phewa, Nepal. Lakes and Reservoirs: Research and Management 2010;15:53-61.

Håkanson L. On the relationship between lake trophic level and lake sediments. Water Research 1984;18:303-14.

Håkanson L. Internal loading: A new solution to an old problem in aquatic sciences. Lakes Reservoirs: Research and Management 2004;9:3-23.

Hickel B. Limnological investigations in Lakes of Pokhara Valley, Nepal. International Review of Hydrobiology 1973;58:659-72.

Impat P. Phewa Tal Watershed Soil Map. Kathmandu, Nepal: Integrated Watershed Management Project, Kathmandu Department of Soil Conservation and Watershed Management; 1980.

Jeelani G, Shah AQ. Geochemical characteristics of water and sediment from the Dal Lake, Kashmir Himalaya: Constraints on weathering and anthropogenic activity. Environmental Geology 2006;50:12-23.

Jha PK, Tiwari J, Singh UK, Kumar M, Subramanian V. Chemical weathering and associated CO_2 consumption in the Godawari River Basin, India. Chemical Geology 2009;264:364-74.

Jones JG. Activities of aerobic and anaerobic bacteria in lake sediments and their effect on the water column. In: Nedwell DB, Brown CM, editors. Sediment Microbiology. London: Academic Press; 1982. p. 107-45.

Jones JR, Knowlton MF, Swar DB. Limnological reconnaissance of water-bodies in central and southern Nepal. Hydrobiologia 1989;184:171-89.

Kato K, Hayashi H. Limnological pre-survey of Lake Phewa, Nepal. Journal of Faculty of Science, Shinshu University 1982;15:27-9.

Khadka UR, Ramanathan AL. Major ion composition and seasonal variation in the Lesser Himalayan Lake: Case of Begnas Lake of the Pokhara Valley, Nepal. Arabian Journal of Geosciences 2013;6:4191-206.

Meybeck M. Atmospheric inputs and river transport of dissolved substances. Proceedings of the Hamburg Symposium; 1983 Aug; IAHS, Hamburg: Germany; 1983. p. 173-92.

Ministry of Forest and Environment (MoFE). Integrated Lake Basin Management Plan of Lake Cluster of Pokhara Valley, Nepal (2018-2023). Kathmandu, Nepal: Ministry of Forests and Environment; 2018.

Ministry of Physical Planning and Works (MoPPW). National Drinking Water Quality Standards and Directives 2005. Kathmandu, Nepal: Ministry of Physical Planning and Works; 2005.

Oli KP. Phewa Lake Conservation Action Plan. Kathmandu, Nepal: Nepal National Conservation Strategy Implementation Program, National Planning Commission, and Government of Nepal; 1997.

Piper AM. A graphic procedure in the geochemical, interpretation of water analysis. Transactions American Geophysical Union 1944;25:914-23.

Poudyal K, Baral H, Keenan RH. Assessing social values of ecosystem services in the Phewa Lake Watershed, Nepal. Forest Policy and Economics 2016;90:67-81.

Pradhan AM, Kim YT. Landslide susceptibility mapping of Phewa catchment using multilayer perceptron artificial neural network. Nepal Journal of Environmental Science 2017;4:1-9.

Pokhara Sub Metropolitan City (PSMC). Water Quality and Sedimentation Management of Phewa Lake. Pokhara, Nepal: Pokhara Sub Metropolitan City; 2007.

Rai AK. Limnological characteristics of Subtropical Lakes Phewa, Begnas, and Rupa in Pokhara Valley, Nepal. Limnology 2000a;1:33-46.

Rai AK. Evaluation of natural food for planktivorous fish in Lakes Phewa, Begnas, and Rupa in Pokhara Valley, Nepal. Limnology 2000b;1:81-9.

Ramsar. On world wetland day lake cluster of Pokhara Valley becomes Nepal's tenth Ramsar Site [Internet]. 2016 [cited 2020 May 20]. Available from: https://www.ramsar.org/news/on-world-wetlands-day-lake-cluster-of-pokhara-valley-becomes-nepals-tenth-ramsar-site.

Ravindra K, Garg VK. Hydro-chemical survey of groundwater of Hisar City and assessment of defluoridation methods used in India. Environment Monitoring and Assessment 2007; 132:33-43.

Regmi RR, Saha SK, Subedi DS. Geospatial analysis of land-use land-cover change modelling in Phewa Lake Watershed of Nepal by using GEOMOD Model. Himalayan Physics 2017;(6-7):65-72.

Ross JD. Erosion and Sedimentation in the Phewa Tal Watershed, Middle Mountain Region, Nepal [dissertation]. Kingston, Ontario, Canada: Queen's University; 1998.

Ross J, Gilbert R. Lacustrine sedimentation in a monsoon environment: The record from Phewa Tal, middle mountain region of Nepal. Geomorphology 1999;27:307-23.

Rowbotham DN, Dudycha D. GIS modelling of slope stability in Phewa Tal Watershed, Nepal. Geomorphology 1998;26:151-70.

Sarah S, Jeelani G, Ahmed S. Assessing variability of water quality in a groundwater-fed perennial lake of Kashmir Himalayas using linear geostatistics. Journal of Earth System Science 2011;120:399-411.

Shrestha P, Janauer GA. Management of aquatic macrophyte resource: A case of Phewa Lake, Nepal. In: Jha PK, Baral SR, Karmacharya SB, Lekhak HD, Lacoul P, editors. Environment and Agriculture: Biodiversity, Agriculture and Pollution in South Asia. Kathmandu, Nepal: Ecological Society (ECOS) and World Conservation Union; 2001. p. 99-107.

Singh AK, Hasnain SI. Environmental geochemistry of Damodar River Basin - east coast of India. Environmental Geology 1999;37:124-36.

Singh AK, Mondal GC, Singh PK, Singh S, Singh TB, Tewary BK. Hydrochemistry of reservoirs of Damodar River Basin, India: Weathering processes and water quality assessment. Environmental Geology 2005;48:1014-28.

Singh VB, Ramanathan AL, Mandal A. Hydrogeochemistry of high-altitude lake: A case study of the Chandra Tal, Western Himalaya, India. Arabian Journal of Geosciences 2016;9:308.

Singh VB, Ramanathan AL, Pottakkal JG, Kumar M. Seasonal variation of the solute and suspended sediment load in

Gangotri glacier meltwater, central Himalaya, India. Journal of Asian Earth Sciences 2014;79:224-34.

Singh VB, Ramanathan AL, Pottakkal JG, Sharma P, Linda A, Azam MF, et al. Chemical characterization of melt-water draining from Gangotri Glacier, Garhwal Himalaya, India. Journal of Earth System Science 2012;121(3):625-36.

Singh VB, Ramanathan AL, Sharma P, Pottakkal JG. Dissolved ion chemistry and suspended sediment characteristics of meltwater draining from Chhota Shigri Glacier, western Himalaya, India. Arabian Journal of Geosciences 2015a;8:281-93.

Singh VB, Ramanathan AL, Sharma P. Major ion chemistry and assessment of weathering processes of the Patsio glacier meltwater, Western Himalaya, India. Environmental Earth Sciences 2015b;73:387-97.

Stallard RF, Edmond JM. Geochemistry of Amazon: The influence of the geology and weathering environment on the dissolved load. Journal of Geophysical Research 1983; 88:9671-88.

Strickland JDH, Parsons TR. Determination of reactive silicate. In: A Practical Handbook of Seawater Analysis. 1st ed. Ottawa, Canada: Supply and Service Canada; 1968. p. 65-70.

Subramanian V. Chemical and suspended sediment characteristics of rivers of India. Journal of Hydrology 1979;44:37-55.

Subramanian V. River transport of phosphorous and genesis of ancient phosphorites. Geological Survey of India 1984; 17(Special):11-5.

Swar DB, Fernando CH. Cladocera from Pokhara Valley, Nepal with notes on distribution. Hydrobiologia 1979a;66:113-28.

Swar DB, Fernando CH. Seasonality and fecundity of Daphnia Lumholtzi Sars in Lake Phewa, Nepal. Hydrobiologia 1979b;64:261-8.

Swar DB, Fernando CH. Some studies on the ecology of limnetic crustacean zooplankton in Lake Begnas and Rupa, Pokhara Valley, Nepal. Hydrobiologia 1980;70:235-45.

Vreca P, Muri G. Changes in accumulation of organic matter and stable carbon and nitrogen isotopes in sediments of two Slovenian mountain lakes (Lake Ledvica and Lake Plannina) induced by eutrophication. Limnology and Oceanography 2006;51:781-90.

Watson CS, Kargel JS, Regmi D, Rupper S, Maurer JM, Karki A. Shrinkage of Nepal's second largest lake (Phewa Tal) due to watershed degradation and increased sediment influx. Remote Sensing 2019;11(4):444.

Yamanaka H, Yoshida M, Arita K. Terrace landform and Quaternary deposits around Pokhara Valley, Central Nepal. Journal of Nepal Geological Society 1982;2:95-112.

Zhu L, Ju J, Wang Y, Xie M, Wang J, Peng P, et al. Composition, spatial distribution, and environmental significance of water ions in Pumayum Co catchment, Southern Tibet. Journal of Geographical Sciences 2010;20:109-20.

Isolation and Molecular Characterization of Polycyclic Aromatic Hydrocarbon Degrading Bacteria from Effluent Water from Weras River Park, Sri Lanka

A.A. Prathiba[1], F. Sumaiya Idroos[1*], and Pathmalal M. Manage[1,2]

[1]Centre for Water Quality and Algae Research, Department of Zoology, Faculty of Applied Sciences, University of Sri Jayewardenepura, Sri Lanka

[2]Faculty of Graduate Studies, University of Sri Jayewardenepura, Sri Lanka

ARTICLE INFO

Received: 29 Feb 2020
Received in revised: 16 Oct 2020
Accepted: 30 Oct 2020
Published online: 27 Nov 2020
DOI: 10.32526/ennrj/19/2020016

Keywords:
Naphthalene/ Anthracene/ Bacterial degradation/ Microplate assay/ Fourier-Transform Infrared Spectroscopy (FTIR)

*** Corresponding author:**
E-mail:
sumaiyaidroos@sci.sjp.ac.lk

ABSTRACT

The present study records the detection of PAHs such as naphthalene and anthracene and isolation of PAHs degrading bacteria from a restaurant site, Weras River Park, in Boralesgamuwa, Sri Lanka. Water samples were collected in seven locations of the study area. Water temperature (°C), pH, and electric conductivity (EC) were measured at the site itself using standard meters. Nitrogen nitrate ($N\text{-}NO_3^-$) and total phosphate (TP) were measured at the laboratory following the standard methods. Following the extraction of PAHs in collected water samples, detection was carried out using the PDA-HPLC diode array method. PAH degrading bacteria were identified using microplate assay. The selected bacteria strains were subjected to degradation kinetic studies following molecular identification by 16S rRNA analysis. Phylogenetic analysis identified *Achromobacter spanius* as potential naphthalene degrading bacteria, where *Alcaligens faecalis* was recorded as an anthracene degrader. Degradation study confirmed that *A. spanius* efficiently degraded naphthalene at the rate of 0.145±0.002 ppm/day, whereas *A. faecalis* degraded anthracene at the rate of 0.181±0.036 ppm/day, respectively. Degradation of structures of the Naphthalene and Anthracene by *A. spanius* and *A. faecalis* was further analyzed by Fourier Transform Infrared Spectroscopy (FTIR). This is the first record on naphthalene degradation by the bacterium *A. spanius*.

1. INTRODUCTION

Polycyclic Aromatic Hydrocarbons (PAHs) are non-polar organic compounds that are comprised of 2 to 7 fused rings and are arranged in linear, angular or clustered structures (Guruge et al., 2008; Kim et al., 2013). Natural and anthropogenic activities such as incomplete combustion of fossil fuels, forest fires, open burning, and the incomplete burning of fuel oils give rise PAHs in the environment (Nkansah, 2012; Witt, 2002). Long term persistence of PAHs in the environment will lead to biomagnification through several fold, leading to adverse aquatic fauna and human health impacts (Guruge et al., 2008; Guruge et al., 2007; Partila, 2013). The bioaccumulation of PAHs in aquatic animals is dependent on several factors, such as the octanol/water partition coefficient (K_{OW}) of each PAH congener, concentration in environmental media, bioavailability, and depuration/excretion of PAHs. PAHs are hydrophobic chemicals that have a high affinity with organic matter in water and sediment compared to the water phase. This trend is more predominant in high-molecular-weight PAHs (more than five-ring) than in low-molecular-weight PAHs because of high K_{OW} values. Typical persistent organic pollutants, such as polychlorinated biphenyls, have the same trend, and high K_{OW} values generally suggest a high bioaccumulation factor. For example, fish are considered to have a higher metabolism capacity and can metabolize/depure PAHs quickly; therefore, a generally positive correlation between the concentration of PAHs in the body and the K_{OW} value is not observed in higher trophic-level fish (Collins et al., 1998; Devi et al., 2016).

Citation: Prathiba AA, Idroos FS, Manage PM. Isolation and molecular characterization of polycyclic aromatic hydrocarbon degrading bacteria from effluent water from Weras River Park, Sri Lanka. Environ. Nat. Resour. J. 2021;19(1):84-94. (https://doi.org/10.32526/ennrj/19/2020016)

PAHs enter into the aquatic environment through the direct deposition of atmosphere while light PAHs comes into the water via rain washout and surface water runoff (Stogiannidis and Laane, 2015; Guruge et al., 2007). A recent study showed the PAHs derived from pyrogenic activities are highly concentrated in urban areas (Abdel-Shafy and Mansour, 2016). Crude oil, fuels and lubricants (Stogiannidis and Laane, 2015; Jiang et al., 2015), oceanic and freshwater oil spills, transportation vessels, boats, storage and use of crude oil (Abdel-Shafy and Mansour, 2016; Liyanage and Manage 2015; Ohura et al., 2015) are the other main identified sources of petrogenic PAHs to the environment. Further, low molecular weight PAHs commonly contained in petrogenic substances have also been recorded (Stogiannidis and Laane, 2015).

PAHs are considered as carcinogens, mutagens and toxic due to their high octanol water (K_{OW}) and organic carbon adsorption (K_{OC}) partition coefficients (Witt, 2002). According to the International Agency for Research on Cancer (IARC), 400 carcinogens out of 900 agents are PAHs (Ohura et al., 2015). Due to low water solubility and electro-chemical stability, PAHs are persist in the environment for a long time and available to bioaccumulate through the food chain (Guruge et al., 2008) and reach high concentrations in soil and many freshwater bodies of the world (Ohura et al., 2015).

Comprehensive studies have been carried out on the carcinogenicity of PAHs to mammals, including humans (Menzie et al., 1992). Briefly, PAHs are transported into cells because of their hydrophobicity and induce gene expression of the cytochrome P450 (CYP) enzyme group. Expressed CYP enzymes metabolize PAHs into additional metabolites. It is important to note that several intermediates in this metabolic pathway can bind to DNA and become mutagenic/carcinogenic. Because of their carcinogenicity, the International Agency for Research on Cancer (IARC) classified three PAHs: benzo(a)anthracene (BaA), benzo(a)pyrene (BaP), and dibenz(a,h)anthracene, as being probably carcinogenic chemicals (Poliakova et al., 2000). Eight PAHs-BaA, chrysene, benzo(b)fluoranthene, benzo(k)fluoranthene, BaP, dibenz(a,h)anthracene, indeno (1,2,3-c,d) pyrene, and benzo(g,h,i)perylene are considered possible carcinogens (Menzie et al., 1992). In aquatic animals, such as fish, epizootic neoplasia is strongly associated with environmental chemical pollution, which has increased exponentially since the 1940s with the growth of synthetic organic chemical-producing industries (Bailey et al., 1984). Certain fish species (e.g., rainbow trout and medaka) are well-established sensitive models for evaluating the effects of exogenous and endogenous factors of chemical carcinogenesis (Bailey et al., 1984; Varanasi et al., 1987). In feral fish, carcinogenic properties of PAHs have also been examined in English sole (*Parophrys vetulus*) and flounder (*Platichthys stellatus*) (Varanasi et al., 1987).

To date many studies have focused on the isolation of PAH degradation by bacteria. Idroos et al. (2015) recorded the degradation of naphthalene by *Stenetrophomonas maltophilia* by 37.5%. Further, Oyehan and Thukair (2017) studied the degradation of the polycyclic aromatic hydrocarbons (pyrene- and phenanthrene) by *Pseudomonas aeruginosa*, *P. citronellolis*, *Ochrobactrum intermedium*, and *Cupriavidus taiwanensis*. Further, Dharmawan et al. (2015) have also reported a similar study on PAH (Fluoranthene and pyrene) degradation by *Burkholderia fungorum* and *Mycobacterium gilvum*.

In Sri Lankan context, most of the recorded studies on PAHs are limited to petrochemical stations (Hamid et al., 2017; Undugoda et al., 2016) and water (Guruge et al., 2007). However, no studies on wastewater released from restaurants and eateries have been addressed. Thus, the present study focuses on quantifying PAHs like naphthalene and anthracene released from effluent waters from a restaurant site. In addition this study also emphasizes the isolation and characterization of PAHs (naphthalene and anthracene) degrading bacteria from the site of effluent water release. Hence, this study, which was carried in 2017, presents the first record on isolation of PAHs (naphthalene and anthracene) degrading bacteria from effluent water released from a restaurant. Consequently, the isolated bacterial strains could be effectively used as a biological agent to treat PAH contaminated sites in the future.

2. METHODOLOGY

2.1 Chemicals

Chemicals used for analysis of water quality parameters were analytical grade (Sigma, Aldrich). HPLC-graded methanol, acetone, dichloromethane, naphthalene and anthracene were obtained from the Department of Zoology and Department of Chemistry, University of Sri Jayewardenepura, Sri Lanka respectively.

Bacteriology grade peptone, yeast extract, sodium chloride, bacteriological agar, and 0.9% saline water needed for bacteriological studies were obtained from Centre for Water Quality and Algae Research, Department of Zoology, University of Sri Jayewardenepura.

2.2 Study area and sampling

Surface water samples were collected from seven sites of Weras River Park (6°50'28.9"N 79°53'37.0"E) representing effluent water releasing sites. The control site was selected from a location which was 200 m away from the effluent water releasing site. Water samples were collected using 1 L sterilized glass bottles. Sampling was carried out from June to September 2017 at seven locations. The sixth and seventh locations were selected as reference sampling points. Water temperature (°C), pH, and conductivity (µS/cm) were measured at the sites using thermometer immersion (Philip Haris, England), pH meter (HACH-HQ 40D) and conductivity meter (HACH-HQ 40D), respectively. Total nitrate and total phosphate concentrations in water were measured according to standard spectrophotometric methods (Total nitrate 420 nm and total phosphate 465 nm) described by American Public Health Association (APHA, 2017).

2.3 Quantification of PAHs

Naphthalene and anthracene extraction was carried out using the modified protocol given by Princewill-Ogbonna and Adikwu (2015). Quantification of naphthalene and anthracene were done using the HPLC system consisting of Agilent 1200 series. A sample volume of 25 µL was injected into a 250×4.6 mm, C18 column at a flow rate of 1 mL/min. Two mobile phases were used for the gradient run (65% Milli-Q water and 35% Methanol). Concentrations of naphthalene and anthracene were determined with a pre-prepared calibration curve of the peak areas at 290 nm for naphthalene and at 375 nm for anthracene, respectively, with an external standard. The HPLC method had a detection limit of 0.5 µg/mL and recoveries for naphthalene and anthracene were obtained greater than 95% with a relative precision of 5%.

2.4 Preparation of calibration curve for naphthalene and anthracene for colorimetric assay

Methylene blue was used as the redox indicator. A concentration series of naphthalene and anthracene was prepared ranging from 0.5 µg/mL to 4 µg/mL and 0.1 mL methylene blue was added for each concentration following measurement of absorption at 609 nm. Calibration plots were developed using the absorbance values and the corresponding concentrations.

2.5 Isolation of PAHs degradation bacteria

Isolation of PAH degrading bacteria was carried out according to Manage et al. (2009).

2.5.1 Enrichment studies

Enrichment of naphthalene and anthracene degrading bacteria was carried out in triplicates for each water and sediment samples in vitro. In the enrichment process, 1 mL of 0.1% naphthalene and anthracene were added separately into each collected 99 mL of effluent water samples.

2.5.2 Isolation of potential PAH degrading bacteria from water sample

Following 14 days of enrichment, 1 mL of sample was removed from each flask and serial dilutions were prepared up to 10^{-3} using sterilized saline solution (0.9% NaCl). Exactly 1 mL of subsample was removed from 10^{-1} to 10^{-3} dilutions and inoculated into sterilized, labeled Petri dishes and then the pour plate method was followed using 1.5% Luria-Bertani (LB) agar medium (peptone 13.1 g/L; yeast extract 4.6 g/L; sodium chloride 4.6 g/L; agar 9.1 g/L) to isolate bacteria. Following two days of incubation, the colonies that appeared on the agar plates were recorded as Colony Forming Unit (CFU/mL) for each plate. Colonies with different morphological features were picked up and inoculated into sterilized liquid LB medium. The liquid cultures were incubated at 28°C overnight, subcultured and repeated streaking on LB agar was followed to prepare pure cultures of bacteria. A portion of each bacteria was stored in LB-glycerol at -20°C for future studies.

2.5.3 Colorimetric screening of PAHs degrading bacteria

This method was modified according to Manage et al. (2009). A loop of morphologically different bacterial strains was transferred into 5 mL of liquid LB medium and incubated overnight at 28°C. The exponentially growing cultures were centrifuged at 10,000 rpm for 20 min and the supernatant was discarded. Bacterial pellets were re-suspended in 0.9% saline solution and incubated at 28°C in a shaking incubator at 100 rpm overnight to exhaust residual

carbon content. Then the bacteria were centrifuged at 100 rpm, the supernatant was discarded, and the remaining pellets were washed three times using filter sterilized saline solution following centrifugation. Finally, the turbidity of bacterial suspensions was equalized (A_{590}=0.35) using a spectrophotometer (SPECTRO UV-VIS double beam PC). Microplates (96 wells) were used to screen naphthalene and anthracene degrading bacteria. Different concentrations of naphthalene (100, 200, and 300 µg/mL) and anthracene (1.0, 1.5, and 2.0 µg/mL) were used for degradation study. Exactly 9 µL of bacterial inoculum in saline solution was added to each well and control wells were treated with 9 µL of filter sterilized saline solution. Subsequently 1 µL of Methylene Blue solution was added to each well and triplicate wells were maintained for each concentration of naphthalene and anthracene. The treated plates were wrapped with wet paper towels and stored in the dark at 28ºC. The absorbance of the plates was read at 0, 3, 6, 9, 12, 18, 24, and 48 h intervals using an Elisa Plate Reader (MULTISKAN EX, Thermo Scientific, USA) at 609 nm. PAH degradation by each bacteria strain was measured using the equation given below (Undugoda et al., 2016).

PAH degradation percentage = 1 – [(Absorbance of sample) / (Absorbance of control)] 100

2.5.4 Degradation kinetics

To study the degradation kinetics of selected PAHs degrading bacteria stains, overnight starved bacteria suspensions were equalized to A590=0.350 and added into 100 mL of sterile lake water, containing either naphthalene (200 µg/mL) or anthracene (1 µg/mL) with 0.1 mL of Methylene blue. The PAHs degradation rates (h) of the bacteria were calculated using the equation below.

$$h = -[(C/C_0)]\ t$$

Where; "C_0" and "C" are the concentration of PAHs at the beginning and at the end of the time interval "t", respectively. Half-life time was calculated as the duration for removal of 50% of the PAHs from the start of each experiment.

2.6 Fourier Transform Infrared Spectroscopy (FTIR)

Depending on the observations of degradation study, an FTIR (Fourier transform infrared spectroscopy) was carried out to study the degradation of naphthalene and anthracene by selected bacteria strains. Overnight starved bacteria suspensions were equalized to A_{590}=0.350 and added into sterile water containing either naphthalene (200 µg/mL) or anthracene (1.0 µg/mL). Flasks were maintained at 28ºC at 100 rpm with continuous shaking. Sample aliquots (1 mL) were removed at 0^{th} and 14^{th} day of incubation and subjected to FTIR analysis.

2.7 Molecular identification of bacteria

Genotypic identification of naphthalene and anthracene degrading bacteria was carried out by amplifying and partial sequencing of the 16S rRNA region of PH1 and PH7 bacterial strains. 16F27 (5'-AGAGTTTGATCMTGGCTCAG-3') and 16R1541 (5'-AAGGAGGT GATCCAGCCGCA-3') primers were employed for the amplification of 16S rRNA region. The PCR reaction mixture (50 µL) contained 20 ng genomic DNA, 0.5 µM of each primer (IDT), 1×Go Taq Green Master Mix (Promega, USA), and 1 mM $MgCl_2$ (Promega, USA). Thermal cycling was performed using a Peltier thermal cycler (MG 25+, 001-31085). The initial denaturation step at 94ºC for 2 min was followed by 30 cycles of DNA denaturation at 94ºC for 10 sec, primer annealing at 55ºC for 20 sec, strand extension at 72ºC for 1 min and final extension at 72ºC for 7 min. DNA sequencing was performed through commercially available service by Macrogen, Korea.

2.8 Statistical Analysis

2.8.1 Cluster analysis

A cluster analysis was carried out using Minitab 17 software to study whether there is a significance difference in Naphthalene and Anthracene concentrations in sampling locations.

2.8.2 Principle Component Analysis (PCA)

Principle Component Analysis (PCA) was carried out using Minitab 14 software to categorize the studied sampling locations depending on analyzed physico-chemical parameters. Reading was as considered as significant when p was ≤0.05.

3. RESULTS

Physico-chemical parameters such as water temperature (ºC), pH, electric conductivity (EC), nitrogen nitrate ($N\text{-}NO_3^-$), total phosphate (TP) which were measured in water samples from seven study locations are given in Table 1.

Table 1. Physico-chemical parameters of water samples in seven locations in Weras Ganga Park

Locations	Temperature (°C)	Conductivity (µS/cm)	pH	NO_3^- (mg/L)	PO_4^- (mg/L)
Location 1	33.0±0.1	399.00±2.65	6.91±0.01	0.72±0.01	0.81±2.20
Location 2	32.4±0.2	478.00±0.58	6.92±0.01	0.04±0.02	0.75±6.72
Location 3	32.2±0.3	403.00±1.53	6.66±0.01	4.53±0.06	0.75±4.58
Location 4	32.5±0.3	330.00±2.00	6.39±0.04	5.28±0.04	0.79±1.27
Location 5	32.1±0.1	332.00±1.00	7.00±0.02	1.91±0.03	0.76±3.36
Location 6	31.2±0.2	264.00±2.52	7.28±0.03	0.45±0.02	0.72±8.33
Location 7	30.7±0.3	249.00±2.08	7.12±0.01	0.11±0.09	0.77±2.54

The highest water temperature of 33.0±0.1°C was recorded in location 1, whereas the lowest was at 30.7±0.3°C in location 7. The conductivity ranged between 249±2 to 478±1 µS/cm, whereas pH ranged between 6.39±0.04 to 7.28±0.03 during the study period. The highest nitrate was recorded at location 4 (5.28±0.04 mg/L) and the lowest recorded at location 2 (0.04±0.02 mg/L). The highest phosphate concentration was recorded in location 1 (0.81±2.20 mg/L) while the lowest was in location 6 (0.72±8.33 mg/L).

Table 2 shows the naphthalene and anthracene concentrations in water samples collected from seven sampling locations of the study. The highest naphthalene and anthracene concentrations were detected from effluent water sampling location 1 whereas the lowest values were detected in the locations 6 and 7 which were the reference points.

Naphthalene degradation potential of PH1-PH5 bacterial strains and anthracene degradation potential of PH6-PH10 bacterial strains were assessed using a colorimetric detection method (Figure 1).

Table 2. Naphthalene and anthracene concentrations in sampling locations

Sampling locations	Naphthalene concentration (µg/mL)	Anthracene concentration (µg/mL)
Location 1	235.21±0.06	1.88±0.05
Location 2	33.36±0.46	1.76±0.01
Location 3	31.09±0.46	1.74±0.01
Location 4	30.64±0.26	1.70±0.01
Location 5	11.14±0.10	1.65±0.01
Location 6	7.32±0.11	1.10±0.02
Location 7	2.75±0.03	0.99±0.02

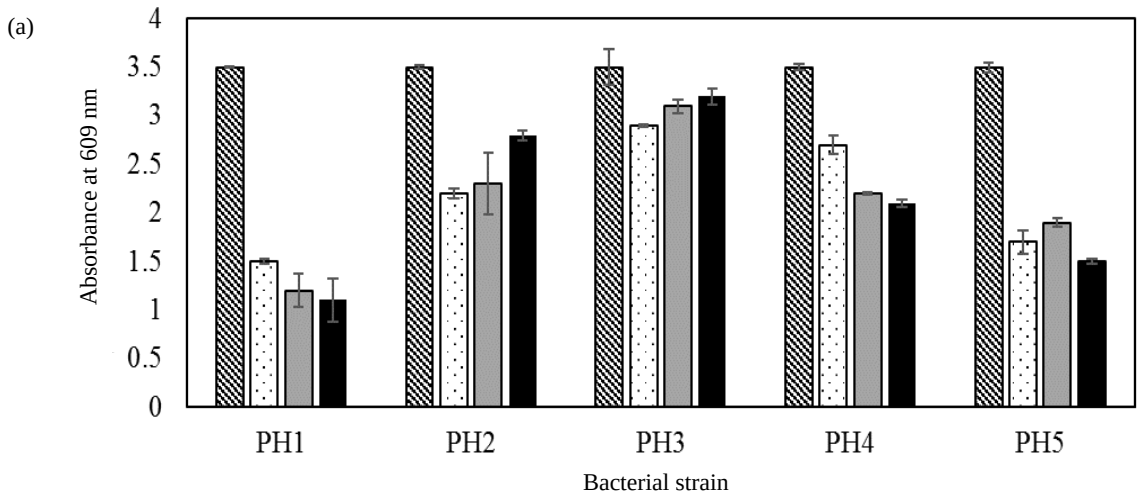

Figure 1. (a) Screening for naphthalene degradation by PH1-PH5 bacterial strains at 24 h of incubation (hatched bars-control, dotted bars-100 µg/mL, ash bars-200 µg/mL, black bars-300 µg/mL). (b) Screening anthracene degradation of by PH6-PH10 bacterial strains at 24 h of incubation (hatched bars-control, dotted bars-100 µg/mL, ash bars-200 µg/mL, black bars-300 µg/mL).

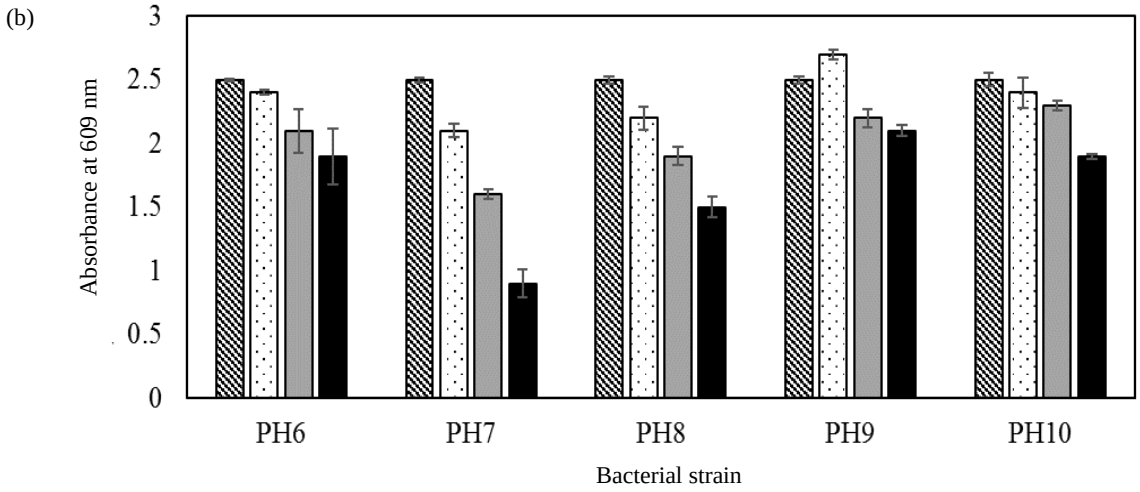

Figure 1. (a) Screening for naphthalene degradation by PH1-PH5 bacterial strains at 24 h of incubation (hatched bars-control, dotted bars-100 µg/mL, ash bars-200 µg/mL, black bars-300 µg/mL). (b) Screening anthracene degradation of by PH6-PH10 bacterial strains at 24 h of incubation (hatched bars-control, dotted bars-100 µg/mL, ash bars-200 µg/mL, black bars-300 µg/mL) (cont.).

According to the colorimetric assay, reduction of absorbance values of wells corresponds to bacterial degradation activity. In the case of naphthalene degradation, PH1 showed the lowest absorption confirming the highest degradation rates. Furthermore, the absorbance value for PH1 was the lowest (1.10±0.01) at 300 µg/mL of naphthalene corresponding to highest degradation. The screening for anthracene degradation confirmed that PH7 as the efficient degrader. Interestingly, PH7 also indicated the lowest absorbance (0.90±0.02) for 2 µg/mL of anthracene proving anthracene degradation ability by the bacterium PH7 is inversely proportional to anthracene concentration (Figure 2).

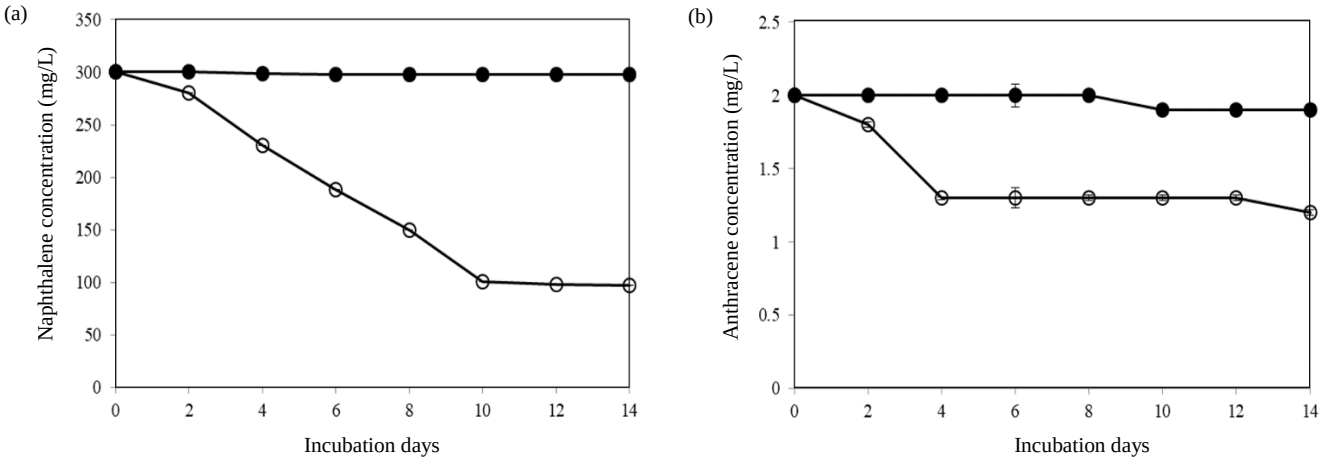

Figure 2. (a) Degradation of naphthalene (300 mg/L) by PH1 (control-closed circles, experiment-open circles). (b) Degradation of anthracene (2 µg/mL is suggested) by PH1 (control-closed circles, experiment-open circles).

The degradation kinetic study confirmed that PH1 (Figure 2(a)) degraded 300 µg/mL of naphthalene up to 99.2 µg/mL within 14 days of incubation whereas PH7 strain degraded 2.00±0.04 µg/mL of anthracene up to 1.02±0.04 µg/mL at the end of 14 days of incubation.

An FTIR analysis further confirmed the naphthalene and anthracene degradation by PH1 and PH7 respectively. According to the FTIR results, the percentage transmission for naphthalene (Figure 3(a) and Figure 3(b)) and anthracene (Figure 4(a) and Figure 4(b)) was reduced after 14 days of incubation.

According to FTIR results the wavelength obtained for anthracene as 2,924 shows complete removal at the 14th day of incubation.

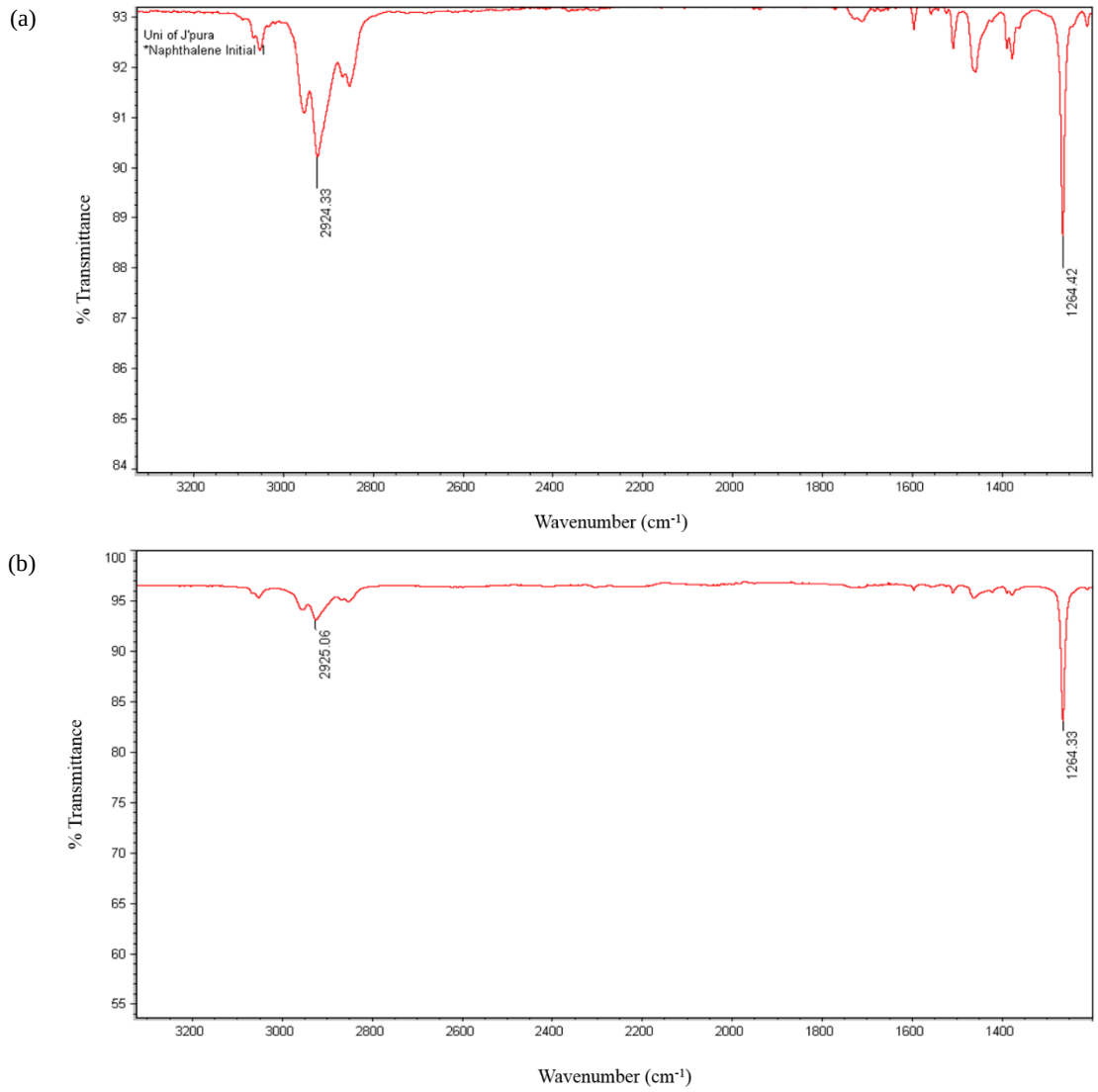

Figure 3. Fourier Transform Infrared Spectroscopy (FTIR) for naphthalene degrading PH1. [(a) 200 µg/mL initial concentration; (b) after 14 days naphthalene concentration]

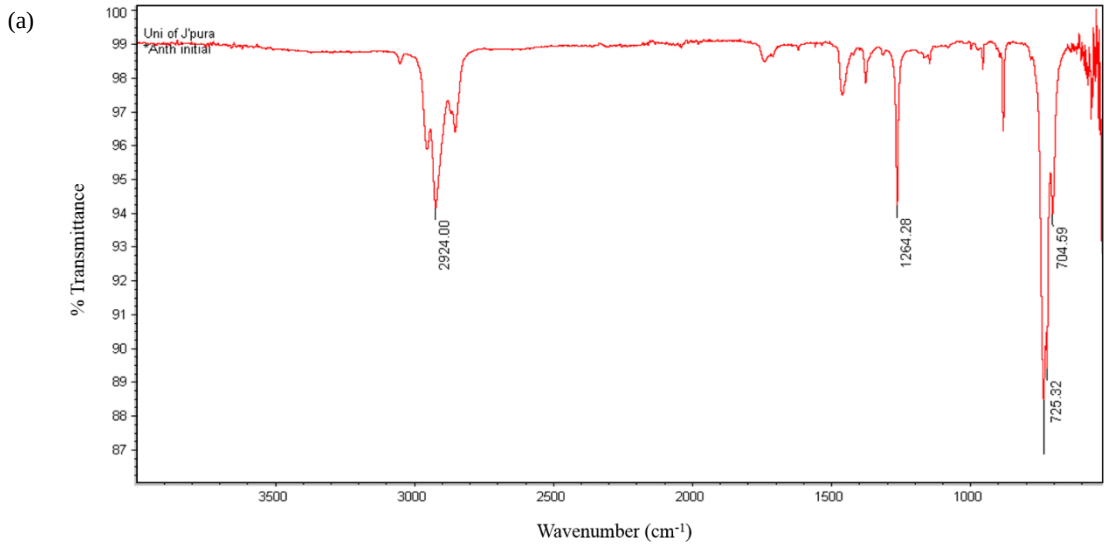

Figure 4. Fourier Transform Infrared Spectroscopy (FTIR) for anthracene degrading PH7. [(a) 200 µg/mL initial concentration; (b) after 14 days anthracene concentration]

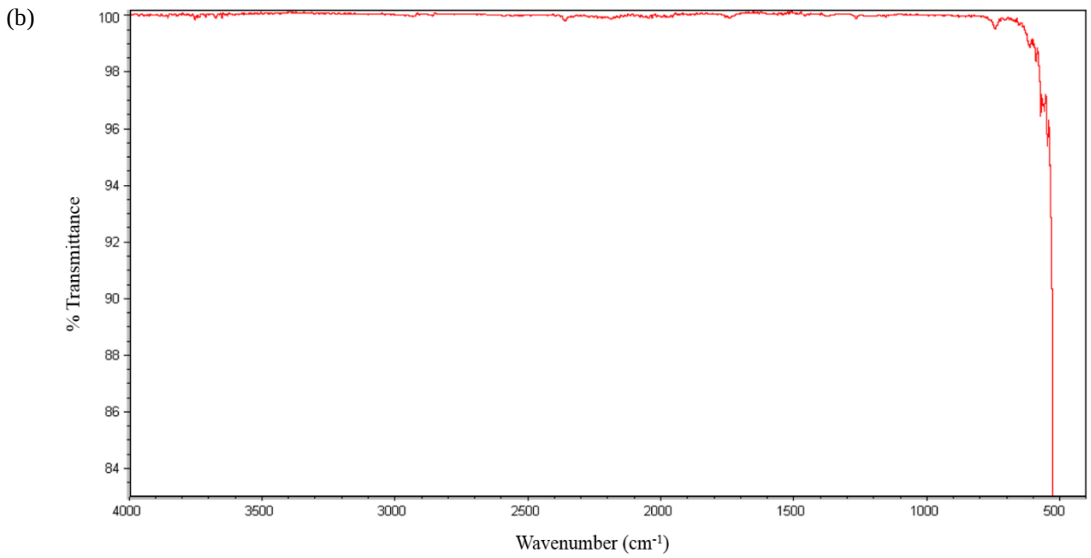

Figure 4. Fourier Transform Infrared Spectroscopy (FTIR) for anthracene degrading PH7. [(a) 200 µg/mL initial concentration; (b) after 14 days anthracene concentration] (cont.)

Morphological characterization of PH1 showed that it was a gram negative, rod shaped and forms light brown colored, circular shaped colonies with irregular margins, whereas PH7 strain was gram negative, rod shaped and forms yellow colored circular shaped colonies with circular margins. The 16S rRNA sequence confirmed that PH1 strain was 98% similar to that of *Achromobacter spanius* and that PH7 strain was 99% similar that of *Alcaligens faecalis* (Figure 5).

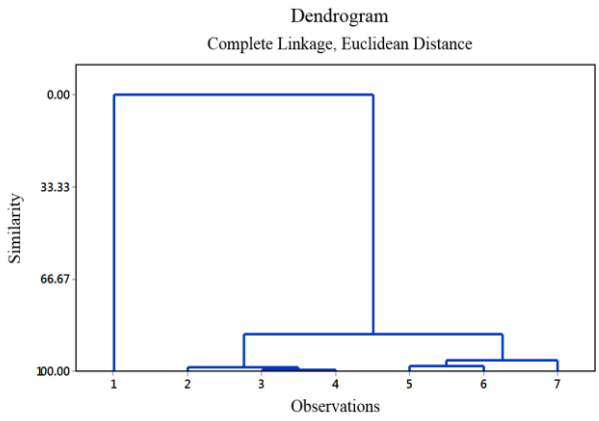

Figure 5. Dendogram showing the clustering of sampling locations based on naphthalene and anthracene concentrations.

The cluster analysis confirmed that location 1, which is the immediate PAH releasing point, occupied a separate cluster denoting high concentrations of naphthalene (235.23±0.06 µg/mL) and anthracene (1.88±0.05 µg/mL) while locations 2, 3, and 4 clustered together with moderate concentrations of naphthalene and anthracene (Figure 6). Locations 5 and 6 showed a different cluster indicating lower low levels of naphthalene and anthracene than locations 2, 3, and 4. Interestingly, location 7 which was away from the immediate PAH releasing site had the lowest concentrations of naphthalene and anthracene (Figure 6).

Furthermore, the PCA categorized the studied sampling sites into three groups based on analyzed physico-chemical properties of collected water samples (Figure 6). The highest water temperature, pH, conductivity, phosphate, naphthalene and anthracene concentration were recorded at location 1 and 2. The maximum concentration for nitrate was recorded at location 3 (4.53±0.06 mg/L) and 4 (5.28±0.04 mg/L). In the case of naphthalene and anthracene contamination, the highest concentrations for naphthalene (235.23±0.06 µg/mL) and anthracene (1.88±0.05 µg/mL) was recorded in location 1 whereas the lowest naphthalene (2.75±0.03 µg/mL) and anthracene (0.995±0.019 µg/mL) concentrations were recorded in location 7. Thus, location 1 and 2 clustered in group A, location 3 and 4 in group B, location 5 in group C and location 6 and 7 in group D (Figure 6).

4. DISCUSSION

This study records the presence of PAH (naphthalene and anthracene) in a restaurant site in Sri Lanka. The water samples obtained from the study area were subjected regular exposure of cooking oil contaminated effluent waters. Water quality parameters revealed that, location 1 has the highest value of temperature (33ºC), phosphate (0.81 mg/L),

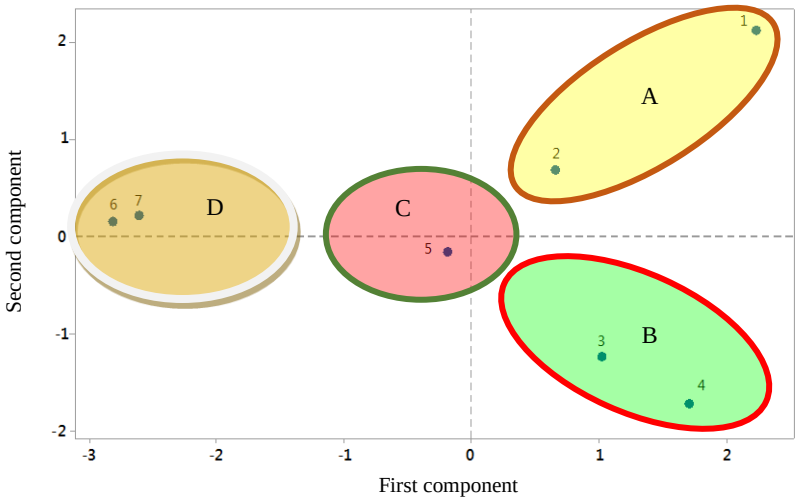

Figure 6. Results of PCA analysis

naphthalene (235.23±0.06 µg/mL) and anthracene concentration (1.78±0.05 µg/mL). This is because location 1 is the immediate wastewater releasing site of the restaurant. However, the nitrate and phosphate concentrations were higher in location 3 (4.53±0.06 mg/L) and 4 (5.28±0.04 mg/L) and this may due to soil, geochemical properties and vegetation type of these sites. During the sampling period it was observed that the Location 3 and 4 cater drinking water needs of domestic animals such as cattle and dogs. Hence, animal droppings to the water in these sites may have resulted in high nitrate concentrations.

According to the industrial wastewater quality standards (BOI, 2011), the temperature of waste water should be at or below 40ºC. The highest value of temperature was recorded as 33ºC at location 1. The temperature of the rest of sampling locations remained below the maximum tolerance limit (40ºC). According to the guide to industrial waste water quality of Sri Lanka (BOI, 2011) water pH should be in the range of 6.0-8.5. The results of the study showed all the sampling locations water pH ranged from 6.39 to 7.12. As stipulated in the wastewater quality guide, nitrate of the industrial and domestic wastewater should be below 50 mg/L. In the study the nitrate concentrations were from 4.53 to 5.28 mg/L. The highest concentration of phosphate (0.080±0.002 mg/L) was recorded at location 1 and the recorded concentrations were below the maximum tolerance limit (1.0 mg/L) given for industrial wastewater quality of Sri Lanka.

In the present study, a colorimetric assay was employed with the methylene blue as the redox indicator to screen naphthalene and anthracene degrading bacteria. When PAH degrading bacteria is present in a microplate well along with PAH and methylene blue, a colour change from blue to colorless would be visualized. This is due to H^+ generated by bacterial metabolism of naphthalene and anthracene. This H^+ together with 2 electrons reduces methylene blue into leucomethylene blue (Hallock et al., 2003). Hence, two bacterial strains, namely PH1 and PH7, were identified as effective naphthalene and anthracene degraders respectively. The 16SrRNA analysis of PH1 and PH7 confirmed the degraders as *Achromobacter spanius* and *Alcaligens faecalis*. It is established that selection of PAH-degrading microorganisms, as with other xenobiotic chemicals, occurs as a result of their previous exposure to this substances in the environment (Lewis et al., 1987). However, these adaptations occur slowly and usually depend on the recalcitrance or biodegradability of the particular substance involved (Tao et al., 2004). PAHs usually have low aqueous solubility, thus are poorly bioavailable for microbial utilization as sole carbon source (Johnsen et al., 2005).

In the present study, naphthalene degradation by *A. spanius* was 66.8±0.02% and the recorded degradation percentage was less than values recorded by Karimi et al. (2015). The results of the studies suggested that the degradation potential is species specific Moreover, Bisht et al. (2010) has recorded 85.3% and 95.8% of naphthalene degradation by the bacterium *B. circulans* (SBA12) and *Kurthia* sp. (SBA4), respectively. Sadighbayan et al. (2016) recorded 57.1% naphthalene degradation by a mixed bacteria consortium from PAH contaminated soil.

In the case of anthracene, *A. faecalis* showed 50.5% degradation. However, less degradation compare to anthracene degradation (55.1%). More or less similar results were recorded when employed

mixed bacterial consortia isolated from soil contaminated with petrochemical by Tao et al. (2004). Barranaco et al. (2004) has recorded two bacterial strains, *B. circulans* (SBA12) and *Kurthia* sp. (SBA4) that degraded anthracene significantly achieving 87.5% and 86.6%, respectively.

The difference for degradation rates of both naphthalene and anthracene by isolated bacteria is specific and is contributed through their unique enzymes secreted during biodegradation (Bisht et al., 2010). Hence the isolated *A. spanius* and *A. faecalis* show different degradation rates for naphthalene and anthracene respectively.

However, it is noteworthy that almost all the studies have been done for the isolation of PAH degradation bacteria in petrochemical sites where high concentrations of PAHs were detected (Undugoda et al., 2016). However, the present study records the isolation of naphthalene and anthracene degrading bacteria from a restaurant site contaminated with cooking oil. Thus, *A. spanius* and *A. faecalis* strains were isolated as potential degraders for naphthalene and anthracene in the present study. However, the recorded degradation percentages of the bacteria *A. spanius* and *A. faecalis* are comparatively low compared to the bacteria recorded by the other studies suggesting previous continuous exposure to particular chemical may enhance the degradation potential.

Interestingly, PAH degrading strains isolated by Dharmawan et al. (2015) showed 100 % removal of PAHs. Gran-Scheuch et al. (2017) also recorded the PAH (Phenanthrene) degradation by *Sphingobium xenophagum* isolated from a diesel oil contaminated soil. According to Gran-Scheuch et al. (2017), *Sphingobium xenophagum* showed 95% removal of Phenanthrene. Hence, it is noteworthy that all recorded studies have isolated PAH degrading bacteria from petroleum oil contaminated sites. However, the present study have deviated from these traditional sites and focused on restaurant effluent water releasing sites. Thus, bacterial strains isolated from the present study shows lower degradation rates as environmental PAH concentration in effluent waters released from restaurant sites have comparatively lesser concentrations of PAHs in comparison to petrochemical stations. The results of this study supports the perspective of the green solution for further development of biotechnological solutions to eliminate of pollutants like naphthalene and anthracene from the aquatic environment.

5. CONCLUSION

This study presents the first record of isolation of naphthalene degrading *Achromobacter spanius* and anthracene degrading *Alcaligens faecalis* strains isolated from a restaurant site. Degradation studies confirmed that *A. spanius* efficiently degrade naphthalene at the rate of 0.145±0.002 ppm/day, whereas *A. faecalis* degraded anthracene at the rate of 0.181±0.036 ppm/day. This is the first study recording an isolation of naphthalene and anthracene degrading bacteria from a restaurant site. Hence, these bacterial strains show comparatively lower naphthalene and anthracene degradations than bacterial strains isolated from petrochemical station sites. Therefore, these isolated naphthalene degrading *Achromobacter spanius* and anthracene degrading *Alcaligens faecalis* strains could be effectively used to treat cooking oil PAH contaminated sites.

REFERENCES

Abdel-Shafy HI, Mansour MS. A review on polycyclic aromatic hydrocarbons: source, environmental impact, effect on human health and remediation. Egyptian Journal of Petroleum 2016;25(1):107-23.

American Public Health Association (APHA) Standard Methods. 23rd ed. Washington, D.C., USA: American Public Health Association; 2017.

Bailey GS, Hendricks JD, Nixon JE, Pawlowski NE. The sensitivity of rainbow trout and other fish species to carcinogens. Drug Metabolism Reviews 1984;15(4):725-50.

Barranaco A, Alonso-Salces RM, Crespo I, Berrueta LA, Gallo B, Vicente F, et al. Polycyclic aromatic hydrocarbon content in commercial Spanish fatty foods. Journal of Food Protection 2004;67(12):2786-91.

Bisht S, Pandey P, Sood A, Sharma S, Bisht NS. Biodegradation of naphthalene and anthracene by chemo-tactically active rhizobacteria of *Populus deltoides*. Brazilian Journal of Microbiology 2010;41(4):922-30.

Board of Investment of Sri Lanka (BOI). Wastewater Quality of Sri Lanka. Colombo, Sri Lanka: Environmental Norms; 2011.

Collins JF, Brown JP, Alexeeff GV, Salmon AG. Potency equivalency factors for some polycyclic aromatic hydrocarbons and polycyclic aromatic hydrocarbon derivatives. Regulatory Toxicology and Pharmacology 1998;28,45-54.

Devi NL, Yadav IC, Shihua Q, Dan Y, Zhang G, Raha P. Environmental carcinogenic polycyclic aromatic hydrocarbons in soil from Himalayas, India: Implications for spatial distribution, sources apportionment and risk assessment. Chemosphere 2016;144,493-502.

Dharmawan R, Nakata H, Ohta H, Niidome T, Takikawa K, Morimura S. Isolation and evaluation of PAH degrading bacteria. Journal of Bioremediation and Biodegredation 2015;6(3):1.

Gran-Scheuch A, Fuentes E, Bravo DM, Jiménez JC, Pérez-Donoso JM. Isolation and characterization of phenanthrene degrading bacteria from diesel fuel-contaminated Antarctic Soils. Frontiers in Microbiology 2017;28:1634.

Guruge KS, Manage PM, Yamanaka N, Miyazaki S, Taniyasu S, Yamashita N. Species-specific concentrations of perfluoroalkyl contaminants in farm and pet animals in Japan. Chemosphere 2008;73(1):210-5.

Guruge KS, Taniyasu S, Yamashita N, Manage PM. Occurrence of perfluorinated acids and fluorotelomers in waters from Sri Lanka. Marine Pollution Bulletin 2007;54(10):1667-72.

Hallock AJ, Berman ES, Zare RN. Ultratrace kinetic measurements of the reduction of methylene blue. Journal of the American Chemical Society 2003;125(5):1158-9

Hamid N, Syed JH, Kamal A, Aziz F, Tanveer S, Ali U, et al. A review on the abundance, distribution and eco-biological risks of PAHs in the key environmental matrices of South Asia. Reviews of Environmental Contamination and Toxicology 2017;240:1-30.

Idroos SF, Manage PM, De Silva BG. Role of *Stenotrophomonas maltophilia* in the degradation of antibiotics and hydrocarbons. Proceeding of the International Conference on Multidisciplinary Approaches; 2015 Sep 11; Golden Rose hotel, Sri Lanka; 2015.

Jiang D, Xin C, Li W, Chen J, Li F, Chu Z, et al. Quantitative analysis and health risk assessment of polycyclic aromatic hydrocarbons in edible vegetable oils marketed in Shandong of China. Food and Chemical Toxicology 2015;83:61-7.

Johnson BA, Farahbod H, Leon M. Interactions between odorant functional group and hydrocarbon structure influence activity in glomerular response modules in the rat olfactory bulb. Journal of Comparative Neurology 2005;483(2):205-16.

Karimi P, Peters KO, Bidad K, Strickland PT. Polycyclic aromatic hydrocarbons and childhood asthma. European Journal of Epidemiology 2015;30(2):91-101.

Kim KH, Jahan SA, Kabir E, Brown RJ. A review of airborne polycyclic aromatic hydrocarbons (PAHs) and their human health effects. Environment International 2013;60:71-80.

Lewis DFV. Molecular orbital calculations and quantitative structure-activity relationships for some polyaromatic hydrocarbons. Xenobiotica 1987;17(11):1351-61.

Liyanage GY, Manage PM. Optimisation of environmental factors on oil degrading bacteria isolated from coastal water and sediments in Sri Lanka. Journal of Tropical Forestry and Environment 2015;5:13-25.

Manage PM, Edwards C, Singh BK, Lawton LA. Isolation and identification of novel microcystin-degrading bacteria. Journal of Applied Environmental Microbiology 2009;75(21):6924-8.

Menzie CA, Potocki BB, Santodonato J. Exposure to carcinogenic PAHs in the environment. Environmental Science and Technology 1992;26(7):1278-84.

Nkansah MA. Environmental Remediation: Removal of Polycyclic Aromatic Hydrocarbons [dissertation]. Norway: University of Bergen; 2012.

Ohura T, Sakakibara H, Watanabe I, Shim WJ, Manage PM, Guruge KS. Spatial and vertical distributions of sedimentary halogenated polycyclic aromatic hydrocarbons in moderately polluted areas of Asia. Environmental Pollution 2015;196: 331-40.

Oyehan TA, Al-Thukair AA. Isolation and characterization of PAH-degrading bacteria from the Eastern Province, Saudi Arabia. Marine Pollution Bulletin 2017;115(1-2):39-46.

Partila AM. Biodegradation of Polycyclic Aromatic Hydrocarbons in Petroleum Oil Contaminating the Environment [dissertation]. Giza, Egypt: Cairo University; 2013.

Poliakova OV, Lebedev AT, Petrosyan VS, Hanninen O, Renzoni A, Sawa D, et al. Accumulation of persistent organic pollutants in the food chain of Lake Baikal. Toxicological and Environmental Chemistry 2000;75,235-43.

Princewill-Ogbonna IL, Adikwu UE. Levels of polycyclic aromatic hydrocarbons in edible vegetable oil sold in Umuahia, main market, Nigeria. IOSR Journal of Environmental Science, Toxicology and Food Technology 2015;9(5):87-92.

Sadighbayan K, Assadi MM, Farazmand A, Monadi AR, Aliasgharzad N, Mobaiyen H, et al. Biodegradation potential of soils in tabriz petroleum refinery for removing solid polycyclic hydrocarbons. Advances in Bioresearch 2016;7(2):57-63.

Stogiannidis E, Laane R. Source characterization of polycyclic aromatic hydrocarbons by using their molecular indices: An overview of possibilities. Reviews of Environmental Contamination and Toxicology 2015;234:49-133.

Tao S, Cui YH, Xu FL, Li BG, Cao J, Liu WX, et al. Polycyclic aromatic hydrocarbons (PAHs) in agricultural soil and vegetables from Tianjin. Science of the Total Environment 2004;320(1):11-24.

Undugoda LJ, Kannangara S, Sirisena DM. Aromatic hydrocarbon degrading fungi inhabiting the phyllosphere of ornamental plants on roadsides of urban areas in Sri Lanka. Journal of Bioremediation and Biodegradation 2016;7(328):2.

Varanasi U, Stein JE, Nishimoto M, Reichert WL, Collier TK. Chemical carcinogenesis in feral fish: Uptake, activation, and detoxication of organic xenobiotics. Environmental Health Perspectives 1987;71:155-70.

Witt G. Occurrence and transport of polycyclic aromatic hydrocarbons in the water bodies of the Baltic Sea. Marine Chemistry 2002;79(2):49-66.

GUIDE FOR AUTHORS

Publication and Peer-reviewing processes of Environment and Natural Resources Journal

Environment and Natural Resources Journal is a peer reviewed and open access journal that is published twice a year (January-June and July-December). Manuscripts should be submitted online at https://ph02.tci-thaijo.org/index.php/ennrj/about/submissions by registering and logging into this website. Submitted manuscripts should not have been published previously, nor be under consideration for publication elsewhere (except conference proceedings papers). A guide for authors and relevant information for the submission of manuscripts are provided in this section and also online at: https://ph02.tci-thaijo.org/index.php/ennrj/author. All manuscripts are refereed through a **double-blind peer-review** process.

Submitted manuscripts are reviewed by outside experts or editorial board members of **Environment and Natural Resources Journal**. This journal uses double-blind review, which means that both the reviewer and author identities are concealed from the reviewers, and vice versa, throughout the review process. Steps in the process are as follows:

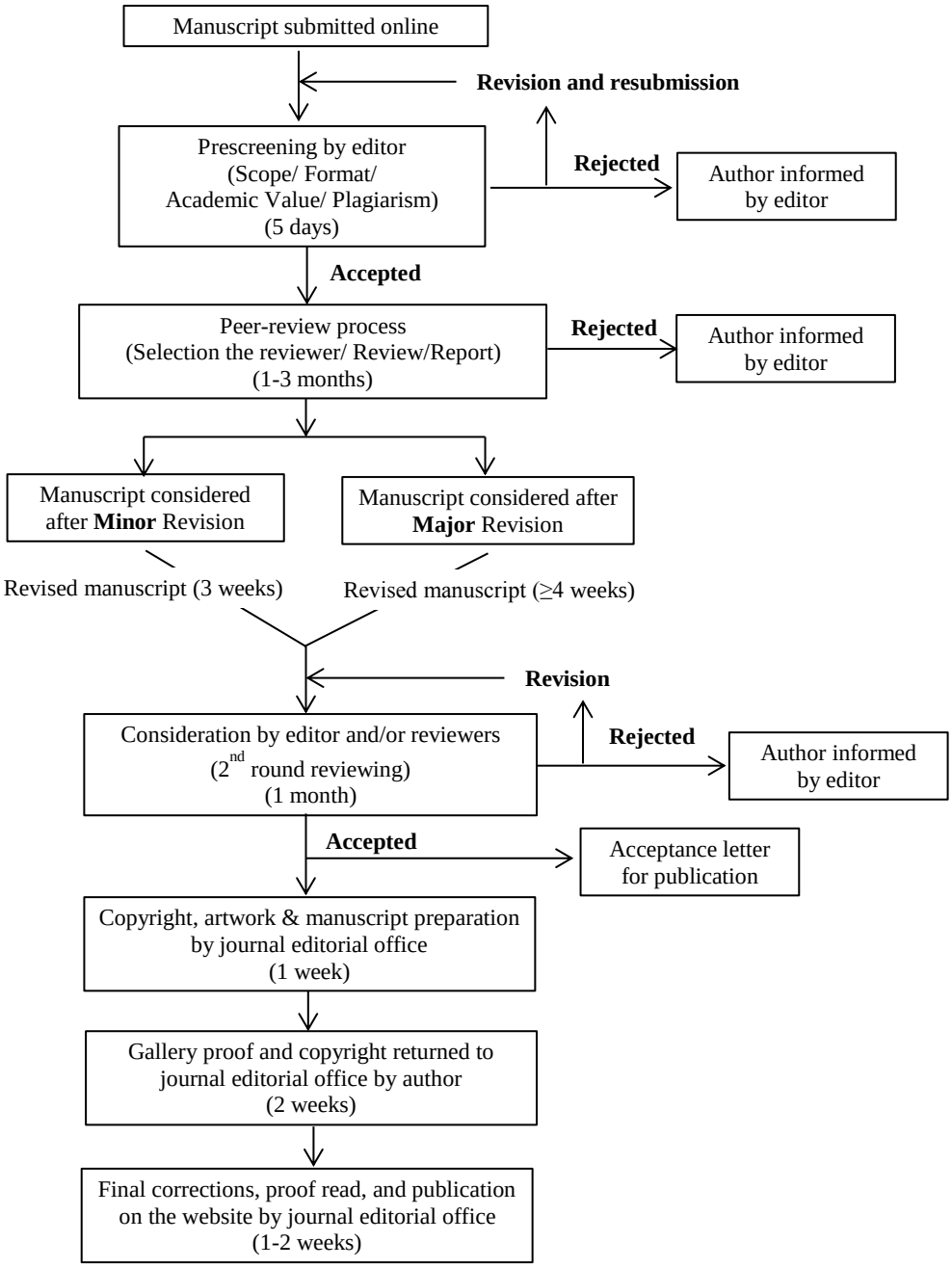

The Environment and Natural Resources Journal (EnNRJ) accepts 2 types of articles for consideration of publication as follows:

- *Original Research Article:* Manuscripts should not exceed 3,500 words (excluding references).
- *Review Article (by invitation):* This type of article focuses on the in-depth critical review of a special aspect in the environment and also provides a synthesis and critical evaluation of the state of the knowledge of the subject. Manuscripts should not exceed 6000 words (excluding references).

Submission of Manuscript

Submitted file(s): The manuscript (A4) must be submitted in Microsoft Word (.doc or .docx).

Reviewers suggestion *(mandatory)*: Please provide the names of 3 potential reviewers with the information about their affiliations and email addresses. *The recommended reviewers should not have any conflict of interest with the authors. Each of the reviewers must come from a different affiliation and must not have the same nationality as the authors.* Please note that the editorial board retains the sole right to decide whether or not the recommended potential reviewers will be selected.

Preparation of Manuscripts

Manuscript should be prepared strictly as per guidelines given below. The manuscript (A4 size page) should be submitted in Microsoft Word (.doc or .docx) with Times New Roman 12 point font and a line spacing of 1.5. *The manuscript that is not in the correct format will be returned and the corresponding author may have to resubmit*. The submitted manuscript must have the following parts:

Title should be concise and no longer than necessary. Capitalize first letters of all important words, in Times New Roman 12 point bold.

Author(s) name and affiliation must be given, especially the first and last names of all authors, in Times New Roman 11 point bold.

Affiliation of all author(s) must be given in Times New Roman 11 point italic.

Abstract should indicate the significant findings with data. A good abstract should have only one paragraph and be limited to 200 words. Do not include a table, figure or reference.

Keywords should adequately index the subject matter and up to six keywords are allowed.

Text body normally includes the following sections: 1. Introduction 2. Methodology 3. Results and Discussion 4. Conclusions 5. Acknowledgements 6. References

Reference style must be given in Vancouver style. Please follow the format of the sample references and citations as shown in this Guide below.

Unit: The use of abbreviation must be in accordance with the SI Unit.

Format and Style

Paper Margins must be 2.54 cm on the left and the right. The bottom and the top margin of each page must be 1.9 cm.

Introduction is critically important. It should include precisely the aims of the study. It should be as concise as possible with no sub headings. The significance of problem and the essential background should be given.

Methodology should be sufficiently detailed to enable the experiments to be reproduced. The techniques and methodology adopted should be supported with standard references.

Headings in Methodology section and Results and Discussion section, no more than three levels of headings should be used. Main headings should be typed (in bold letters) and secondary headings (in bold and italic letters). Third level headings should be typed in normal and no bold, for example;

2. Methodology

2.1 Sub-heading

2.1.1 Sub-sub-heading

Results and Discussion can be either combined or separated. This section is simply to present the key points of your findings in figures and tables, and explain additional findings in the text; no interpretation of findings is required. The results section is purely descriptive.

Tables Tables look best if all the cells are not bordered; place horizontal borders only under the legend, the column headings and the bottom.

Figures should be submitted in color; make sure that they are clear and understandable. Please adjust the font size to 9-10, no bold letters needed, and the border width of the graphs must be 0.75 pt. *(Do not directly cut and paste them from MS Excel.)* Regardless of the application used, when your electronic artwork is finalized, please 'save as' or convert the images to TIFF (or JPG) and separately send them to EnNRJ. The images require a resolution of at least 300 dpi (dots per inch). If

a label needed in a figure, its font must be "Times New Roman" and its size needs to be adjusted to fit the figure without borderlines.
All Figure(s) and Table(s) should be embedded in the text file.

Conclusions should include the summary of the key findings, and key take-home message. This should not be too long or repetitive, but is worth having so that your argument is not left unfinished. Importantly, don't start any new thoughts in your conclusion.

Acknowledgements should include the names of those who contributed substantially to the work described in the manuscript but do not fulfill the requirements for authorship. It should also include any sponsor or funding agency that supported the work.

References should be cited in the text by the surname of the author(s), and the year. This journal uses the author-date method of citation: the last name of the author and date of publication are inserted in the text in the appropriate place. If there are more than two authors, "et al." after the first author' name must be added. Examples: (Frits, 1976; Pandey and Shukla, 2003; Kungsuwas et al., 1996). If the author's name is part of the sentence, only the date is placed in parentheses: "Frits (1976) argued that . . ."

In the list of references at the end of the manuscript, full and complete references must be given in the following style and punctuation, arranged alphabetically by first author's surname. Examples of references as listed in the References section are given below.

Book
Tyree MT, Zimmermann MH. Xylem Structure and the Ascent of Sap. Heidelberg, Germany: Springer; 2002.

Chapter in a book
Kungsuwan A, Ittipong B, Chandrkrachang S. Preservative effect of chitosan on fish products. In: Steven WF, Rao MS, Chandrkachang S, editors. Chitin and Chitosan: Environmental and Friendly and Versatile Biomaterials. Bangkok: Asian Institute of Technology; 1996. p. 193-9.

Journal article
Muenmee S, Chiemchaisri W, Chiemchaisri C. Microbial consortium involving biological methane oxidation in relation to the biodegradation of waste plastics in a solid waste disposal open dump site. International Biodeterioration and Biodegradation 2015;102:172-81.

Published in conference proceedings
Wiwattanakantang P, To-im J. Tourist satisfaction on sustainable tourism development, amphawa floating marketSamut songkhram, Thailand. Proceedings of the 1st Environment and Natural Resources International Conference; 2014 Nov 6-7; The Sukosol hotel, Bangkok: Thailand; 2014.

Ph.D./Master thesis
Shrestha MK. Relative Ungulate Abundance in a Fragmented Landscape: Implications for Tiger Conservation [dissertation]. Saint Paul, University of Minnesota; 2004.

Website
Orzel C. Wind and temperature: why doesn't windy equal hot? [Internet]. 2010 [cited 2016 Jun 20]. Available from: http://scienceblogs.com/principles/2010/08/17/wind-and-temperature-why-doesn/.

Report organization
Intergovernmental Panel on Climate Change (IPCC). IPCC Guidelines for National Greenhouse Gas Inventories: Volume 1-5. Hayama, Japan: Institute for Global Environmental Strategies; 2006.

Remark

** Please be note that manuscripts should usually contain at least 15 references and some of them must be up-to-date research articles.*

** Please strictly check all references cited in text, they should be added in the list of references. Our Journal does not publish papers with incomplete citations.*

Mahidol University

Wisdom of the Land

Research and Academic Service Section, Faculty of Environment and Resource Studies, Mahidol University
999 Phutthamonthon 4 Rd, Salaya, Nakhon Pathom 73170, Phone +662 441-5000 ext. 2108 Fax. +662 441 9509-10
E-mail: ennrjournal@gmail.com Website: https://www.tci-thaijo.org/index.php/ennrj